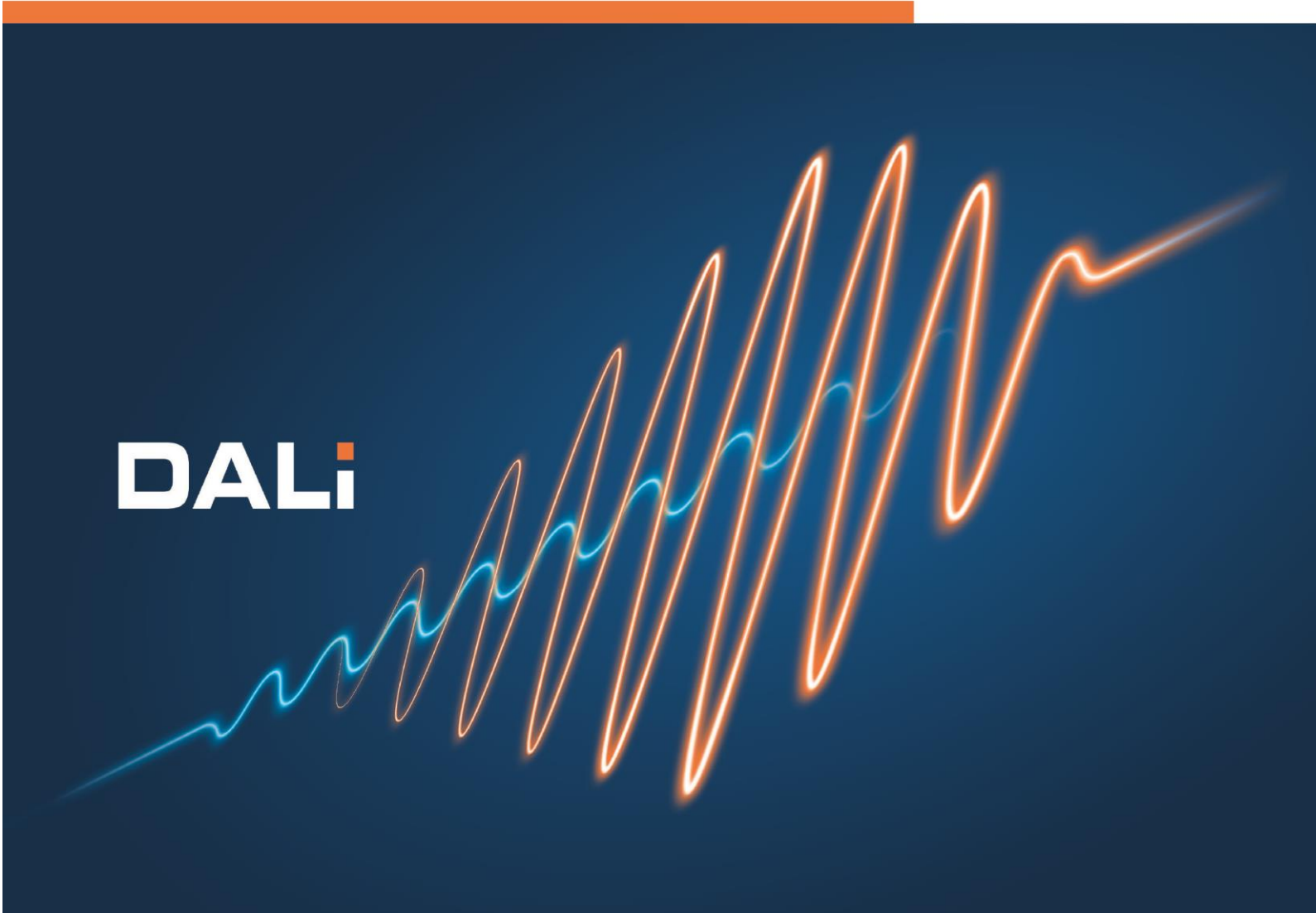


DALI – Dresden Advanced Light Infrastructure

Conceptual Design Report

DALi



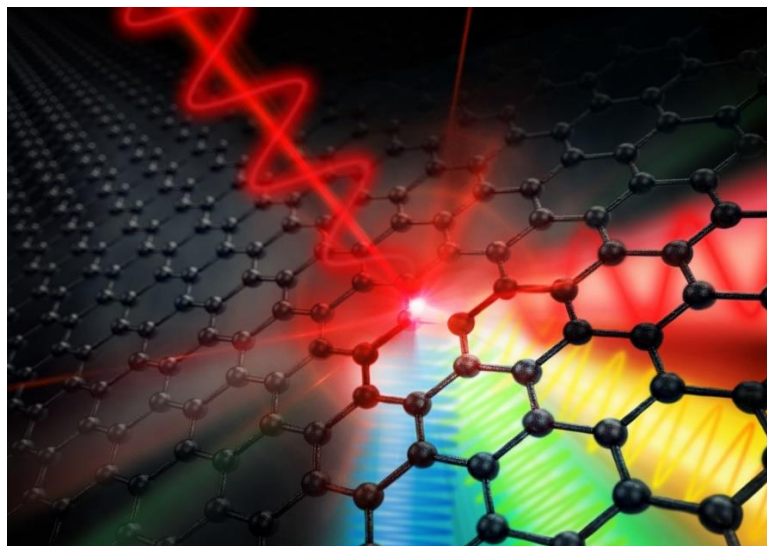
Helmholtz Research Infrastructures

CONCEPTUAL DESIGN REPORT FOR A LARGE INVESTMENT OF CATEGORY B (>50 M€)

DALI

Proposal for a new THz light source with a multitude of probes

The DALI project comprises the succession of the present ELBE facility by a high-field THz radiation source with world-class beam parameters in combination with secondary radiation.



Project Information

Name: Dresden Advanced Light Infrastructure (acronym: DALI)

Research field(s): Matter / From Matter to Materials and Life

Coordinating Helmholtz center: Helmholtz-Zentrum Dresden-Rossendorf (HZDR)

Helmholtz centers and external partner institutions: TU Dresden

Category B: Intended for the German National Roadmap for Large-Scale Infrastructures

Description: DALI will be an electron-accelerator-based facility for high-field terahertz (THz) combined with advanced photon and UED probes as well as a secondary positron source. This infrastructure will be operated as a user facility (LK II) for the study of matter by the national and international scientific community.

DALI project team

Project leaders	Prof. Dr. Manfred Helm Prof. Dr. Thomas Cowan Prof. Dr. Ulrich Schramm
Project manager	Klaus Knöfel
Building, infrastructure	Dirk Reichelt
Accelerators, radiation sources	Prof. Dr. Peter Michel Dr. Ulf Lehnert
User stations, instrumentation	Dr. Stephan Winnerl Dr. Jan-Christoph Deinert Dr. Andreas Wagner
Scientific Director of HZDR	Prof. Dr. Sebastian Schmidt
Administrative Director of HZDR	Dr. Diana Stiller

Contributors

From the Helmholtz-Zentrum Dresden – Rossendorf:

Dr. Ellen Adams	Dr. Andre Arnold	Dr. Maik Butterling
Prof. Dr. Thomas Cowan	Dr. Jan-Christoph Deinert	Dr. Pavel Evtushenko
Prof. Dr. Karim Fahmy	Michael Freitag	Dr. Gowrishankar Hallilingaiah
Prof. Dr. Manfred Helm	Dr. Guido Juckeland	Mathias Justus
Dr. Sven Kiele	Dr. J. Michael Klopf	Dr. Uwe Konrad
Isabell Kösterke	Dr. Sergey Kovalev	Dr. Michael Kuntzsch
Dr. Ulf Lehnert	Dr. Maciej O. Liedke	Prof. Dr. Peter Michel
Dr. Raffael Niemczyk	Dr. Thales de Oliveira	Dr. Alexej Pashkin
Dr. Anton Ryzhov	Gudrun Sauerbrey	Prof. Dr. Roland Sauerbrey
Prof. Dr. Sebastian Schmidt	Dr. Christof Schneider	PD Dr. Harald Schneider
Dr. Barbara Schramm	Prof. Dr. Ulrich Schramm	Dr. Rico Schurig
Mike Siemon	Reinhard Steinbrück	Dr. Jochen Teichert
Dr. Andreas Wagner	Dr. Stephan Winnerl	Dr. Rong Xiang
Dr. Klaus Zenker		

External experts:

Prof. Dr. Stefano Bonetti, *Univ. Ca' Foscari, Venice, Italy & Univ. Stockholm, Sweden*
Prof. Dr. Mischa Bonn, *MPI for Polymer Research, Mainz, Germany*
Prof. Dr. Michael Gensch, *Institute of Optical Sensor Systems, DLR Berlin, Germany*
Prof. Dr. Isabella Gierz, *Univ. Regensburg, Germany*
Dr. Maksim Grechko, *MPI for Polymer Research, Mainz, Germany*
Prof. Dr. Markus Gühr, *Deutsches Elektronen Synchrotron DESY, Hamburg, Germany*
Prof. Dr. Stefan Kaiser, *TU Dresden, Germany*
Dr. Susanne Kehr, *TU Dresden, Germany*
Dr. Hirohito Ogasawara, *SLAC National Accelerator Laboratory, Menlo Park, USA*
Dr. Debanjan Polley, *LBNL & UC Berkeley, California, USA*
Prof. Dr. Sascha Preu, *TU Darmstadt, Germany*
Prof. Dr. Dmitry Turchinovich, *Univ. Bielefeld, Germany*
Dr. Peter Zalden, *European XFEL, Schenefeld, Germany*

Main editors:

Prof. Dr. Manfred Helm, Dr. Sven Kiele, Dr. Ulf Lehnert, Dr. Alexej Pashkin

Contents

List of Figures	I
List of Tables	II
Abbreviations	4
Preface	7
Executive Summary	8
1 Overview.....	11
1.1 Introduction	11
1.2 Key parameters of the facility	12
1.3 List of experimental stations	15
2 Scientific Potential (“Scientific Case”).....	16
2.1 Science with THz radiation	18
2.1.1 Superconductivity and highly correlated systems	19
2.1.2 THz nonlinear optics.....	21
2.1.3 THz radiation to stimulate surface chemical reactions	23
2.1.4 Ultrafast and nonlinear spin dynamics.....	24
2.1.5 Non-equilibrium dynamics of water and aqueous solutions in the THz range	26
2.1.6 Ultrafast nonlinear dynamics on nanoscale.....	28
2.1.7 Application-oriented research	30
2.1.8 Biological materials	31
2.2 Probing structural dynamics by ultrafast electron diffraction (UED).....	33
2.2.1 Ultrafast structural dynamics of quantum materials.....	34
2.2.2 UED to study the excited-state dynamics of isolated molecules.....	35
2.3 Science with positrons	36
2.3.1 Probing defect kinetics with positron annihilation lifetime spectroscopy	36
3 Methods and Experimental Stations Enabling New Science with DALI.....	39
3.1 Pump-probe experiments	39
3.2 Time-resolved ARPES.....	41
3.3 Liquid jet	43
3.4 UED system.....	44
3.5 High-intensity Positron Source (HiPS).....	45
3.6 Direct electron beams.....	47
3.7 Central computing infrastructure and data management	48
3.7.1 Central computing infrastructure	48
3.7.2 DALI measurement and control data	50
3.7.3 Experiment planning, simulation, scheduling and execution	51
3.7.4 Open science and European partnerships	52
3.7.5 Sustainable and secure long-term operation	52
4 Machine Design	54
4.1 Physics concept.....	54
4.1.1 Machine overview and main beam parameters	54
4.1.2 Machine operation, sources and timing	55
4.1.3 Electron gun beam dynamics	56
4.1.4 Electron beam transport	57
4.1.5 High-pulse energy THz source	58
4.1.6 High-pulse-energy, high-repetition-rate MIR-THz source	64
4.1.7 Optical beam propagation	67
4.1.8 Short-pulsed positron source.....	68
4.1.9 Ultra-fast electron diffraction.....	69
4.2 Injectors	71
4.2.1 High repetition rate injector for FEL.....	71
4.2.2 High bunch charge injector for super-radiant THz/positron.....	72

Contents

4.2.3	Operational experience	76
4.2.4	Injector test setup.....	79
4.2.5	Alternative guns	79
4.3	Accelerator modules	81
4.3.1	Introduction	81
4.3.2	Basic setup of the ELBE type accelerator module	83
4.3.3	SRF cavities.....	85
4.3.4	Power requirements and fundamental power coupler	88
4.3.5	SRF Infrastructure.....	89
4.3.6	Cryomodule upgrade options and modifications	91
4.4	Magnets	93
4.5	Undulators.....	94
4.5.1	Undulators for the mid-IR source	94
4.5.2	Undulators for the THz sources	95
4.6	Beam dumps.....	96
4.7	Kickers for parallel beams operation	98
4.8	High-power RF systems	103
4.8.1	RF power amplifier technology.....	104
4.8.2	RF waveguide infrastructure	105
4.9	Low-level RF systems.....	105
4.9.1	Digital LLRF	105
4.9.2	Alternatives	106
4.9.3	Long term stability	106
4.9.4	Cost estimate	107
4.10	Timing system.....	107
4.11	Synchronization and longitudinal feedback systems	108
4.11.1	RF master oscillator.....	108
4.11.2	Synchronization system.....	109
4.11.3	Feedback systems.....	109
4.12	Machine protection system	111
4.12.1	MPS architecture	111
4.12.2	Beam loss interlocks.....	111
4.12.3	RF interlocks.....	112
4.12.4	Vacuum inrush detection	112
4.12.5	Radiation damage prevention	113
4.12.6	MPS on operation level.....	113
4.13	Beam diagnostics	113
4.13.1	Beam current monitors	113
4.13.2	Beam position monitors	113
4.13.3	Arrival time monitors	117
4.13.4	Beam profile monitors.....	117
4.13.5	Longitudinal phase space diagnostics	118
4.13.6	Beam loss monitors	118
4.14	THz and FEL diagnostics.....	119
4.14.1	Compressed bunch THz sources	119
4.14.2	Modulated bunch THz sources	121
4.14.3	FEL oscillator.....	122
4.15	Control system	123
4.15.1	Existing solutions	124
4.15.2	Considerations for DALI.....	125
4.16	Vacuum system	125
4.17	Radiation safety / shielding.....	127
4.18	Personnel safety system.....	127
4.19	Cryogenic system	128
4.20	Power and auxiliary supplies	130
4.21	Integration into a DALI building.....	131
5	Strategic Importance and Impact	134

5.1	Strategic importance of DALI.....	134
5.1.1	Strategic importance for HZDR and the Helmholtz Association	134
5.1.2	Strategic importance for the region, Germany and Europe	136
5.1.3	Uniqueness in a worldwide context	137
5.1.4	Attractiveness to external users	142
5.2	Impact of DALI	143
5.2.1	Regional and supra-regional economic effects.....	143
5.2.2	Sustainability	145
5.2.3	Public acceptance, stakeholder and communication.....	145
6	DALI Project Management.....	147
6.1	Planned governance structures (during construction & operation)	147
6.1.1	Management during the DALI project phase	147
6.1.2	Management during the operation phase.....	148
6.2	Operation regime, access management and user operation	149
6.3	Building options	150
6.4	Schedule and work breakdown structure	150
6.5	Risk management and mitigation	152
6.5.1	Technical risks.....	152
6.5.2	Other risks.....	153
7	Financial Framework	154
7.1	Project scope	154
7.2	Project costs	154
7.3	Cost profile.....	156
7.4	Operational costs.....	156
7.5	Costs of the phase-out	156
7.6	Funding scenarios	156
7.7	Economic risk assessment	157

List of Figures

Figure 1: Principle layout of the DALI facility.....	12
Figure 2: Energies of various THz excitations and strong-field THz applications.	16
Figure 3: Illustration of Higgs oscillations in a superconductor.....	20
Figure 4: Temporal asymmetry of electron heating and cooling rates in graphene	22
Figure 5: THz-induced surface chemical reactions.	24
Figure 6: Resonant narrowband excitation of an antiferromagnetic (AFM) mode in NiO.....	25
Figure 7: Schematics of the hydrogen bond network and THz vibrations in liquid water.	27
Figure 8: Schematics of FEL-based scattering-SNIM.	28
Figure 9: Examples for devices applications to be investigated at DALI.	30
Figure 10: Proof-of-principle for TFISH generation	32
Figure 11: Pair distances in CF_3I	35
Figure 12: Fate of positrons in matter.	37
Figure 13: Distribution of DALI sources and table-top sources to the experimental stations	39
Figure 14: Overview over the main pump–probe techniques	40
Figure 15: Scheme of a (multicycle) THz pump – tr-ARPES probe experiment.	42
Figure 16: THz pump – THz Kerr effect / TFISH probe setup at TELBE.	43
Figure 17: Schematics of the positron annihilation lifetime setups EPOS at ELBE	45
Figure 18: Schematics of the UHV chamber for in-situ defect characterization.	46
Figure 19: The new HZDR Data Center.....	50
Figure 20: Heliport scheme	51
Figure 21: Schematic overview of the accelerators and secondary sources.	54
Figure 22: Two-parameter optimization of the SRF gun beam dynamics using ASTRA.....	56
Figure 23: Spectral density (a, left) and pulse energy (b, right) of a single-cycle CDR source. .	59
Figure 24: Spectral power density	61
Figure 25: Spectral power density on the screen.....	61
Figure 26: Output pulse energy at the fundamental resonance frequency of a wiggler.....	63
Figure 27: Envelopes of the optical mode in the ring resonator of the oscillator FEL.	64
Figure 28: Small-signal gain per round-trip for different wavelength and FEL parameters.	65
Figure 29: Saturation power of the FEL oscillator	66
Figure 30: Propagation of a THz optical beam out from the accelerator vault.	67
Figure 31: Envelopes of the optical beam.....	68
Figure 32: ELBE type thermionic DC gun.	72
Figure 33: Photograph of the SRF gun II cold mass	73
Figure 34: The cut-out view of the ELBE SRF gun	74
Figure 35: Cavity performance expressed as a function of the intrinsic quality factor and the accelerating field.	76
Figure 36: Overview of quantum efficiency (QE), beam hours and total extracted charge of all Cs_2Te cathodes used in SRF gun II so far.....	77
Figure 37: Representative plot of cavity gradient and extracted current for a typical user beam time.	78
Figure 38: The layout of the proposed diagnostic beam line in the injector test cave.....	79
Figure 39: QWR normal conducting RF gun and the injector beam line used for LCLS-II facility.	80
Figure 40: Cross section of LCLS-II HE quarter wave resonator (QWR) SRF gun.....	80
Figure 41: Photograph of a cryomodule.....	82
Figure 42: Cross-section of the ELBE type cryomodule with the most important components. .	83
Figure 43: Cross section view of a complete nine-cell cavity.	86
Figure 44: Vertical test results of two RI made 9-cell TESLA cavities	87
Figure 45: RF power requirements as a function of beam current	88
Figure 46: Cross section view at the cold part of the FPC (left) and warm part of the FPC with interlock diagnostic and doorknob waveguide transition (right).	89
Figure 47: ELBE cavity tandem in ISO 4 cleanroom after final assembly and leak check.	90
Figure 48: Proposed clean room complex	91
Figure 49: Proposed SRF test cave.....	91

Figure 50: The most advanced ELBE type cryomodule (left) compared to its ancestor (right).	92
Figure 51: Wavelength tuning range of an undulator with 100 mm period length.....	95
Figure 52: Wavelength tuning range of an undulator with 300 mm period length.....	96
Figure 53: Aluminum body with stainless steel cooling coil entering from below.	97
Figure 54: Graphite body with stainless steel vacuum vessel for guiding the cooling water.....	98
Figure 55: Mechanical design and field strength of the resonant kicker cavity.....	101
Figure 56: Mechanical design of the ELBE strip-line kicker.	102
Figure 57: Deflection field strength in the cross-section view.	102
Figure 58: Simulated F-parameters of the strip-line kicker assembly.....	103
Figure 59: Solid-state power amplifier cabinet with combiner and circulator.	104
Figure 60: Schematic view of the elements of the feedback loop.	110
Figure 61: Machine protection system overview.	112
Figure 62: Strip-line (left) and button type (right) pickups for beam position monitoring.....	114
Figure 63: Simple BPM detection scheme for a 10 MHz band pass system.....	114
Figure 64: 2D CAD drawing of the ELBE strip-line BPM (left) and a KEK strip-line BPM (right).	116
Figure 65: XFEL cold button BPM + pickup (left) and XFEL warm button BPM + pickup (right).	116
Figure 66: Libera Single Pass E.....	117
Figure 67: Pulse-to-pulse detection scheme.	120
Figure 68: Layout of existing diagnostics for FELBE FELs.	122
Figure 69: Layout of the method for shot-to-shot detection of the CEP of each FEL pulse.	123
Figure 70: Acc. Helium supply Low pressure circuit I	129
Figure 71: Low pressure circuit II: UED lab.	129
Figure 72: DALI machine layout.	130
Figure 73: Rooms for technical equipment and user laboratories on the first floor.....	131
Figure 74: Layout of the new DALI building.....	132
Figure 75: Possible locations for a new DALI building on the HZDR campus.	133
Figure 76: Photon science facilities in Germany.....	135
Figure 77: THz pulse energies versus repetition rate	140
Figure 78: Organizational chart of the DALI project.	147
Figure 79: DALI organizational chart.	148
Figure 80: Schedule of the DALI project (based on construction start in 2027).	151
Figure 81: DALI work breakdown structure.	151

List of Tables

Table 1: Key electron beam parameters of the proposed DALI user facility.....	13
Table 2: Photon beam parameters of the proposed facility available for user experiments.....	14
Table 3: Beam parameters for positron sources.....	14
Table 4: Forecast of DALI data volumes and data bandwidth	49
Table 5: Electron beam requirements for secondary positron beam generation.	69
Table 6: Simulated UED performance for the ELBE SRF Gun.	70
Table 7: Overview of the DALI injectors.	71
Table 8: Requirements for the photocathode drive laser(s).	75
Table 9: Comparison of the LINAC	82
Table 10: Technical specifications of the ELBE type cryomodule.....	84
Table 11: TESLA cavity parameters.....	85
Table 12: Overview of further developments of the ELBE type	92
Table 13: Comparison of the respective advantages and disadvantages of the two beam dump variants.	98
Table 14: Properties of deflecting structures acting as beam spreaders.....	99
Table 15: Beam parameters considered for the beam separator design (left) and important normal conducting RFDC parameters are also highlighted (right).	100
Table 16: Reference oscillator frequencies needed for DALI.....	109

<i>Table 17: Achievable resolutions of a 10 MHz, 1.3 GHz band pass electronic for different BPMs.</i>	115
<i>Table 18: Example control system configuration for EPICS and Tango</i>	124
<i>Table 19: Power consumption scenarios of the acc. modules and distribution system.</i>	128
<i>Table 20: Other accelerator-based THz facilities.</i>	139
<i>Table 21: Worldwide positron facilities.</i>	142
<i>Table 22: Cost estimation for the DALI facility (given in T€)</i>	155
<i>Table 23: Cost profile for the DALI implementation (given in T€).</i>	156

Abbreviations

1D, 2D	one-, two-dimensional
ADC	analog-to-digital converter
AIDA	apparatus for in-situ defect analysis
AFM	antiferromagnetic
ALICE	Accelerators and Lasers In Combined Experiments
AMC	advanced mezzanine card
AMOC	age-momentum correlation
ARPES	angle-resolved photoelectron spectroscopy
ASTRA	A Space charge TRacking Algorithm
BLM	beam loss monitor
BPM	beam position monitor
CDR	coherent diffraction radiation
CDR	conceptual design report
CDW	charge density waves
CEBAF	Continuous Electron Beam Accelerator Facility
CEP	carrier envelope phase
CER	coherent edge radiation
CPLD	Complex Programmable Logic Device
CW	continuous wave
DAC	digital-to-analog converter
DALI	Dresden Advanced Light Infrastructure
DBA	donor-bridge-acceptor
DC	direct current
DCLS	Dalian Coherent Light Source
DCM	differential current monitor
DESY	Deutsches Elektronen-SYNchrotron
ELBE	electron accelerator with high brilliance and low emittance
EOM	electro-optical modulator
EOS	electro-optic sampling
EOSC	European Open Science Cloud
EPICS	Experimental Physics and Industrial Control System
EPOS	ELBE positron source
ERL	Energy Recovery Linac
ESFRI	European Strategy Forum on Research Infrastructures
ESS	European Spallation Source
EuXFEL	European X-Ray Free-Electron Laser
FAT	factory acceptance test
FC	Faraday cup
FEL	free-electron laser
FELBE	FEL Source at ELBE
FET	field effect transistor
FHG	fourth-harmonic generation
FIS	“Forschungsinfrastruktur”, research infrastructure
FMEA	Fehlermöglichkeits- und Einflussanalyse (error mode and impact analysis)
FPGA	Field Programmable Gate Array
FRM II	Forschungsreaktor München II
FTE	full-time equivalent
FTIR	Fourier-transform infrared
FTS	fast-tripping system
GPS	Global Positioning System
GUI	graphical user interface
HEB	hot electron bolometer
HGHG	high-gain harmonic generation
HHG	high-harmonic generation
HiPS	High-intensity Positron Source
HLD	High Magnetic Field Laboratory Dresden

HMI	human machine interface
HOM	high order mode
HPR	high-pressure rinsing
HRA	hazard and risk analysis
HZDR	Helmholtz-Zentrum Dresden – Rossendorf
IBC	Ion Beam Center
ICT	integrating current transformer
LCLS	LINAC Coherent Light Source
LEAPS	League of European Accelerator-based Photon Sources
LHC	Large Hadron Collider
LED	light-emitting diode
LEED	Low-energy electron diffraction
LHe	liquid helium
LINAC	linear accelerator
LK II	“Leistungskategorie II”
LLRF	low-level radiofrequency
LN2	liquid nitrogen
MAC	Machine Advisory Committee
MePS	Monenergetic Positron Source
MESA	Mainz Energy-Recovering Superconducting Accelerator
MicroTCA	Micro-Telecommunications Computing Architecture
MIMPS	multiplexed photoionization mass spectrometry
MIR	mid-infrared
MO	master oscillator
MPS	machine protection system
MRF	Micro Research Finland Oy
MU	master unit
μBI	micro-bunching instability
NC	normal conducting
NEG	non-evaporable getter
NEPOMUC	Neutron induced positron source munich
NIR	near-infrared
OR	optical rectification
OSAT	onsite acceptance test
PCA	photoconductive antenna
pELBE	Positron beamline at ELBE
PITZ	Photo Injector Test Facility
PoF	program-oriented funding
PoIFEL	Polish Free-Electron Laser
PLC	Programmable Logic Controller
PMT	photomultiplier tube
PPLN	periodically poled LiNbO ₃
PSS	Personnel Safety System
PY	person years
QE	quantum efficiency
QWR	quarter wave resonator
REMPI	resonance-enhanced multiphoton ionization
RHEED	Reflection high-energy electron diffraction
RI	Research Instruments GmbH
RF	radiofrequency
RFDC	RF deflecting cavity
RMS	root mean square
ROBIS	Rossendorf Publications Repository
RODARE	Rossendorf Data Repository
RTM	rear transition module
SAC	Scientific Advisory Committee
SASE	self-amplified spontaneous emission
SC	superconducting
SCADA	Supervisory Control and Data Acquisition
SFG	sum frequency generation

SIL	safety implementation level
SLAC	Stanford Linear Accelerator Center
SPONSOR	Slow Positron Beam of Rossendorf
SRF	superconducting radiofrequency
s-SNIM	scattering scanning near-field infrared microscopy
SSA	solid-state amplifier
SSA	solid-state power amplifier
TARLA	Turkish Accelerator and Radiation Laboratory at Ankara
TCAV	transverse deflecting cavity
TDR	technical design report
TDS	time-domain spectroscopy
TDS	transversal deflection structure
TELBE	THz Source at ELBE
TEUFEL	THz Emission from Undulators and Free-Electron Lasers
TFISH	THz field-induced second-harmonic generation
TFLN	thin-film LiNbO ₃
TMD	transition-metal dichalcogenide
tr	time-resolved
TRHEPD	total-reflection high-energy positron diffraction
TR-PES	time-resolved photoelectron spectroscopy
UED	ultrafast electron diffraction
UHV	ultrahigh vacuum
URC	user representatives committee
US	ultra-sonic
UPWR	ultra-pure water rinsing
UV	ultraviolet
VM	vector modulator
VUV	vacuum ultraviolet
XPS	X-ray photoelectron spectroscopy
XUV	extreme ultraviolet

Preface

This conceptual design report (CDR) of the Dresden Advanced Light Infrastructure (DALI) represents an advancement to a higher degree of detailedness and concreteness compared to the “preliminary CDR” published in 2020. There is one significant, qualitative change, however, that should be mentioned already here: The presented CDR of DALI focusses on sources for THz radiation and positrons only while the vacuum ultraviolet (VUV) free-electron laser (FEL) was ~~revoked~~. Originally, HZDR has proposed DALI for about 200 Mio. €. The large inflation, in particular the extreme increase of construction costs would have caused to significantly exceed (at least by a factor of two) the initially intended budget, bringing it to a level that would not be manageable anymore by a medium-size but multi-programmatic research center such as HZDR. Therefore, a priority setting was necessary. The review process of the preliminary CDR and of the PoF review has resulted in a strong recommendation to push forward the THz science, considering the exciting scientific case as well as the unique in-house competence. With this priority we keep the price cap at the originally intended level. This necessary modification was discussed and fully endorsed by the DALI project team, the HZDR scientific advisory board (WBR), the scientific-technical council (WTR) and the HZDR advisory board.

Sebastian M. Schmidt

Executive Summary

As a successor to the present ELBE facility, which has been operating at HZDR since 2004, we propose to build the **Dresden Advanced Light Infrastructure (DALI)**: a suite of advanced **accelerator-based THz sources that are continuously tunable over the frequency range from 0.1 THz to 30 THz**. Furthermore, the proposed DALI THz sources would deliver ultrashort pulses that are fully coherent, extremely intense, and transform-limited with relatively narrow bandwidth ($\approx 10\%$ spectral bandwidth), thus providing exceptionally high fields within a few cycles of radiation. Based on a concept utilizing a pair of superconducting 50 MeV electron linear accelerators (LINAC), the **THz sources** will provide radiation with high pulse energy (up to $100 \mu\text{J} - 1 \text{ mJ}$) at a high but flexible repetition rate (up to 1 MHz), an unprecedented combination of both parameters being a factor of at least 100 larger compared to what is available to date. The accelerator-based THz sources of DALI will be combined with a wide range of tabletop laser-based sources as well as an ultrafast electron diffraction (UED) instrument to directly probe the ultrafast THz-driven structural dynamics. With a sub-100 fs synchronization, this combination of photon and UED sources will provide a worldwide unique THz facility and open a wealth of new avenues for investigations of nonlinear and high-field-driven phenomena in matter.

The THz frequency range encompasses a number of elementary and collective low-energy excitations in matter. Examples are spin waves in magnetically ordered systems, intra-exciton transitions in semiconductors, quantum-confined states in nanostructures, order parameters or energy gaps in high-temperature superconductors, phonons in semiconducting or dielectric crystals, rotational transitions in molecules, and vibrations of large biomolecules. The variety of low-energy excitations gets even richer when external fields are applied, e.g. when magnetic fields enable electron spin resonances or cyclotron resonances. While probing these low-energy excitations in linear THz spectroscopy experiments has been well established for many decades, strong excitation requires intense, tunable THz radiation pulses that are still not widely available. In particular, ultrastrong excitation of low-energy transitions resulting in highly nonlinear interactions, which can for example initiate phase transitions or the breaking of covalent bonds, has been demonstrated only in a small number of highlight examples so far. It is particularly attractive that THz excitation enables the selective addressing of the aforementioned excitations. This is a major advantage compared to excitation with ultrashort optical pulses, which concurrently excite the electronic system, thereby potentially masking the dynamics of interest. Recent observations indicate that intense THz fields may also play a key role in (ground-state) surface chemistry, which is relevant for catalysis, and in THz-driven membrane transport in biological structures. Moreover, such a THz source would be especially suited for experiments with liquid jets, which have hardly any restrictions on the average power they can withstand.

Present-day table-top laser-based THz sources have demonstrated comparable pulse energies (mostly based on optical rectification in LiNbO_3) at frequencies below 3 THz, but at repetition rates of 1 kHz and less. For the high frequencies of 20 – 30 THz, parametric amplification and optical frequency mixing are employed, however with relatively low efficiency at these MIR frequencies. The intermediate THz frequencies from 3 to 15 THz remain the most difficult to generate with table-top sources, although progress was recently made using optical rectification in organic crystals. Latest developments in Yb-based fiber or disk lasers, on the other hand, promise systems with higher repetition rate and thus higher average power. However, estimates indicate that an **accelerator-based THz source** will significantly outperform table-top systems in the combination of pulse energy, spectral brightness, and repetition rate in the foreseeable future.

Calculations show that it is not possible to properly cover the whole spectral range from 0.1 to 30 THz using one and the same accelerator-based THz generation mechanism. Due to

constraints related to electron bunch charge and bunch length compression, the customary methods for producing high-power coherent undulator radiation from 50 MeV electron bunches will be limited to frequencies lower than 3 THz. To achieve higher frequencies up to 30 THz, the electron beam has to be longitudinally density-modulated by an external laser (optical klystron). To this end, the most appropriate external laser will effectively be a free-electron laser (FEL) oscillator, as it provides continuous tunability and high peak fields at high repetition rate.

At the new DALI facility, THz radiation will therefore be generated by:

- A **superradiant** undulator (0.1 – 3 THz, 10 – 15% bandwidth, pulse energy up to 100 μ J – 1 mJ, repetition rate up to 1 MHz, carrier envelope phase stable, conceptually similar to the present TELBE source; it is considered to actually implement two undulators with different period numbers and bandwidths).
- A **superradiant** undulator driven by a modulated electron beam (3 – 30 THz, few-percent bandwidth, pulse energy up to 100 μ J – 1 mJ, repetition rate up to 1 MHz)
- An FEL oscillator, which can act both as a modulator and as a narrowband THz source (3 – 30 THz, 1 – 2% bandwidth, a fixed 10 MHz repetition rate, and 1 – 10 μ J pulse energy). A cavity dumper is under development to enable an increase in pulse energy to 10 – 100 μ J accompanied by a variable repetition rate up to 100 kHz.
- In addition to the multicycle narrowband sources, a single-cycle broadband source based on coherent diffraction radiation (or a similar mechanism) will also be provided. Instead of selectively exciting a single specific mode, it will utilize the achievable ultrahigh electric field of several MV/cm, which is comparable to the intrinsic electric fields in atoms to non-resonantly drive matter into highly non-equilibrium dynamic configurations.

To drive the suite of THz sources described above, two separate electron injectors will be needed, one with 1 nC bunches at a repetition rate of up to 1 MHz for the superradiant sources and one with 100 pC bunches at 10 MHz for the FEL oscillator that will provide the electron bunch modulation or cavity-dumped FEL pulses.

To exploit the full research potential of the intense DALI THz sources, it is of key importance to utilize advanced probing techniques. By incorporating synchronization methods with lowest possible timing jitter, these different probing techniques can deliver in-depth information on the THz-driven response of materials with extraordinary temporal resolution. For example, probing with femtosecond white-light pulses allows the monitoring of ultrafast changes to the bandgaps of semiconductors and dielectrics. In addition, probing using near-field techniques gives insight into nonlinear dynamics on nanometer length scales. Utilizing (weak) broadband THz pulses, one can perform THz time-domain spectroscopy (THz-TDS) to obtain the complex dynamic conductivity of materials, which will for example reveal the field-driven opening or collapsing of superconducting gaps. Optically sampling of THz harmonic emission processes sheds light on complex nonlinear light-matter interaction, e.g. due to excitation of collective modes in matter (Higgs oscillations in superconductors, amplitudons in density-wave systems, etc). Time- and angle-resolved photoemission spectroscopy (tr-ARPES) directly reveals the energy dispersion of occupied electronic states and can thus indicate how the band structure and occupation are altered by intense THz fields. Ultrafast electron diffraction, on the other hand, provides insights into the underlying structural changes within the lattice or the molecular conformation. Thus, the selective addressing of low-energy excitations by intense THz pulses, combined with the tools of tr-ARPES and UED to monitor the changes induced in the electronic and structural properties, respectively, will enable a new quality of solid-state research.

Compact light sources based on advanced laser plasma accelerators may complement the high-field sources of the DALI facility for dedicated low-repetition-rate applications. Ultrafast high-power laser-driven sources with variable photon energy enable unprecedented probing capabilities as well as highest transient fields and serve as a technology development platform for future applications.

Building upon the exceptional success and high demand for the pELBE positron source, a **High-intensity Positron Source (HiPS)** based on bremsstrahlung production will complement the DALI light sources, thus opening up unique experimental conditions for materials science, chemistry, solid-state physics, and semiconductor research. Positron annihilation in matter serves as an excellent tool for depth-resolved studies of open-volume defects and nanoscale porosity in bulk samples and thin films. The experience gained at the existing ELBE positron source (EPOS) in defect studies and porosimetry in materials will be extended by new types of in-situ defect analysis and characterization, focusing on dynamical effects of defect migration and development by means of laser-induced charge carrier manipulation, high- and low-temperature annealing, and ion irradiation. High electron bunch charges and pulse repetition rates of 1 – 5 MHz constitute ideal conditions for positron annihilation lifetime measurements of depth-resolved open-volume defects, such as point defects, precipitations, and grain boundaries in metals, alloys, ceramics, polymers, and (ionic) liquids, and of material porosities with sizes ranging from 0.2 to 35 nm. In addition to addressing fundamental issues in defect-related phenomena in semiconductors, metal alloys, insulators and polymers, application-oriented studies will focus on materials development for energy materials, high-speed information processing and transmission, and membrane technology.

The new DALI facility will thus encompass light sources and particle sources with unmatched characteristics that are optimally suited for research related to questions of high societal impact, as outlined in the scientific cases in Chapter 2. The combination of intense tunable coherent THz beams tuned to drive the specific processes of interest, with a wide range of synchronized tabletop photon sources and ultrafast electron beams will enable unprecedented scientific insights. Furthermore, the unique positron source and instrumentation proposed within the DALI concept will deliver unprecedented insight into the growth and formation of materials and structures critical for advanced technologies. Realizing this combination of sources essentially requires a dedicated large-scale facility, making DALI unique for the foreseeable future.

1 Overview

1.1 Introduction

The major grand challenges of mankind in the decades to come are (i) the energy- and climate transformation of our societies, (ii) to maintain physical and mental health of an aging population, and (iii) to create a transparent and modern digital world. One of the key methods to approach these global objectives is material research of natural occurring and engineered matter and structures. Success depends critically on the availability of instruments that can unravel the structure and function of matter at different size, energy, and time scales. DALI will explore a totally new and unknown domain and will therefore add a powerful new tool to tackle the Sustainable Development Goals¹ mentioned above. The basis will be the possibility to investigate matter and to understand processes on the smallest length and time scales, and the ability to shape materials properties and to steer the processes resulting of this knowledge.

To meet the very challenging requirements of the user community, a new architecture of accelerator-based radiation sources is required. The proposed facility will be based on two superconducting electron accelerators generating beams with energies up to 50 MeV. The accelerated sub-picosecond electron bunches will be used to generate ultrashort pulses of fully coherent high intensity THz radiation. The narrowband THz radiation will be continuously tunable over the spectral range of 0.1 – 30 THz (10 – 3000 μm in wavelength). The THz beams will be combined with a wide range of synchronized tabletop laser-based sources as well as other advanced probes, including ultrafast electron diffraction (UED) and time-resolved angle-resolved photoelectron spectroscopy (tr-ARPES). The portfolio of photon and electron sources will be complemented by secondary positron beams offering unrivalled capabilities for materials science. Spin-polarized positrons will be produced from radioisotopes for investigation of specific spin dependent phenomena.

As the successor of ELBE, DALI will be operated as an international user facility, building on the extensive experience gained while serving users of ELBE with THz radiation and positron beams amongst others over almost a quarter of a century. The strength of DALI will be the possibility to combine narrowband THz radiation with continuous tunability across one of the most challenging regions of electromagnetic spectrum in ultrashort pulses at high and flexible repetition rates synchronized with advanced probes for measuring ultrafast dynamics in matter. The THz and positron sources will be directed to a variety of specific user laboratories with excellent conditions for scientists from materials sciences, physics, chemistry, biology and medicine as well as from environmental sciences. Research topics will comprise of studies such as high-temperature superconductivity, dynamic control of the properties or function of matter, the role of water in life processes, and the switching of processes in cell membranes just to name a few.

In the recently established Helmholtz Photon Science Roadmap, DALI, PETRA IV, and BESSY III were identified as essential and fully complementary upgrades of the existing landscape of accelerator-based light sources in Germany, and indispensable for maintaining the competitiveness of Germany as a world-leading location for research.

DALI was presented in the context of the evaluation of the Helmholtz Research Field *Matter* for the preparation of the fourth period of the program-oriented funding (PoF IV). The reviewers explicitly recommended the implementation of DALI, pointing out the THz revolution expected to arise from the new facility.

¹ <https://sustainabledevelopment.un.org>

The construction phase of DALI is expected to extend from 2027 to 2033. The costs are estimated at 229 M€. Operational costs, which will be covered by HZDR, are assumed to amount to 23 M€ per year.

1.2 Key parameters of the facility

The principle layout of the new DALI facility is shown in Figure 1. Two superconducting CW RF accelerators generate electron beams of 50 MeV with the bunch charge and repetition rate characteristics required for the respective secondary sources. THz radiation is generated in appropriate standard undulators and guided into the user laboratories. The radiation will be available to users at 9 individual experimental stations (see Section 1.3). In addition to the electromagnetic radiation, positron beams and a UED facility will also be made available to users. The new facility will be housed either in a new building about 89 m long and 76 m wide or within the existing ELBE hall. A comparison of costs and other considerations for both options is presented in Section 4.21.

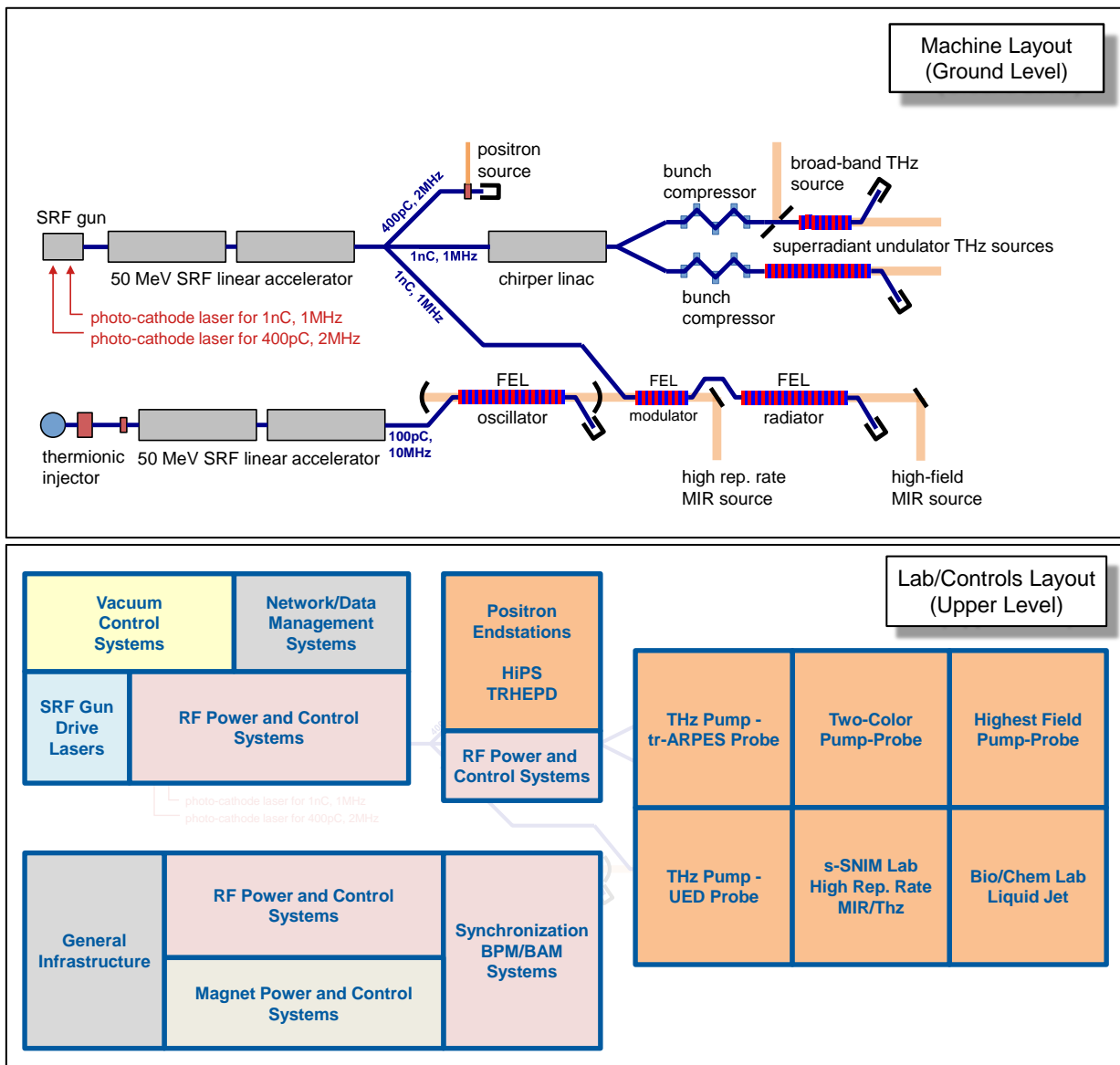


Figure 1: Principle layout of the DALI facility.

Two electron accelerators will generate 50 MeV electron beams, with the parameters given in Table 1. The acceleration of the high bunch charge of 1 nC, provided at a repetition rate of up to 1 MHz, is the most important electron beam parameter for the new superradiant THz source, delivering a photon pulse energy up to a few hundred μJ , which is about two orders of magnitude higher than the presently operating source, TELBE. This combined with the proposed concept of using the continuously tunable FEL radiation to premodulate the 1 nC bunches at the desired radiation frequency will extend the spectral range for the narrowband superradiant emission by one order of magnitude beyond the present capabilities of the existing TELBE source. Both new photon sources will take full advantage of the high average current of 1 mA provided by the CW SRF LINAC technology developed and used already today at HZDR's radiation source ELBE.

Table 1: Key electron beam parameters of the proposed DALI user facility based on two superconducting RF CW accelerators.

Parameters	MIR-THz FEL-oscillator	Superradiant THz and Positrons
Electron beam energy	50 MeV	50 MeV
Bunch charge	100 pC	1 nC
Electron pulse length	Few ps	200 fs – few ps
Transverse emittance	<15 mm·mrad	<15 mm·mrad
Bunch repetition rate	10 MHz	100 kHz – 1 MHz
Average beam current	1 mA	1 mA

Undulators and FELs will then convert the electron beams into THz radiation with the properties given in Table 2. The main purpose of the new DALI facility is to increase the pulse energy of the MIR and THz pulses by about two orders of magnitude from the presently available few μJ to a few hundred μJ . The high-energy photon pulses will be provided at a repetition rate of up to 1 MHz. The combination of high MIR-THz pulse energy and high repetition rate will be unique worldwide and is unprecedented to date.

All beams can be synchronized with each other to a jitter down to less than 10 fs, so that a large number of possibilities for pump–probe experiments at the experimental stations can be made available to the users. Pulse-resolved detection schemes will furthermore enable sub-cycle time resolution in all THz-based experiments up to the 30 THz regime.

The Gaussian THz beams feature excellent focusing properties, resulting in high peak fields. For example, considering a numerical aperture of 0.5, peak fields of 1 MV/cm are expected for the broadband source, and 0.5 MV/cm (at low frequency) up to 700 MV/cm (at high frequency) for the narrowband source. Furthermore, the possibility to manipulate the polarization of the THz beam in the lab to create, for example, beams with orbital angular momentum can provide benefits for beam focusing and propagation, as well as the ability to drive more exotic transients in materials.

Additionally, certain user experimental stations will be equipped for combining any of the DALI photon beams with a UED probe beam to study photon-driven structural dynamics, while secondary positrons generated by the LINAC-accelerated electron beams will be available simultaneously with the DALI photon beams.

Table 2: Photon beam parameters of the proposed facility available for user experiments.

Parameter	Superradiant MIR-THz	Broadband THz	MIR-THz FEL Oscillator
Wavelength range	10 μm – 3 mm	120 μm – 3 mm	10 – 120 μm
Frequency range	0.1 – 30 THz	0.1 – 2.5 THz	2.5 – 30 THz
Pulse energy	100 – 1000 μJ	100 μJ	10 μJ
Repetition rate	0.1 – 1 MHz	0.1 – 1 MHz	10 MHz
Pulse length (RMS)	0.2 – 15 ps	0.2 ps	1 – 25 ps
Peak power	20 – 500 MW	500 MW	~1 MW
Photons per pulse	10^{16} – 10^{18}	10^{18}	10^{13}
Photon energy	0.4 – 125 meV	0.4 – 10 meV	10 – 125 meV
Bandwidth	0.5 – 15 %	100%	0.5 - 3.0 %

Table 3: Beam parameters for positron sources.

Parameter	Positron Annihilation Lifetime Spectroscopy	High-intensity Positron Source, microbeam	High-intensity Positron Source TRHEPD, open-beam port
Repetition rate	100 kHz – 1 MHz	100 kHz – 1 MHz	1 MHz
Positron rate	$5 \times 10^9 / \text{s}$	$1 \times 10^8 / \text{s}$, remoderated	$1 \times 10^7 / \text{s}$, remoderated
Time spread	<150 ps FWHM	<500 ps FWHM	–
Beam diameter	5 mm	50 μm	1 mm, low divergence
Positron kinetic energy	500 eV – 30 keV	5 eV – 8 keV	10 keV – 20 keV

The beam parameters for user experiments with secondary positron beams are listed in Table 3. While the setup for high-intensity positron annihilation lifetime spectroscopy features the highest average positron intensity on the samples for depth-dependent free-volume and porosity studies, the positron microbeam utilizes positron remoderation in order to achieve a brightness enhancement and thus enable small beam foci for position-resolved 4D annihilation lifetime studies. Total-reflection high-energy positron diffraction (TRHEPD) will be enabled at the open-beam port, which is available for other user setups as well.

1.3 List of experimental stations

DALI will comprise various experimental stations, which will ensure the optimum use of its accelerator-based sources for science and technology.

User stations involving the accelerator-based MIR-THz radiation sources:

- (U1) User stations for optical **single-color MIR-THz pump–probe spectroscopy**, based on DALI's broad- and narrowband THz sources, respectively.
- (U2) **Dual-color optical pump–probe stations** involving DALI's broad- and narrowband THz sources, respectively, in combination with synchronous table-top laser systems. The latter include mode-locked fs laser oscillators, μJ to mJ amplifiers, and frequency conversion to MIR and UV/Vis wavelengths. A table-top THz high-field source will also be provided.
- (U3) **MIR-THz scattering near-field infrared microscopy (s-SNIM)** stations, both for room temperature and for cryogenic temperatures, also including options for nonlinear s-SNIM pump–probe experiments.
- (U4) A user lab for **MIR-THz pump – ARPES probe experiments**. This will include a table-top XUV source based on femtosecond laser technology with nonlinear frequency conversion, offering few 10 fs XUV pulses for experiments on MIR-THz-driven dynamics with highest demands on temporal resolution.
- (U5) User stations for **experiments involving fluid jets**, in particular for investigations on THz-induced dynamics in aqueous materials, especially biological and chemical specimens.
- (U6) One user endstation will be equipped with a **UED instrument** for measurement of the **ultrafast structural dynamics** driven by any of the DALI THz sources or to track the structural changes in molecules resulting from selective photoionization by the HHG XUV source.

User stations utilizing the positron beams:

- (U7) User station for **ultrafast in-situ defect analysis and characterization** using the High-intensity Positron Source (HiPS)
- (U8) **Microbeam user station utilizing a high-brightness positron microbeam** for the study of nanoscale-patterned surfaces (by 2D/3D scans) as well as for surface investigations of the first monolayer using positron diffraction techniques, such as total-reflection high-energy positron diffraction (TRHEPD). The microbeam will allow high-resolution temporal and high-resolution spatial annihilation and Doppler-broadening experiments to be performed at very high positron beam intensities.
- (U9) Versatile **open-beam port** for users with dedicated own experimental setups.

2 Scientific Potential (“Scientific Case”)

The core strength of DALI will be its uniquely **intense and flexible accelerator-based THz sources** in conjunction with electron- and positron-based diagnostics and state-of-the-art ultrafast laser infrastructure. DALI will therefore enable an unprecedented opportunity to **study strong-field THz-driven low-energy modes in all kinds of matter on all relevant length- and timescales**.

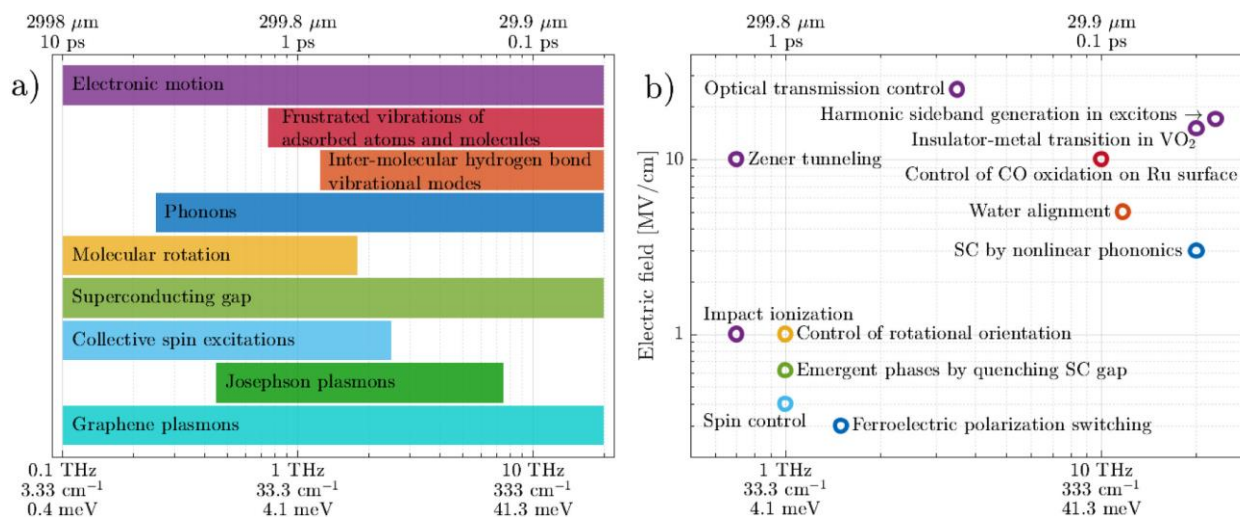


Figure 2: Energies of various THz excitations and strong-field THz applications. (a) Fundamental excitations in solids and molecular systems in the THz region. (b) Examples of applications of strong-field THz light. Figure adapted from Ref. 2.

The DALI THz sources will bridge the gap in the electromagnetic spectrum spanning from 0.1 THz to 30 THz. This energy region marks the transition from the realm of electronics to that of optics and is therefore characterized by the onset of numerous quantum effects related to low-energy modes in matter. These are the excitation of, e.g., vibrational and rotational modes, spin dynamics, and more intricate collective phenomena and quasiparticles, which are roughly summarized in Fig. 2(a).² Access to these phenomena using a specifically tailored, resonant source will offer new fundamental insights into a number of intricate phenomena, from high-temperature superconductivity to catalytic activity as well novel ultrafast and efficient schemes for transmitting and storing information. In this way, the fundamental understanding of technologically relevant processes can contribute directly to overcoming societal challenges: The need for more efficient chemical processes, extremely broadband wireless communication, ultrafast and efficient data processing, and elementary biological processes, among others.

This Chapter starts with an introduction to a number of highly relevant scientific areas for which the availability of the DALI THz sources is expected to lead to significant breakthroughs. This is followed by the presentation of a broad range of scientific cases, which exemplify the unique potential of DALI.

Dynamics of phase changes – The development of new materials has made it possible to harness correlated and quantum effects in an increasing number of applications, yet many theoretical predictions for new phases or states of matter remain elusive to experimental verification. Since these exotic phases of matter in its electronic ground state are often predicted

² P. Salén et al., Phys. Rep. **836–837**, 1-74 (2019)

to exist far from equilibrium, they are not thermally accessible. Thus, high-field THz pulses provide a unique pathway to transiently access the necessary non-equilibrium conditions selectively and without parasitic excitation of the electronic states. Thanks to the broad tunability of the DALI THz sources, one can selectively drive individual modes to access and drive the predicted phases, thereby changing both quantum and macroscopic properties of matter. In combination with the advanced probing methods provided by the complementary DALI photon and UED sources, it will be possible to determine the electronic and structural distributions that reveal these hidden phases, and consequently to guide the design of new materials and structures such that the desired properties can more readily be accessed and utilized.

Ultrafast spin and lattice dynamics – Future information technologies require ever faster processing and transfer of data with minimal dissipation, and miniaturization down to the quantum level. Ideal candidates for fulfilling these requirements are materials systems which allow ultrafast energy and information transfer between charge currents, and lattice and spin degrees of freedom. Remarkably, the THz frequency range naturally coincides with the intrinsic frequencies, wavelengths and rates of lattice vibrations (phonons), spin waves (magnons) and electron transport, respectively. Therefore, interrogating and driving the relevant phenomena specifically, using the intense and flexible DALI THz sources, is the key to disentangling the relevant complex ultrafast processes. The unique THz parameters at DALI are therefore enabling an unprecedented insight into novel spintronic and magnonic applications, which extend towards quantum computing applications, and elementary magnetic processes in general.

Catalysis – All industrially relevant chemical reactions are triggered by structural excitation, i.e. low-energy modes, such as (frustrated) rotations, vibrations, etc. THz radiation from DALI will allow selective optical excitation of such modes with highest flexibility, enabling highest control of such reactions on the fastest time scales (needs >1 MV/cm field strength in 10 THz frequency range, which is only reachable with an accelerator-based source). Photoelectron spectroscopy can directly probe the electronic structure, and thereby the chemical state of the sample. Recent advances in laser technology will provide sufficiently powerful XUV sources at high repetition rate. Electron diffraction using the UED source can probe related structural changes. By providing all these methods together, DALI can generate comprehensive and complete ultrafast movies of catalytic reactions at surfaces.

Solvation Water Dynamics – Water is the solvent of life - the structure, function, and reactivity of biomolecules, ranging from small ions to complex proteins, are controlled by water. Intermolecular vibrational and rotational motions of the water network, such as the breaking and reforming of hydrogen bonds, occur on the picosecond timescale. Thus, THz frequencies directly probe these collective hydrogen-bond dynamics, and provide insight into the biomolecule solvation shell. DALI, with its intense and tunable source, will allow selective excitation of solvation shells for specific biomolecules, allowing for the first insights into the nonlinear dynamics and energy flow pathways of biomolecule-solvent coupling. The unique properties of DALI allow for the expansion of water research to the field of biology.

Defect kinematics with positron beams – Time-resolved investigations of defect kinematics require both an intense positron source as well as timings down to ns and ps, which can be delivered by DALI. The main scientific impact is foreseen from pump-probe experiments where exotic magnetic and structural phases or defect-related quantum states are excited using alternating electric fields, ions, or monochromatic light and probed with positrons. Studies of electron spin-dependent phenomena will be addressed using a spin-polarized positron beam from radioisotope production, and the potential of using an accelerator-driven spin-polarized positron source will be evaluated. Dynamic processes associated with the migration of vacancy-like

defects and their interactions within the crystal matrix are of crucial importance to grasp ion-induced nanopattern formation, ionic-transport-driven magnetic switching, and elusive sub-bandgap quantum states in semiconductors and insulators.

These and further important challenges that can be addressed using the DALI facility are described in the following sections. These scientific applications are based to a great extent on input from the scientific community of interested external users. To foster intense communication between machine specialists, HZDR in-house scientists, and external experts from inside and outside Germany, HZDR organized several dedicated topical workshops. The unique and powerful combination of photon, electron, and positron sources will serve these scientific needs while also opening up the possibility to perform entirely new studies of matter and dynamics not yet foreseen.

2.1 Science with THz radiation

Many elementary and collective low-energy excitations in matter, which govern phenomena of high technological and fundamental relevance, fall into the THz frequency range. These excitations include energy gaps in high- T_c superconductors, intersubband/intersublevel transitions in low-dimensional semiconductors, phonons in crystalline semiconducting and insulating materials, cyclotron or electron spin resonances between magnetically confined states, as well as rotational and vibrational transitions in molecules. Furthermore, the interaction with THz radiation results in various quasiparticles, such as dressed exciton polaritons or surface-plasmon polaritons.

While most of these excitations have been studied extensively by linear THz spectroscopy experiments, strong excitation inducing nonlinear phenomena requires intense tunable THz radiation pulses that are still not routinely available. Ultrastrong excitation of these low-energy transitions results in highly nonlinear behavior, which can for example initiate both electronic and structural phase transitions, breaking of covalent bonds, and high-order nonlinear or non-perturbative effects. In this respect, the DALI light source will pave the way to unprecedented studies of ultrastrong light–matter interaction at THz frequencies.

In particular, selective and even resonant excitation by intense, spectrally narrow THz pulses becomes possible using an accelerator-based source, which is a major advantage with respect to THz generation from femtosecond optical pulses. For example, in highly correlated systems, optical excitation typically results in the creation of hot free electrons that indirectly influence the ordering of spins, can trigger phonons, and interact with bound electrons of the system. As a result, it becomes difficult or even impossible to disentangle and understand the manifold dynamics. THz radiation, on the other hand, can be used to excite phonons or magnons in a selective manner. The intense radiation pulses can strongly interact directly with the low-energy excitations, resulting in new dressed states of matter. Another strong point of THz radiation in controlling materials is the possibility of monitoring the amplitude and phase of the electromagnetic wave (rather than just the intensity) and to do this with sub-cycle temporal resolution. This provides comprehensive information on the response dynamics.

In addition to the resonant excitation of low-energy modes with comparably narrowband THz pulses, intense single-cycle THz pulses enable experiments where the THz field can be viewed as a strong transient DC bias. Strong electric fields can significantly alter the properties of materials. In case of moderate fields (few tens of kV/cm), the interaction with THz pulses can lead to strong nonlinearities in the optical properties of materials, resulting in THz harmonics emission, as demonstrated for a number of Dirac materials. Another example is the THz-induced bandgap

in the 2D material bilayer graphene. For even stronger transient fields, electrons are accelerated and swept through the entire Brillouin zone of a crystal, resulting in Bloch oscillations. When THz field strengths become comparable to the crystal fields ($\sim 1 \text{ V/nm} = 10 \text{ MV/cm}$), one can expect that energy bands in semiconductors break up into a Wannier–Stark ladder, i.e. delocalized Bloch states are converted into localized Wannier–Stark states. While these phenomena are primarily of fundamental scientific interest, the outcome of these studies can be highly relevant for the development of future (opto-)electronic devices. As device dimensions shrink and electronic switching times become faster, mature electronic engineering relies on the information how standard semiconductors and novel materials such as 2D materials react to strong electric fields on femto- to picosecond time scales. Strong transient DC fields are further envisioned to stimulate and steer chemical reactions at surfaces. By the collective excitation of frustrated vibrational modes of chemical species bound to a surface, it may be possible to directly control its catalytic activity. Thereby, one may gain a comprehensive insight into fundamental catalytic processes, which is of exceedingly high technological and environmental value. The transient DC fields of strong THz pulses may further shed light on transport processes of ions across cell membranes, which can provide insights into a number of hitherto poorly understood elementary processes in biology. In addition, the THz frequency range overlaps with low frequency motions of protein hydration water, which plays a key role in the functionality of these fundamental building blocks of life. Developing suitable sources and techniques at DALI can therefore be a key to the understanding elementary processes such as protein folding or substrate binding.

In order to exploit the full research potential of an intense THz source, various probing techniques (user stations U1 – U6 in Section 1.3) that are tailored to the processes of interest are of key importance. These optical or electronic techniques, all synchronized to the THz source operating with minimum timing jitter, deliver in-depth information on the reaction of materials upon intense THz excitation. For example, probing with femtosecond white-light pulses allows one to monitor bandgaps of semiconductors and dielectrics. Raman- and Brillouin light scattering enable insights into a wealth of material properties and their ultrafast THz-driven dynamics.

From THz time-domain spectroscopy (THz-TDS) utilizing (weak) broadband pulses, the complex dynamic conductivity of materials can be obtained, which for example will indicate superconducting gaps. Time- and angle-resolved photoemission spectroscopy (tr-ARPES) directly reveals the energy dispersion of occupied and excited states and can thus indicate how the electronic band structure and occupation are altered by intense THz fields. Electron diffraction, on the other hand, provides insights into THz field-driven structural changes.

The dynamics driven by high-field THz pulses cover a wide range of physical processes, as seen above. Consequently, the sample types that can be investigated are not only limited to solids. Experiments on soft matter and, in particular, liquids are also possible. Here, liquid jets offer a possibility to examine samples that require constant refreshing and circumvent the need for windows, which may perturb the sample signal.

In summary, the selective addressing of low-energy excitations by intense THz pulses, combined with specific tools to monitor the changes induced in the electronic system, the band structure, and its occupation as well as structural properties, will enable a new quality of research in a broad range of sample systems.

2.1.1 Superconductivity and highly correlated systems

Tailored ultrafast light pulses have opened new ways for controlling the complex behavior of quantum materials. To perform control without significantly heating the electronic system,

collective modes are resonantly excited in the system by narrowband THz pulses with high spectral brightness in order to induce tailored nonlinear interactions.³

The range of typically 0.1 – 15 THz allows for direct coupling to **superconducting or other correlated gaps** or for driving collective excitations inside these gaps. One prominent example is inducing Josephson plasma solitons in cuprates.⁴ Even direct excitation of the complex superconducting order parameter, the **Higgs amplitude mode**, has been realized in the s-wave superconductor NbN.^{5,6} For the important class of high- T_C superconducting cuprates, such excitation and future control of the Higgs mode are more challenging due to their d-wave order parameter, which results in strong damping and dephasing. In recent experiments at TELBE, phase-resolved third-harmonic THz spectroscopy has revealed not only a driven Higgs response, but also a new collective mode that directly couples to the superconducting order,^{7,8} thus shedding new light on the interplay of external modes with high- T_C superconductivity. The high DALI pulse energies will allow the application of pulse shaping and wave-mixing schemes for selective quenching and control of the complex ordered phase⁹ by finite momentum transfer. Momentum-dependent quenches would even make “Higgs spectroscopy” possible, identifying unknown order parameters via different symmetries of their collective modes.⁸ For sizable excitation fluence pulses, in particular under wave-mixing geometries, required pulse energies at DALI are estimated to be at least one order of magnitude larger than presently available at TELBE.

In particular, the aspect of inducing momentum-dependent quenches and controlling order parameters with unconventional symmetries requires a time- and momentum-resolved probe.⁹

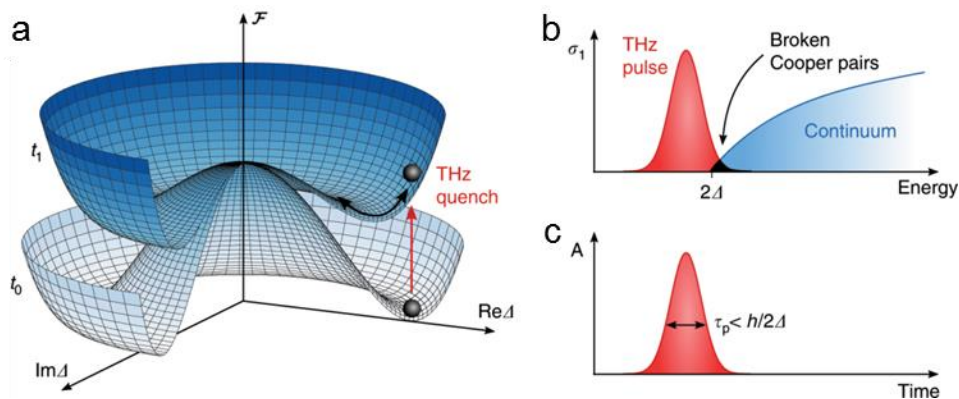


Figure 3: Illustration of Higgs oscillations in a superconductor. a) Free-energy landscape \mathcal{F} of a superconductor as a function of the real and imaginary parts of the superconducting gap. After a quench, the free energy is suddenly changed, exciting the superconducting condensate and leading to collective Higgs oscillations, indicated by a black arrow. The red arrow indicates a quench induced by a THz pump pulse. b) Higgs excitation mechanism using a THz pump pulse. The pump pulse overlaps only slightly with the quasiparticle continuum indicated in blue. The Mexican hat shrinks due to the breaking of Cooper pairs. c) To excite the Higgs oscillation, the pulse must fulfil the non-adiabaticity condition in the time domain. Figure adapted from Ref. 9.

³ M. Först et al., Nat. Phys. **7**, 854 (2011)

⁴ A. Dienst et al., Nat. Mater. **12**, 535 (2013)

⁵ R. Matsunaga et al., Phys. Rev. Lett. **111**, 057002 (2013)

⁶ R. Matsunaga et al., Science **345**, 1145 (2014)

⁷ H. Chu et al., Nat. Commun. **11**, 1793 (2020)

⁸ S. Kaiser, Phys. Scr. **92**, 103001 (2017)

⁹ L. Schwarz et al., Nat. Commun. **11**, 287 (2020)

Here, XUV photons by high-harmonic generation (HHG) will enable probing by **time- and angle-resolved photoemission spectroscopy (tr-ARPES)**¹⁰ and will open up a full view on the dynamics of the transient band structure of the driven system. For cuprate superconductors, this would require high momentum to be reached to cover the full nodal-to-antinodal region and high energy resolution to probe the collective gap dynamics. For correlated systems showing quantum phase transitions, tuning by external parameters (magnetic fields, pressure, strain, etc.) for probing scaling laws or looking for phase separation on the nanoscale will be important to identify the nature of these quantum transitions.

Besides THz-induced quenching, **light-induced superconductivity** is another intriguing phenomenon, which can be triggered in cuprate superconductors by driving low-frequency phonon modes^{8,11} or in doped fullerenes K_3C_{60} by local excitation of molecular vibrations.¹² Exploring the possibility of long-lived metastable states via dynamical stabilization requires high-field narrow-bandwidth multicycle pulses in the 0.1 – 30 THz regime (typical phonon range of oxide perovskites, 2D-TMDs, etc.) or up to 60 THz (for molecular vibrations in organic crystals).

More generally, periodic driving of solids with strong light fields can be used to change the band structure of solids and therefore their electronic properties. In this way, it might also be possible to turn a metal into a (topological) insulator¹³ or even a superconductor.¹² Besides resonant excitation of infrared-active phonon modes (used for light-induced superconductivity), another approach for changing the electronic properties is based on off-resonant coherent modulation of the momentum of the Bloch electrons (**Floquet engineering**).¹⁴ Here, the coherent interaction between light field and Bloch electrons (giving rise to Floquet–Bloch states) is expected to induce topological phase transitions¹³ or dynamical localization of charge carriers¹⁵ resulting in a light-induced metal-to-insulator transition.

This type of experiments requires quasi-monochromatic pump pulses tunable from THz to MIR frequencies with MV/cm field strength and at least 100 kHz repetition rate. The induced changes in band structure will be probed by **tr-ARPES**. Limitations in this type of experiments may arise from the possibility of sample heating, pump-induced space charge broadening of the band structure, and photoelectron streaking. Pioneering experiments¹⁶ have shown that these problems can be handled.

In summary, versatile high-field THz pulses tunable over a wide frequency range to address collective excitations or drive collective order parameters will allow unprecedented control of quantum materials: Switching between selected phases or creating new phases of matter will explore new physical effects and open a new avenue of functionalizing materials for applications.

2.1.2 THz nonlinear optics

In contrast to the selective excitation of distinct degrees of freedom in a solid, such as phonons, magnons, etc., the strong and comparably slowly varying field of the THz pulses can easily accelerate free electrons near the Fermi level, leading to extreme transport phenomena. As the THz photon energies lie far below interband resonances in bulk semiconductors, notable variations in the electronic occupation occur via intraband transitions, which can eventually induce

¹⁰ A. K. Mills et al., *Rev. Sci. Instrum.* **90**, 083001 (2019)

¹¹ D. Fausti et al., *Science* **331**, 189 (2011)

¹² M. Mitrano et al., *Nature* **530**, 461 (2016)

¹³ T. Oka et al., *Phys. Rev. B* **79**, 081406 (2009)

¹⁴ T. Oka et al., *Annu. Rev. Con. Mat. Phys.* **10**, 387 (2019)

¹⁵ D. H. Dunlap et al., *Phys. Rev. B* **34**, 3625 (1986)

¹⁶ J. Reimann et al., *Nature* **562**, 396 (2018)

strong nonlinear optical effects in a material. Compared to nonlinear experiments with single-cycle THz pulses, permitting for delta-like excitation of the material of interest, quasi-monochromatic, multicycle nonlinear driving, which is one of the key strengths of the DALI sources, allows one to strongly amplify the nonlinear response of the material, making use of its natural recovery/relaxation dynamics. Such dynamics usually do not contribute significantly to the nonlinear response probed in the single-cycle regime; however, it can lead to a significant enhancement of the measurable nonlinearity of the probed system. One recent example of such a response is THz high-harmonic generation (HHG) in graphene,¹⁷ which makes use of the extremely short sub-picosecond time scale of electron relaxation in graphene. This can occur between subsequent THz electric-field maxima within a multicycle driving THz field, thus enhancing the observable nonlinearity, as demonstrated in Figure 4.

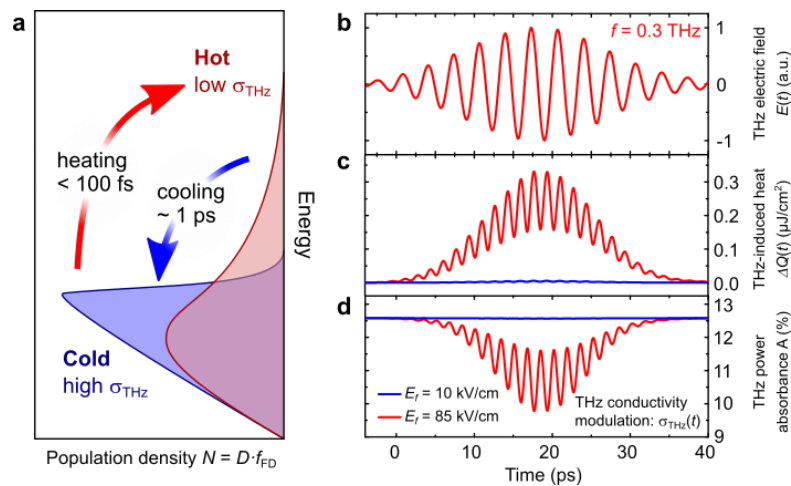


Figure 4: Temporal asymmetry of electron heating and cooling rates in graphene (a) leads to a situation where the application of a THz driving field (b) to the graphene electron population results in electronic heat accumulation $\Delta Q(t)$ (c) and hence in the temporal modulation (d) of the THz absorbance $A(t)$ and of the conductivity of graphene $\sigma(t)$. In these calculations, the driving field (b) oscillates at the fundamental frequency $f=0.3$ THz. Blue and red lines in (c) and (d) correspond to driving-field peak amplitudes of 10 kV/cm and 85 kV/cm, respectively. The field strength of 10 kV/cm represents the regime of small-signal nonlinearity (no substantial modification of the sample properties on the time scale of the interaction with the THz wave), whereas the field strength of 85 kV/cm leads to considerable electron heating and thus to a substantial decrease in the absorption of graphene at the peak of interaction. Adapted from Ref. 17.

Yet another advantage of quasi-monochromatic THz driving is the possibility to quantify the THz-range i^{th} -order nonlinear optical coefficient of the material $\chi^{(i)}$ in HHG-type experiments, producing spectrally clean high harmonics with quantifiable field strength, which can be directly related to the pump field at the fundamental driving frequency.¹⁷

Resonant excitation of lattice vibrational modes (phonons) has been demonstrated as an efficient tool for non-equilibrium control of solids commonly known as *nonlinear phononics*.¹⁸ THz-driven coherent lattice vibrations with a large amplitude can induce a desirable lattice deformation via the anharmonic phonon coupling.¹⁹ In this way, it becomes possible to access metastable ferroelectric order in quantum paraelectrics²⁰ like SrTiO₃ or light-induced superconducting state

¹⁷ H. Hafez et al., Nature **561**, 507 (2018)

¹⁸ R. Mankowsky et al., Rep. Prog. Phys. **79**, 064503 (2016)

¹⁹ A. von Hoegen et al, Nature **555**, 79 (2018)

²⁰ T. F. Nova et al, Science **364**, 1075 (2019)

discussed in Section 2.1.1. Moreover, recently the phonon pumping has been utilized for ultrafast optical control of magnetization.^{21,22}

Finally, elementary excitations of the magnetic subsystem – magnons – can be also excited by coherent THz radiation.²³ Although the coupling between the magnetic field component of the THz radiation and ordered spins is much weaker than the THz electric field coupling to the electron or the lattice subsystems, recent progress in generation of extremely high THz fields and their enhancement by specially designed antenna structures has enabled first demonstrations of nonlinear magnon interactions.^{24,25} In certain cases, the nonlinear phononics and magnonics approaches can be combined to exploit a direct spin-lattice coupling.²⁶

Therefore, DALI is uniquely suited to explore THz nonlinearities in different material systems based on both non-resonant (Drude-like, Debye-like) and resonant (phonons, magnons, quantized electronic states) excitations. The ability to measure under cryogenic conditions and in high magnetic fields further adds to the scope of possible experiments. The high field strength offered by DALI will extend the scope of nonlinear processes further to the regime of optical Bloch oscillations. If the quasi-momentum $\hbar k$ of an electron in the crystal field is altered by an electric field E such that its k reaches the edge of the Brillouin zone before the electron is scattered, it is Bragg-reflected.²⁷ As a result, it is traversing the Brillouin zone again, leading to charge oscillations in real and reciprocal space. This effect would be another source of extremely nonlinear behavior, enabling HHG in a broad frequency range spanning several octaves.

2.1.3 THz radiation to stimulate surface chemical reactions

Apart from accelerating free background electrons, high THz field transients can induce ionic motions in crystals and even single molecules. On surfaces, these motions have a strong impact on the chemical bonds, both intramolecular and between molecules and surface. Consequently, this makes THz excitation a highly promising tool for investigating catalytic processes.

A vast number of economically important processes in the chemical and energy industry rely on heterogeneous catalytic processes, which are chemical reactions of molecules adsorbed on the surface of a solid substrate. Heterogeneous catalytic reactions are driven thermal excitations, which include phonons (substrate lattice vibration) and vibrational motions of the adsorbed molecule (frustrated rotations and translations), see Figure 5A. Frustrated rotations and translations are important attributes of adsorbed molecules. They are THz-frequency collective vibrations of the adsorbed molecule and the substrate surface, which play important roles in a wide variety of processes on the substrate surface, including diffusion, heat transport, and the chemical reactivity of adsorbed molecules. It is the excitation of these frustrated vibrations that mediates the collision between the adsorbed reactant molecules to transform them into the product by breaking or forming chemical bonds, as visualized in a recent ultrafast X-ray spectroscopy study.²⁸ Ways to stimulate chemical reactions on surfaces can be developed by exciting the frustrated vibrations of adsorbed molecules by high-field THz radiation around 10 THz, matching the frustrated vibrational motions of adsorbed species on the surface.

²¹ D. Afanasiev et al., *Nat. Mater.* **20**, 607 (2021)

²² A. Stupakiewicz et al., *Nat. Phys.* **17**, 489 (2021)

²³ T. Kampfrath, *Nat. Photonics.* **5**, 31 (2011)

²⁴ S. Schlauderer et al., *Nature* **569**, 383 (2019)

²⁵ J. Lu et al., *Phys. Rev. Lett.* **118**, 207204 (2017)

²⁶ E. A. Mashkovich et al., *Science* **374**, 1608 (2021)

²⁷ O. Schubert et al., *Nat. Photon.* **8**, 119–123 (2014)

²⁸ H. Öström et al., *Science* **347**, 978–982 (2015)

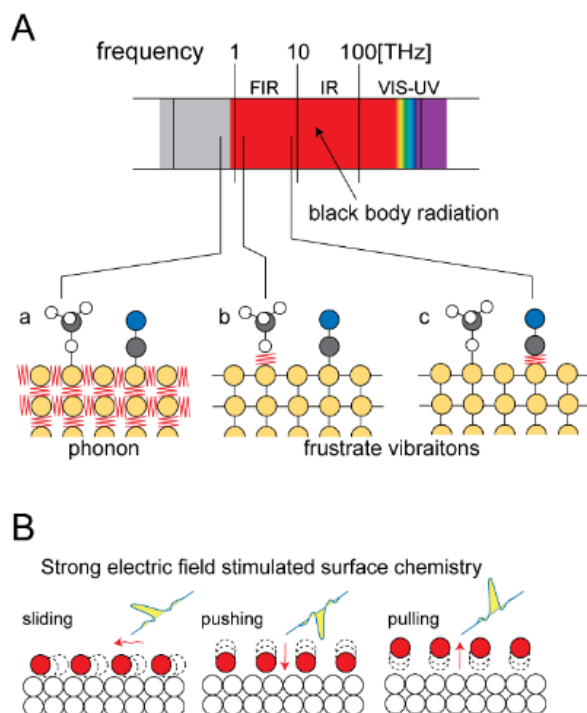


Figure 5: THz-induced surface chemical reactions.

A) Excitation at surfaces. a) Lattice vibration of the substrate (phonon), b) and c) frustrated vibrational motion of weakly and strongly adsorbed species, respectively. The arrows indicate the maximum frequency of black-body radiation at room temperature.

B) Excitation of frustrated motions collectively using half-cycle electric field pulses in different directions to the surface.

The aforementioned study has demonstrated that the intense THz radiation can be used to stimulate a chemical reaction between adsorbed CO molecules and atomic O on a Ru surface.²⁹

Not only the frequency of THz radiation, but also the strong and directional electric field is of significant interest. The coherent and broadband character of THz radiation from the accelerator will enable the generation of a strong electric field in excess of 10^9 V/m (or 0.1 V/atom). We envision the use of this strong electric field to collectively excite frustrated vibrational motions in order to drive chemical reactions³⁰ (Figure 5B). In conjunction with theoretical modeling, this method will shed light on the elementary steps of catalytic processes. The THz-driven molecular dynamics at the surface can be probed using a number of different methods. Highly promising is the use of tr-ARPES (see Section 3.2), which directly yields the field-induced changes to the electronic structure and, therefore, the chemical state. Furthermore, structural information can be gathered by time-resolved diffraction methods.³¹

2.1.4 Ultrafast and nonlinear spin dynamics

Exploring and controlling ultrafast spin dynamics with THz pulses

Ultrafast, coherent control of spin dynamics has recently been enabled by the appearance of intense THz sources, both table-top (laser-based)^{32,33} and accelerator-based.³⁴ Ferro-, ferri-, and antiferromagnetic systems have been investigated with this type of radiation.^{23,35} The possibility of resonantly driving well-known magnetic resonances in antiferromagnetic systems is opening

²⁹ J. L. LaRue et al., Phys. Rev. Lett. **115**, 036103 (2015)

³⁰ H. Ogasawara, D. Nordlund, A. Nilsson, "Ultrafast Coherent Control and Characterization of Surface Reactions using FELs", SLAC-PUB-11503 (2005)

³¹ M. Greif et al., Struct. Dyn. **2**, 035102 (2015)

³² A. G. Stepanov et al., Opt. Mater. Express **4**, 870–875 (2014)

³³ M. Jazbinsek, IEEE J. Sel. Top. Quantum Electron. **14**, 1298–1311 (2008)

³⁴ B. Green et al., Sci. Rep. **6**, 22256 (2016)

³⁵ S. Bonetti et al., Phys. Rev. Lett. **117**, 087205 (2016)

up new studies of nonlinear spin dynamics aimed at switching the antiferromagnetic order on ultrafast time scales and has also led to the observation of a new spin resonance in ferromagnetic thin-film samples, possibly consistent with the existence of spin nutations at ultrafast time scales.³⁶ A benchmark experiment demonstrating the efficiency of the narrowband THz radiation from the TELBE source for driving of an antiferromagnetic resonance in NiO is illustrated in Figure 6. The spin deflection achieved for the narrowband accelerator-based source exceeds by more than an order of magnitude the deflection induced by a state-of-the-art broadband laser-based THz source.

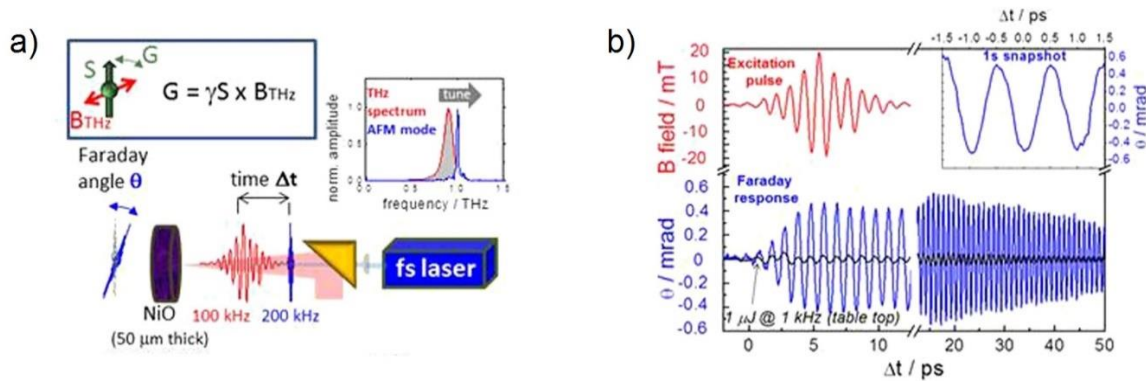


Figure 6: Resonant narrowband excitation of an antiferromagnetic (AFM) mode in NiO.

a) The transient THz B-field from a multi-cycle TELBE pulse is utilized to launch a coherent antiferromagnetic spin wave. The spin deflection is probed by the transient Faraday rotation of a delayed fs laser pulse. The resonant excitation provides a spectral density per pulse that is 36 times larger than achievable from a broad-band tabletop THz source. b) Transient Faraday rotation angle θ (blue-solid) plotted over delay time Δt between THz (red-solid) and laser probe pulses. The measurement shows that the spin precession evolves coherently over several tens of picoseconds. Due to the orders of magnitude higher spectral density at the resonance frequency, the amplitude of the THz-driven spin deflection is considerably increased compared to coherent excitation by a state-of-the-art high-field table-top THz source of similar pulse energy (black-solid line). Adapted from Ref. 34.

Another promising route for controlling magnetic order is the excitation of phonon modes that are coupled to the magnetic subsystem.^{22,37} Furthermore, the coherent excitation of chiral phonons that generates an effective magnetic field inside a sample provides another possibility for ultrafast spin control. Recent theoretical³⁸ and experimental³⁹ studies demonstrated the high potential of this approach. The required excitation frequencies for driving the relevant phonon modes are typically in the range between 5 and 15 THz. At the same time, both types of phononic magnetization control demand high THz fluences in excess of 1 mJ/cm² that are not available currently at the FELBE free-electron laser, but will be feasible using the DALI superradiant THz-MIR source.

The envisaged development of DALI will allow these areas to be explored further. At the moment, the choice of samples investigated is largely limited by those exhibiting resonances in the narrow 0.2 – 1 THz range. Many more antiferromagnetic systems with material-tunable resonances (such as orthoferrites) could be explored, and the coupling with phonon modes at even higher frequency could be investigated in greater detail. It is worth mentioning that very little is known

³⁶ K. Neeraj et al., Nat. Phys. **17**, 245–250 (2021)

³⁷ A. S. Disa et al., Nature **617**, 73–78 (2023)

³⁸ D. M. Juraschek et al., Phys. Rev. Research **4**, 013129 (2022)

³⁹ T. Nova et al., Nat. Phys. **13**, 132–136 (2017)

about magnetism in this frequency range, and unexpected experimental evidence may appear while performing experiments at DALI. From a fundamental point of view, this is motivated by the access to the energy scales between the spin-orbit and exchange interactions. Finally, this frequency range would open up access to an intense source resonant with the bandgap of many topological materials with their unique spin-locking properties in the topological surface states. The spin dynamics in these systems are yet largely unexplored, and DALI would allow for novel investigations on those materials as well.

2.1.5 Non-equilibrium dynamics of water and aqueous solutions in the THz range

Molecular dynamics and structural properties – In the low-frequency regime, electromagnetic pulses exert a transiently varying torque on molecular dipoles, such as water. The response of water to this change of electric fields is dominated by motions with relaxation times of 8, 1, and 0.1 ps. These Debye-type relaxation mechanisms dominate the susceptibility for slow variations up to the THz frequency range. The molecular motions corresponding to these relaxations have been investigated for centuries – yet there are several conflicting models to decompose the dielectric susceptibility of water into individual processes,^{40,41} which implies that the motion is essentially not known. Computer simulations fail to accurately reproduce the complex anomalies of water dynamics,⁴² even with recent advances in the field.⁴³

Earlier studies of the interaction of water with slowly varying electric fields were limited by the resulting heating, but some studies indicate that dielectric saturation begins at around 500 kV/cm. For the response of water, the frequency dependence between 0.1 and 20 THz is particularly insightful, because these frequencies will allow specific excitations to be driven out of equilibrium, potentially enabling an isolation of their impact on the molecular network.

The resulting structural modulation of water can be probed optically, by detecting the dielectric anisotropy via the THz Kerr effect^{44,45} or by probing the loss of centrosymmetry (a structural probe) by THz field-induced second-harmonic generation (TFISH).⁴⁶ These techniques provide information on the relaxation dynamics of the oriented water network. This will help to identify the underlying motions and also enable studies of the same motions at supercooled temperature, offering the instrumentation to probe the dynamics of the low-temperature liquid phase of water, which was recently resolved by its different atomic structure.⁴⁷

A separate UED setup (see Section 3.4) might also be considered as a probe to determine the molecular structure after THz excitation of a very thin liquid jet of a few 100 nm thickness. These jets can now be readily generated by gas-dynamic virtual nozzles.⁴⁸ Using this technique, the structure corresponding to the fundamental relaxation mechanism of liquid water can be directly resolved.

On the microscopic scale, the environment provided by water is characterized by a complex and highly dynamic network of intermolecular hydrogen bonds.⁴⁹ The structure and fluctuations of the

⁴⁰ A. Y. Zaslavsky, *Phys. Rev. Lett.* **107**, 117601 (2011)

⁴¹ N. Q. Vinh et al., *J. Chem. Phys.* **142**, 164502 (2015)

⁴² G. A. Cisneros et al., *Chem. Rev.* **116**, 7501 (2016)

⁴³ C. Hölzl, H. Forbert, and D. Marx. *Phys. Chem. Chem. Phys.* **23**, 20875 (2021)

⁴⁴ M. C. Hoffmann et al., *Appl. Phys. Lett.* **95**, 231105 (2009)

⁴⁵ P. Zalden et al., *Nat. Commun.* **9**, 1 (2018)

⁴⁶ D. J. Cook et al., *Chem. Phys. Lett.* **309**, 221 (1999)

⁴⁷ K. H. Kim et al., *Science* **358**, 1589 (2017)

⁴⁸ J. D. Koralek et al., *Nat. Commun.* **9**, 1 (2018)

⁴⁹ Y. Marcus, *Chem. Rev.* **109**, 1346–1370 (2009)

hydrogen bond network can facilitate some reactions and hinder others. For example, hydrophobic interactions help to fold proteins and cell membranes in biology.⁵⁰ In industry, these interactions hinder the full recovery of petroleum from an oil reservoir.⁵¹ Given the high impact of water, a comprehensive description of its microscopic structure and dynamics is strictly necessary for any quantitative and predictive models. However, many aspects of microscopic water behavior remain elusive and require new experimental methods. Complementary to the probing of comparably slow rotational dynamics (see above), the DALI light source will enable **nonlinear THz spectroscopy**^{52,53} of water, particularly in the >10 THz frequency regime.

THz vibrations of water are highly collective and delocalized (see Figure 7). Thus, these vibrations are sensitive probes for the extended water structure and thermally excited collective dynamics. Insights that have recently been obtained using linear THz absorption spectroscopy prove the efficacy of this approach.^{54,55} However, it is challenging to resolve several critical characteristics of a molecular system using linear absorption spectroscopy. Revealing the inhomogeneity of the hydrogen bond network, anharmonicity of the intermolecular forces, pathways, and rates of the thermal energy transfer requires nonlinear THz spectroscopy. Recent studies have demonstrated the potential of nonlinear THz techniques at capturing water dynamics.^{56,57} Proof of principle experiments conducted at FELBE showed that strong anisotropy can be induced in both liquid jets as well as static liquid cells.⁵⁸ The further development and application of novel nonlinear techniques are still currently limited by the lack of intense, broadband, and tunable light sources in this spectral range. The prospective DALI light source will greatly advance the THz spectroscopic methods for water research, and allow for expansion into the fields of biology (see Section 2.1.8), atmospheric chemistry, and catalysis.

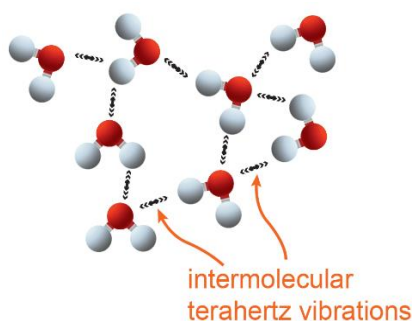


Figure 7: Schematics of the hydrogen bond network and THz vibrations in liquid water.

A specific example of nonlinear spectroscopy at DALI will be 2D THz spectroscopy, an analog of the widely used 2D spectroscopies in the MIR, visible, and ultraviolet spectral ranges. 2D THz spectroscopy will enable the direct measurement of the inhomogeneity, anharmonicity, and couplings for the intermolecular motions in liquid and solid water (ice). With the improved

⁵⁰ P. Ball, *Chem. Rev.* **108**, 74–108 (2008)

⁵¹ A. Bhardwaj et al., *J. Dispers. Sci. Technol.* **14**, 87–116 (1993)

⁵² M. C. Hoffmann, “Nonlinear Terahertz Spectroscopy”, in *Terahertz Spectroscopy and Imaging*; K.-E. Peiponen, A. Zeidler, M. Kuwata-Gonokami Eds.; Springer 2013; pp 355–388

⁵³ A. Shalit et al., *Nat. Chem.* **9**, 273–278 (2016)

⁵⁴ M.-C. Bellissent-Funel et al., *Chem. Rev.* **116**, 7673–7697 (2016)

⁵⁵ G. Schwaab, F. Sebastiani, and M. Havenith, *Angew. Chem. Int. Ed.* **58**, 2–16 (2018)

⁵⁶ F. Novelli et al., *Applied Sciences* **10**, 5290 (2020)

⁵⁷ F. Novelli et al., *J. Phys. Chem. B.* **124**, 4989-5001 (2020)

⁵⁸ F. Novelli et al., *Phys. Chem. Chem. Phys.* **24**, 653 (2022)

understanding of the nature of intermolecular motions in neat water, we will be able to address the nature of these motions in the aqueous solutions of inorganic and organic ions and molecules, from simple ions to proteins. The resulting new detailed models will allow the quantitative evaluation of the role of THz vibrations in the thermodynamics of complex systems, such as protein–ligand complexes and colloids.

2.1.6 Ultrafast nonlinear dynamics on nanoscale

Scattering scanning near-field infrared microscopy (**s-SNIM**), schematically depicted in Figure 8, enables the nanoscopic investigation of matter with a wavelength-independent resolution of a few 10 nm. Beating the diffraction limit by far, this method allows for fundamental examination of novel materials particularly concerning their local variation of physical properties, including local charge density distribution and mobility, local structural properties, as well as infrared-to-THz spectral response that may be affected e.g. by phononic, plasmonic, and magnonic excitations and related surface modes. Moreover, as s-SNIM is based on atomic force microscopy, complementary information at the very same local sample position can be recorded, including topography, surface potential, local conductivity, and piezoelectric response. Current emerging applications include semiconductor nanostructures, phase transitions in complex oxides, unusual polaritonic responses in van der Waals materials,⁵⁹ and viscous flow of electronic Dirac fluids.⁶⁰ Recently, s-SNIM operation was also demonstrated for the liquid-phase environment, enabling spatial-spectral analysis of soft matter in its intrinsic aqueous phase. This makes the technique very promising to study the dynamics of separate biological cells in their normal state, which is difficult to achieve with other techniques.⁶¹

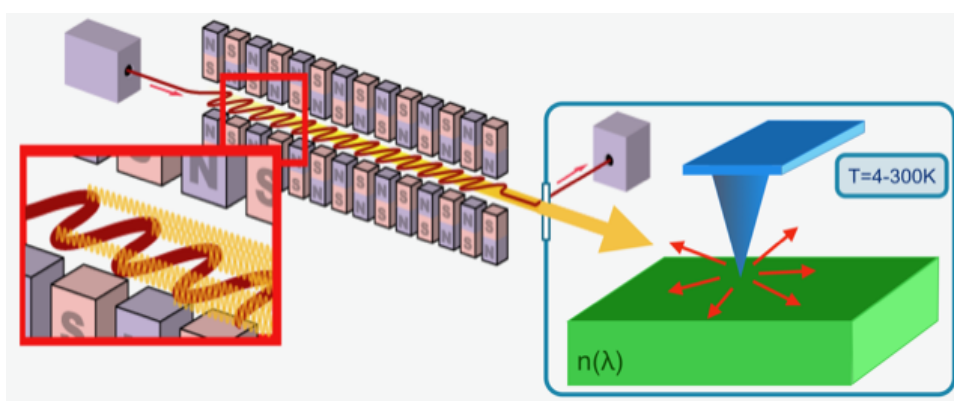


Figure 8: Schematics of FEL-based scattering-SNIM.

DALI will also enable **nanoscale polaritonic interferometry studies** of a variety of collective excitation modes, **including plasmons, phonons, and magnons**, thus providing direct access to their energy–momentum dispersion in a broad range of frequencies. The high photon flux of DALI would allow direct visualization of the yet unobserved magnon polaritons by combining low-temperature nanoscopy with specially developed magnetic probes of nitrogen vacancies.

Vertical stacking of a variety of two-dimensional materials (semimetallic, magnetic, insulating, semiconducting, among others) into **van der Waals heterostructures** opens up a plethora of

⁵⁹ T. V. G. de Oliveira et al., *Adv. Mat.* **33**, 2005777 (2021)

⁶⁰ M. J. H. Ku et al., *Nature* **583**, 537 (2020)

⁶¹ B. T. O'Callahan et al., *Nano Lett.* **20**, 4497 (2020)

new physical phenomena that result from interlayer orbital hybridization. Controlled layer twisting additionally allows for the generation of spatial heterogeneities that are fundamentally at the nanoscale. Utilizing the exceptional DALI frequency tunability, stability, and high fields would allow linear/nonlinear imaging and nanospectroscopical studies at their native length scales.

Exploiting the fast and fully automated frequency tuning, high pulse energies, and controlled repetition rates of DALI will enable **THz photothermal nanoscale spectroscopy** techniques. Nanochemistry, biochemical, and medical research should directly profit from direct access of spectroscopic information at the nanoscale.

The strength of s-SNIM in combination with the DALI THz source is twofold. First, DALI can provide a unique wavelength range with an extremely wide spectral coverage that is not accessible with table-top sources. Second and most importantly, DALI delivers high field strengths that enable studies of nonlinear light–matter interactions, including non-perturbative phenomena in the strong-coupling regime.

In general, both narrowband and broadband excitation will be of interest. Usually, s-SNIM operation is based on CW light sources or sources pulsed in the MHz range, where the laser repetition rate is much higher than the cantilever oscillation frequency. The pulse energies of table-top sources with MHz pulse rates are too low for nonlinear near-field spectroscopy. Even for an intense light source like FELBE, most s-SNIM studies are in the linear regime as the average power limitation (maximum ~ 50 mW to avoid destruction of the tip) limits the pulse energy to a few nJ. Nevertheless, FELBE allowed a first demonstration of nonlinear transport in semiconductor nanowires studied by s-SNIM.⁶² Most nonlinear phenomena, in particular non-perturbative effects, require orders of magnitude higher pulse energies. DALI is ideal for providing these intense pulses in a wide spectral range. Moreover, the repetition rate is adjustable, so the average power does not exceed the limit. Special s-SNIM operation modes with low-repetition-rate sources (in the kHz range) have been successfully demonstrated.⁶³

Such a high-field source for nonlinear THz science opens up the possibility to study novel dynamical effects that cannot be observed with linear spectroscopy. For example, Higgs spectroscopy reveals new insights into high-temperature superconductors,⁷ and THz HHG has great potential for future THz nanoelectronics.¹⁷ These techniques typically require semi-narrowband driving fields of THz radiation on the order of 100 kV/cm that are not possible to achieve with modern laser technologies at MHz repetition rates. For these reasons, combining the DALI THz source with time-resolved s-SNIM will provide novel opportunities to understand nonlinear THz light–matter interactions in materials, such as topological nanowires, quantum dots, nanostructured devices, superconductivity of twisted graphene bilayers, and disordered materials.⁶⁴ All such studies will not only provide better understanding of fundamental physics at the nanometer scale, but are very relevant for future high-frequency electronics, as most steps of signal manipulation (generation, detection, amplification) require nonlinear response of matter.

In addition, synchronous laser-based sources covering the wavelength range from the visible to the THz regime will be combined with accelerator-based sources for time-resolved s-SNIM via pump–probe techniques.

⁶² D. Lang et al., *Nanotechnology* **30**, 084003 (2019)

⁶³ H. Wang et al., *Nat. Commun.* **7**, 13212 (2016)

⁶⁴ K. Zhao et al., *Nat. Phys.* **15**, 904 (2019)

2.1.7 Application-oriented research

Clearly, DALI is aimed as a facility for outstanding basic research. Nevertheless, user experiments at a forefront facility of DALI will also target application oriented research. This will mainly be related to applications in research laboratories. Basically, the goal is to boost the whole field of experiments with intense THz fields. A straightforward example is to study the limits of nonlinear materials for THz generation. At DALI, intense THz pulses can be utilized to study the nonlinear THz transmission and the destruction threshold of these materials. Importantly, the THz limits can be explored disentangled from the limits placed by the optical excitation. Furthermore, varying the repetition rate, one can easily distinguish thermal effects related to average power from other effects, e.g. multiphoton excitation of phonons that are related to the peak THz intensity.

The combination of the DALI THz source with many ultrafast probing techniques requires ultrafast detection and arrival time monitoring. This triggers the development of ultrafast broadband detectors that are valuable for a wider research community. Examples for such detector developments have been started at FELBE, where field-effect transistors with wide spectral range, short electronic response time, low-noise operation at room temperature and robustness against intense THz pulses have been demonstrated.^{65,66} These detectors are used at various THz facilities and have the potential as a commercial product. Generally, detector, modulator, ultrafast switching and frequency multiplication devices can be tested and characterized at DALI (Figure 9). Frequency multiplication is an important driver for THz technology as it allows to make use of compact, cost-efficient electronic sources at lower frequencies to realize higher output frequencies.

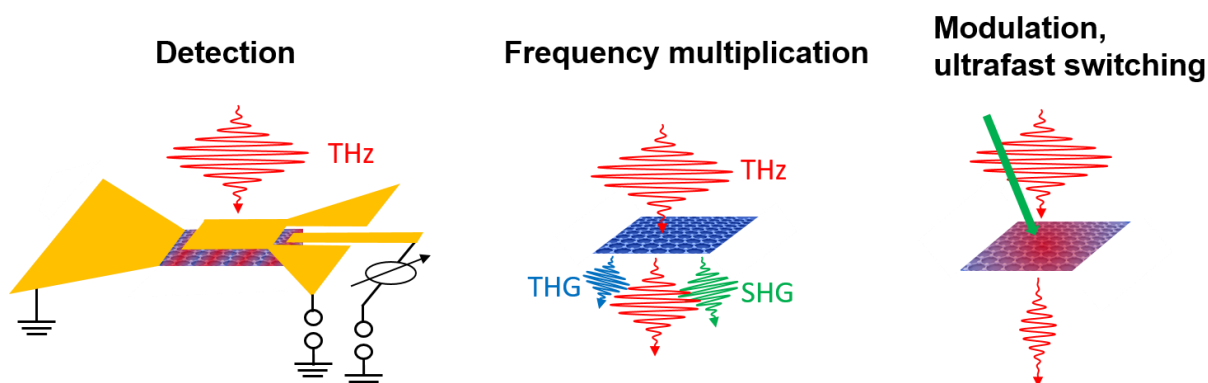


Figure 9: Examples for devices applications to be investigated at DALI.

Another promising material for THz technology is graphene. Its unique optical and electronic properties enable to use it as an ultrafast detector for THz and infrared pulses.^{67,68} In contrast to detectors based on field-effect transistors that are sensitive only below 10 THz, graphene-based detectors demonstrated a fast sub-100 ps rise time for pulses in a broad spectral range from THz to the visible. The detector employs a large area graphene active region with interdigitated electrodes that are connected to a log-periodic antenna to improve the long-wavelength collection efficiency, and a silicon carbide substrate that is transparent throughout the visible regime. The

⁶⁵ S. Preu et al., *Opt. Express* **21**, 17941–17950 (2013)

⁶⁶ S. Regensburger et al., *IEEE T. THz Sci. Techn.* **8**, 465–471 (2018)

⁶⁷ M. Mittendorff et al., *Opt. Express* **23**, 28728–28735 (2015)

⁶⁸ M. Mittendorff et al., *Appl. Phys. Lett.* **8**, 021113 (2013)

detector exhibits a noise-equivalent power of approximately $100 \mu\text{W}\cdot\text{Hz}^{-1/2}$ and is characterized at wavelengths from 780 nm to 500 μm .

THz technology enters wider markets in the area of security applications, non-destructive testing, environmental monitoring and wireless communication. Developing and advancing this technology requires studies from the material to the device and to the system level. In particular, developing mass-market applications at certain frequencies requires advanced THz instrumentation operating in a much wider frequency and power range than the product under development. DALI can enable testing and developing new cutting edge instrumentation.

2.1.8 Biological materials

Dielectric spectroscopy,⁶⁹ nuclear magnetic resonance,⁷⁰ and time-resolved infrared spectroscopy⁷¹ have revealed the existence of ordered water structures in the hydration shell of biomolecules. Recently, their expected correlation with heat capacity changes has been proven by static THz spectroscopy.⁷² In contrast to spectroscopic approaches, which sample molecular states of the solvent and the solute at equilibrium, the high intensity and repetition rate of the planned THz source will allow deviations from equilibrium to be induced by the polarization of hydration shells and of dipoles within electric-field-sensitive proteins in cell membranes. This enables entirely new experimental approaches that address fundamental questions regarding the role of hydration shell structure and dynamics in the cellular process. For example, structure formation in protein domains of low complexity is thought to be highly dependent on the solvation/desolvation of their side chains,⁷³ and was recently confirmed by linear THz spectroscopy.⁷⁴

Transitions from protein–solvent to protein–protein contacts depend on the release and/or fusion of independent hydration shells and thus on interfacial water orientation and dynamics. Here, the prime interest of a large biophysical science community concerns i) the recently discovered liquid–liquid phase transitions⁷⁵ of many disease-related proteins carrying these low complexity domains and ii) the introduction of electric-field-driven processes in cell membrane proteins such as voltage-gated channels. Small volume samples, such as for proteins, are possible, and can be probed in liquid cells or hydration-controlled sample compartments. Dedicated sample delivery methods, such as liquid jets, have been installed, and proof-of-principle experiments have been conducted at TELBE (see Figure 10). These demonstrate that the scientific fields will profit from THz experiments in an unprecedented fashion by using an optical probe laser to detect THz-pump-induced nonlinear effects by second-harmonic generation. Competition of low-complexity domains for hydration water is assumed to be a critical factor that induces protein phase separation in the living cell and that may be directly affected by water orientation in strong THz fields. The synchronized optical probing further enables simultaneous coupling to fluorescence markers that show the folding states of proteins in order to correlate these with the measured dielectric relaxation times. A highly demanded application is conducting these experiments in

⁶⁹ N.Q. Vinh, S.J. Allen, and K.W. Plaxco, *J. Am. Chem. Soc.* **133**, 8942–8947 (2011)

⁷⁰ F. Persson, P. Söderhjelm, and B. Halle, *J. Chem. Phys.* **148**, 215103 (2018)

⁷¹ D. Laage, T. Elsaesser, and J. T. Hynes, *Chem. Rev.* **117**, 10694–10725 (2017)

⁷² F. Böhm, G. Schwaab, and M. Havenith, *Angew. Chem. Int. Ed.* **56**, 9981–9985 (2017)

⁷³ S. S. Ribeiro et al., *Nat. Rev. Chem.* **3**, 552–561 (2019)

⁷⁴ J. Ahlers et al., *Biophys. J.* **120**, 1266–1275 (2021)

⁷⁵ S. Alberti, A. Gladfelter, and T. Mittag, *Cell* **176**, 419–434 (2019)

living cells with ultimate performance and additional optical monitors of cell physiology. The required microscopic setup is currently being installed at TELBE.

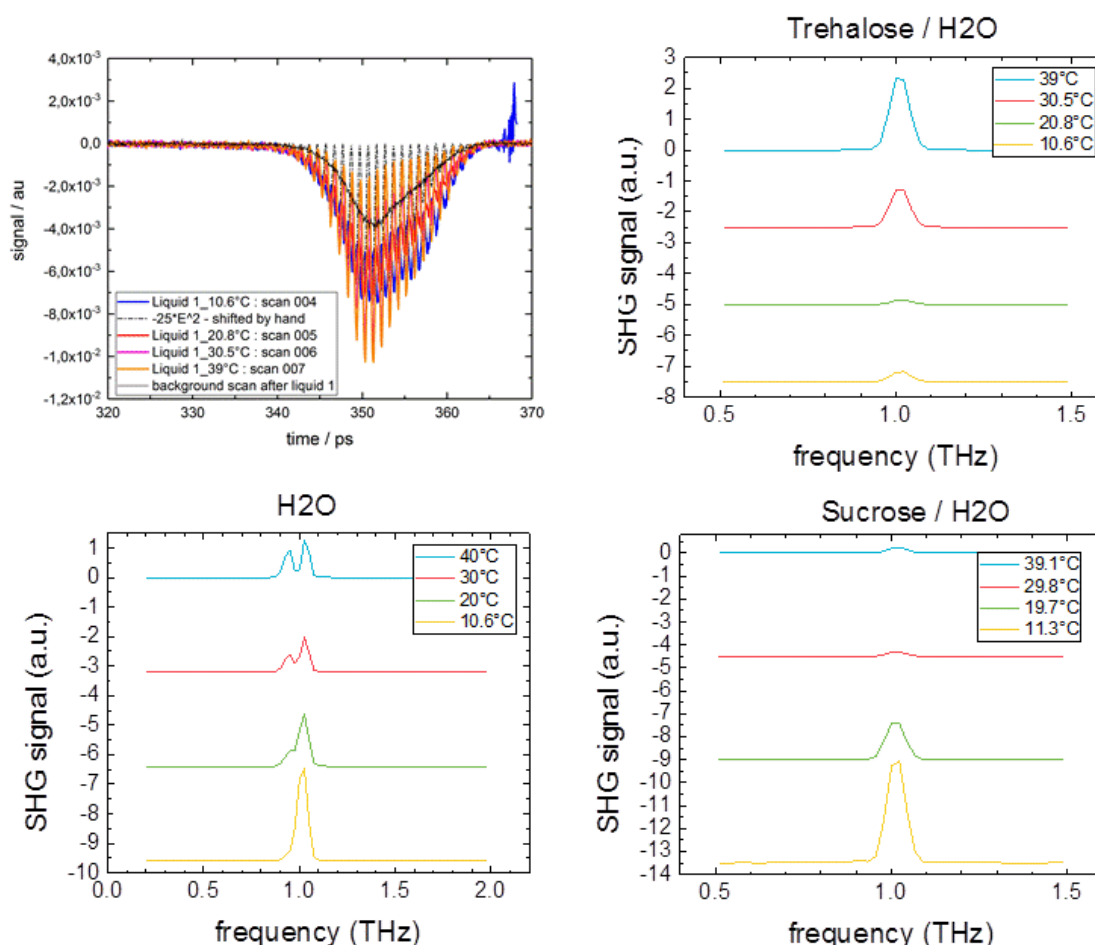


Figure 10: Proof-of-principle for TFISH generation in aqueous sugar solutions in a liquid jet. The figure shows the THz-induced oscillation of the probe light (400 nm) at 1 THz, i.e. twice the frequency of the 0.5 THz excitation pulses. The temperature dependence of the TFISH signal is solute-specific, as shown here for the discrimination between the chemically similar sugars sucrose and trehalose. Trehalose, but not sucrose, is synthesized in many lower animals to confer draught resistance, probably by stabilizing specific water structures at their cell membrane interfaces.^{76,77} The demonstrated chemical sensitivity for solvent–solute interactions in the TFISH experiment shows that the underlying solvent–solute interactions can be studied in a liquid jet.

Furthermore, THz single-cycle pulses will provide strong (10 – 30 MV/m) individual electric field pulses that are in the range of typical transmembrane electric fields in eukaryotic cells, so that voltage-dependent processes are expected to become inducible for the first time at high repetition rates to study primary reactions in voltage-gated membrane proteins and in transmembrane ion transporters. The thorough analysis of THz-induced phenomena in proteins requires genetic engineering and complementary, mostly infrared and fluorescence-spectroscopic studies, which are feasible on site at the Institute of Resource Ecology at HZDR and within the well-established research network within the “Physics of Life” excellence cluster at TU Dresden.

⁷⁶ J. H. Crowe, F. A. Hoekstra, and L. M. Crowe, *Annu. Rev. Physiol.* **54**, 579–599 (1992)

⁷⁷ C. Erkut et al., *Curr. Biol.* **21**, 1331–1336 (2011)

2.2 Probing structural dynamics by ultrafast electron diffraction (UED)

Electron diffraction is a powerful tool for examining the structure of matter and is highly complementary to X-ray diffraction measurements. For example, X-ray diffraction is sensitive to the electron distribution, while electron diffraction is sensitive to the nuclear distribution. Also, when comparing these two types of probe beams, electrons cause less damage to the sample due to the larger scattering cross section compared to X-rays.⁷⁸ On the other hand, X-rays probe deeper into samples. And while electron diffraction covers a larger range of reciprocal space due to the smaller de Broglie wavelength, X-rays offer higher reciprocal space resolution.⁷⁹

Utilizing ultrashort electron bunches further enhances electron diffraction by enabling time-resolved or ultrafast electron diffraction (UED). Typically, UED has been performed with electrons at hundreds of keV, but the modest beam energy limits the penetration depth of the electrons, and space charge effects limit the temporal resolution. The recent development of MeV energy electron sources for UED enables deeper probing and sub-100 fs resolution.^{80,81} For the larger interaction volume of gas phase samples, the higher beam energy of MeV-UED also greatly reduces the velocity mismatch between the optical pump pulse and the electron probe pulse.^{82,83}

To achieve the full potential of UED, one must first initiate the dynamic conditions of interest. In previous UED measurements, this was achieved with ultrashort optical pulses, which couple directly to the charge carriers and only indirectly with the atomic distribution. The high-field coherent THz sources of DALI provide a new powerful and unique means for driving structural, molecular, and atomic dynamics directly. Furthermore, the ELBE SRF electron gun – which has already demonstrated robust high-performance operation for high bunch charge – is well suited to deliver the extremely-low-emittance ultrashort electron bunches required for a MeV-UED source.

The combination of a high-field coherent THz pump and a keV-UED or MeV-UED probe at DALI is highly relevant for studies of condensed matter systems. For example, by measuring how high-field-driven structural dynamics affect phenomena such as charge density waves (CDW),^{84,85} superconductivity,⁸⁶ and other correlated systems that exhibit properties highly dependent on the underlying lattice structure (e.g. insulator–metal transitions),^{87,88} a breakthrough could be made in the presently incomplete understanding of electron–lattice coupling.

Reaction dynamics are another process for THz pump – UED probe experiments. The potential barrier of certain reaction processes can be reduced significantly when molecules present particular orientations or conformations.⁸⁹ High-field multicycle THz radiation is ideal for driving

⁷⁸ R. J. D. Miller, *Science* **343**, 1108 (2014)

⁷⁹ M. Stefanou, et al., *Chem. Phys. Lett.* **683**, 300–305 (2017)

⁸⁰ J. Yang et al., *Nat. Commun.* **7**, 11232 (2016)

⁸¹ K. Floettmann, *Nucl. Instrum. Methods Phys. Res. A* **740**, 34–38 (2014)

⁸² X. Wang and P. Musumec, *Report of the Basic Energy Sciences Workshop on the Future of Electron Sources*, SLAC National Accelerator Laboratory (2016); <https://doi.org/10.2172/1616511>

⁸³ E. Hall et al., *Future of Electron Scattering and Diffraction*, US Department of Energy, Washington, DC, United States (2014), <https://doi.org/10.2172/1287380>

⁸⁴ N. Erasmus et al., *Phys. Rev. Lett.* **109**, 167402 (2012)

⁸⁵ T.-R. T. Han et al., *Phys. Rev. B* **86**, 075145 (2012)

⁸⁶ F. Carbone et al., *Proc. Natl. Acad. Sci.* **105**, 20161 (2008)

⁸⁷ M. Gao et al., *Nature* **496**, 343 (2013)

⁸⁸ V. R. Morrison et al., *Science* **346**, 445–448 (2014)

⁸⁹ H. Jean-Ruel et al., *J. Phys. Chem. B* **117**, 15894–15902 (2013)

large-scale molecular motion and conformational changes,⁹⁰ and the combination of photoelectron spectroscopy and UED probes can resolve the dynamics of the structural, conformational, and molecular orientations throughout the reaction process. Understanding these processes can lead to greater efficiencies and reduce unwanted byproducts in many types of chemical reactions.

In all of these types of studies, significant benefits arise from the high repetition rate and collocation of the DALI photon and UED sources. Signal-to-noise and data statistics clearly benefit from the high repetition rate in all types of measurements, but this is particularly important for dilute gas phase measurements. Also, the high fluence (pulse energy) of the photon sources and the higher bunch charge that is possible in a MeV-UED system (relative to keV-UED) would enable single-shot measurements of irreversible processes, such as chemical reactions.

2.2.1 Ultrafast structural dynamics of quantum materials

While astounding electronic properties such as superconductivity, CDW, and insulator–metal phase transitions have long been predicted theoretically, it has only more recently become possible to fully study some of the materials and structures exhibiting these properties. These phenomena arise from the correlated motions within the electron system, and these correlations are related to the interaction between the electrons and the lattice. Measuring the structural changes that occur when these types of materials transition to the highly correlated phase provides insight into the electron–lattice interaction and how it gives rise to these properties. Furthermore, detecting the ultrafast transient processes that occur in such phase transitions can reveal previously undetected non-equilibrium phases.

The phases of matter where these exotic electronic properties are manifest often depend on the energetics of the system, and for example may only exist at low temperature. In some cases, such as in vanadium dioxide (VO₂), it has long been observed that the phase transition between the insulating and metallic phase occurs close to room temperature and is accompanied by a transformation of the lattice structure.^{91,92,93} But a full understanding of the underlying physics remains incomplete, particularly in light of more recent discoveries of the existence of a transient metallic phase that can be driven by an ultrafast optical excitation.^{94,95,96} It was later confirmed by optical pump – UED probe studies that this photoinduced transient metallic phase results from a reorganization of the charge density that is not accompanied by a structural transformation.⁸⁸ The understanding and control of the non-thermal insulator–metal phase transition of VO₂ and similar materials have great promise for ultrafast optical switching.

Similarly, very recent optical pump – UED probe studies of the layered rare-earth tritelluride, LaTe₃, detected the existence of a transient photoinduced CDW, which competes with the equilibrium CDW.⁹⁷ A slight lattice anisotropy in the *a*–*c* plane allows a CDW to form only along the *c*-axis. Under photoexcitation by an ultrashort optical pulse, the equilibrium CDW weakens and a CDW along the *a*-axis appears. The appearance of the *a*-axis transient CDW is attributed to the photoinduced generation of topological defect/anti-defect pairs, which locally disrupt the *c*-axis equilibrium CDW and allow the transient CDW to form along the *a*-axis. The UED measurements clearly revealed the possibility to optically access pathways to new ordered

⁹⁰ L. A. Pellouchoud and E. J. Reed, *Phys. Rev. A* **91**, 052706 (2015)

⁹¹ F. J. Morin, *Phys. Rev. Lett.* **3**, 34–36 (1959)

⁹² J. A. S. Barker, H. W. Verleur, and H. J. Guggenheim, *Phys. Rev. Lett.* **17**, 1286–1289 (1966)

⁹³ H. W. Verleur, A. S. Barker, and C. N. Berglund, *Phys. Rev.* **172**, 788–798 (1968)

⁹⁴ A. Pashkin et al., *Phys. Rev. B* **83**, 195120 (2011)

⁹⁵ T. L. Cocker et al., *Phys. Rev. B* **85**, 155120 (2012)

⁹⁶ A. Cavalleri et al., *Phys. Rev. Lett.* **87**, 237401 (2001)

⁹⁷ A. Kogar et al., *Nat. Phys.* **16**, 159–163 (2020)

phases within materials, and even greater control may become possible if one considers resonant THz excitation of the non-equilibrium ordered phase.

It is important to note that for the UED measurements of V. R. Morrison et al.,⁸⁸ the electron energy was limited to 95 kV with a repetition rate of 1 kHz, which required 12.5 minutes to acquire at each pump–probe delay. A. Kogar et al.⁹⁷ utilized both keV- and MeV-energy UED systems, also at low repetition rate, and found that the transient a -axis scattering is better resolved by the MeV-UED measurement due to the reduced background scattering from the sample substrate. For the proposed DALI UED system, there are clear advantages to the higher repetition rate in addition to the wider range of MIR-THz pump beams provided by the suite of DALI photon sources.

2.2.2 UED to study the excited-state dynamics of isolated molecules

Nature is full of sophisticated molecular building blocks that selectively and efficiently transfer light energy from the sun into other forms of energy, such as changes in chemical bonds, charge separation, or heat. The energy transformation occurs on electronically excited states of the molecules by a highly intertwined motion of electrons and nuclei on an ultrafast time scale. Changes in molecular geometry can induce electronic transitions, which determine the fate of energy distribution within the molecule. This phenomenon cannot be described within the

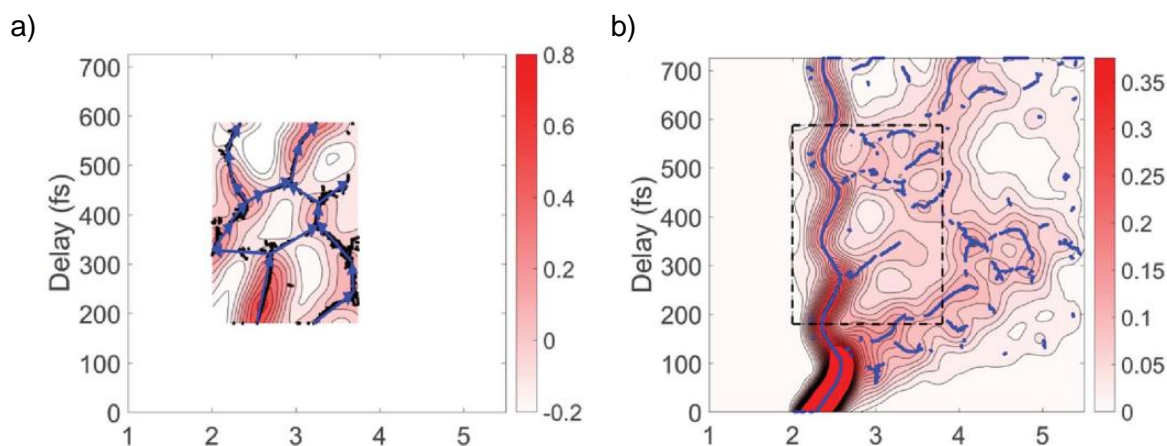


Figure 11: Pair distances in CF_3I . (a) Experimental pair distances resulting from the Fourier transform of experimental scattering patterns of CF_3I . The data are shown as a function of delay between the UV pump pulse and the electron probe pulse. (b) Simulated ab-initio pair distances of C-I within CF_3I . The vibrational wavepacket is launched on a Rydberg state of CF_3I by a two-photon process. The C-I distance undergoes a regular vibrational motion between 2 and 3 Å together with a bifurcation at a conical intersection, allowing population to reach out to longer pair distances. The chosen region in the experiment shows the bifurcation at the conical intersection around 300 fs and a recombination of the two parts at about 450 fs in agreement with the simulation (adapted from Ref. 100).

framework of the Born–Oppenheimer approximation and presents a continuing challenge for quantum simulations as well as for experiments aimed at finding these crucial transitions. The direct characterization of geometry changes in isolated molecules with atomic accuracy on an ultrafast time scale has recently become possible due to advances in relativistic UED.⁹⁸

At SLAC, the first gas phase experiments with 100 fs time resolution have allowed the spatial imaging of molecular rotational⁸⁰ and vibrational wavepackets.⁹⁹ Building up on these

⁹⁸ S. P. Weathersby et al., Rev. Sci. Instr. **86**, 073702 (2015)

⁹⁹ J. Yang et al., Phys. Rev. Lett. **115**, 173002 (2016)

experiments, a prototype dissociation reaction of CF_3I and the ring opening process on cyclohexadiene have been studied.^{100,101} In the context of CF_3I , it was even possible to observe the nuclear motion in the vicinity of a so-called "conical intersection", a prototype topology for nuclear–electron coupling. Figure 11 shows the experimental results of wavepacket bifurcation and recombination together with ab-initio simulations of the process.¹⁰⁰

The results above were obtained at the SLAC MeV e- source with 100 fs pulse duration, about 10 fC bunch charge and 120 Hz repetition rate. While UED experiments at repetition rates on the order of 100 Hz are limited to chemicals of high vapor pressure, 1 MHz sources will serve to investigate a large set of important building blocks having typically lower vapor pressure, such as nucleobases. In comparison to X-ray sources, unique new opportunities exist for electron sources. X-rays interact via Thompson scattering, which limits the interaction with the electrons of molecules due to unfavorable scaling with particle mass. Electrons, however, scatter off both molecular electrons and nuclei, making them ideal tools for the observation of subtle changes, such as in proton transfer.

2.3 Science with positrons

The interaction with positrons, the antiparticles of electrons, offers a unique tool for investigating lattice defects in materials science, solid-state physics, chemistry, and electronics in a non-destructive way. Mechanisms of defect formation, defect migration, and defect annealing on the atomic scale, ranging from grain boundaries, dislocations, single-atom and cluster vacancies to nanoscale voids and surface effects are fundamentally important for the understanding of material features and functionalities by altering their electrical, mechanical, dielectric and magnetic properties. Positrons therefore serve as highly sensitive and highly mobile probes for non-destructive studies bridging the gap between fundamental studies and technological applications where defect engineering leads to tailored material characteristics and enhanced performance, e.g. in CMOS circuits (low-k materials), magnetic switching, surface chemistry and catalysis, membranes, high-entropy alloys, radiation-hard materials, and solar cell materials.

2.3.1 Probing defect kinetics with positron annihilation lifetime spectroscopy

Based on the experience gained at the existing EPOS positron source at ELBE and on various requests by a growing strong user community from research centers and universities all over the world, experimental applications of the proposed DALI positron source cover materials research,¹⁰² solid-state physics,¹⁰³ semiconductors, chemistry,¹⁰⁴ and more. Being the antiparticles of electrons, positrons and related measures, such as positron annihilation lifetimes, the energy and momentum distributions of annihilation photons, and the possible formation of positronium – the bound state of electron and positron – are highly sensitive to local electron densities in matter and materials as well as to open-volume defects inside the lattice. For this reason, studies of crystal imperfections are now one of the dominant applications of positron annihilation spectroscopy. Due to typically large diffusion lengths in matter (~ 100 nm), implanted positrons test up to 10^6 host atoms and imperfections, resulting in a sensitivity to crystal defects on the ppm concentration level.¹⁰⁵ Moreover, the annihilation lifetime strongly depends on the

¹⁰⁰ J. Yang et al., *Science* **361**, 64 (2018)

¹⁰¹ T. J. A Wolf et al., *Nat. Chem.* **11**, 504 (2019)

¹⁰² A. Quintana et al., *ACS Nano* **12**, 10291 (2018)

¹⁰³ T. Kosub et al., *Nat. Commun.* **8**, 13985 (2017)

¹⁰⁴ G. Panzarasa et al., *Macromolecules* **50**, 5574 (2017)

¹⁰⁵ J. Čížek, *J. Mater. Sci. Technol.* **34**, 577 (2018)

type of defect (single up to clusters of vacancies), while the annihilation gamma-ray energy tests the local electron momentum distribution and thus the chemical environment of defects. The annihilation lifetime, Doppler-broadening of the annihilation photons, and angular correlation of the annihilation radiation serve as sensitive tools for fundamental and applied studies of local electron densities in materials. Large open volumes in porous materials lead to the formation of positronium (Ps). Again, the annihilation lifetime of the spin-parallel state (ortho-Ps) tests the size of voids in porous materials ranging from sub-nm to 100 nm. In contrast to intrusion techniques (LN_2 , Hg), the positronium lifetime method is applicable for closed porosity¹⁰⁶ and can be applied in thin films down to a few 10 nm thickness.

Physics at the positron beamline experimental station AIDA (Apparatus for In-situ Defect Analysis) at the existing EPOS focuses on probing the evolution of vacancy-like defects and their conglomerates fully in-situ as a function of time in order to answer fundamental questions arising when approaching the nanoscale as well as more applicable challenges (e.g. in semiconductor manufacturing). Among those fundamental studies, we attempt to understand the formation of non-equilibrium vacancies generated during noble-gas ion irradiation¹⁰⁷ and their dependence on

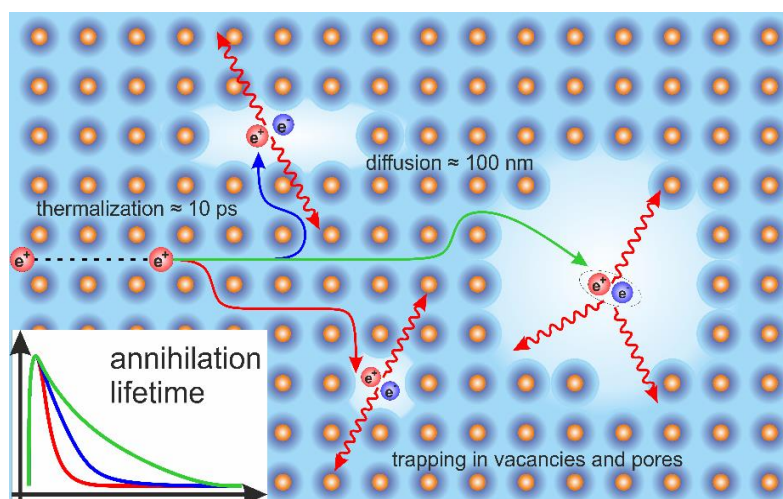


Figure 12: Fate of positrons in matter. After rapid thermalization, positrons diffuse about 100 nm before being trapped in open-volume defects or forming positronium inside larger voids.

intrinsic parameters such as initial defect concentration and system temperature. First insights into the damage produced by ion implantation in materials aid in developing models of damage evolution.¹⁰⁸ Another fundamental open question regards the kinetics of vacancies and their clustering leading to surface nanopatterns (holes, voids, sponges) on semiconductor and metal surfaces upon ion irradiation.¹⁰⁹ Until now, more application-oriented investigations involving positron annihilation spectroscopy have concentrated on the influence of defects on the magnetic phase transition between ferromagnetic and paramagnetic states, where the excess of vacancies serves as accelerating stimulus for magnetic reordering processes in FeAl thin films.¹¹⁰ Electric-

¹⁰⁶ A.G. Attallah et al., Sci. Rep. **13**, 7765 (2023)

¹⁰⁷ H. Wiedersich, Radiat. Eff. **12**, 111–125 (1972)

¹⁰⁸ S. Argawal et al., Sci. Adv. **6**, eaba8437 (2020)

¹⁰⁹ R. Böttger et al., Appl. Phys. A **113**, 53–59 (2013)

¹¹⁰ J. Ehrler et al., Acta Mater. **176**, 167–176 (2019)

field-controlled magnetic switching driven by complex defects has been achieved in Co_3O_4 systems.¹¹¹ An obvious extension of the current studies will involve investigations of defect kinetics in both aforementioned magnetic systems during continuous ion irradiation and voltage biasing, respectively. Similar processes have been and are studied in different material classes, for example FeRh ¹¹² and FeV in the case of magnetic phase transitions, and in oxides and nitrides for voltage-controlled magnetic switching¹¹³. Another example where kinetics plays an essential role is a mechanism of nanopore formation in ultralow-k thin films, which is so far not entirely understood. The low-k materials are candidates for insulating dielectrics in digital circuits. Although many of these kinetic processes could be successfully studied using positrons at the existing EPOS, the sensitivity to kinetic effects was limited to slower processes that last at least a few minutes (due to the actual positron intensity). In contrast, a more intense positron beamline would provide access to faster processes in the range of seconds, thus expanding possible user cases, such as studies of the first seconds of fast precipitation processes in Al alloys, which help to control the material properties of age-hardenable Al alloys.¹¹⁴

The overall aim will be to perform pump–probe experiments down to picosecond time scales for dynamical processes of defect evolution and annealing, for example laser pump – positronium probe experiments, to study the dynamics of laser-induced paramagnetic centers in porous materials,¹¹⁵ which are of great interest for electronic and optical applications. Illumination of wide-gap semiconductors, such as AlN or diamond (future candidates for electronic applications), with sub-bandgap monochromatic light in light pump – positron probe studies allows the self-consistent determination of optical absorption cross sections and of the vacancy concentration,¹¹⁶ which is essential for proper applications. Future strategic topics that require the “high-intensity all in-situ approach” and that can only be conducted by implementing AIDA at DALI are: i) observation of defect evolution during magneto-ionic transport and memristive switching, ii) evaluation of sub-bandgap defect levels in insulators and semiconductors by means of monochromatic light illumination, iii) kinetics of thermally activated semiconductor dopants, and iv) low-angle grain boundary engineering in high-temperature type II superconductors.

¹¹¹ J. de Rojas et al., *Adv. Funct. Mater.* **30**, 2003704 (2020)

¹¹² W. Griggs et al., *APL Mater.* **8**, 121103 (2020)

¹¹³ J. de Rojas et al., *Nat. Commun.* **11**, 5871 (2020)

¹¹⁴ L. Resch, *J. Mater. Sci.* **53**, 14657 (2018)

¹¹⁵ D. B. Cassidy et al., *Phys. Rev. B* **75**, 085415 (2007)

¹¹⁶ J. M. Mäki et al., *Phys. Rev. Lett.* **107**, 217403 (2011)

3 Methods and Experimental Stations Enabling New Science with DALI

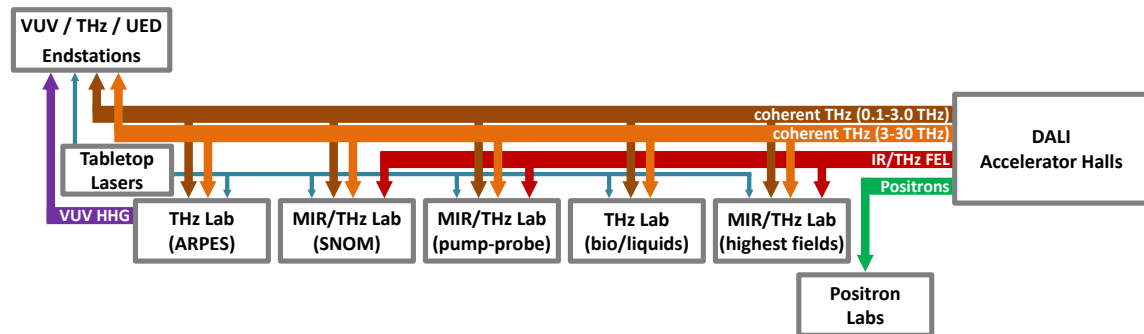


Figure 13: Distribution of DALI sources and table-top sources to the experimental stations and labs.

3.1 Pump–probe experiments

Nonlinear interactions of intense THz radiation with matter can be investigated simply by monitoring the parameters of the transmitted radiation as a function of its intensity, such as changes in transmission (e.g. in z-scan experiments), polarization state, or spectral content, e.g. by cross-phase modulation or by registering harmonics generated in the sample. Beyond that, pump–probe spectroscopy is the most powerful technique to study the effect of intense THz radiation in a time-resolved way. In pump–probe experiments, the change induced by intense pump pulses is monitored by non-disturbing probe pulses of variable delay. In the following, the main pump–probe experiments (as summarized in Figure 14) envisioned for the DALI facility are discussed along with important technical aspects.

- Degenerate pump–probe experiments** – In degenerate pump–probe experiments (user stations U1), a beam from the DALI source is split into an intense pump and a weak probe beam. Hence, the system is probed at the same photon energy as the excitation. Utilizing incoherent detection of the probe beam, this technique can be performed in a jitter-free manner with a temporal resolution determined by the pulse duration. Performing experiments with sub-cycle temporal resolution is enabled by coherent detection using nonlinear crystals for electro-optic sampling (EOS). This technique allows one to monitor amplitude and phase changes related to changes in the complex optical constants (refractive index, dielectric constant, dynamic conductivity) with sub-cycle temporal resolution. This requires a near-infrared femtosecond laser that is synchronized to DALI (user stations U2). By nature, this introduces a jitter, which will be minimized in several steps using cutting-edge technology. Firstly, by using drift-compensated fiber links and ultrastable laser oscillators for the accelerator-based DALI source, the jitter can be minimized down to <500 fs. Next, implementing arrival time monitors at the experimental stations and using phase-locked feedback loops operating at harmonics of the repetition rate allows long-term drifts to be suppressed and jitter to be reduced to the <100 fs level. Finally, implementing post-mortem data analysis using precise THz-based arrival time monitors makes it possible to reach <10 fs temporal resolution, as has already been demonstrated at TELBE. Here, optimized hardware and algorithms, developed for the TELBE light source and for DESY, will handle large data volumes at high repetition rates, compress, and process them. The data analysis and data compression will be performed online, and the results of ultrafast measurements will be available during the experiments.

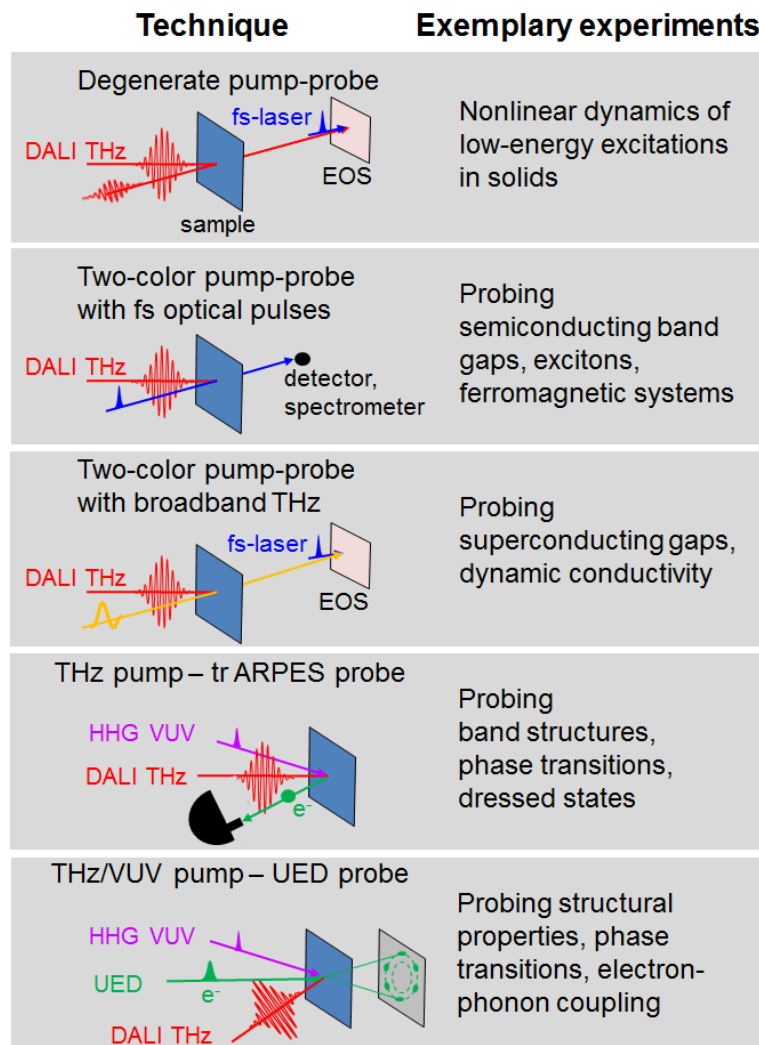


Figure 14: Overview over the main pump–probe techniques at the DALI THz facility.

- Two-color probing with femtosecond optical pulses** – Using femtosecond laser pulses precisely synchronized to the DALI source makes it possible to study various MIR-THz-induced ultrafast dynamics in solid-state systems, such as semiconducting bandgaps and excitons as well as ferromagnetic systems, via various electro- or magneto-optic (Kerr) effects. Hence, the DALI experimental stations will be equipped with near-infrared femtosecond lasers that are synchronized to DALI (see above, user stations U2). There will be different lasers optimized for different experimental configurations, e.g. wavelength tunability or ultimately short pulse duration. Furthermore, the spectral range for probing with femtosecond pulses can be easily extended from the near-infrared towards the MIR (<20 μm) and UV (e.g. 400 nm, 266 nm) via nonlinear optical processes. In particular, the generation of femtosecond supercontinuum pulses via self-phase modulation and their detection with a spectrometer yield information in a wide spectral range with femtosecond time resolution.
- Two-color probing with broadband THz radiation** – The DALI THz sources will cover basically the full THz range (0.1 – 30 THz) with intense pulses. The spectral width will be 10 – 15% for the lower frequencies (0.1 – 3 THz) and as low as a few percent for the higher

frequencies. It will be extremely useful to combine this rather narrowband pumping with broadband THz probing (user stations U2). For example, this will allow the monitoring of superconducting gaps while pumping phonons in a superconductor, or the monitoring of the dynamic conductivity in order to observe a metal–insulator transition induced by a strong THz electric field. To this end, broadband THz pulses will be generated via nonlinear processes (mainly optical rectification and difference frequency generation), and the THz transients will be recorded via EOS, providing amplitude and phase information. The synchronized femtosecond near-infrared sources are ideally suited to generate broadband THz probe pulses and to provide gating pulses for detection via EOS. The DALI pump radiation will be suppressed by spectral filtering, spatial filtering, and demodulation techniques.

- **Probing by time-resolved ARPES (tr-ARPES)** – Time-resolved, angle-resolved photoemission spectroscopy (tr-ARPES, user station U4) is a powerful method to directly observe the energy dispersion of occupied states. When used as a probe technique, it reveals changes in occupation and moreover changes in the band structure itself, induced by the pump beam. For tr-ARPES, an extreme ultraviolet (XUV) light source (photon energy ~ 20 eV, wavelength ~ 62 nm) is envisioned. It will be based on high-harmonic generation (HHG) in a noble gas jet (e.g. Ar, Kr) driven by a few-mJ femtosecond near-infrared laser synchronized to the DALI THz sources. As for many other pump–probe experiments, the range of 100 – 500 kHz is highly attractive. It offers much higher signal-to-noise ratio compared to systems operating at 1 kHz. Repetition rates above 1 MHz, on the other hand, restrict experiments to materials with rather short recovery times and may introduce heating issues.
- **Probing with UED** – An endstation equipped with a UED instrument (user station U6) will enable users to directly probe the structure of matter under dynamic conditions. In condensed matter systems, this is a powerful technique for measuring the underlying structural dynamics in photon-driven phase transitions or for directly monitoring the dynamics of specific lattice modes that provide the critical electron–phonon coupling that give rise to correlated phenomena. The tunability of the high-field MIR-THz sources of DALI provides an ideal tool for driving these types of non-equilibrium dynamics in condensed matter systems through resonant excitation of the relevant lattice modes. A commercial keV-UED system can provide the performance required for condensed matter samples, but R&D is also currently underway to investigate the ELBE SRF gun to provide higher energy electrons for MeV-UED. The ELBE SRF gun would extend the UED measurements to gas-phase and liquid-phase systems where the larger sample volume requires fully relativistic electrons to minimize the velocity mismatch between the electrons and the photon pulse. The ELBE SRF gun would also provide the unique capability of MeV-UED at high repetition rates, thus delivering unprecedented signal-to-noise ratios in the study of dilute gas-phase and liquid-phase samples. An MeV-UED instrument based on the ELBE SRF gun would create entirely new possibilities for tracking the structural dynamics in biological and chemical systems prepared or functionalized using the DALI MIR-THz sources.

3.2 Time-resolved ARPES

The combination of high-field THz excitation and tr-ARPES probing (user station U4) will enable groundbreaking experiments on THz-induced phenomena at surfaces and molecular-solid interfaces, covering a broad scope of scientific challenges and thus greatly expanding the scientific capabilities of the DALI facility.

As explained above, the main advantage of THz pumping, compared to the traditionally used optical excitation in the near-infrared or visible spectral range in a tr-ARPES experiment, is that it

allows one to *directly* excite the specific low-energy fundamental modes, such as lattice vibrations, magnons or free carriers, while avoiding parasitic higher-energy excitations of the electronic system. The direct access to the electronic band structure $E(\mathbf{k})$ of a THz-driven solid offered by tr-ARPES enables an unprecedented view on the dynamics of emergent phenomena in complex solids or molecular-solid interfaces. The THz pump – tr-ARPES probe experimental station (see Figure 15) will allow the investigation of not yet fully understood phenomena, such as charge order and high- T_C superconductivity, or surface chemistry and catalysis, which are examples of scientific questions with a potentially enormous technological impact on our society.

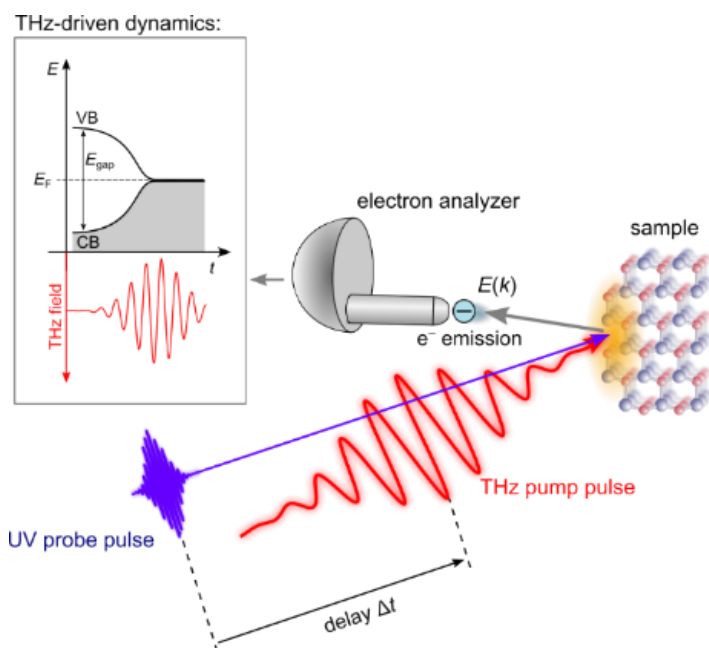


Figure 15: Scheme of a (multicycle) THz pump – tr-ARPES probe experiment.

A first THz pump pulse drives the sample into a non-equilibrium state, which is probed by a second time-delayed UV light pulse that causes photoemission of electrons. The electron analyzer shows a direct image of the band dispersion $E(k_{||})$. The inset shows a hypothetical THz-driven insulator–metal transition, made evident by the closing of the gap around the Fermi level E_F .

DALI is the ideal facility for realizing this project. It offers high-field THz pump pulses at worldwide unique high repetition rates (>100 kHz), which exceed that of any typical high-field THz laser-based source by about two orders of magnitude. This results in a superior dynamic range in experiments, enabling an unprecedented reduction of the THz – tr-ARPES measurement time to below 1 hour, which is a typical surface degradation time for most systems. A THz – tr-ARPES experimental station will thus offer the academic community in Germany and worldwide the possibility to perform THz – tr-ARPES measurements on a large variety of material classes for the first time. The unique quasi-monochromaticity and frequency tunability of the DALI THz sources in the range 0.1 – 30 THz is furthermore ideally suited to drive specific low-energy excitations in matter selectively, e.g. into an excited spin but electronic ground state. In this way, it will be possible to e.g. isolate the signatures of THz-driven lattice or spin mode nonlinearities (i.e. clearly resolved higher harmonics of the pump THz field) in the response of the ARPES-probed electronic structure of materials. Establishing the proposed THz pump – tr-ARPES experimental station and eventually making it available to the broad user community requires a number of technological and scientific challenges to be tackled. A new station is currently under construction at the TELBE THz source, which will serve as a test facility to explore and solve these challenges. Most importantly, the strong interaction of nascent photoelectrons with the THz field (THz streaking) needs to be understood and implemented into the experimental analysis. Furthermore, solving the intricacies of generating sufficiently high THz fields at a precise position on a sample under ultrahigh vacuum (UHV) conditions will be a major step in the first phase of the THz-ARPES project and is of scientific interest on its own. As mentioned above, first

pioneering experiments using a low-repetition-rate light source at moderate THz fields have recently shown the viability of the THz pump – tr-ARPES method and potential ways to overcome detrimental effects of THz streaking.^{16,117}

3.3 Liquid jet

The selective non-thermal THz excitation of low-energy degrees of freedom offers novel strategies to explore elementary processes in materials that are in their electronic and/or vibronic ground state. While these types of experiments are already routinely performed on solids, setups for chemical and particularly life science applications are still in their infancy. Here, a liquid-jet setup, which is currently being developed and established at TELBE, will enable pump–probe experiments that make use of the high repetition rate and pulse-resolved data acquisition, resulting in a superior dynamic range compared to table-top THz sources (user station U5). Using a liquid jet as the sample environment has the advantages that i) the issue of average heating of the liquid is mitigated so that even highest pulse energies can be used, and ii) the jet allows studies of ultrafast (fs) dynamics of long-lived (up to seconds) product phases, as occurring in photoreceptors. Additionally, the absence of window materials circumvents any artifacts from interactions of the THz pulses with the window material.

First preliminary measurements conducted at TELBE demonstrate the feasibility of this method and the important role of a high-field high-repetition-rate THz source: the worldwide first observation of the THz Kerr effect in a liquid jet was made at TELBE (see Figure 16), and further experiments in water using the THz field-induced second-harmonic (TFISH) method yielded strong signals whose origin point at hitherto unrecognized interaction mechanisms.

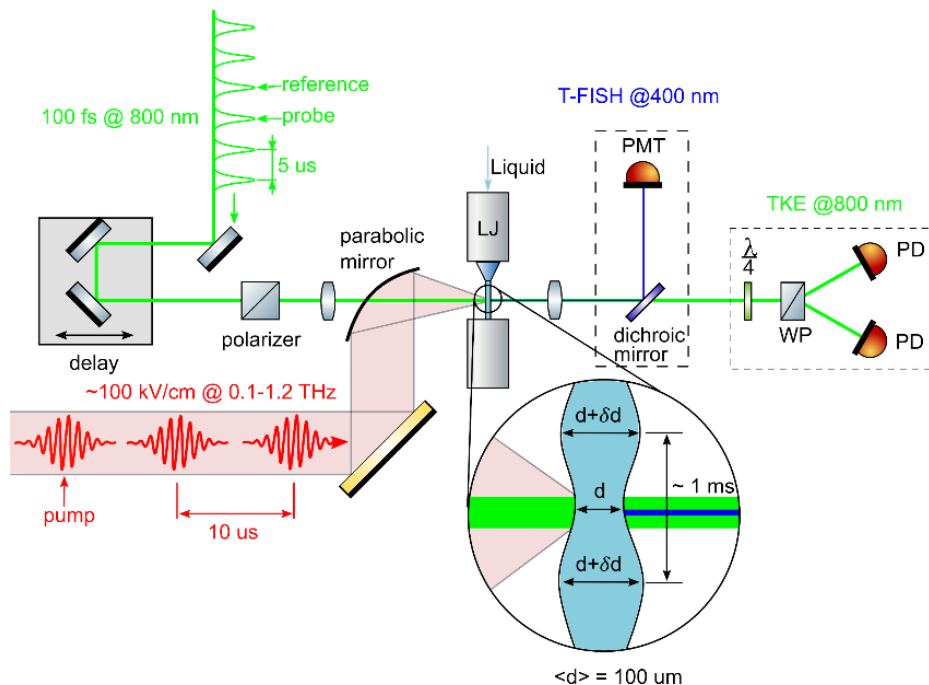


Figure 16: THz pump – THz Kerr effect / TFISH probe setup at TELBE.

THz pulses from the TELBE undulator source (red) are focused into a liquid jet to sub-mm spot sizes. The Kerr rotation or generation of 400 nm harmonics is probed by 100 fs near-infrared laser pulses (green).

¹¹⁷ K. Waltar et al., Opt. Express **26**, 8364 (2018)

3.4 UED system

As an integral part of the new DALI radiation source, we propose to include instrumentation for measuring the ultrafast structural dynamics in matter driven by the high-field pulses of the DALI THz sources (user station U6). The instrumentation will be provided by a commercial keV-UED instrument and/or an MeV-UED instrument based on the ELBE SRF gun. The standard UED measurement is a pump–probe experimental method based on an ultrashort photon pump pulse and a UED probe pulse. In the UED technique, the ultrafast photon pulse drives the sample into an excited, usually non-equilibrium state. The pump pulse may induce chemical, electronic, or structural transitions, and after a specified time delay, a sub-picosecond electron bunch (typically ~100 fs FWHM) is incident upon the sample. The diffraction pattern of the scattered electron bunch contains structural information about the sample with atomic resolution on the time scale of the electron bunch.⁷⁸ By varying the delay of the UED bunch, a time-resolved picture of the dynamics of the nuclear distribution can be produced.

While commercially available UED instruments operating at around 100 keV provide exemplary performance for measurements of condensed matter systems, there are several advantages that can be realized when utilizing MeV energy electrons for UED measurements. The electron sources for MeV-UED systems have lower emittance and higher brightness than keV-UED systems, i.e. an increased coherence length, and thus access to a larger range of reciprocal space.⁷⁸ Ultrarelativistic beams allow an improved time resolution below 100 fs due to suppressed space-charge broadening of the bunches and a much smaller velocity mismatch between the probe electrons and the pump laser pulses in extended gaseous samples.^{82,83} Also, while keV-UED systems are limited to probing the surface states of condensed matter systems, the higher electron beam energy of MeV-UED allows for probing bulk samples without causing damage.⁷⁸ The proposed MeV-UED system based on the ELBE SRF gun can deliver electrons with kinetic energies up to 5 MeV, which is the favored energy range for MeV-UED measurements. Furthermore, with the higher bunch charge made possible with MeV-UED, some measurements are possible in a single shot (critical for nonreversible processes).

Measurements of dilute gas phase samples will benefit significantly from the unique combination of the high repetition rate and the MeV beam energy of the CW SRF gun design proposed for the DALI MeV-UED source, dramatically improving the signal-to-noise ratio and reducing measurement times. Condensed matter samples generally must be limited to rep. rates of a few kHz though due to the low thermal conductivity of the ultrathin samples (< 100 nm). Nonetheless, both the commercial keV-UED and the proposed ELBE SRF gun-based MeV-UED systems and associated photocathode drive lasers will utilize the same underlying high rep. rate and CW RF operation as the DALI accelerator systems, which offers a significant advantage with regard to synchronization of the UED instrument with the MIR-THz photon sources.

One advantage offered by a keV-UED instrument over MeV-UED are the space and radiation shielding requirements. A keV-UED instrument can fit in a relatively compact ~ 2 m x 2 m space on an optical table and requires only modest localized radiation shielding. The higher beam energy and larger footprint of the MeV-UED instrument will necessitate being housed within a small radiation shielded enclosure. The space and radiation shielded needed for an MeV-UED system is incorporated in the planned layout of the radiation enclosure for the DALI accelerator and would not require any additional structure or construction, but will require additional photon transport lines from the DALI MIR-THz sources. Furthermore, since the liquid-He consumption of the ELBE SRF gun-based MeV-UED instrument would be small, the liquid-He requirements can be shared with the He liquefier for the primary superconducting accelerator systems of the proposed DALI facility.

3.5 High-intensity Positron Source (HiPS)

The High-intensity positron Source (HiPS) at the DALI facility will consist of three main parts covering state-of-the-art positron techniques (user stations U7 – U9). The installation of a high-brightness positron source at a superconducting CW accelerator operating at around 1 MHz repetition rate combines a perfectly matched time structure for positron annihilation lifetime experiments (~ 100 ps in bulk metals up to 142 ns for the vacuum decay of ortho-Positronium) with a high average current for high-dynamic-range secondary experiments. Operating HiPS at the 50 MeV, 1 MHz, 1 mA beamline will increase the available secondary positron yield by a factor of 15 compared to the existing EPOS positron source.

The HiPS source will utilize the unique liquid-metal technology that was developed for the electron-to-bremsstrahlung converter of the neutron time-of-flight experimental station¹¹⁸ at the existing ELBE facility. This high-power converter will substantially increase the available positron production yield by allowing higher primary beam intensities and power densities.

In contrast to intense positron sources that employ neutron capture gamma rays for pair production (for example the NEPOMUC source at FRM-II in Garching, Germany), an accelerator-based source imprints the time structure of the driving beam directly onto the secondary source, making this technology favorable for precise annihilation lifetime studies.

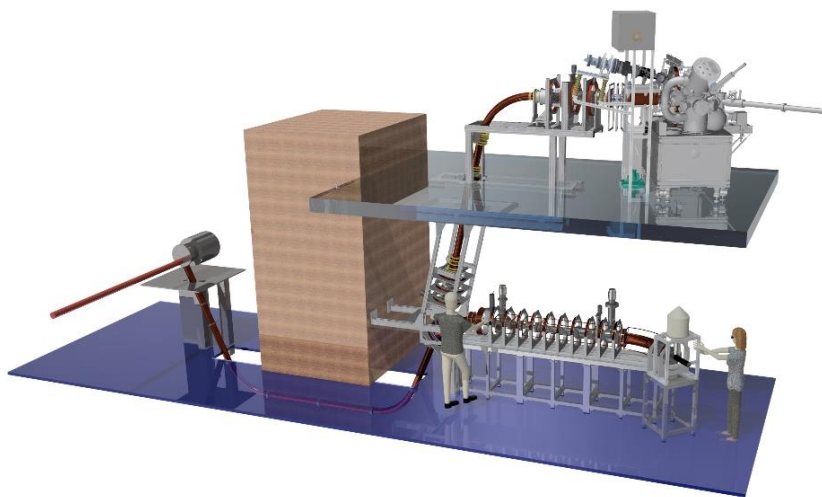


Figure 17: Schematics of the positron annihilation lifetime setups EPOS at ELBE, including the AIDA UHV chamber for in-situ defect characterization on the upper platform.

The three main parts of HiPS are:

1. A modified version of the existing EPOS ultrafast apparatus for in-situ defect analysis (AIDA, see Ref. 119) and for characterization focusing on dynamical effects of defect migration and development by means of laser-induced charge carrier manipulation, high- and low-temperature annealing, and ion irradiation will be installed at the low-energy positron annihilation lifetime beamline HiPS. Based on the experience with the already existing in-situ experimental station, the new AIDA will be a UHV cluster system consisting of a deposition/measurement chamber and a gas reactor chamber. It provides a unique combination of pulsed positron beam with defect states modification techniques, i.e. annealing, ion irradiation, and high-pressure gas loading. Hence, it enables the possibility to

¹¹⁸ E. Altstadt et al., *Ann. Nucl. Energy* **34**, 36–50 (2007)

¹¹⁹ A. Wagner et al., in: *AIP Conf. Proc.*, 2018: p. 040003

study defect kinetics as a function of several variables, e.g. temperature, ion fluence and energy, and gas loading pressure. In addition, materials deposition can be realized using up to four evaporation sources and a 3-magnetron sputtering chamber connected in-situ to the deposition/measurement chamber. Complementary to positron annihilation spectroscopy, sheet resistance measurements can be utilized to probe for defects. External light sources, e.g. LED, monochromatic Xe lamp, or laser radiation, can be used as drivers for transitions of the defect charge state by means of photon excitation of electrons captured at sub-bandgap vacancy states (carrier trapping) or, in the case of laser radiation, for defect modification in the pump–probe fashion.

At DALI's 50 MeV, 1 MHz, 1 mA beamline, the effective positron rate will be around a factor 10 to 100 higher compared to other intense positron sources. As a result, measurement times can be reduced to a sub-minute range. This is essential for the study of fast kinetic processes within complex systems, such as voltage-induced ionic motion in thin films and switchable ferromagnetism,^{120,121} which is of great interest for new types of nanoscale electronic devices. The very high sensitivity of positron annihilation to vacancy-like defects and smallest changes in concentration constitutes an ideal probe for studies of temperature-induced kinetic processes, such as thermally activated vacancy diffusion, which plays an important role in industrial applications, like the recently discovered positive effect of low-temperature annealing of RF cavities on their performance.¹²² Although these kinetic processes have successfully been studied using positrons at the existing EPOS, the sensitivity to kinetic effects has been limited to slower processes that last at least a few minutes (due to the actual positron intensity), whereas the more intense HiPS beamline will provide access to faster processes in the range of seconds, expanding possible user cases.

Furthermore, the beamline characteristics allow for the study of complex systems with wide ranges in positron lifetimes that are not accessible with other techniques, such as tailored nanoporous metallic structures,¹²³ which serve as new types of quantum dot solar cells, (bio-)sensors and materials for hydrogen storage, and materials for quantum information processing.

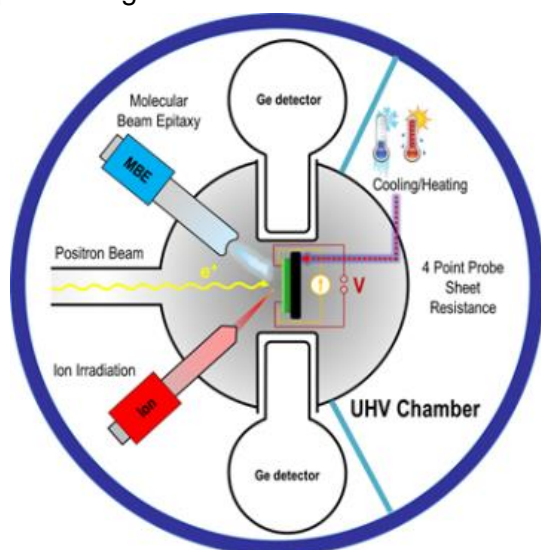


Figure 18: Schematics of the UHV chamber for in-situ defect characterization.

¹²⁰ Z. Tan et al., ACS Nano. **17**, 6973 (2023)

¹²¹ A. Quintana et al., Small **14**, 1704396 (2018)

¹²² A. Grassellino et al., "Accelerating fields up to 49 MV/m in TESLA-shape superconducting RF niobium cavities via 75C vacuum bake", arXiv:1806.09824 (2018)

¹²³ A. Barranco, A. Borrás, A.R. González-Elipé, and A. Palmero, Prog. Mater. Sci. **76**, 59–153 (2016)

2. A high-brightness positron microbeam will serve for the study of nanoscale-patterned surfaces (by 2D/3D scans) as well as for surface investigations of the first monolayer using positron diffraction techniques, such as total-reflection high-energy positron diffraction (TRHEPD).

In contrast to standard electron diffraction techniques (LEED and RHEED), the diffraction pattern obtained by positron diffraction depends only on the atoms on the topmost surface (since the surface is repulsive to positrons). This unique feature of showing sensitivity to the top surface layer gives new insights into state-of-the-art 2D materials such as graphene or single metal layers. Furthermore, since TRHEPD is based on the self-interference of an elastically scattered positron, just as the other diffraction techniques, it is very sensitive not only to the positions of the atoms but also to the species of atoms.^{124,125} Realizing positron diffraction at the high-intensity DALI source will result in improved signal-to-noise ratio in the obtained diffraction patterns due to the intensified beam, which makes it possible to observe clearer patterns within much shorter measurement times on the order of hours or below. In that case, even kinetic surface processes such as the arrangement of atoms or molecules at surfaces can be studied, which is of utmost importance for the design of new types of sensors and membranes.

Combining the positron diffraction facility with the planned tr-ARPES spectrometer using THz radiation, DALI will become a worldwide unique user facility for state-of-the-art surface studies.

3. A versatile open-beam port, like at the intense positron source FRM-II in Garching, is of great interest for users with dedicated own experimental setups (e.g. for in-situ hydrogen loading during a measurement¹²⁶). Thanks to the high intensity of the HiPS facility and the unique features of the pulsed beam, coincidence measurements of the positron lifetime and of the time-resolved momentum distributions of positron–electron annihilation photons (referred to as positron age–momentum correlation, AMOC) can be realized in minutes instead of hours. These measurements are of great interest for probing the elemental environment around the free volume in polymers in relation to ionic diffusion through a particular polymer chain, for highly selective gas separation by finely controlled structures, etc.¹²⁷

3.6 Direct electron beams

The existing ELBE facility serves a broad user community with a wide range of applications employing the direct electron beam for detector developments,¹²⁸ radiation biology,¹²⁹ materials research,¹³⁰ and radiation hardness investigations.¹³¹ The successful implementation of a fast beam kicker at ELBE allows high-resolution timing experiments to be performed with reduced repetition rates in a parasitic mode of operation for energy-dispersive secondary neutron experiments and high-energy bremsstrahlung production. Given further requests from internal and external users, a direct electron beamline and/or secondary beam source could be

¹²⁴ T. Hyodo et al., *J. Phys.: Conf. Ser.* **791**, 012003 (2017)

¹²⁵ Y. Fukaya et al., *J. Phys. D: Appl. Phys.* **52**, 013002 (2019)

¹²⁶ M. O. Liedke et al., *J. Appl. Phys.* **117**, 163908 (2015)

¹²⁷ K. Sato et al., *Macromolecules* **42**, 4853–4857 (2009)

¹²⁸ Z. Liu, et al., *Nucl. Instrum. Methods Phys. Res. A* **959**, 163483 (2020)

¹²⁹ L. Laschinsky et al., *Radiat. Environ. Biophys.* **55**, 381 (2016)

¹³⁰ J. Ji et al., *Sci. Rep.* **6**, 31238 (2016)

¹³¹ J. C. Costa et al., *IEEE J. Electron. Dev. Soc.* **7**, 1182 (2019)

established at the new DALI facility close to the beam dump of the 50 MeV, 10 MHz accelerator driving the optical ring resonator.

3.7 Central computing infrastructure and data management

The computing and data management infrastructure of the large-scale research institution DALI must take into account the following main requirements:

- a central computing infrastructure for simulation, data transfer, data processing/analysis and long-term archiving of primary, secondary and publication data,
- seamless interfaces for the pre-processing and transfer of measurement and control data,
- infrastructure and digital workflows for a complete FAIR digital data lifecycle, consisting of planning, simulation, scheduling and execution of experiments from user registration to publication of results,
- policies and technical solutions making sure that the research is embedded in the international research landscape and the criteria of modern open science are met,
- concepts and measures to ensure sustainable and effective long-term operation of the facility.

The HZDR is in an excellent position with regard to the computing infrastructure, as a new data center will go into operation in Dresden-Rossendorf in 2024, for which important requirements for the future operation of the DALI were already taken into account. The results of numerous projects with HZDR's national and international partners are incorporated into the planning and design of DALI.

The design concept for implementing the aforementioned main requirements is presented in the following sections.

3.7.1 Central computing infrastructure

The starting point for designing the central computing infrastructure relies on the number of experiments, the data volume, the data rates and the requirements for processing and storing the data. For the planning, the experience gained at the ELBE Facility, especially at the FELBE and TELBE experiments, is essential.

The new facility DALI will support the simultaneous operation of both THz and Positron experiments. As before at ELBE, DALI will be operated in shifts with 12h per shift resulting in a number of approximately 375 shifts per year. A portion of the shifts will be needed for machine development and settings preparation. Given the novelty of the THz sources planned for DALI, additional shifts are also needed for accelerator-only R&D to investigate the new methods for THz production and improve performance. This reduces the available user shifts to ~ 280 per year. We consider running THz and positron experiments simultaneously for 50% of the user shifts. It will also be possible to run two THz sources at once (possibly even 3 THz sources at once), but this will require scheduling user shifts with beam parameter requirements that are compatible for running simultaneously. As an initial estimation, 25% of THz user shifts could be compatible with running two sources simultaneously.

By far the highest data rates for the current TELBE beamline are generated by pulse-resolved measurements, which typically generate several GB of data per minute. Pulse-resolved measurements will also be relevant for DALI, and the higher pulse repetition rate here can mean up to a factor of 10 compared to TELBE data rates. For the Positron experiments an increase of

up to a factor of 100 above current pELBE statistics is forecasted, which accounts for the transition from static to time-resolved measurements.

Table 4: Forecast of DALI data volumes and data bandwidth

DALI Parameter	Forecasted values	Resulting Requirement	Data Center Requirement
User shifts	280 / a		
THz Experiments (6-8 end stations)	260 / a		2,5 PB / a
Raw Data Volume / shift	1 TB	260 TB / a	
Derived Data Volume / shift	3 TB	780 TB / a	
Control Data / shift	100k variables + 24k error codes at 1 kHz	1,5 PB / a	
Positron Experiments (1-2 end stations)	210 / a		
Raw Data Volume / shift	0,1 TB	26 TB / a	1,6 PB / a
Derived Data Volume / shift	0,3 TB	78 TB / a	
Control Data / shift	100k variables + 24k error codes at 1 kHz	1,5 PB / a	
Bandwidth to Data Center	max. 3 THz + 1 Positron experim. simultaneously	100 Gb / s	100 Gb / s
Archiving			
Experiments Data 10 a			41 PB / 10 a
Publication Data >10 a (RODARE Repository)	150 published data sets / a	200 TB / a	2 PB / 10 a (redundant)

The following numbers should represent a rough estimate for the number of user shifts/year in the “normal” first phase of DALI operations.

The above figures can be used to estimate the data center and network infrastructure requirements for DALI. It should be assumed that the requirements will continue to increase due to technical developments, including higher resolutions and shorter repetition rates. In addition, it is very important that the infrastructure for data storage has the highest availability and that there are secure access options for external users as well.

The HZDR is currently building a new, modern data center, which will go into operation in early 2024. Requirements from DALI have already been incorporated into the planning of this data center, so that the capacity and rack space, energy, cooling capacity and high throughput network can be provided locally at the site. By operating the existing data center as a backup facility, on-demand availability as well as the long-term and sustainable provision of data is securely guaranteed. High bandwidth fiber links to the central data storage facilities will be provided for each end station.

In addition to memory capacity and network throughput, significant high performance computing capacity is also required for:

- the simulation of the experiments,
- the processing and analysis of the raw data,
- fast feedback loops to analyze the real-time data against expected values,

- allocation and analysis of control data for monitoring and optimal operation of the machines.

For more than 20 years, HZDR has been operating HPC clusters that can be sized to meet the aforementioned requirements. Extensive experience has existed for many years with the use of accelerators, such as GPU and FPGA. These enable a particularly energy- and resource-efficient operation of the DALI IT infrastructure.



Figure 19: *The new HZDR Data Center*

3.7.2 DALI measurement and control data

DALI will produce a gigantic amount of data, both for the monitoring and control of the machine itself, and by the detectors of the user experiments. Real-time preprocessing directly on the experiment, combined with intelligent reduction and compression, enables DALI to operate in a resource-efficient manner and ensures consistent linkage of the machine data with the experiment data. This is essential to ensure provenance and traceability of the data.

The bandwidth currently implemented for TELBE is sufficient and is ultimately limited by the write speed to the central data storage rather than the data transfer speed. Continuing development of FPGA-based data processing will enable more local real-time data processing, which will also keep the data bandwidth requirements from growing too fast. This development has already been started for the ELBE facility.

The frequency for archiving of signals depends on the signal. Some signals (e.g. BPM, BAM, etc.) will require archiving at rates above a kHz, while some signals (e.g. vacuum, magnets, etc.) will require slower archiving rates of a Hz or an even lower rate. The current process to archive these signals can be improved (e.g., every value is saved, rather than only saving values when a change happened, combined with the use of dedicated time series databases), to reduce the data archiving requirements in a DALI implementation. More detailed descriptions of the

requirements for LLRF feedback signal analysis and archiving is described in the corresponding chapter.

3.7.3 Experiment planning, simulation, scheduling and execution

Each experiment starts with the users' request, which is evaluated, selected and planned accordingly. At HZDR, the software GATE, originally developed at Helmholtz-Zentrum Berlin (HZB) for BESSY, has proven itself for this purpose. It is used for ELBE, but also for the Ion Beam Center (IBC). For the IBC, the software was also further adapted for rolling beam time allocation to better serve industry users. This feature also opens up new opportunities for DALI to better serve customers from industry, as experience has shown that they need faster access to experiments.

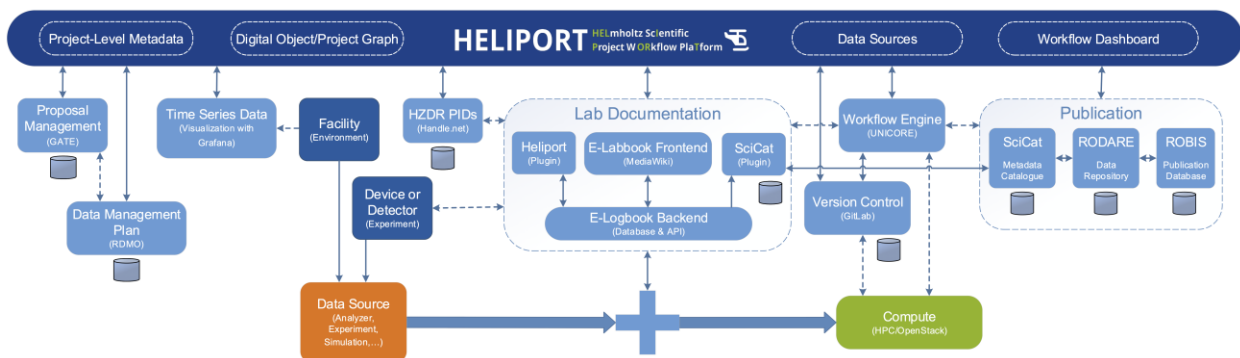


Figure 20: Heliport scheme including available applications, services as well as data sets for a specific experiment (each resource or digital object has a unique identifier).

The system GATE accompanies the user through the course of an experiment from the application to the publication of the results. As a project of the Helmholtz Metadata Platform, the HELIPORT software was developed at the HZDR together with partners (e.g. FZJ, HI Jena, GFZ). This software makes it possible to link the data and metadata of all steps of the experiment's lifecycle, to assign them with unique identifiers (see Figure 20) and to publish the resulting data sets (e.g. on RODARE). In addition, it is possible to register analysis workflows and thus, together with the software used, make them visible, traceable and reproducible for all participants in an experiment. For the DALI data management, appropriate structures, tools and an access rights management will be created to ensure that all data are treated according to FAIR principles.

After completion of the experiment, the results are published, both the scientific publication and the associated data and software. With the components ROBIS (scientific publication), RODARE (data publication) and Helmholtz Codebase (software publication), HZDR has already developed the necessary infrastructures to provide the results with unique identifiers (DOI). Of course, users can also publish their results in other international or discipline specific repositories.

3.7.4 Open science and European partnerships

DALI, the new large-scale European research facility, will be developed according to the latest principles of open science. Like ELBE, DALI will be an important player in the “League of European Accelerator-based Photon Sources” (LEAPS) and LaserLab Europe. For many years, joint solutions for the management of data, users and software have been developed within LEAPS and the European Open Science Cloud (EOSC). The HZDR was and is actively engaged in developing the EU projects PANOSC, ExPaNDS, LEAPS-INNOV, EVERSE.

Within these projects, policies and technical solutions were developed that will be used for DALI. These include, among others, the PANOSC Data Policy Framework, LEAPS data strategy,¹³² the Virtual Infrastructure for Scientific Analysis (VISA) and the PAN Training and e-Learning platform, hosted at the HZDR.

On the national level the HZDR is engaged at the National Research Data Infrastructure Germany (NFDI). It is a member of the consortium DAPHNE4NFDI (Data from Photon and Neutron Experiments), which establishes an open and FAIR infrastructure for data management at facilities for research with photons and neutrons.

For the Helmholtz Association, the platform Helmholtz federated IT Services - HIFIS was developed, which provides Helmholtz researchers and partners with cloud services and software services that support collaboration and scientific workflows. The HZDR is driving this platform as one of the leading centers. It will enable DALI users and scientists to carry out all planning, communication, preparation and follow-up of the projects using the state-of-the-art technology. In addition HZDR participates actively in the entire incubator initiative.

3.7.5 Sustainable and secure long-term operation

Particular attention must be paid to ensuring that all components of DALI are developed in a sustainable manner, including the computing and data management infrastructure.

This concerns in particular:

- an energy- and resource efficient operation,
- provision of automated processes to ensure quality and reduce manual effort,
- uninterrupted research with comprehensive monitoring and appropriate support structures,
- ensuring security especially against cyber attacks.

A new local data center is available for operating the computing infrastructures, which was built according to the latest energy efficiency requirements (see Section 3.7.1). In addition, energy-saving accelerators (GPU, FPGA) and optimized methods and procedures, e.g. for compression and AI-supported evaluation of the data, will be applied for DALI. This is also a central focus for continuous innovation and optimization of all components. In addition, the planned mail-in and assisted remote experiments will help to reduce the carbon footprint caused by travel requirements. In addition we expect this to have also a high attractiveness to non-expert users and users from industry, resulting in lowered access barriers and accelerated innovation cycles.

The manual cleaning and processing of the huge amounts of data from DALI is very time-consuming and should be automated as far as possible. The workflow tools for this will be implemented primarily by the HELIPOINT project, which is described in Section 3.7.3. This guarantees both the quality and the reproducibility of the processes.

¹³² A. Götz, E. le Gall, U. Konrad et al., Eur. Phys. J. Plus **138**, 617 (2023)

With a sophisticated surveillance system, faults in individual components or workflows can be detected early in order to detect defects and minimize downtime. With more than 100,000 readings, this is a special challenge that can only be mastered with the state-of-the-art methods and digital solutions. For this purpose, new methods of artificial intelligence will be used, the development of which has already begun.

Cyber attacks are a permanent threat to all types of digital infrastructures these days. The necessary resilience against these threats is essential for the operation of a large device and must be taken into account in the design right from the start. Since this threat already exists today, the Helmholtz Association's ROCK-IT (Remote, Operando Controlled, Knowledge-driven, IT-based) project was recently launched with a time line of 2023 till end of 2025. The ROCK-IT core partners are DESY, HZB, HZDR, and KIT, together with key users from science and industry. The objectives of the dedicated work package of ROCK-IT are:

- secure network and data transfer
- identity management and remote access
- IT security operating concept

The solutions will be implemented and tested at a demonstrator facility and will be available for integration into the DALI project. The implementation of all low energy consuming measures will be closely discussed with best practiced facilities such as KARA¹³³ at KIT.

¹³³ https://www.kit.edu/kit/english/pi_2022_072_designing-large-accelerators-for-energy-efficiency-and-sustainability.php

4 Machine Design

4.1 Physics concept

4.1.1 Machine overview and main beam parameters

The scientific case outlined above asks for powerful radiation sources for a large span of radiation wavelengths and with a variety of important parameters. This section describes the machine design developed to fulfill this need. The radiation frequencies range from 0.1 to 30 THz covering 10 μm to 3mm in wavelength. The challenge consists in providing the required combination of high pulse energy and spectral bandwidth/brightness, variable repetition rate, and wavelength tunability for all of these frequencies. There is no single source able to cover the complete range of wavelengths and parameters. The following Figure 21 should serve as an overview of the design to be described now.

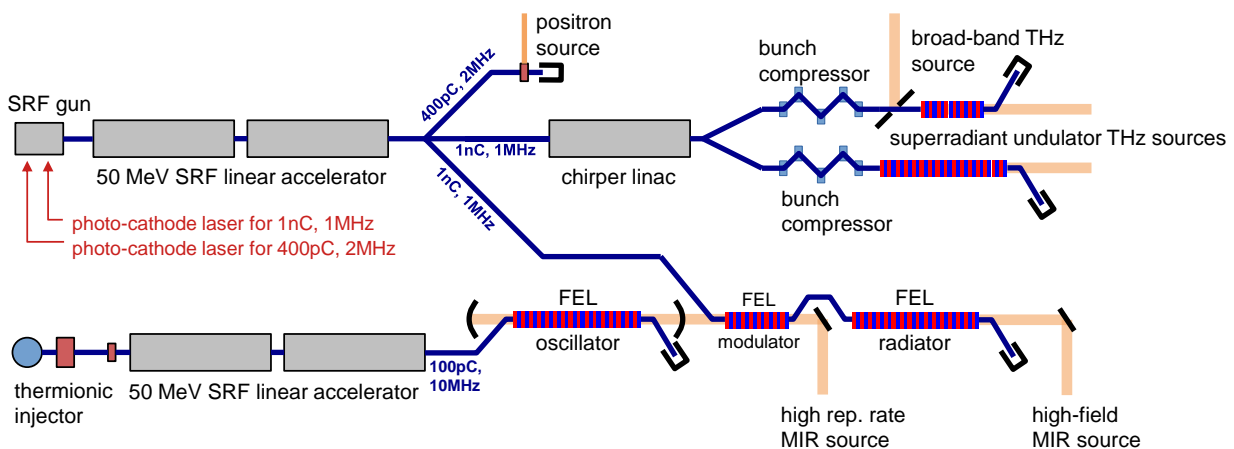


Figure 21: Schematic overview of the accelerators and secondary sources.

All radiation sources will be driven by CW superconducting linear accelerators. This is due to the fact that many experiments benefit from sources operating at a high repetition rate. Also, the stability of the machine is improved by the capability of running diagnostics and feedback loops continuously. Most experiments require high radiation fields and pulse energies but many targets cannot handle extremely high average powers. Therefore, we attempt to provide a flexible timing of the radiation pulses spanning the complete range from single shots on demand up to 1 MHz of continuous repetition. Radiation pulse energies and powers for the coherent photon sources scales by the square of the driving charge, so, we will provide a high bunch charge electron beam to yield the maximum output. The limit is set by the present technology of the electron source which is able to deliver about 1nC of charge at the required repetition rates with sufficient beam quality. At the maximum repetition rate of 1 MHz this yields a beam current of 1 mA, which at the maximum beam energy of 50 MeV results in a maximum beam power of 50 kW.

For long radiation wavelengths it is possible to just compress the complete electron bunch to a limit where it emits fully coherent radiation in either of two undulators with different numbers of periods, selected according to user requirements concerning spectral bandwidth. This mode of radiation production will be utilized for the THz sources. For wavelengths shorter than approximately 100 μm this is no longer possible and a different scheme needs to be applied. To achieve superradiant emission at these shorter wavelengths, we must provide a seed which is then modulated onto the electron beam and amplified such that finally fully coherent radiation is

produced in an undulator (radiator) from an electron beam sliced into micro-bunches with a spacing equal to the desired wavelength.

To generate the necessary seed radiation we will use a free-electron laser oscillator that will be driven by a separate linac. The bunch repetition rate of the beam generated by this linac has to match the round-trip frequency of the optical resonator of the FEL which will be about 10 MHz. With an average beam current of 1 mA the bunch charge in this linac will reach 100 pC which can easily drive an oscillator FEL with sufficient gain. With a maximum beam energy of 50 MeV, the shortest radiation wavelength of 10 μm can be reached.

A positron source similar to the one presently operated at ELBE will also be part of the DALI facility. It will be driven by the high-charge linac but with a slightly different set of parameters. Bunch charges up to 400 pC at 2 MHz repetition rate will provide a much higher average positron flux than the pELBE source.

4.1.2 Machine operation, sources and timing

In order to deliver as much user beam time as possible it should be possible to simultaneously operate essentially all of the radiation and particle sources. While the FEL oscillator for the mid-IR is obviously independent from the other end-stations all other sources are driven by the high-charge linac and need special means of beam distribution. It is envisaged to run interleaved bunch trains tailored for each source through that linac and distribute those using kickers and septum magnets for separation. It needs to be mentioned, though, that the beam energy is linked across the whole facility. It is not possible to accelerate interleaved bunch trains to different energies in the same linac. When running the modulator/radiator IR source also both linacs have to operate at the same beam energy.

The total amount of beam current that can be accelerated is limited by the capabilities of the linac, its RF couplers and RF power amplifiers. The high charge linac will be designed for a maximum beam current of 1 mA yielding a beam power of 50 kW at maximum energy of 50 MeV. The positron source is the most power-hungry target requiring 400pC of bunch charge at 2 MHz repetition rate, thus, already consuming 80% of the available beam current. While it is operating at full power 1 nC bunches with a repetition rate of 100 kHz would be available to each of the THz and mid-IR sources. Higher repetition rates up to 1 MHz at the THz/IR sources can only be delivered by cutting down the average beam current to the other end-stations.

To separate the bunches out of the beam for the positron source we plan on using a transversely deflecting resonant kicker cavity operating at 2 MHz detuning from an integer sub-harmonic of the accelerator frequency. In this kicker all bunches with 2 MHz repetition rate receive the same deflection, while those bunches intended for the THz/IR sources are interleaved in the opposite phase and get separated. Both bunch trains need different charges – 400 pC for the positron source and 1 nC for the THz/IR sources. As it is difficult to modulate the photo-cathode laser of the gun on a pulse-to-pulse basis we will use two independent lasers irradiating the same photo-cathode to generate the two interleaved bunch trains from the SRF gun. A high signal-to-noise ratio in the positron decay experiments requires a suppression of electrons emitted as dark current from the SRF gun at times when no laser pulse is present. This can be achieved with a kicker right after the gun dumping all unwanted beams or with a chopper in the positron beam path.

Parallel operation of several possibly independent sources poses significant challenges to the timing/synchronization system as well the machine protection (interlock) system. In order to guarantee maximum independence of all users, all beam options need to be ramped up and when necessary switched off (interlocked) without disrupting the other beam lines. Special care has to

be taken to cope with beam-beam dependencies introduced by varying RF loading of the linacs. Sophisticated feedback, ramp and tuning algorithms need to be developed to satisfy this need. Also, the beam diagnostics elements operated in beam lines with more than one beam present have to be designed to distinguish between the different parallel beams.

The synchronization of both electron beam sources is of particular importance for the IR sources. Ideally, one wants to supply the user with a carrier-envelope stable optical pulse phase-locked to the master oscillator. The envelope of the out-coupled pulse in the radiator is given by the bunch form of the high-charge beam. The radiation phase, however, is defined by the oscillator cavity which will therefore need an active stabilization of the cavity length. Still, the oscillator cavity can be detuned by some integer wavelengths which increases the gain and improves the stability of the oscillator because the optical pulse from the oscillator will be longer than the out-coupling electron pulse. A stable temporal overlap is needed to ensure a stable modulation seeding the radiator beam line.

4.1.3 Electron gun beam dynamics

The operation of the DALI THz facility requires a 1 nC electron beam with a repetition rate of 0.1-1 MHz and high beam brightness. Only photo-injectors can be considered for these very high charges and peak currents. Few options exist and are reviewed with respect to technical questions in Section 4.2. Here we consider the beam dynamics of the SRF gun only due to its successful service in the existing ELBE facility in user operation.

The low transverse emittance is required to stay below the diffraction limit and maximize the FEL parameter ρ , which leads to a reduction of FEL gain length, an increase of FEL saturation power, and an increase of FEL bandwidth.¹³⁴ A small (slice) energy spread is essential to achieve highest compression in the bunch compressor for the super-radiant radiation source and is also vital for a high efficiency of the FEL process. As the electron beam brightness in the undulators is ultimately limited by the longitudinal and transverse emittance of the electron beam at gun exit, a study of the achievable beam qualities is necessary.

Figure 22 shows the transverse and longitudinal emittance achievable with a 1 nC bunch charge from the HZDR SRF gun when a gun gradient of 30 MV/m is reached. The simulations were

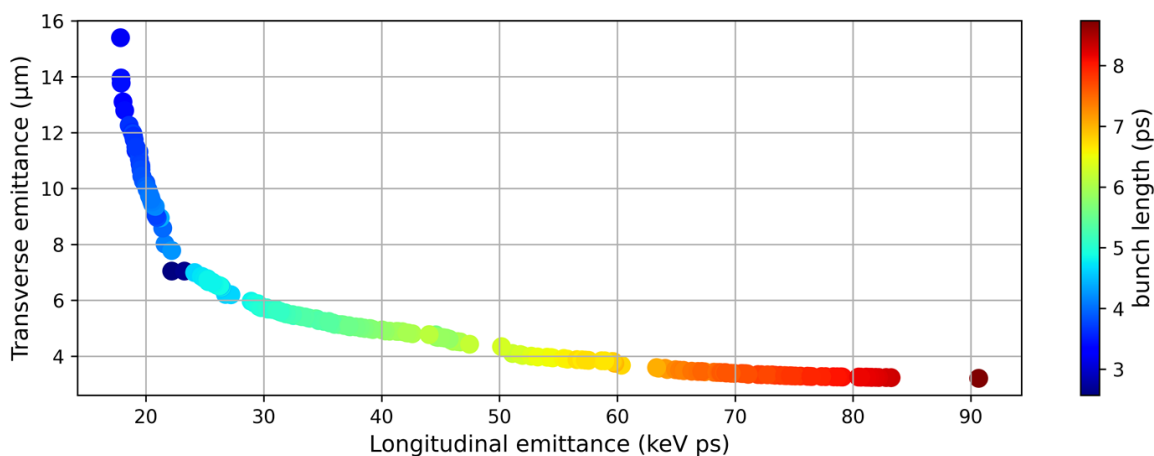


Figure 22: Two-parameter optimization of the SRF gun beam dynamics using ASTRA.

¹³⁴ Z. Huang and K.-J. Kim, Phys. Rev. ST Accel. Beams **10**, 034801 (2007)

carried out in ASTRA¹³⁵ and assumed electron emission from a Cs₂Te cathode with a laser pulse of temporal Gaussian and transverse flattop shape.

The longitudinal and transverse beam emittance are coupled; the transverse emittance for example can be reduced when choosing a smaller laser spot size of the cathode at expense of a larger longitudinal emittance and vice versa. Since the laser pulse dimensions, RF emission phase, and magnetic focusing strength determine the beam qualities they can be used to tune the SRF gun for a particularly low transverse or longitudinal emittance as required for certain demands during user operation. Besides this, a more sophisticated laser system might allow for laser pulse shapes which would further reduce the emittance.

While different alternatives may be considered (see Section 4.2 below), we conclude that the SRF electron gun in operation and under continuous development at ELBE is fully able to deliver the necessary beam properties required by DALI.

4.1.4 Electron beam transport

A magnetic beam transport system will be designed to guide the beam from the electron sources through the accelerators to the different end stations and to ensure optimum beam parameters for their operation. While this sounds straightforward, a number of effects need to be considered in order to preserve the initial quality of the beam and to avoid degradation of critical parameters. While the general design can follow proven principles that have been applied to the ELBE beamlines, the high bunch charge delivered by DALI creates challenges for the electron beam transport and must be considered in more detail.

In general, due to the high charge and short bunch length desired for the DALI beam, space charge interactions within the electron bunch play more significant role than was the case in the ELBE designs. Even small density fluctuations in regions of small beam size and high charge density will lead to intra-beam energy modulations which again can be turned into density modulations in dispersive sections. While this process, when not taken care of, can lead to a micro-bunching instability of the whole beam transport, in the present designs it only leads to some increase of the slice energy spread of the beam which, nevertheless, is a parameter that crucially influences the limits of bunch compression. The process cannot be entirely avoided but will be minimized by a careful design. It is expected that this growth of the energy spread can be controlled to much lower values than those considered as a worst-case scenario in the following estimations of the possible radiation source output.

A process that needs special consideration is the intra-beam interaction mediated by coherent synchrotron radiation in bending sections. DALI utilizes a high-charge beam with short bunch length to use coherent synchrotron radiation as a source but such radiation will also be produced in other places and act on the beam. For all dispersive sections of the DALI beam transport it will be a major design target to minimize the beam degradation (mainly growth of the transverse emittance) of the beam.

Another form of collective interaction within the electron bunch is mediated by wake fields produced by the electron bunch when moving through an environment with varying boundaries. The action of these wake fields onto the beam can distort the time dependent (slice) energy of the beam and, thus, severely influence the bunch compression that relies on eliminating first and second order correlations within the bunch. The mechanical design of the beam line should address the necessity of wake field reduction and simulations must define an upper limit (budget) to the allowed distortions.

¹³⁵ afm Website, <http://www.desy.de/~mpyflo/>

The tools that are needed to study all these collective processes in the DALI beam transport do exist and are widely used already. It will be a subject of the TDR to deliver a complete start-to-end simulation of the beam transport. First simulations of the most critical sections have already been performed and show the feasibility of the proposed design and its ability to reach the required parameters.

4.1.5 High-pulse energy THz source

Bunch compression

For efficient generation of coherent undulator radiation, a bunch length much shorter than the wavelength is required. For generation of 30 THz ($\lambda \approx 10 \mu\text{m}$), a bunch length shorter than 10 fs would be needed. This is not achievable with the present state-of-the-art accelerator technology for bunches with 1 nC charge. For a medium energy machine (<100 MeV) like being discussed here certain limits for the peak current cannot be exceeded. In the present study this limit is assumed as 4 kA which has been found in bunch compressor simulations. Imposing this limit implies that very short bunches can only contain a limited amount of charge. The bunch charge itself is limited by the capabilities of the electron gun which is assumed to 1 nC here. Staying within the peak current limit a 1 nC bunch can be compressed down to 100 fs (r.m.s.) bunch length but not further down.

The longitudinal bunch compression is achieved by first accelerating the beam in a LINAC at an off-crest phase of the RF waveform to introduce a time–energy correlation in the longitudinal phase space. Then the beam is passed through a magnetic beam delivery system (bunch compressor) where the path length depends on the energy. One strongly limiting factor for the bunch compression is the second-order time–energy correlation introduced by the LINAC due to the cosine-like time dependence of the accelerating field. For optimal bunch compression, the second-order time–energy correlation needs to be eliminated.

For this, we intend to utilize a magnetic nonlinear bunch compressor, where the first- and second-order correlations of the phase space can be adjusted independently. Beam dynamics considerations¹³⁶ show that the major limiting factor for longitudinal bunch compression is the uncorrelated (slice) energy spread. Such considerations show that, for instance, when a beam with an initial RMS bunch length of 6 ps is accelerated from 10 MeV to 50 MeV 30 degrees off-crest in a 1.3 GHz LINAC, then for the final bunch length of about 10 fs, a slice energy spread of about 2 keV would be required. Practically, in an accelerator system suitable for an MIR-THz source and for a bunch charge of 1 nC, one should expect the slice energy spread to be almost two orders of magnitude higher. The slice energy spread is determined first by the electron source. Modern electron guns typically generate beams with a slice RMS energy spread of a few keV.¹³⁷ However, the slice energy spread does not stay constant during acceleration and beam transport, and grows due to longitudinal space charge driven micro-bunching instability.¹³⁸ The theory of micro-bunching instability shows that the most influential parameters determining the amount of growth of the slice energy spread are the initial slice energy spread generated by the electron gun, and the peak current.¹³⁹ Application of the 1D linear theory of micro-bunching instability predicts that the average slice energy spread would grow from a few keV to about 50 keV, assuming acceleration from 10 MeV to 50 MeV and a 50 m long system. This growth will limit the bunch compression of the 1 nC bunch at 50 MeV to about 200 fs RMS bunch length. This estimation assumes that 1D linear theory is sufficiently accurate and that the micro-bunching

¹³⁶ P. Emma, Handbook of Accelerator Physics and Engineering, 2nd edition (2005)

¹³⁷ Z. Huang, et al., Proceedings of PAC'2005, Knoxville, USA (2005)

¹³⁸ E. L. Saldin, E. A. Schneidmiller, and M.V. Yurkov, DESY Report No. TESLA-FEL-2003-02, (2003)

¹³⁹ Z. Huang, et al., Phys. Rev. ST Accel. Beams **7**, 074401 (2004)

instability starts from shot noise. In reality, the space charge is 3D and not a 1D effect, and real injector beams can have an initial modulation (bunching factor) larger than the one given by the shot noise. The robustness and applicability of these assumptions must be thoroughly studied during the technical design phase.

Broad-band Sources

Besides the relatively narrowband MIR and THz pulses generated by undulators, single-cycle broadband THz pulses are also required. Such pulses have a dual purpose. When generated by the same electron bunch that is used for undulator radiation generation, the single-cycle pulses are used to time-stamp the undulator radiation pulses and achieve very high temporal resolution.¹⁴⁰ Such pulses are also used as broadband high-field pump beams when sufficiently high pulse energy is achieved. Presently, at ELBE, such pulses are generated via the CDR mechanism, providing few 100 nJ pulse energy. The performance of this source is in good agreement with theoretical predictions.¹⁴¹ Assuming the same high-charge electron beam parameters as used for the coherent undulator radiation estimations, i.e., a bunch charge of 1 nC, an RMS bunch length of 200 fs, and a beam energy of up to 50 MeV, we expect that a CDR source would generate single-cycle pulses with a pulse energy of about 100 μ J. Figure 23a shows the spectral density of such a source calculated for different beam energies, assuming a perfectly conducting radiator with a radius of 50 mm, a central aperture with a radius of 2.5 mm, and radiation collection within a cone with a half-angle of 250 mrad, which is typical for such setups and close to the practical limits. The pulse energies calculated assuming a Gaussian longitudinal bunch distribution and integrating in the range from 0.01 THz to 2.5 THz are shown in Figure 23b for three different RMS bunch lengths. When developing the technical design of the new source, we will consider other mechanisms for single-cycle THz pulse generation. These need to include coherent synchrotron radiation and coherent edge radiation from a single bending magnet, as well as coherent Cherenkov radiation from a dielectrically loaded waveguide. The aim of the new developments here will be to further substantially increase the pulse energy and to develop sources that do not require the beam to pass through a relatively small aperture as is the case with the CDR source.

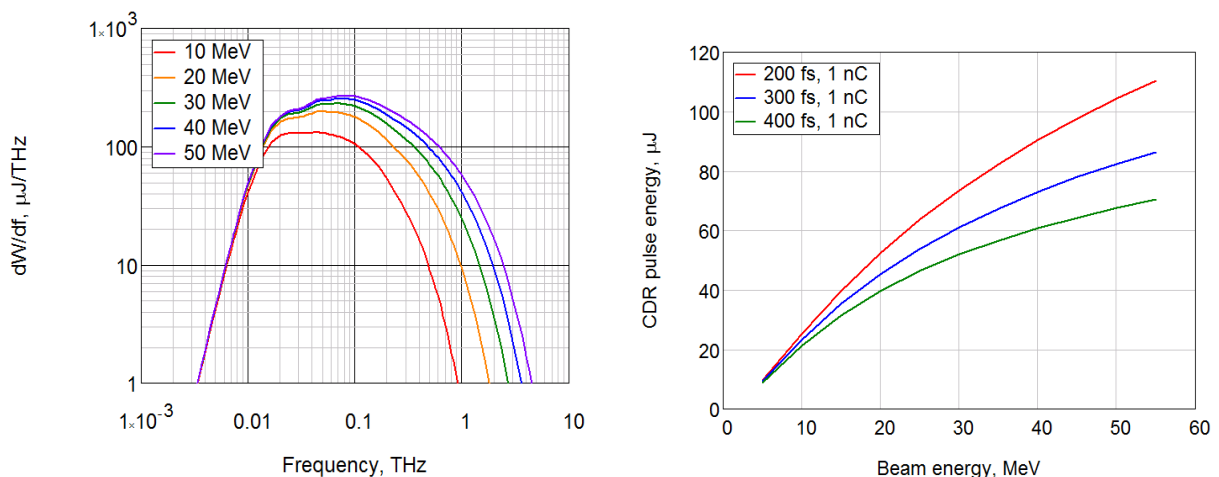


Figure 23: Spectral density (a, left) and pulse energy (b, right) of a single-cycle CDR source.

¹⁴⁰ S. Kovalev et al., Struct. Dyn. **4**, 024301 (2017)

¹⁴¹ S. Casalbuoni et al., Phys. Rev. ST Accel. Beams **12**, 030705 (2009)

Undulator Source Parameters

Resonance Condition: Insertion devices are usually characterized by the K parameter which gives the ratio of the transverse momentum the beam particles acquire on their trajectory to the longitudinal momentum. The maximum deflection angle is K/γ (γ being the relativistic factor).

Usually, a distinction is made between undulators ($K < 1$) and wigglers ($K > 1$) as the radiation properties differ due to interference. Our devices qualify as wigglers in most cases. As we are mostly interested in long radiation wavelengths produced from high beam energies we need large K values to fulfil the resonance condition

$$\lambda = \frac{\lambda_U}{2\gamma^2} \left(1 + \frac{K^2}{2} + \gamma^2 \theta^2 \right) \quad (1)$$

Far-field radiation properties: In the far field the optical beam can be approximated as a Gaussian beam with a Rayleigh range

$$Z_R = L_U / 2\pi \quad (2)$$

($L_U = N_U \lambda_U$ is the length of the undulator). Such a beam is characterized by a (virtual) beam waist of $\sigma_{RMS} = \sqrt{\lambda L_U} / 4\pi$ (or $w_0 = \sqrt{\lambda L_U} / 2\pi$) and an opening angle $\theta_{RMS} = \sqrt{\lambda / L_U}$. For calculation of the power of the usable optical beam we define a central cone containing most of the radiated power.

$$\theta_{cen} = \frac{1}{\gamma^* \sqrt{N_U}} = \sqrt{\frac{2\lambda}{L_U}} \quad (3)$$

One should note that this is twice as large as the diffraction cone and reflects the fact that constructive interference of the wavefronts emitted from the individual undulator periods is limited in emission angle. The quantity $\gamma^* = \gamma / \sqrt{1 + K^2/2}$ appearing in the definition is the relativistic factor of the co-moving average frame of reference of the electron beam inside the undulator.

The spectral distribution of the emitted radiation can be derived from the interference of radiation emitted from the individual undulator periods.¹⁴² The resulting spectral line shape to be observed on the emission axis is obtained as

$$L\left(\frac{N \Delta\omega}{\omega_1}\right) = \left(\frac{\sin^2\left(\frac{\pi N \Delta\omega}{\omega_1}\right)}{N^2 \sin^2\left(\frac{\pi \Delta\omega}{\omega_1}\right)} \right) \quad (4)$$

This function drops to half its maximum value when $N \Delta\omega / \omega_1 \sim 0.5$ and so we can take the bandwidth of the fundamental wavelength as $1/N_U$.

The properties of the radiation fields are illustrated here showing the radiation field of a 1nC charge produced in a wiggler with 8 periods and $K_{RMS} = 2$ at 1 THz observed on a screen in 10 m distance from the wiggler center. The central cone has an opening angle of 16 mrad in this case. The numerical simulation was done using TEUFEL.¹⁴³ Figure 24 shows the spectral power density

¹⁴² J. A. Clarke, The Science and Technology of Undulators and Wigglers (2004).

¹⁴³ U. Lehnert, TEUFEL – THz Emission from Undulators and Free-Electron Lasers,

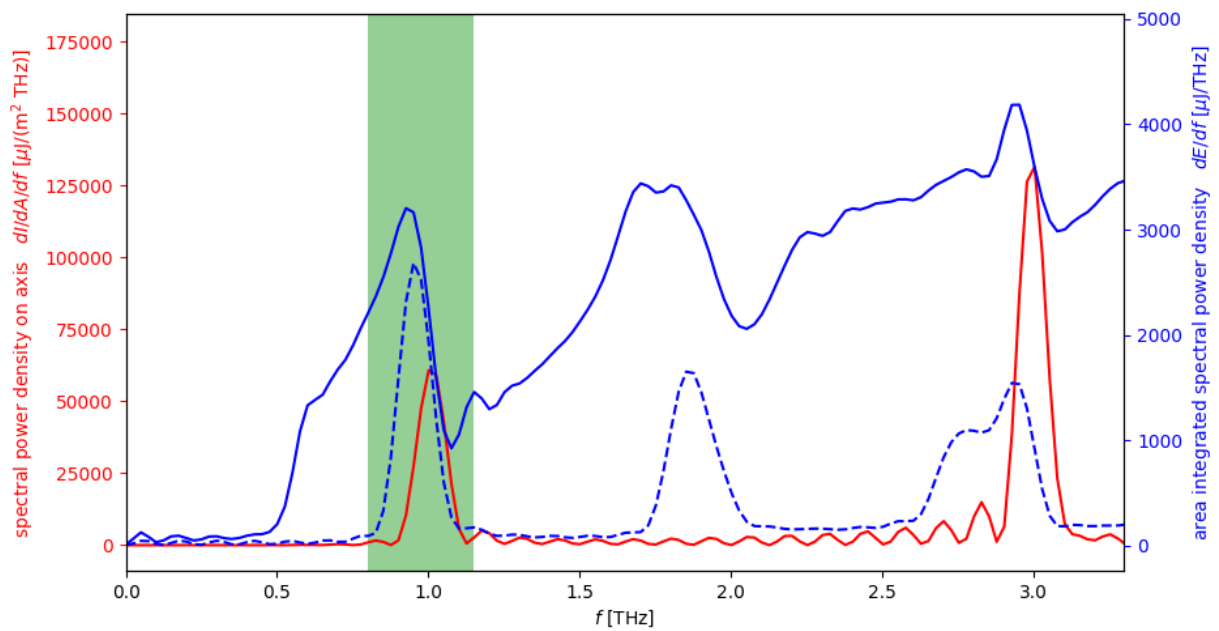


Figure 24: Spectral power density on-axis (red), integrated over the central cone (dashed blue) and integrated over the whole field shown (solid blue).

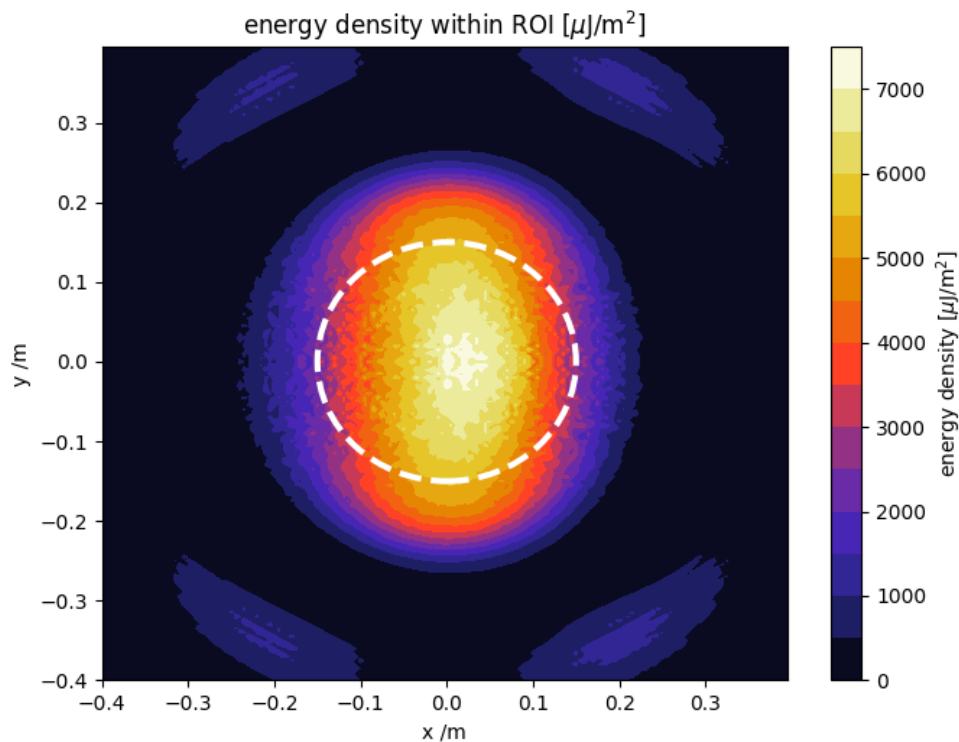


Figure 25: Spectral power density on the screen only considering spectral content within the green shaded range of interest in the shown spectrum. Some far off-axis content of the second harmonic Doppler-shifted into the same frequency is visible in the outer parts of the screen. The white circle depicts the size of the central cone.

on axis and integrated over the screen area. Contributions from higher harmonics are clearly visible, the second (as are all other even harmonics) is suppressed on axis.

In Figure 25 the spatial distribution of the emitted radiation is visualized, the spectrum was limited to the green shaded range of interest shown in the spectrum. The radiation outside the central cone is emitted at lower frequencies than the resonance frequency, as is to be expected from the off-axis behavior of Eq. (1).

Radiation pulse energy: Estimates of the radiation output generated by charged particles inside undulators can be found in various textbooks. A thorough derivation is given by Clarke,¹⁴⁴ an easy-to-follow presentation is given by Attwood.¹⁴⁵ Here we just cite (Clarke p.68) the spectral energy density on axis

$$\left. \frac{d^2W}{d\omega d\Omega} \right|_{\theta=0} = \frac{Q^2 N^2 \gamma^2}{4\pi\epsilon_0 c} L \left(\frac{N\Delta\omega}{\omega_n} \right) \frac{n^2 K^2}{(1 + K^2/2)^2} \left[\mathfrak{S}_{\frac{n-1}{2}}(\xi) - \mathfrak{S}_{\frac{n+1}{2}}(\xi) \right]^2 \quad (5)$$

$$\xi = \frac{n K^2/4}{1 + K^2/2}$$

Often we are interested in the power density of the fundamental emission frequency on axis in which case we have to integrate over the spectrum. The integration then yields for the fundamental frequency

$$\left. \frac{dW}{d\Omega} \right|_{\theta=0} = \frac{Q^2 N \gamma^2}{2\epsilon_0 \lambda} \frac{K^2}{(1 + K^2/2)^2} [\mathfrak{S}_0(\xi) - \mathfrak{S}_1(\xi)]^2 \quad (6)$$

One should notice the scaling of the power density with the design parameters. As can be expected from physics reasoning it scales linearly with the number of undulator periods and quadratically with the charge. Also important is the linear scaling with the frequency of the emitted radiation.

To arrive at the total radiation energy emitted into the central cone one has to integrate over the solid angle. While so far we have computed the radiation of a single point charge only, we now have to extend that description to an extended electron bunch consisting of many particles. This is done by introducing a form factor $F(\lambda)$ describing the longitudinal distribution of the charge compared to the radiation wavelength. This factor approaches unity for a point charge or very short bunch and drops to zero when the bunch length grows to be equal to the wavelength. Alike the bunch charge the square of the form factor enters the equation for the pulse energy.

$$E_{cen} = F^2(\lambda_n) \frac{\pi Q^2}{2\epsilon_0 \lambda_n} B_n(K) \quad (7)$$

$$B_n(K) = \frac{K^2}{1 + K^2/2} [\mathfrak{S}_0(\xi) - \mathfrak{S}_1(\xi)]^2$$

In Eq. (7) all terms depending on the strength of the magnetic field of the undulator are comprised into one term $B_n(K)$. It turns out that this term only differs from unity when the undulator strength K is smaller than 2, so, we can neglect it for coarse estimates. This formula is now rather easy to evaluate and we have done so for a bunch charge of 1nC and assuming bunch compression to reach a form factor of $F^2=0.5$. Figure 26 shows the accessible radiation pulse energy for the THz frequency range of interest. The bunch length (assumed a Gaussian shape) needed to reach

¹⁴⁴ J. A. Clarke, The Science and Technology of Undulators and Wigglers (2004)

¹⁴⁵ D. Attwood, <https://people.eecs.berkeley.edu/~attwood/srms/2007/Intro2007.pdf>

$F^2=0.5$ is shown on the upper scale. For frequencies above one THz this leads to unrealistically short bunch lengths. Experience from high-energy machines show that at our beam energy a peak current of 4 kA cannot be exceeded without serious degradation of the bunch quality. To stay within this limit the bunch charge would have to be reduced when one wants to generate higher frequencies.

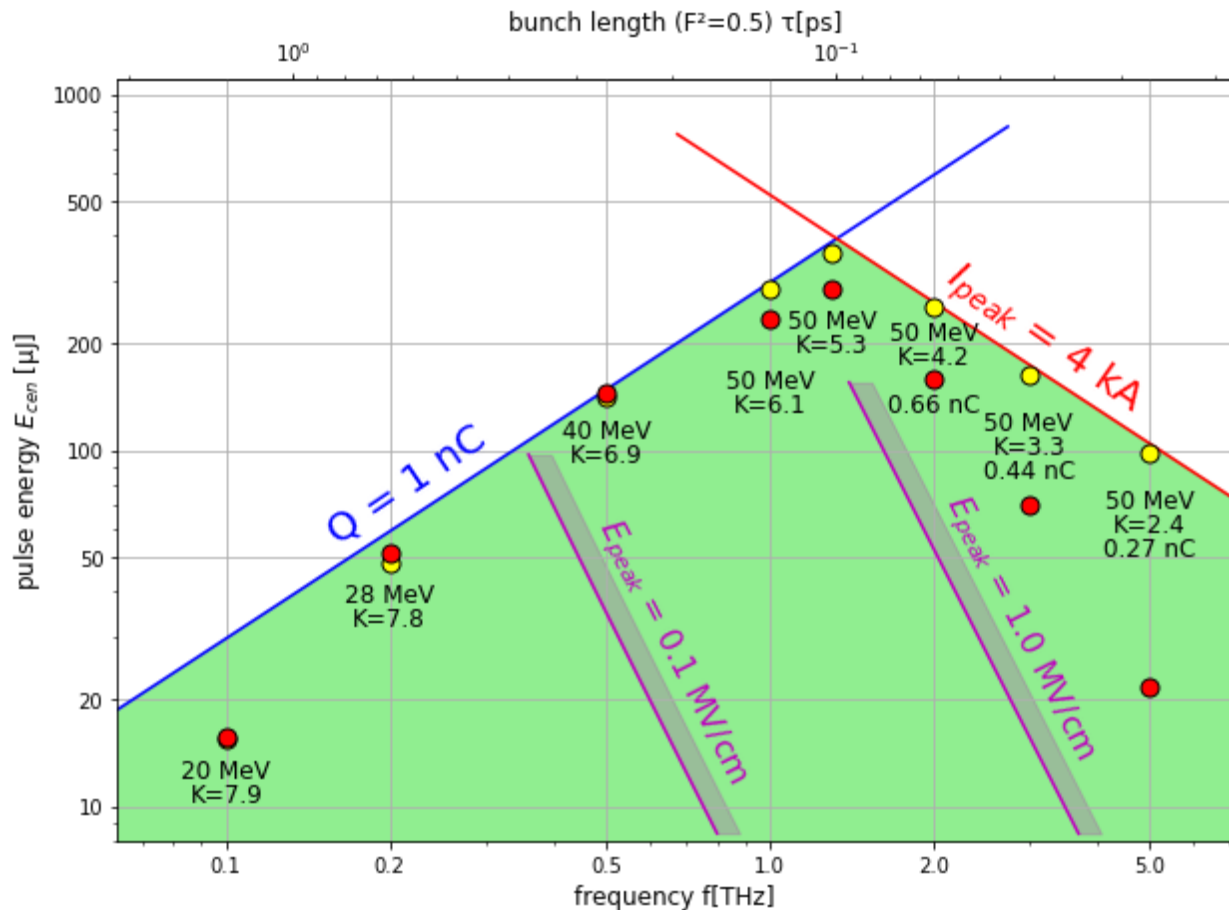


Figure 26: Output pulse energy at the fundamental resonance frequency of a wiggler with 8 periods of 300 mm generated by a Gaussian bunch compressed to a form factor of 0.5.

The validity of that prediction has been verified using the TEUFEL simulation code. The yellow dots in Figure 26 were obtained with an idealized bunch of negligible transverse emittance and energy spread with the bunch length yielding $F^2=0.5$. Obviously, the estimation is in very good agreement with the simulation at all but the very lowest frequencies. The disagreement at 0.1 THz originates from the very large opening angle of the emitted radiation cone while the acceptance angle of the simulation was assumed with a finite value given by the size of the vacuum chamber inside the undulator.

In addition, the effect of realistic beam properties was studied in simulations shown as red dots. The transverse emittance of the electron beam was assumed as $\epsilon_n=5$ mm mrad but this is of minor influence. The major effect comes from the large energy spread of the beam which – given a certain longitudinal emittance – is needed to reach the specified bunch length. The value of the emittance used here was 100 keV ps which is significantly larger than the values obtained in the simulations of the electron source parameters where it is possible to reach 20 keV ps. So, this

simulation presents a worst-case scenario considering substantial degradation of the beam quality during the transport and bunch compression which is not expected to occur in that severity.

Many experiments mostly care about the reached peak field rather than the total pulse energy. The accessible field strength was estimated by simulating the focusing of the radiation pulse with a 2" parabola of 150 mm focal length onto the target. As shown, THz fields above 1 MV/m can be reached for frequencies above 1.5 THz.

4.1.6 High-pulse-energy, high-repetition-rate MIR-THz source

At frequencies higher than 3.0 THz a good longitudinal form factor of the bunch cannot be obtained any more by compressing the full bunch. One way to overcome this limitation is to use a beam that is longitudinally modulated with the periodicity of the desired radiation wavelength. We argue that, given the requirement of a pulse repetition rate between 100 kHz and 1 MHz, the most suitable way to modulate the beam longitudinally on the scale from 10 μm to 250 μm is to employ the mechanisms used in an optical klystron or a laser heater. There, the longitudinal density modulation is obtained via a two-step process. First, the electron beam energy is modulated by co-propagating the electron beam together with an optical beam in an undulator. The mean beam energy, the wavelength of the external optical beam, the undulator period, and its K parameter are arranged so as to satisfy the FEL resonance condition. This leads to a net energy exchange between the external optical mode and the electron beam with the periodicity of the optical mode. In the second step, the energy-modulated beam is passed through a beam transport section with longitudinal dispersion. This results in the modulation of the longitudinal density of the electron beam again with the periodicity of the external optical mode. The detailed description of this process can be found in ¹⁴⁶ and references therein. Here, we only summarize the results and list the most relevant parameters. We also assume the capability to induce the energy modulation amplitude to be three times larger than the slice energy spread. Under such conditions, a bunching factor of ~ 0.5 at the first harmonic can be achieved.

FEL oscillator

An FEL oscillator can easily provide the necessary electric-field amplitude for modulating a high-charge electron beam inside its optical cavity. In this case, the out-coupling from the resonator can be minimized, so that only a very small fraction of the intra-cavity power, necessary for the FEL system monitoring and diagnostics, leaves the optical cavity. The FEL oscillator modeling, which assumes the use of an undulator with a period of 100 mm and 40 periods as well as an

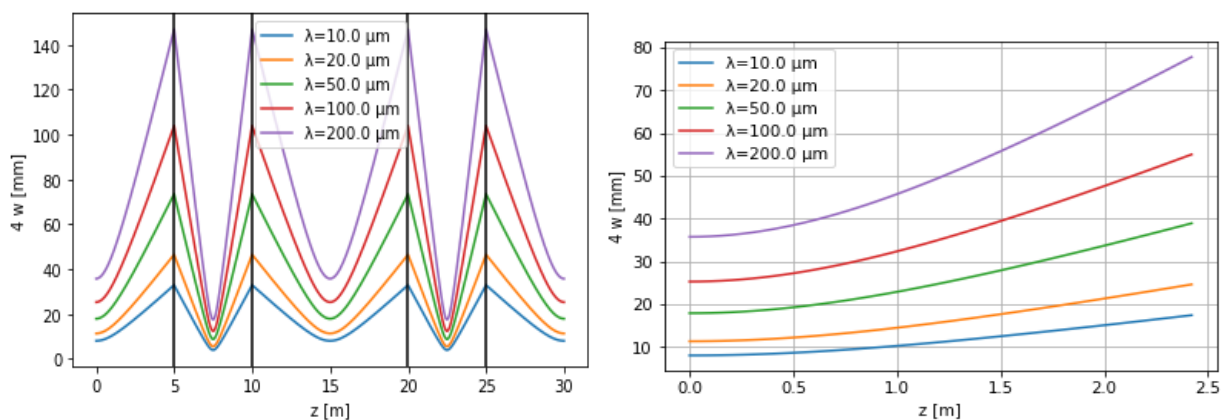


Figure 27: Envelopes of the optical mode in the ring resonator of the oscillator FEL.

¹⁴⁶ L. H. Yu, Phys. Rev. A **4**, 5178-5193 (1991)

electron beam with parameters as presently used at ELBE (bunch charge of 77 pC, RMS pulse length of 0.5 ps, longitudinal emittance of 50 keV ps, transverse normalized emittance in both planes of 10 mm mrad, and Rayleigh length of the optical resonator of 1 m), shows that for any wavelength in the required range, the intra-cavity pulse can provide electric fields at least five times higher than required. As this could result in an unwanted over-bunching we also consider using a smaller out-coupled fraction of the FEL beam to modulate the high-charge electron beam.

For the oscillator we envisage a rectangular optical resonator with a round-trip frequency of 10 MHz. Given the constraints of the vault a 10 m by 5 m size yields a suitable shape. To accommodate the limited cross-section of the beam inside the undulators a stable symmetric design was chosen with a Rayleigh length of $L_R=1.25$ m in the undulator sections and another cross-over with $L_R=0.3$ m in the perpendicular sections. The stability parameter of the resonator computes as $g_2=0.012$ indicating a very stable setup. The optical beam envelope and a zoomed-in section near the undulator center are shown in Figure 27. For an undulator length of 4 m an undulator gap (clear aperture) of 50 mm is just sufficient to transport beams with up to 100 μm wavelength with small losses. Larger gaps are considered unrealistic given the large field strength required to obtain the necessary undulator parameter for long wavelengths.

A somewhat larger Rayleigh length up to 1.6 m could be used. In that case, the stability parameter would increase to $g_2=0.070$ which is still very stable. The beam size at the ends of the undulator would be slightly lower, from $4w=48$ mm down to $4w=45$ mm at 100 μm wavelength at the expense of an increased beam size at the undulator center. This would decrease the coupling to the electron beam, thereby, reducing the gain but also increasing the saturation power.

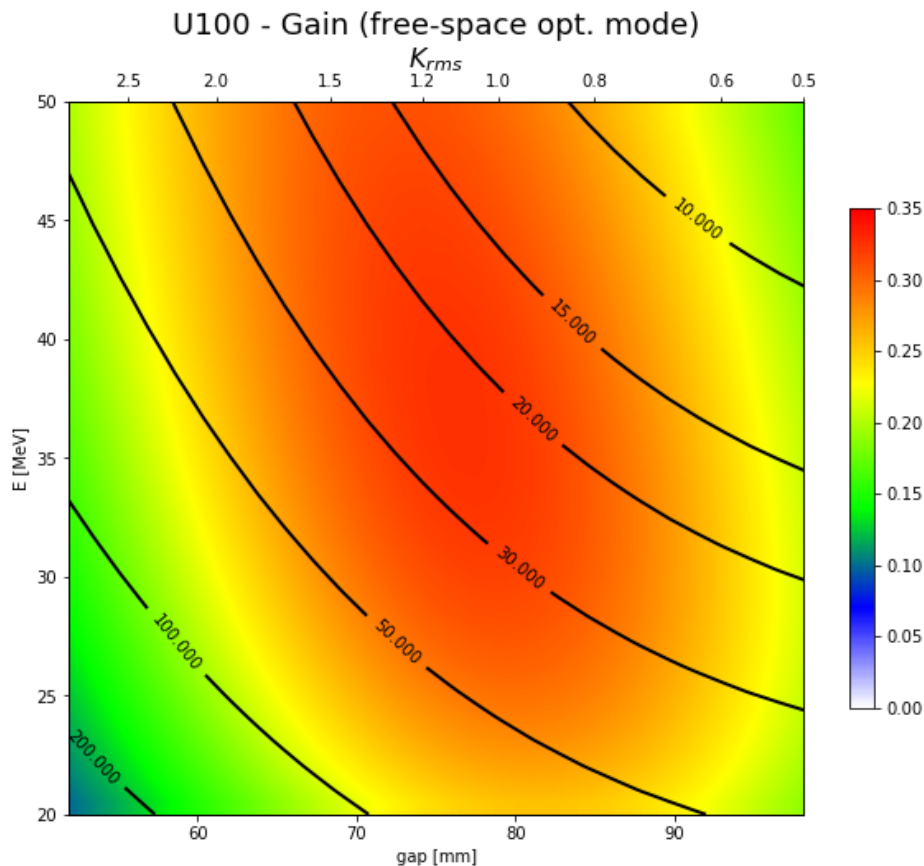


Figure 28: Small-signal gain per round-trip for different wavelength and FEL parameters.

We have used linear FEL theory to get an estimate of the FEL gain in the oscillator. A 50 pC bunch charge at 1 ps bunch length delivers a peak current of 20 A. For the electron beam a matched β in vertical direction and $\beta=1.0$ m in horizontal direction were assumed. A beam energy spread of 50 keV was assumed independent of the total beam energy. The computed small-signal gain (see Figure 28) is well sufficient (above 30% per round-trip) for all wavelengths of interest.

Calculations with GENESIS (steady-state) were performed to determine the saturation point of the oscillator and the possible out-coupled power. For 10 μ m radiation wavelength the beam energy was chosen at 50 MeV and with a bunch charge of 50 pC at a bunch length of 1 ps a peak current of 20 A was obtained. It can be seen that the single-pass gain drops as the power in the cavity builds up. We assume that half the round-trip losses of the optical resonator are actual out-coupled power while the same amount is lost due to diffraction. Initially the round-trip gain of the optical intensity corresponds to the value indicated in Figure 29. Depending on the chosen out-coupling fraction the power will rise up to the indicated level during startup of the FEL.

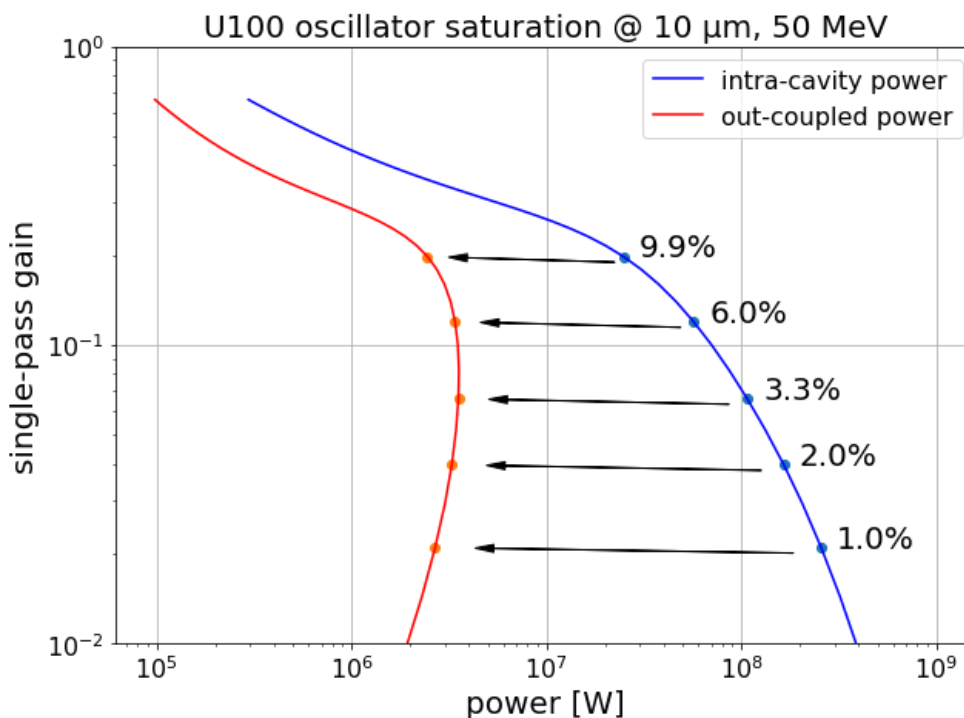


Figure 29: Saturation power of the FEL oscillator (blue: intra-cavity, red: out-coupled) for different out-coupling fractions.

FEL modulator

The optical beam of the oscillator FEL is used to imprint an energy modulation at the intended radiation frequency onto the high-charge electron beam. This is done by overlapping the beams in an undulator at resonance frequency. The intention here is to obtain a substantial energy modulation – significantly exceeding the slice energy spread of the beam – but not yet a temporal bunching of the electrons. Otherwise, coherent synchrotron radiation in the electron beam transport from the modulator to the radiator could deteriorate the beam quality.

It is subject to ongoing studies whether the intra-cavity beam of the FEL oscillator or an out-coupled beam should be used for modulating the high-charge beam. The optimum power for modulation is somewhere in the few 10^6 to few 10^7 W range depending on the wavelength. This also depends on the optical mode size in the modulator and the chosen length of the undulator.

At short wavelength even in a modulator of only 10 periods length when placed intra-cavity high bunching factors up to 50% are expected at the saturation intensity of the oscillator. On the other hand, at the longest wavelengths a rather long modulator of 40 periods can barely reach a sufficient energy modulation when driven by the out-coupled beam. Further studies taking into account the radiation gain processes inside the modulator are needed to decide about the optimum configuration to be used.

FEL radiator

The radiator receives a high-charge electron bunch energy-modulated at the desired radiation frequency. The electron beam transport between the two will be a synchronous achromatic design – the R_{56} of the radiator alone is sufficient to turn the energy modulation into a bunching. Over the radiator length along with the increasing bunching a radiation field is building up, ideally reaching full saturation at the undulator end. The optimum length of that radiator strongly depends on the dynamics of the evolving FEL interaction between the beam and the optical field and needs to be studied further to arrive at a detailed design. The current baseline assumes an intra-cavity modulator of 10 periods and a radiator of 40 periods length, both with the same parameters as the undulator used in the oscillator.

4.1.7 Optical beam propagation

The different photon sources of DALI will deliver ultrashort pulses spanning the THz and MIR spectrum with exceptionally high brightness. As shown in sections 4.1.5 and 4.1.6, the intensity distribution and divergence of the photon beam can have a complex spectral dependence. It is critical to preserve the spectral, temporal, and transverse mode from the source to the user labs. The beams will be propagated from the DALI sources to the user labs above the accelerator enclosure by a set of mirrors in an evacuated transport line. Due to the strong divergence, especially at the longer wavelengths, it will be necessary to use a combination of focusing and flat mirrors to manage the beam size throughout the transport. We will utilize a combination of optical propagation tools to calculate the propagation of the diversity of DALI photon sources.

Basic Gaussian transport calculations will be used to establish the optical acceptance of potential layouts for each beam transport. Gaussian beam propagation is not computationally intensive, thus allowing for relatively easy determination of certain parameters such as the focal length and size for each mirror. This type of calculations will be useful to examine several different potential layouts, but has limitations since it only considers a single wavelength and does not include information about the wavefronts and phases of the optical pulse.

One example – the propagation of the THz undulator radiation from an 8-period undulator – is shown in Figure 30. The initial optical beam was obtained from a TEUFEL simulation, the subsequent propagation done with a diffraction propagation algorithm. For visibility the diameter of the optical mode is exaggerated by a factor of 2. Due to the strong divergence of the radiation produced in an undulator and the necessity to capture a possibly large acceptance angle a first focusing mirror needs to be placed as close as possible to the beam exits from the undulator. Another narrow focus needs to be placed at a convenient location for a vacuum window separating the accelerator UHV from the optical beamlines. Then the beam is directed towards the ceiling of the accelerator vault and

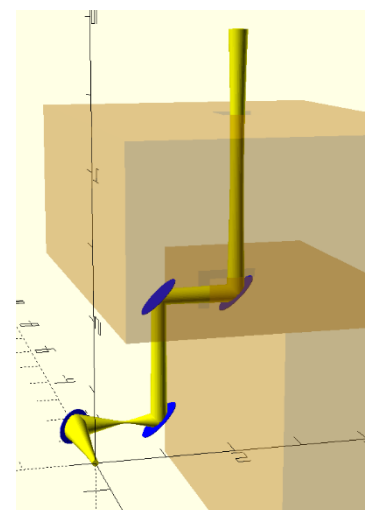


Figure 30: Propagation of a THz optical beam out from the accelerator vault.

into the wall. Inside the wall another mirror directs the beam towards the upper floor where the optical laboratories are situated. The complicated guiding of the beam through wall and ceiling is necessary for radiation protection. But it should also be mentioned that due to strong diffraction effects the beam rapidly diverges and every few meters focusing mirrors are required to keep the optical beam size under control. Figure 31 shows the optical beam envelopes of that example.

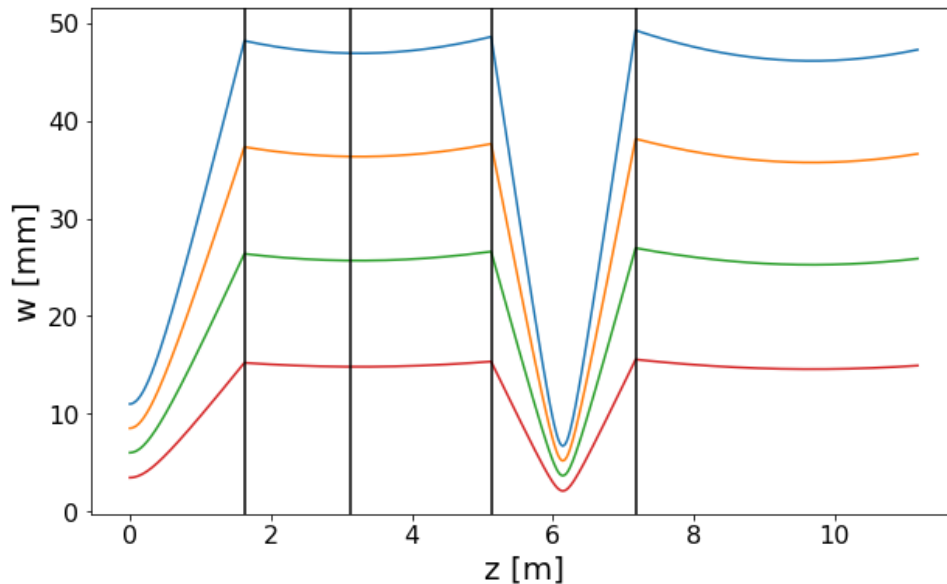


Figure 31: Envelopes of the optical beam for the propagation of undulator radiation out from the accelerator vault. Shown are 4 different wavelengths (0.3, 0.5, 1.0 and 3.0 THz).

This kind of design work and propagation simulation needs to be done for all sources and all beam paths to the experimental stations. For single frequencies, however, Gaussian beams can be used as an approximation of the true optical beam and fast propagation algorithms be used for the initial design stage. Once a small number of potential optical transport layouts are established from Gaussian beam calculations, more rigorous simulations of the beam transport will be performed using diffraction propagation codes such as the in-house code used here, the one built into OCELOT¹⁴⁷ or the SRW¹⁴⁸ code. These types of codes provide full information and tracking of the wavefronts, phases, intensity distribution, and divergence from the source as a function of wavelength. These simulations will thus facilitate refinement of the optical transport to ensure that the required spectral, spatial, and temporal distribution can be reliably transported to the user labs and experimental end stations.

4.1.8 Short-pulsed positron source

The high-charge injector/accelerator section will be used to generate secondary low-energy positron beams for defect characterizations and porosity analysis for a wide range of materials. Given by the longest annihilation lifetimes of ortho-positronium states, the spin-parallel quasi-atom consisting of one electron and one positron, of 142 ns in vacuum, the beam repetition rate

¹⁴⁷ <https://github.com/ocelot-collab/ocelot>

¹⁴⁸ O. Chubar, P. Elleaume, Synchrotron Radiation Workshop (SRW). <https://github.com/ochubar/SRW>

has to stay below around 20 MHz in order to avoid pulse to pulse overlapping in lifetime measurements.

Based on the experience gained at the ELBE secondary positron source pELBE, a suitable converter will generate a high-flux bremsstrahlung beam which enable positron-electron formation from pair-production for all energies from $2 m_e c^2$ up to the electron end point energy. Inside a polycrystalline Tungsten moderator foil of 5 μm thickness impinging positrons quickly lose their kinetic energy by collisions down to thermal energies. Moderated positrons are then re-emitted with about 2 eV kinetic energy due to the negative positron work function in Tungsten. Negative work functions do not exist for electrons.

Table 5: Electron beam requirements for secondary positron beam generation.

Electron beam energy	Average beam current	Bunch charge	Repetition rate	Transversal emittance	Pulse length
50 MeV	800 μA	400 pC	2 MHz	<15 mm mrad	< 10 ps

Crystal defects inside the Tungsten moderator which are generated by impinging electrons, photons, and neutrons will diminish the moderation efficiency and the secondary positron yield. Operating at high enough electron beam intensities and with sufficient thermal insulation temperatures crystal defects start to anneal at temperatures of about $2/3 T_m$, the melting temperature of Tungsten of 3700 K. The operation of pELBE has shown stable moderator conditions for several years without efficiency degradations. The overall conversion efficiency at pELBE of 65000 $e^+/\mu\text{A}$ electron beam current at 35 MeV beam energy will result in at least a factor of 8 higher positron beam intensity compared to the actual implementation.

Annihilation lifetime measurements require high signal-to-noise ratio of about $10^6:1$ which necessitates low dark current operations and an effective suppression scheme by beam-kicking (see Section 4.8).

The low-energy positron beam at DALI will outperform all other facilities of that kind in operation worldwide.

4.1.9 Ultra-fast electron diffraction

An important capability for THz-driven dynamics enabled by DALI is the possibility to directly drive modes coupled to the structure of matter. This can open pathways to transient phases in condensed matter or functionalize molecules to facilitate biological or chemical processes. To achieve a complete understanding of the THz-driven structural dynamics ultrafast electron diffraction (UED) will provide an ideal probe. A commercial¹⁴⁹ table-top keV-UED system can provide atomic resolution in reciprocal space and temporal resolution of a few hundred femtoseconds for condensed matter samples.

As an alternative or in addition to a commercial keV-UED instrument, an investigation of utilizing the ELBE SRF gun to drive an MeV energy electron beam as a UED source is underway. As described in Section 3.4, the higher beam energy provides several advantages in terms of the possibility for improved reciprocal space resolution, temporal resolution, and particularly the capability for measuring extended gas and liquid phase samples.

¹⁴⁹ DrX Works, <https://drx.works/systems/ultrafast-electron-diffraction-ued/>

The ELBE SRF gun design has already demonstrated excellent performance and robust long-term reliability driving beam for the existing coherent THz source at ELBE (TELBE). Simulations have shown that operation of the existing ELBE SRF gun design at 10 fC (~ 62,500 electrons) could deliver the performance required for a UED instrument. A detailed list of the UED parameters simulated for two operational modes with the ELBE SRF gun is shown in Table 6. The high-repetition-rate stroboscopic mode is optimal for dilute gas phase samples and for maximal signal-to-noise ratio. The single-shot mode can be utilized in experiments in which higher bunch charge is preferred. Demonstration experiments using the existing ELBE SRF gun for UED are planned to take place in the next few years.

Table 6: Simulated UED performance for the ELBE SRF Gun.

Parameter	Stroboscopic mode and gas phase experiments	Single-shot experiments
RF peak field	20.5 MV/m	
RF frequency	1.3 GHz	
Photocathode material	Cu (with 0.5 $\mu\text{m}/\text{mm}$)	
Quantum efficiency of photocathode	2×10^{-5}	
Drive laser wavelength	260 nm	
Drive laser temporal width	50 fs RMS	
Drive laser lateral width	50 μm diameter	
Repetition rate	100 kHz – 13 MHz	< 100 kHz
Electron beam kinetic energy	4 MeV	
Bunch charge at gun	10 fC (62,500 e-)	20 fC – 100 fC (1.2×10^5 – 6.25×10^5 e-)
Bunch charge after collimator	1 – 10 fC	10 fC – 50 fC
Relative energy spread	1.7×10^{-4} – 7.3×10^{-4}	1.0×10^{-4} – 1.3×10^{-4}
Normalized RMS emittance	6.8 – 13.5 nm	6.6 – 17.6 nm
Electron bunch length at target	< 50 fs	< 100 fs
Electron beam size at target	400 μm	500 μm
Spatial coherence length	10 nm	12 nm
Pump laser spot size	150 μm	
Temporal resolution	50 fs	100 fs
Gas sample size	150 μm	N/A
Electron beam size at detector	20 μm	
Average current	1 nA – 130 nA	< 50 nA
Electrons per second	6.3×10^9 – 8.1×10^{11}	< 3.1×10^{11}

While the choice to provide a keV-UED or an MeV-UED instrument is contingent upon the interim progress of the development of the ELBE SRF gun for MeV-UED, the DALI project anticipates

the development of such an apparatus, e.g., by foreseeing the need for additional cooling capacity of the Helium cryo-plant, the space within and the layout of the DALI accelerator hall and space for the photocathode drive laser system, access to the UED bunker and the ability to operate the UED experiment independently from the rest of the DALI facility.

4.2 Injectors

For accelerator-based light sources, electron injectors belong to the most crucial technologies. All injector subsystems must fulfill stringent requirements in order to reliably deliver high quality beams.

According to the parameter request of different beam lines for DALI project, we should consider the following different injectors (see Table 7). A DC gun with a thermionic cathode will be used as the high repetition rate injector for mid-IR FEL oscillator. An SRF gun with a photocathode will serve as the high bunch charge injector generating effectively two beams in parallel – for the super-radiant THz beam line and positron beam line.

Table 7: Overview of the DALI injectors.

	high rep. injector	high charge injector	fs-pulse injector
task	oscillator mid-IR FEL	super-radiant IR-THz & e ⁺	UED
Bunch charge (pC)	100 pC	1 nC /400 pC	10 - 100 fC
Rep. Rate	10 MHz	0.1 - 1 MHz	0.1 - 13 MHz
Mean beam current	1 mA	1 mA	
Beam Energy	250 keV	>5 MeV	3 - 5 MeV
Transv. emittance	10 μm	< 10 μm	0.01 μm
Long. emittance	50 keV·ps	<115 keV ps	N/A
Pulse length	tbc	tbc	50 - 100 fs

4.2.1 High repetition rate injector for FEL

As an electron source for the FEL oscillator the ELBE thermionic DC Gun (as shown in Figure 32) will be adopted. It provides a pulsed electron beam for the superconducting main accelerator. The pulsed electron beam delivered by the injector has an energy of 235 keV, a bunch charge up to 100 pC and an average beam current of 1.0 mA. The repetition frequency of the pulses can be set to 10 MHz. It consists of a DC high voltage electron source with a gridded thermionic cathode at high-voltage potential and an anode on ground with an electrostatic acceleration potential of -250 kV. The emitted electron current is modulated by the grid voltage forming pulses of about 500 ps length. These electron bunches enter the sub-harmonic buncher that runs at a frequency of 260 MHz (one fifth of the working frequency). The bunches are first compressed in the subsequent drift path by the energy modulation produced in the buncher. They are further compressed in the following 1.3 GHz fundamental buncher before entering the first superconducting cavity. Five magnetic lenses and some steering magnets belong to the beam optics. A macro-pulse generator and deflector coils allow to cut out pulse trains with lengths

between 0.1 and 35 ms at repetition rates up to 25 Hz. Diagnostic devices are installed for beam characterization as well as for optimization control during accelerator operation.

The electron source has been operating very reliably for the last 20 years at the ELBE accelerator, where it also serves as a source for the free electron laser, which has very similar requirements to the FEL oscillator for DALI.

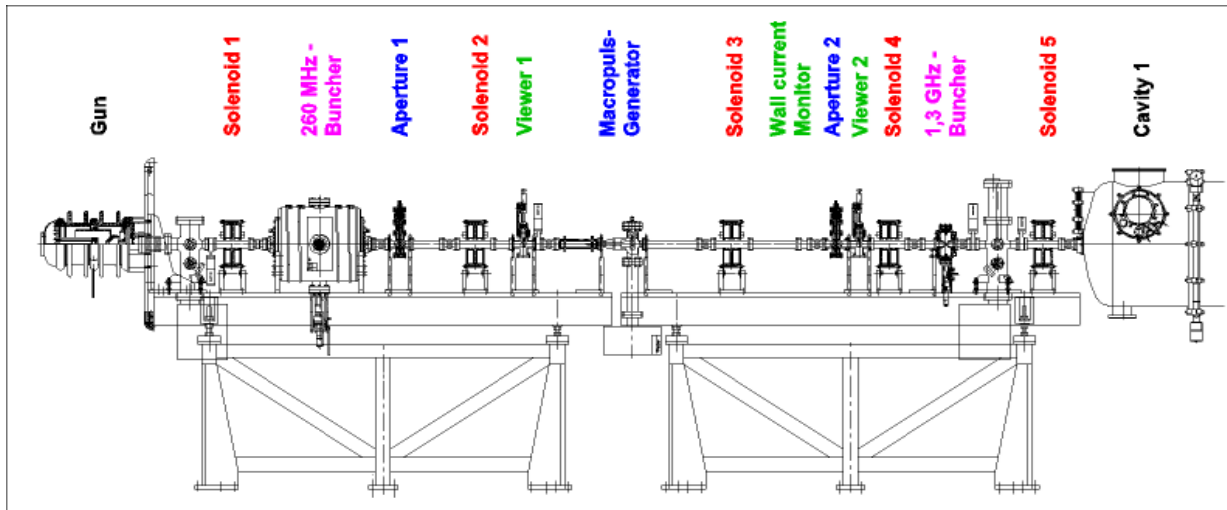


Figure 32: ELBE type thermionic DC gun.

4.2.2 High bunch charge injector for super-radiant THz/position

The success of continuously operated (CW) sources for medium and far-infrared radiation as well as for ultrafast time-resolved electron diffraction (UED) is closely linked to the development of a high-brightness CW electron source. It is a general consensus that a superconducting radio-frequency photoelectron injector (SRF gun) is a promising candidate for this purpose.¹⁵⁰ In SRF guns, the cathode is placed directly in the radio frequency (RF) cavity, which results in photoelectrons generated by laser pulses, being immediately accelerated in the strong electric field. This is reducing the space charge effect and resulting in a low beam emittance and high brightness at the exit of the gun. Since RF losses for superconducting cavities are low (max. some 10 W) even in CW operation and at high accelerating fields, this concept is superior to all others. Although even higher fields can be achieved in a normal conducting (NC) RF injector, CW operation is only possible by significantly reducing the field strength due to the quadratic dependence of the RF power dissipation.

The idea of using a SC gun cavity is now 35 years old and was originally proposed by University Wuppertal.^{151,152} After the idea was brought years later to HZDR, the first beam ever was produced in a proof-of-concept experiment based on a half-cell TESLA cavity. 8 years later and with a much more advanced 3.5 cell gun cavity, the injection into the ELBE linac and generation of radiation from IR-FEL were demonstrated.¹⁵³ In 2014, the gun was then replaced by the most advanced

¹⁵⁰ X. Wang and P. Musumec, Workshop on the Future of Electron Sources, 2016

¹⁵¹ H. Chaloupka et al., Proc. of 4th SRF Workshop, 1989

¹⁵² A. Michalke, et al., Proc. of 5th SRF Workshop, 1991

¹⁵³ J. Teichert et al., Nucl. Instrum. Methods Phys. Res. Sect. A **743**, 114-120 (2014)

version to date (Figure 33), which is now used for routine user operation to produce THz radiation and neutrons.¹⁵⁴

Due to the many years of successful development in the field of SRF guns, it is obvious to propose a similar electron source that is based on the latest developments for the project described here.

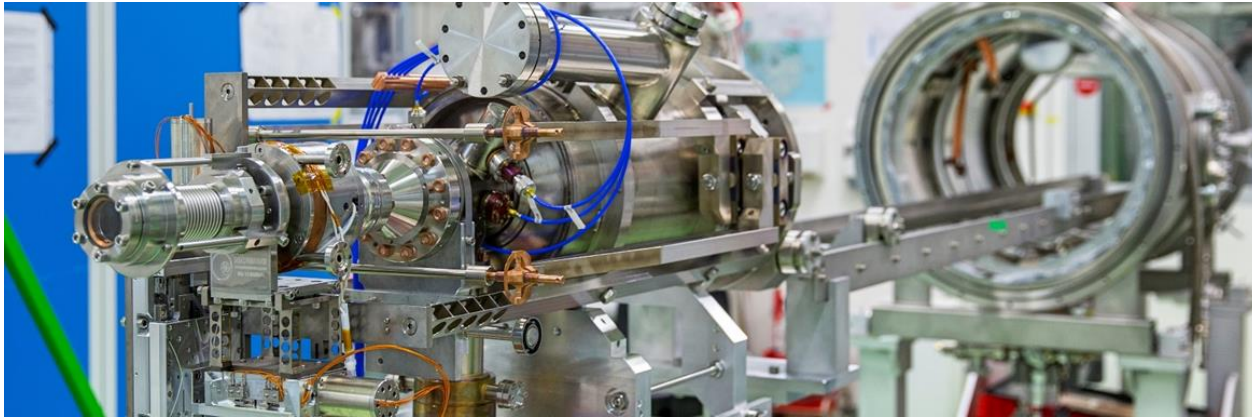


Figure 33: Photograph of the SRF gun II cold mass, right before the wedding with its cryostat.

ELBE-type SRF gun

The advantage of the HZDR concept is its compactness. The gun is just 1.3 m in length and less than 1 m in diameter. Thus, after a very short distance, the electron bunch is already relativistic and short enough for further acceleration. As a consequence, no buncher or booster is needed, which significantly simplifies the beam transport and reduces the overall effort.

The core of the gun is the cold mass consisting of a $3\frac{1}{2}$ cell 1.3 GHz Nb gun cavity and a choke cell, both surrounded by a LHe vessel (Figure 34). On one side of the cavity, the cathode ends almost flush with the back-wall of the first half cell. The cathode is mounted in a multi-purpose cooling and support system, that provides a temperature of 77K and allows cathode transfer into the cold gun. In addition, thermal and electrical isolation from the cavity is realized to provide a DC bias for the multipacting suppression. Last but not least, the cathode is moved by remote stepper motors to find the best RF focus. At the other side of the cavity, literally the gun exit, the fundamental RF power coupler, two HOMs loads, and a superconducting solenoid on a motion stage are assembled. The latter provides early beam focusing.

Essential subsystems of injector

a) Cryomodule

The main purpose of the cryomodule is the isolation of the 2K cold-mass from room temperature. Its design is based to a great extent on the experience gained from the ELBE LINAC module. It consists of a stainless-steel vacuum vessel, a μ -metal shield to reduce earth magnet field inside and a liquid nitrogen shield for pre-cooling. The latter is also used for cathode cooling. The mechanical support for the cold-mass is made by thin titanium spokes which allow for proper alignment at all times. The two cavity tuners consists of a lever gear pair each, that are moved in vacuum on a cold and dry lubricated spindle drive. This in turn is connected via stainless steel bellows to the drive unit located outside the cryostat. They provide sufficiently large tuning range,

¹⁵⁴ J. Teichert et al., *Physical Review Accelerators and Beams* **24**, 033401 (2021)

high resolution, low hysteresis, long lifetime and low cryogenic loss. Finally, for liquid He level control a separate reservoir and an electrical heater are installed.

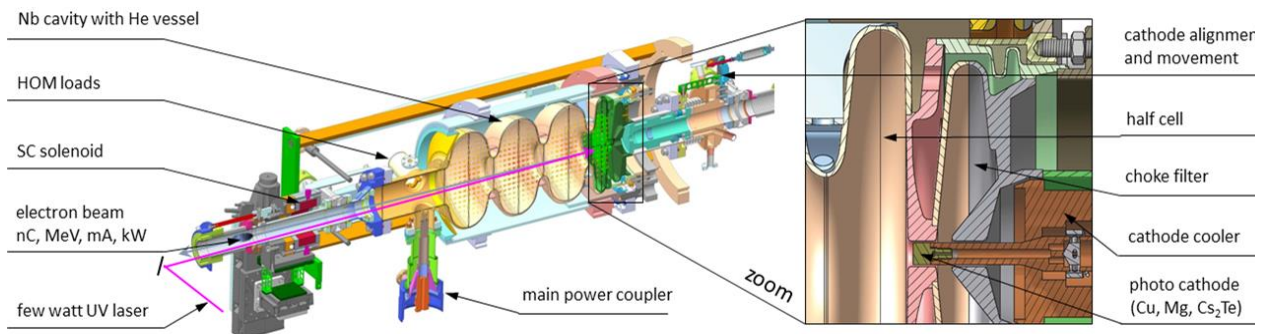


Figure 34: The cut-out view of the ELBE SRF gun (cold mass) shows the 3.5 cell cavity and the associated components. The zoomed in view on the right gives more details about the cathode, the half cell and the choke cell.

b) Photocathode and laser

High performance and stable operation of a photocathode in an SRF photoinjectors has always been a challenge. In general, photoinjectors require that the cathode possesses high enough QE, practically reasonable lifetime, low thermal emittance and short response time. For operation in high electric field, cathodes need to be particle free, have a smooth surface and produce not too much of dark current.

High QE allows to reduce power requirements for the drive laser, while small thermal emittance and short response time are essential for transverse and longitudinal bunch structure. The choice of photocathode material must be made taking into account the drive laser system. For example, to generate 1 nC bunch charge with a 10% QE photocathode (Cs_2Te), laser pulse energy of 50 nJ on the cathode would be required, while with a 0.01% QE (metal), correspondingly, 50 μJ .

Based on the requirements of the DALI facility, the work on photocathodes will be conducted in the following step-by-step mode: metallic photocathode for gun commissioning; Cs_2Te photocathode for routine operation; study of new photocathodes.

The prepared photocathode should be transferred to the gun through a load lock system. The whole system should preserve a particle free environment under extremely high vacuum of 10^{-11} mbar and prevent the contaminants reaching the cathode surface during a cathode exchange. Meanwhile, a QE measurement system should be integrated into the cathode transport chamber so that more data can be collected during the storage.

Parallel operation of one of the THz sources together with the positron source while using one SRF gun as injector is foreseen. The requirements to electron beam parameters for the THz and positron sources are significantly different though, which in turn means different requirements to laser pulses in terms of energy, duration, temporal and perhaps also spatial shape, as well as different repetition rates.

The most straightforward and flexible way to alternately combine laser pulses with different parameters on the cathode, which would allow completely independent variations of the parameters, is usage of two independent laser sources. The beams from the two sources can be combined and made collinear at a point in the laser room and then propagate further to the

cathode through the same laser beam line. Required laser power on the cathode can be calculated from needed beam current (I_{beam}) and quantum efficiency (QE) of the cathode:

$$P_{UV} = \frac{I_{beam} hc}{QE \lambda e} \quad (8)$$

where h is Planck constant, c — speed of light, λ — laser wavelength, e — elementary charge. Power losses on the way from the laser output to the cathode have to be taken into account. Years of beam operation with an SRF gun at ELBE enable us to estimate power (pulse energy) of UV laser output required for a given beam current (bunch charge) fairly easily. The Laser pulse energy in Table 8 is calculated under the assumption that the transmittance of the laser beam transport is 10% (losses for beam shaping on a hard aperture are taken into account) while the quantum efficiency of the photo cathode is 1%.

Table 8: Requirements for the photocathode drive laser(s).

	Laser 1	Laser 2
Purpose	THz	Positrons
Rep. rate	10...200 kHz	2 MHz
Pulse energy (bunch charge)	5 μ J (1 nC)	2 μ J (400 pC)
Pulse duration (FWHM RMS)	7 3 ps	7 3 ps

Building lasers with such parameters will not require a fundamentally new development. The new generation of NEPAL photocathode lasers developed and being built at DESY for EuXFEL, FLASH and PITZ is capable of providing >10 μ J pulses at 258 nm at 1 MHz in 1 ms bursts.¹⁵⁵ One of the key reasons DESY needed to develop their own “home-built” laser system is their need for very specific burst pattern, where every burst consists of two sections of pulses of different duration and energy.

Requesting “Laser Science and Technology” department at DESY to build two photocathode lasers for DALI seems to be a reasonable approach, which would, as an additional benefit, deepen the cooperation between DESY and HZDR. Alternatively, given that building a laser for the CW mode of operation is principally simpler than building a laser for a burst mode, commercially available laser can be considered as a nearly ready-made solution.

c) Other subsystems and infrastructure

The subsystems, such as high-power RF system, low level RF, liquid helium and liquid nitrogen are planned together with the LINAC modules. The vacuum system is separated in cryostat or isolation vacuum ($\leq 10^{-6}$ mbar), beam line vacuum ($\leq 10^{-9}$ mbar) and cathode storage and transport vacuum ($10^{-10} \sim 10^{-11}$ mbar). The periphery infrastructure includes temperature-stabilized laser room with transport pipes for laser transport, a photocathode lab with cleanroom environment and an ISO4 cleanroom for SRF cavity and beam line assembly (Figure 48).

¹⁵⁵ C. Li et al., Photocathode Laser Development for Superconducting X-Ray FEL at DESY, IPAC (2021)

4.2.3 Operational experience

RF operation

At HZDR, experience in operation with the first SRF gun has already gathered since 2007. However, as this source was still a prototype and not intended for routine operation, this section focuses on our experience with the second improved SRF gun II. One of the most important questions arises from the interaction of a normal-conducting cathode vaporized with the photoactive layer and the superconducting resonator, which is extremely demanding in terms of an absence of particulates. Experience with gun II shows that due to the complex processes during cleanroom assembly, a performance deterioration of up to 30% compared to the last vertical test is to be expected. However, the assembly took place in the USA at that time and the degradation could also have been significantly caused by the air transport. The SRF guns planned for DALI will be assembled in a cleanroom next to the accelerator, so that less degradation can be expected here. But more important is the finding, that with the exception of the first Cs_2Te cathode, which had a serious design issue, all subsequent cathodes (30 cathodes in total) have caused no further degradation in cavity performance over the past eight years.

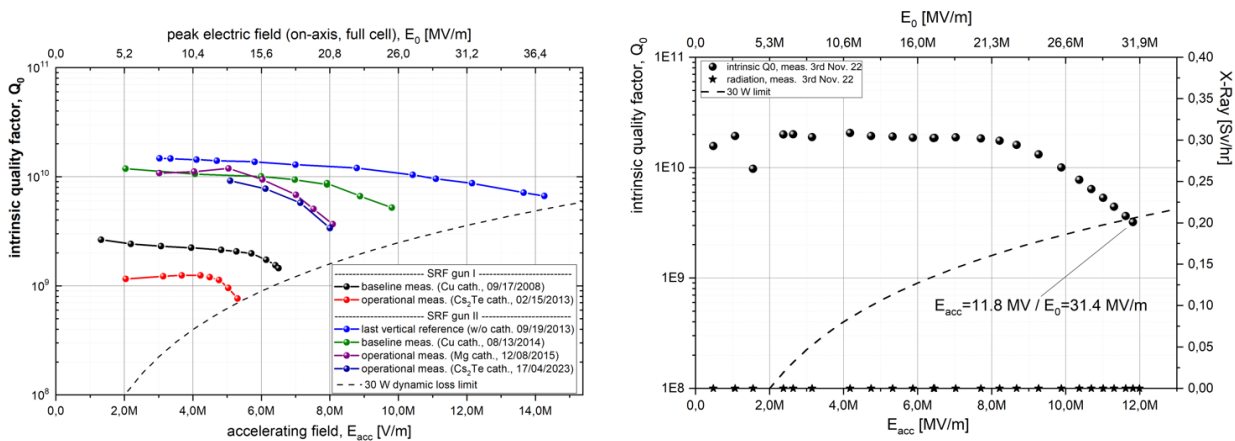


Figure 35: Cavity performance expressed as a function of the intrinsic quality factor and the accelerating field. The left plot shows the performance of SRF gun I and II at different points in time, while the right plot shows the result for SRF gun III (currently under construction) after successfully passing the vertical acceptance test.

Nevertheless, it remains to be emphasized that the performance achieved so far is not sufficient to extract a bunch charge of 1 nC with a sufficient beam quality, as targeted in this project. This would require at least an on-axis RF field of $E_0=30$ MV/m. However, this value is quite realistic, since it was achieved and often exceeded in all vertical tests of our gun cavities (Figure 35). Combined with a well-prepared clean room assembly, similar to that for TESLA 9 cell cavities, it is expected to preserve the performance all the way into the accelerator bunker. Just as an example, Gun II already achieved a value of 26 MV/m before the faulty Cs_2Te cathode was installed, and even 1-2 MV/m more would have been possible at that time.

Among many other RF parameters, the short-term stability / jitter of the acceleration field is certainly the most important. Main source of disturbance is the excitation of the mechanical Eigenmodes of the cavities by the various vibrations from all rotating objects such as vacuum- and water pumps, air condition but also from stochastic sources. Via different transfer media these may then excite one or more mechanical Eigenmodes and an undesired resonant oscillation built up. Microphonics measurements at SRF gun II show that some of these resonances could be

attributed to membrane pumps and the compressors of LHe machine but some sources remain unknown. The overall frequency detuning was found to be 7 Hz (RMS), which results in a phase noise already reduced by the LLRF system down to good values of 0.02° or 43 fs (both RMS)¹⁵⁶. However, further improvements can be expected, as the used cavity was found to be mechanically very soft and a new cavity will have a higher mechanical stiffness.

Photo cathode operation

To date, 30 different photo cathodes (2 Cu, 12 Mg, 16 Cs₂Te) have been used in the SRF gun-II. After commissioning with pure Cu, Mg was used as an interim solution until the issue with Cs₂Te overheating was solved. Since 2020, only the Cs₂Te on Cu plugs have been used. The preparation is done in-house and to a large extend successful. We manage to maintain the QE from storage near the gun over months up to its transfer into the gun. But once there they all behave differently, in terms of multipacting, QE during operation and lifetime/robustness. As shown by the statistics plot (Figure 36) some maintain good QE of 1% and more, but others barely reach half a percent. Nevertheless, on average a cathode is used for 500 h of beam time and lasts at least for ¼ in the gun. The latter is typically limited by warm up of LHe machine.

Since the lifetime, according to what was observed so far, does neither depend on the overall extracted charge nor on the duration in the gun, but rather on its chemical composition, it is planned to optimize the cathode preparation process by improved analytical methods, such as X-ray photoelectron spectroscopy (XPS). Such a system is already in use and corresponding experience is available. In addition, it is planned to use molybdenum instead of pure copper as the cathode substrate, as molybdenum itself has no chemical reaction with Cs₂Te coating.

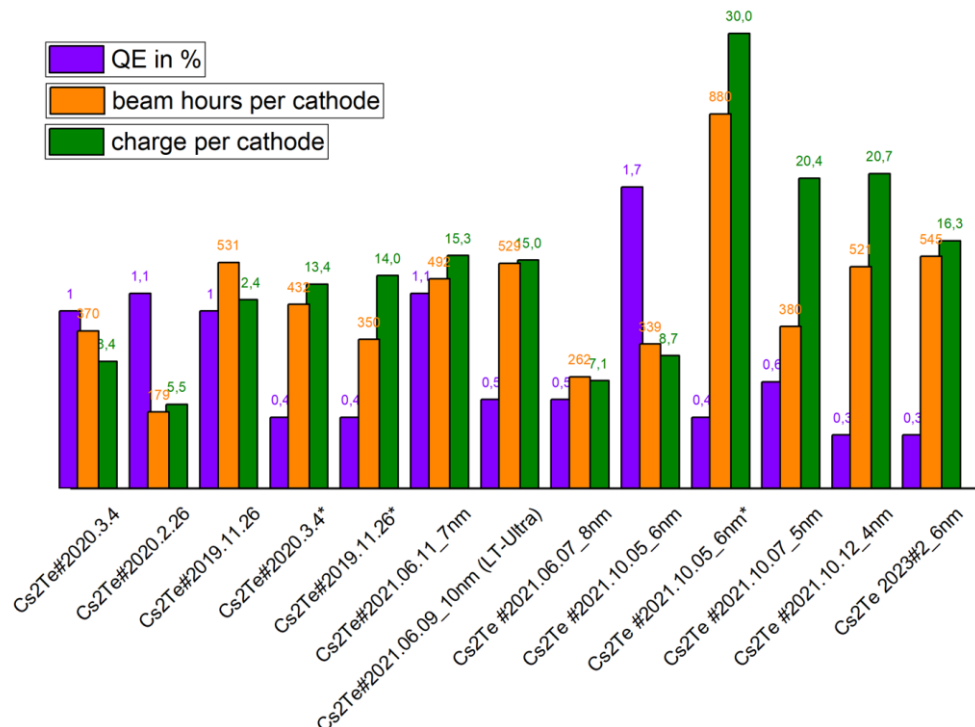


Figure 36: Overview of quantum efficiency (QE), beam hours and total extracted charge of all Cs₂Te cathodes used in SRF gun II so far.

¹⁵⁶ A. Arnold et al., Proceedings of the International Conference on RF Superconductivity (2021)

Beam operation

SRF-Gun II was commissioned in 2014 and is being used in routine operation since 2018. It is mainly used as an injector for the most demanding user experiment in terms of stability and bunch charge, the generation of THz radiation. In addition, however, the source is also used for neutrons production, as it is clearly superior to the thermionic injector in terms of bunch charge and beam energy. Distributed over a year, this results in an average of about 1800h beam time, which corresponds to about 40% of the total ELBE beam time to be allocated.

In both cases, the gun delivers a 4 MeV beam with a bunch charge of 200-250 pC and a repetition rate up to 250 kHz in CW. It is running very stable and reliable over many days w/o any trips. An example is shown by Figure 37 during a neutron run end of last year, when a total of 15 C was extracted within 8 days. Although users are currently requesting rather low currents, we have already accelerated up to 400 μ A into a beam dump 5m downstream the beam line and there is no limitation known to achieve the nominal beam current of 1 mA. Last but not least the bunch charge was already extracted up to 600 pC downstream into the faraday cup, but to push this value to 1 nC a higher RF field is mandatory.

To characterize the electron source, various electron beam parameters were determined in the past years. These include the energy and energy spread as a function of the emission phase, the transverse emittance for different bunch charges, and the bunch length at the entrance of the first ELBE linac.¹⁵⁷ All measured values agree well with the predicted simulation results, and the source can be considered as understood and an extrapolation of the expected beam parameters at higher acceleration gradients and bunch charges is quite permissible.

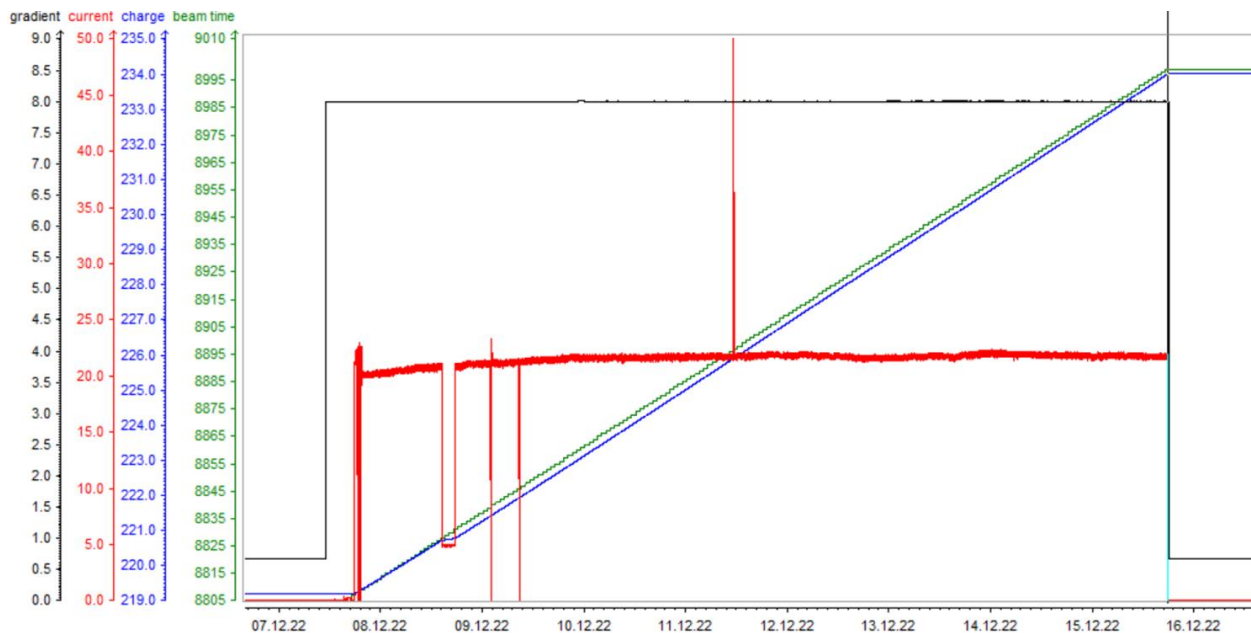


Figure 37: Representative plot of cavity gradient and extracted current for a typical user beam time. Here the gun was running very stable and reliable w/o any trips and a total of 15 C was extracted within 8 days.

¹⁵⁷ J. Teichert et al., Physical Review Accelerators and Beams **24**, 033401 (2021)

4.2.4 Injector test setup

As the most critical system, the performance of injectors must be carefully investigated and optimized in advance. A separate test cave with independent access and all subsystems is strongly suggested. This allows the qualification and characterization of the SRF gun before it is installed at the accelerator. At the same time, it also allows a replacement to be provided as a “hot spare”, that has already been tested and is just waiting to be deployed.

The layout of the proposed diagnostic beam line of the SRF gun is presented in Figure 38. The diagnostics will support measurements of transverse projected emittance, slice emittance, longitudinal emittance, energy and energy spread, spatial profile, beam halo and dark current. A quadrupole triplet serves for focusing and optimal matching of the beam for the various measurement options. Furthermore, it enables larger tuning scope of the gun solenoid for emittance compensation studies. Bunch length and longitudinal phase space measurements can be performed by means of a transverse deflecting cavity and the 180° dipole magnet. The deflecting cavity is normal conducting and operated in pulses mode, which is sufficient for diagnostic purposes. Transverse emittances can be measured with slit masks in screen stations 2 or 4 and the subsequent screens. The position of screen station 4 corresponds to the intended distance between SRF gun and first accelerator module entrance where the transverse emittance should have its minimum. Using the transverse deflection cavity, slice emittance measurements are possible. For this purpose, the slice slit in screen station 3 and the slit mask in screen station 4 are used. The figure does not show the correction quadrupoles, steerers, BPMs and integrating current transformers (ICTs) which complete this diagnostic beam line.

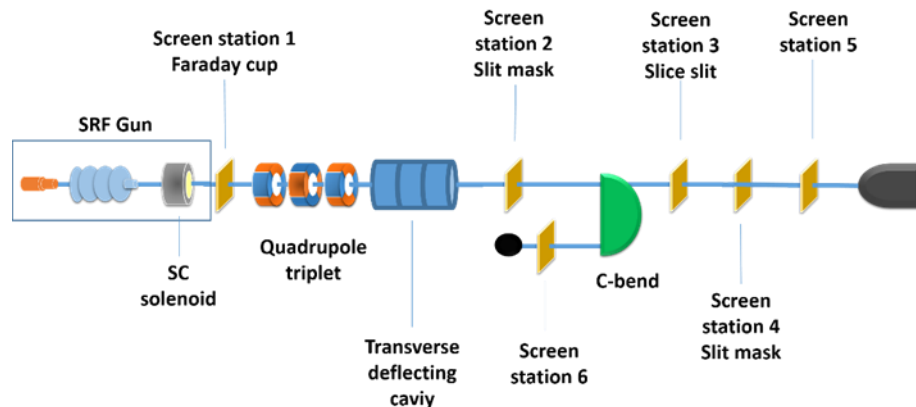


Figure 38: The layout of the proposed diagnostic beam line in the injector test cave.

4.2.5 Alternative guns

Besides the ELBE SRF gun, there are also other types of CW electron sources in operation or under design.¹⁵⁸ Among them, QWR normal conducting RF gun (VHF gun) developed at LBNL/SLAC and QWR SC RF gun developed for LCLS-II HE would be possible alternative candidates for the DALI high charge injector.

a) QWR NC RF gun (VHF gun)

One of the alternative CW electron guns is the quarter wave resonator (QWR) NC gun currently being used at LCLS-II and in future for Shanghai XFEL.^{158,159} Figure 39 shows a schematic layout

¹⁵⁸ F. Zhou, C. Adolphsen, D. Dowell, R. Xiang, *Front. Phys.* **11**, 1150809 (2023)

¹⁵⁹ F. Zhou et al., *Physical Review Accelerators and Beams* **24**, 073401 (2021)

of this CW normal conducting RF gun at LCLS-II. The single-cell gun cavity is designed for CW operation at 185.7 MHz, the seventh sub-harmonic of the 1.3 GHz SC linac frequency. The LCLS-II gun provides voltage gain of ~650 kV, corresponding to a photocathode gradient of ~17.5 MV/m. Two RF ports are powered by 60 kW solid-state amplifiers (SSA). Twelve non-evaporable getter (NEG) pumps around the outer cavity keep the gun vacuum in the low 10^{-9} Torr scale to achieve reasonably long lifetimes of the Cs₂Te photocathode. The gun is cooled via five separate water circuits with a flow about 40 gallons-per-minute. There is a two-cell buncher with 1.3 GHz NC RF cavity, powered by SSA of 7.6 kW, in order to compress the bunch length, and two solenoids for beam focusing and emittance compensation.

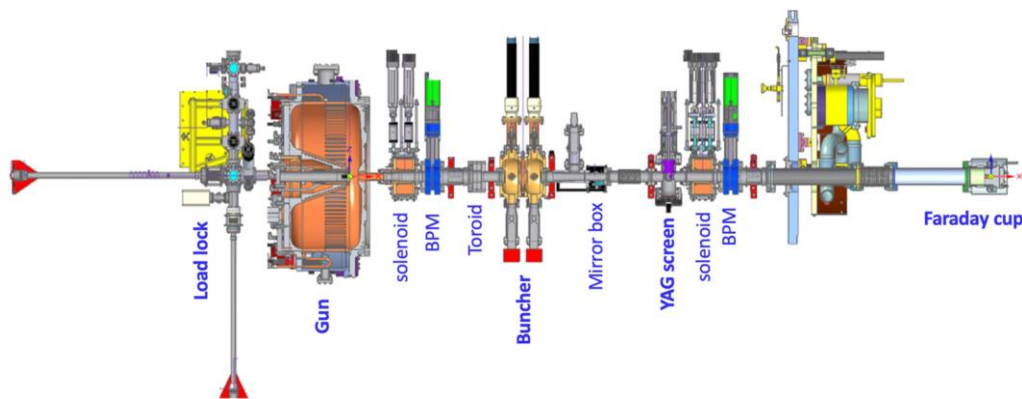


Figure 39: QWR normal conducting RF gun and the injector beam line used for LCLS-II facility.

However, compared to the SRF gun, the disadvantage of CW NC gun is the request of high RF power, cooling water and extra buncher in beam line. Moreover, the low energy of electron beams between the injector and the first linac makes the space charge effect significantly higher than that with ELBE SRF gun, especially for high bunch charge beams.

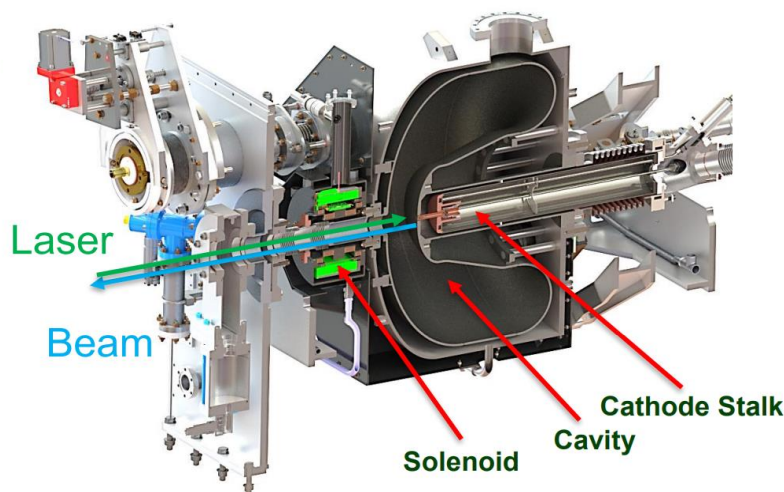


Figure 40: Cross section of LCLS-II HE quarter wave resonator (QWR) SRF gun.

b) QWR SRF gun

Another type of CW RF gun is QWR SRF gun, for example the new LCLS-II HE SRF gun developing under cooperation SLAC/MSU/ANL/HZDR¹⁶⁰ (shown in Figure 40). This 185.7 MHz SRF cavity is designed with the goal of achieving a photocathode gradient of at least 30 MV/m. The photocathode is held by a coaxial fixture (“cathode stalk”) for thermal and electrical isolation from the cavity body. The system must allow for precise alignment of the photocathode, particle-free photocathode exchange, cryogenic (55-70K) or warm (273-300K) photocathode operating temperatures, and DC biasing to inhibit multipacting. There is an SC solenoid installed at the exit for focusing and emittance compensation.

This gun concept is beyond-state of art and very promising as a low emittance CW source.¹⁶¹ However, this gun is primarily designed to provide beams of 100 pC bunch charge with ultra-low emittance, but not for high bunch charge purpose. The prototype gun will be tested within the next years. Afterwards one can verify, whether the parameters can match the DALI design requirement.

4.3 Accelerator modules

4.3.1 Introduction

In order to minimize the development effort for DALI with regards to cavity and cryomodule, a new development of both is not sought. Instead, the cryomodule developed for the electron linear accelerator ELBE (Figure 41) as well as adapted TESLA cavities are planned to be used. To avoid misunderstandings, this does not mean that a 20-year-old technology will be the basis of the new machine. The opposite is the case. Due to constant developments at HZDR and by the company Research Instruments GmbH (RI), which manufactures the same under license, the module is still state of the art. The same applies to the cavities. Based on the worldwide experience, the TESLA design, which has established itself as the quasi-standard for electron linear accelerators, will be used for the DALI machine as well. This guarantees the greatest possible cost-benefit ratio, since only established knowledge and technologies will be used.

At the moment four ELBE type modules and two comparably constructed SRF-Gun modules have been built and operated at the HZDR. Additionally, RI has produced another six modules for the ALICE ERL in Daresbury, the TARLA FEL in Ankara¹⁶² as well as for the MESA ERL in Mainz¹⁶³ and currently another four modules are being built for the Polish Free-Electron Laser (PoFEL) in Świerk near Warsaw.¹⁶⁴ With this, RI is the only commercial supplier that offers compact superconducting accelerator modules for CW operation. In sum, there are currently experiences in the design, construction and operation of a total of ten cryomodules of this type, which may be considered sufficient to realize a project as described in this document.

Of course, XFEL / LCLS-II modules could also be an alternative, but these are neither commercially available nor does HZDR have an expertise comparable to the ELBE type modules. In addition, due to the size of 12m and the weight of 7.8t an expensive cleanroom and assembly infrastructure would be required to maintain the modules and to be able to repair them in the event of an accident. Of course, a maintenance agreement with DESY might be an option, but this will hardly allow short response time in the event of a problem. Thus, the entire module would

¹⁶⁰ S. J. Miller et al., Proc. 21th Int. Conf. RF Superconductivity (2023)

¹⁶¹ LCLS-II-HE SRF Gun Technical Specification and SOW, 2021

¹⁶² A. Aksoy, U. Lehnert, Nucl. Instrum. Methods Phys. Res. A **762**, 54-63 (2014)

¹⁶³ F. Hug, et al., Proceedings. of the 2016 Linac Conference, East Lansing, USA (2016)

¹⁶⁴ P. Czuma et al., Proceedings of 13th International Particle Accelerator Conference (2022)

have to be removed for quick repair and a complete spare part module needs to be available at all time. This is ultimately more expensive than having only one ELBE module as a spare part on the shelf. In addition, the modular design of the ELBE type offers more flexibility, so that in this early design phase, different layouts with different energies can be realized very easily just by scaling the module number.



Figure 41: Photograph of a cryomodule of the ELBE type installed in the accelerator tunnel at HZDR.

Nonetheless, the XFEL module with its 8 cavities will be briefly discussed below. An advantage is undoubtedly the high energy gain, so that it could represent a more compact alternative to the ELBE module. This might be at least true for beam energies greater than 100 MeV as discussed for the VUV FEL part that was originally included in the DALI Pre-CDR. However, as shown in Table 9, this strongly depends on the anticipated gradient of the cavities and the required final energy of the LINAC. All data is taken from chapter 4 of the XFEL TDR.¹⁶⁵ It should also be noted that the XFEL construction always requires a cryogenic feed and end cap at the beginning and

Table 9: Comparison of the LINAC for 50, 100 and 150 MeV using XFEL or ELBE type modules (12.5 MV/m per Cavity).

		based on XFEL module(s)	based on ELBE modules
50 MeV	static loss + dyn. 2K loss	1x25 W + 4x15 W = 85 W	2x10 W + 4x15 W = 80 W
	length	12 m	2x3.5 m + 1.0 m = 8.0 m
	weight	8 t	2x1.5 t = 3 t
	cost estimate	3.2 Mio € ¹⁾ + Feed- and Endcap	2x2.4 Mio € = 4.8 Mio € ²⁾
100 MeV	static loss + dyn. 2K loss	1x25 W + 8x15 W = 145 W	4x10 W + 8x15 W = 160 W
	length	12m	4x3.5 m + 3x1.0 m = 17.0 m
	weight	8t	4x1.5 t = 6 t
	cost estimate	3.2 Mio € ¹⁾ + Feed- and Endcap	4x2.4 Mio € = 9.6 Mio € ²⁾ €

¹⁾ private communication Elmar Vogel (DESY)

²⁾ based on official 2023 quote for 5 modules

¹⁶⁵ M. Altarelli et al. (eds.), XFEL Technical Design Report, DESY 2006-097

end of the module. These require space and cause additional costs (both not known yet). In general, the XFEL design is rather optimized for long SRF LINACs by incorporating the cryogen supply and eliminating hot-cold transitions between the modules to save space. For short SRF LINACs, other designs can ultimately be more cost and space efficient.

4.3.2 Basic setup of the ELBE type accelerator module

The ELBE type cryomodules contain two XFEL 9-cell cavities with a resonant frequency of 1.3 GHz (see section 4.3.3). They are operated in superconducting state at a temperature of 2K and for this purpose both cavities are enclosed by helium filled titanium vessels. Both vessels are firmly connected to each other to a so-called tandem string (Figure 42). This stable structure is suspended in the center of the cryomodule by 6 tension rods that are attached with manipulators for precise radial alignment from the outside. The fundamental power couplers for the required RF power are located centrally below the tandem.

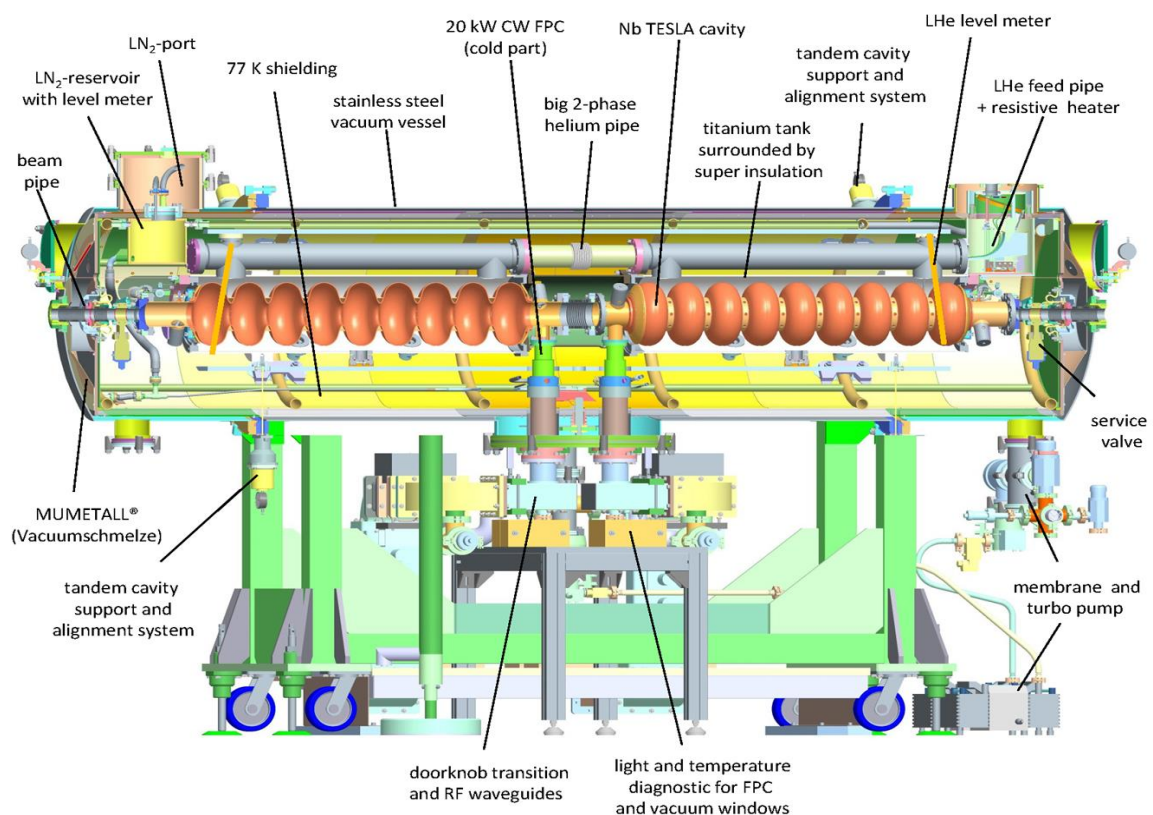


Figure 42: Cross-section of the ELBE type cryomodule with the most important components.

The vessels are filled with superfluid helium, whereas the evaporating helium is being collected by a 2-phase helium gas return pipe with a capacity of ~ 4 g/s and returned to the helium plant. During regular operation, helium is filled exclusively via this line.

The beam line vacuum system consists of the two 9-cell cavities that are interconnected via a flexible 2K bellows, followed on both sides by a beam line transition with DN40 vacuum gate valve to room temperature. A short bellows compensates for length change while the resonator is tuned in the direction. The gate valves serve to protect the cavity tandem against contamination by particles which are almost unavoidable during transportation and subsequent installation of the beam line in the tunnel. Due to the limited space in the module, compact valves of the VAT series 01 are used. These have a guaranteed permeability of $\mu_r < 1.05$ and thus do not constitute as

source for additional magnetic fields. This is of particular importance, since these magnetic fields are frozen in the niobium during phase transition to superconducting state and thus increase the surface resistance and deteriorate the quality factor of the cavities. As our cavities are operated continuously, highest quality factors are desirable in order to minimize the dynamic losses into the helium.

In order to bridge the thermal gradient between the 2 K cold cavity and the beam line at room temperature, two bellows assembly are used. These offer a correspondingly large thermal length with a short mechanical length at the same time. The first bellow realizes the transition from VAT valve (near 2K) to the intermediate thermal shield (77 K) whereas the second bellow is arranged between the thermal shield and the accelerator beam line. The joint of both bellows is anchored to the thermal shield in order to remove the heat. In addition to the thermal shield also a magnetic shield encloses the tandem to reduce external magnetic fields such as earth's magnetic fields.

Like the cavity tandem, also the module itself is largely symmetrical. It consists of a mid-part and two end caps which together form a vacuum vessel. In order to prevent heat convection to the 2K cold tandem the vessel is evacuated to at least $1e-6$ mbar (so called isolation vacuum). The whole vessel is made of stainless steel 1.4301 and rests on a frame equipped with transport wheels and pedestals. Adjusting screws and sliding faces allow the transversal and longitudinal adjustment of the vacuum vessel by ± 10 mm. The mid-part has a large flange at the bottom (ISO-K DN500) to access the main couplers (see Section 4.3.4). Both end caps have flanges for electrical feedthroughs as well as for helium and nitrogen connections (all ISO-K DN250). The electrical feedthroughs can be optionally mounted on both sides. Likewise, also the waveguide connections for the main couplers can be led through on both sides of the module, so that an easy adaptation to external conditions later in the tunnel/cave is possible.

Table 10: *Technical specifications of the ELBE type cryomodule.*

Mechanical specification	
length from flange to flange	3450 mm
width (of the underframe)	1050 mm
max. height (without LN2 connection)	1830 mm
weight	1.5 t
Operating data	
frequency @ 2K	1300.000 (± 0.05) MHz
tuning range	± 120 kHz ¹⁾
cavity bandwidth	110 Hz
FPC (fundamental power coupler)	≥ 15 kW
accelerating gradient per cavity	≥ 12.5 MV/m
Cryogenic performance	
static losses of the cryomodule at 2K	< 10 W ²⁾
static losses of the cryomodule at 77K	< 100 W ²⁾
dynamic losses at 25 MV (CW operation)	< 30 W (corresponds to $Q_0 \geq 1.0e10$) ³⁾

¹⁾ for ELBE type lever tuner, XFEL scissor tuner achieves ± 300 kHz plus ± 400 kHz by piezo stack

²⁾ measured value for modules used at the ELBE LINAC

³⁾ RI guarantees < 25 W and $Q_0 \geq 1.25 \times 10^{10}$ which they have recently demonstrated for MESA

The sealing of all feedthroughs and flange connections are realized by O-rings and ISO-K standard. In addition, the module has several maintenance openings through which repairs or

adjustments can be carried out without having to dismantle the end cap of the vacuum vessel, as this always requires breaking the beam line vacuum. All technical specifications are summarized in Table 10.

4.3.3 SRF cavities

Design

The used cavities are about 1m long structures consisting of nine individual cells that are operated in the superconducting state at a frequency of 1.3 GHz. The design is based on the well-known TESLA specification¹⁶⁶, but they are made following the latest version according to the European XFEL project (Figure 43). High purity niobium with RRR>300 is used as material and the entire production, surface preparation and documentation are done as for the XFEL series production. Therefore, all XFEL specifications and test steps are used as defined by DESY. Following this procedure, high accelerating fields and quality factors can be achieved. All parameters of the cavity are summarized in Table 11.

Table 11: TESLA cavity parameters.

type of accelerating structure	standing wave
accelerating mode	TM010, π mode
fundamental frequency, f_0	1.3 GHz
design gradient, E_{acc}	12.5 MV/m
quality factor Q_0 at E_{acc}	$\geq 1.0 \times 10^{10}$
dynamic loss, P_{diss}	15 W
active length, L	1.038 m
R/Q ¹⁾	518 Ω
$E_{\text{peak}}/E_{\text{acc}}$	2.0
$B_{\text{peak}}/E_{\text{acc}}$	4.26 mT/(MV/m)
Lorentz force detuning	1 Hz/(MV/m) ²

¹⁾ we define the shunt impedance by the relation $R = V^2/(2P)$, where P is the dissipated power and V the peak voltage in the equivalent parallel LCR circuit.

Fabrication

The fabrication procedure of the cavities consists of deep drawing and EB welding of the parts into a cavity assembly. This procedure is well established and has more than 20 years of industrial fabrication experience. Half cells are produced from 2.8 mm thick Niobium discs pressed into shape using a set of dies. Two half cells are joined at the iris with an EB weld to form a dumbbell. And after proper cleaning, eight dumbbells and two end group sections are finally assembled in a precise fixture to the final cavity.

Since even tiny surface contaminations are potentially harmful as they decrease the quality factor and may even lead to a thermal breakdown/quench of the superconductor, a perfect cleaning of the inner cavity surface is of highest importance. Cavity treatment and assembly is therefore

¹⁶⁶ B. Aune et al., Phys. Rev. ST Accel. Beams **3**, 092001 (2000)

carried out in ISO 4 (ISO 14644-1) clean rooms and the preparation is done following the XFEL standard for industrial production.

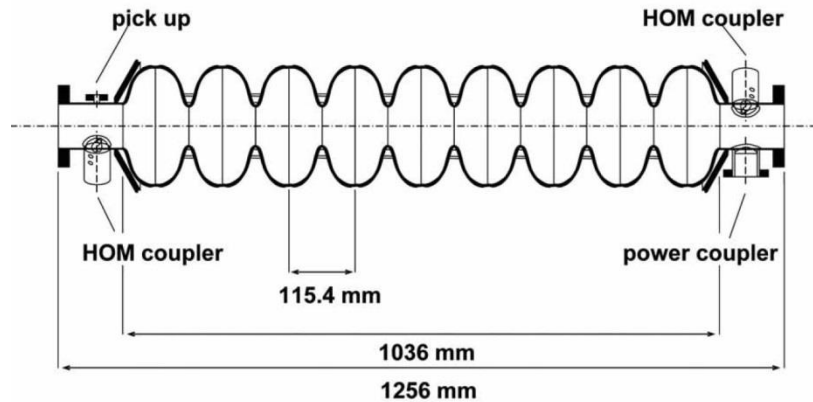


Figure 43: Cross section view of a complete nine-cell cavity.

Cavity performance

RF performance tests for SRF cavities are a crucial tool for quality control. Right after production the performance is determined by measuring quality factor Q as a function of the accelerating gradient in so called a vertical test. The needed infrastructure is available at DESY and frequently used by RI and other external users. Just to give an example for the today's standard; the recently procured RI made 9-cell TESLA cavities for ELBE have achieved accelerating gradients of $E_{acc} = 35$ MV/m and beyond (see Figure 44, left).

Despite this outstanding value, a significant reduction in performance during CW operation later at the accelerator are to be expected. Frequently discussed reasons are:

- Particulate contamination during cleanroom assembly of the cavity and the entire periphery,
- Particulate contamination during operation due to their migration into the cavity, particulates are produced by moving beam line elements such as shutters, screen stations, beam kickers
- Surface contamination from outgassing of beam line elements, associated with formation of surface deposits and adsorbates
- Higher residual magnetic field than in the vertical test due to less efficient μ -metal shielding

The gradient currently guaranteed by Research Instruments RI is $E_{acc} = 12.5$ MV/m at a quality factor of $Q_0 = 1.25 \times 10^{10}$. This value can be considered as conservative, since it is also achieved by the almost 20-year-old ELBE cavities but with the exception of the Q_0 (Figure 44, right). Higher gradients, especially with a significantly higher quality factor can be achieved with the so-called N-doping developed for LCLS-II¹⁶⁷. This involves, in addition to the XFEL standard preparation an increase of the furnace degas temperature from 800 to 900° C followed by the actual n-doping at 800° C in a 25 mTorr nitrogen atmosphere and later a fast cooldown between 15K and 9K. The latter is important for a proper magnetic flux expulsion. However, N-doping requires a reduction

¹⁶⁷ J. N. Galayda, Proceedings of 9th International Particle Accelerator Conference (2018)

of the residual magnetic field to 5 mG or 0.5 μT , which clearly requires a double layer of high-permeability magnetic shielding and a demagnetized vacuum vessel.

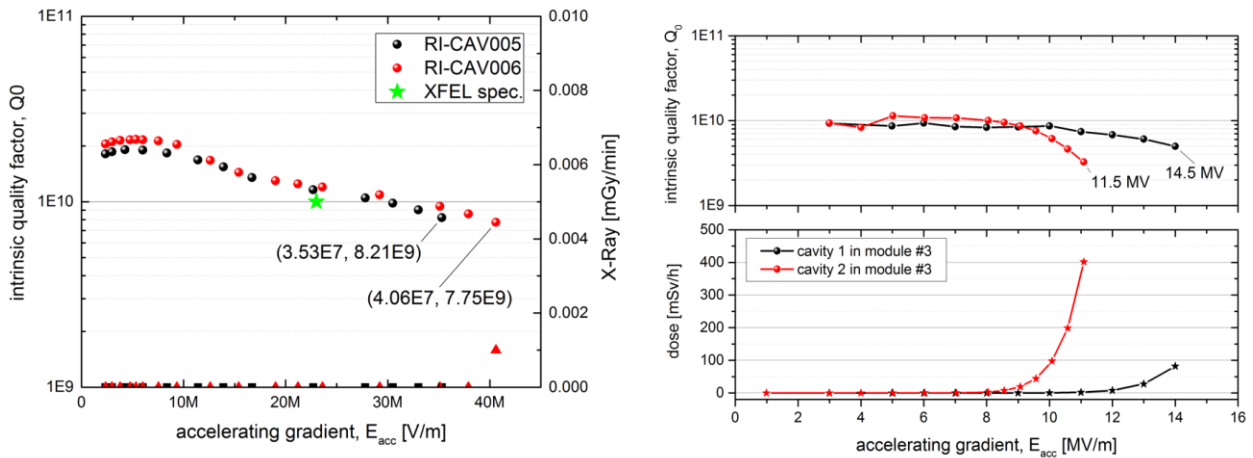


Figure 44: Vertical test results of two RI made 9-cell TESLA cavities (left) and the usable operational gradients of two almost 20 years old TESLA cavities installed in the ELBE accelerator tunnel.

According to M. Checchin at the last SRF conference on 25-30 June 2023, who presented the most recent results from SLACs LCLS-II commissioning, TESLA type cavities produced and processed based on the latest technology easily achieve $Q_0 > 2.7 \times 10^{10}$ as well as $E_{\text{acc}} > 18 \text{ MV/m}$ on average in the cryomodules. And even 24 MV/m could be demonstrated for the first 5 LCLS-II-HE cryomodules.¹⁶⁸ But even more important for our project are the most recent on-site commissioning results of both MESA modules built by RI. For all four cavities an unloaded quality of at least 1×10^{10} at 12.5 MV/m could be demonstrated (private communication Timo Stengler, MESA).

In addition to quality factor and gradient so called microphonics is another important parameter. It describes the excitation of the mechanical Eigenmodes of the cavities by the various vibrations in its environment. Relevant sources are all rotating objects such as vacuum- and water pumps, air conditioning, compressors of the helium plant and also stochastic sources such as road traffic or seismic movements of the basement. These sources are connected via different transfer media, such as beam pipe, RF waveguide, basement and support frames but also via the liquid helium itself to the cavity. If the excitation spectrum after transmission coincides with the mechanical eigenmode spectrum, undesired resonant excitation may happen. These have to be damped by suitable design measures on the transmission line or the cryomodule or the cavity itself. Since this is only possible within limits, a feedback system, the low-level RF (LLRF) is used to stabilize amplitude and phase of the RF field (see Section 4.10). For the project described in this document, both the transmission path and the excitation spectrum are still unknown. However, the measured behavior of the cavities operated at ELBE can serve as an estimate for microphonics to be expected. For these cavities, significant frequency components can be identified at approximately 10, 25, 50, 65, 75, 135, 165, 200, 265, 280 Hz, that eventually add up to a total frequency noise of $\sigma_f < 1 \text{ Hz}$ (RMS) or 10 Hz (pk-pk), respectively. Based on these results no stability problems due to microphonics are to be expected.

¹⁶⁸ M. Checchin, Pre-Press Proceedings of 21st SRF Conference, Michigan, USA (2023).

4.3.4 Power requirements and fundamental power coupler

In the currently discussed design, a beam current of $I_b=1$ mA and an accelerating voltage of $V_{acc}=12.5$ MV per cavity are anticipated. Assuming that the acceleration will occur near crest and because of the relatively large bandwidth in combination with the low microphonics, the incident and reflected power P_i and P_r can be determined by the following two simple equations, a more complex consideration is not necessary:

$$P_i = P_{diss} \frac{(1 + \beta + P_b/P_{diss})^2}{4\beta} \text{ and } P_r = P_i - P_b - P_{diss} \text{ with } P_{diss} = \frac{V_{acc}^2}{Q_0 \times r_s} \quad (9)$$

For reasonable gradients, the forward and reflected power is plotted as a function of the beam current (see Figure 45). This consideration can be important, because all currents between 0 mA and 1 mA typ. occur during accelerator tuning. Especially the reflected power for low currents and high gradients can become challenging because of the resulting standing wave. However, as the bandwidth is comparatively small, stable operation even at ambitious 15 MV with full reflection is not expected to be a problem.

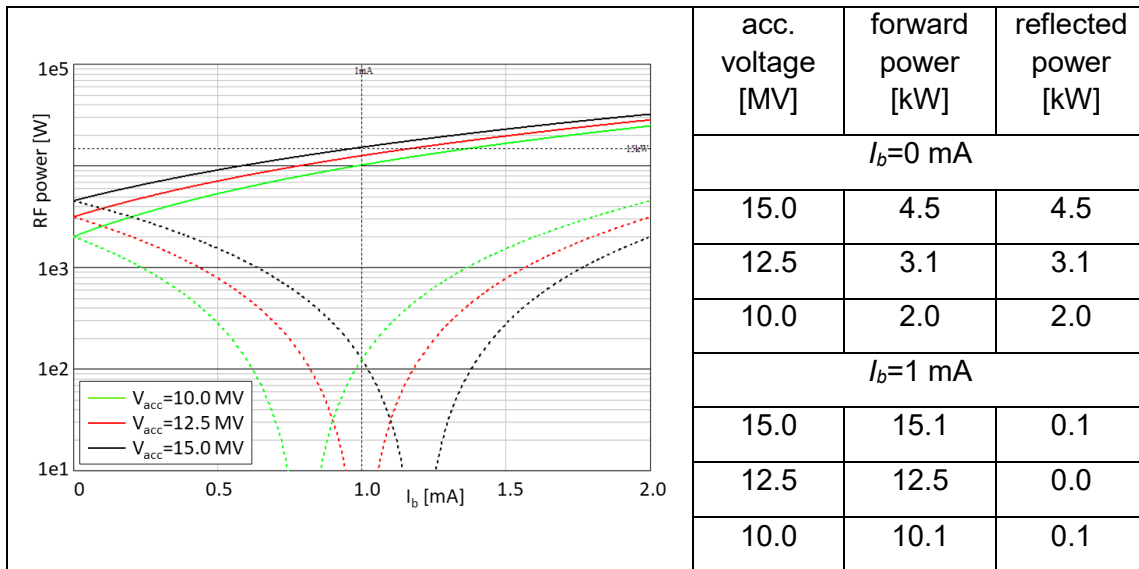


Figure 45: RF power requirements as a function of beam current for different accelerating voltage.

The required RF power of 15 kW is based on a maximum reasonable acceleration voltage of 15 MV and a nominal beam current of 1 mA. An additional 5 kW is added to compensate for cavity detuning due to helium pressure fluctuations and microphonics and to handle higher beam currents if necessary. The resulting 20 kW per cavity can be covered by modern solid-state RF power amplifier (SSPA) as explained in detail in Section 4.9.

In order to transport the power into the cavity, a fundamental power coupler (FPC) of the ELBE type is proposed. These couplers are working very reliably at ELBE and withstand an average power up to 20 kW (traveling wave) during routine operation. As the inner conductor is not moveable the external Q needs to be adjusted carefully before the final assembly by selecting the correct antenna length. Typical values are $3e6 < Q_{ext} < 2e7$ which is in good agreement with the anticipated value for DALI.

The cold part of the coupler is formed by a coaxial waveguide whose inner and outer conductors are connected to a conical ceramic, the cold window. It separates the beam line vacuum from the

insulation vacuum and is cooled by liquid nitrogen. A warm part on the other hand is realized by so-called Doorknob that transforms the coaxial into a rectangular WR650 waveguide, which is closed by a second vacuum barrier, the warm window made from quartz glass.

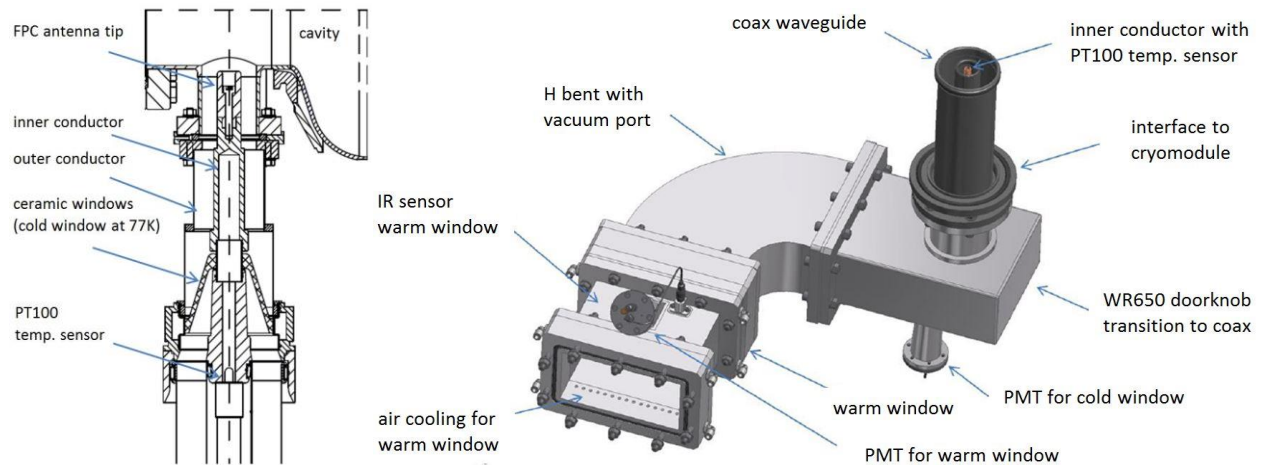


Figure 46: Cross section view at the cold part of the FPC (left) and warm part of the FPC with interlock diagnostic and doorknob waveguide transition (right).

In order to protect both coupler parts in case of unexpected events several measures are realized. Photomultiplier tubes (PMT H5783 or H11901 from Hamamatsu), one for the cold window and one for the warm window are used to detect light discharge. Additionally, the inner conductor of the FPC and the cold window is cooled by LN2 and the temperature is monitored by PT100. The warm window on the other hand is cooled by a constant airflow and monitored by Raytech IR temperature sensors and the coupler vacuum is measured by vacuum gauge (Pfeiffer IKR060). Whenever a certain threshold of at least one sensor is exceeded the RF is switched off. The fastest interlock with shutdown time of <math><1\text{ ms}</math> is realized by the PMTs.

4.3.5 SRF Infrastructure

Cleanroom complex

Since it is planned to have the cryomodules manufactured by industry, the need to assemble them in a suitable clean room is initially eliminated. However, during the 20 years of operation of the ELBE accelerator, it has become apparent that minor and major damages to the module can occur for various reasons. Also, contamination of the cavities caused by particle migration from adjacent beamlines cannot be ruled out. For these reasons, an infrastructure must be provided that allows a cryomodule to be completely dismantled, re-rinse its cavities and to re-assembled the cold string under ISO 4 clean room conditions (see Figure 47). Even if repairing a module would never be necessary, assembling the SRF gun requires the same infrastructure anyway. And last but not least the beampipe and beam line elements close to the cryomodules need to be cleaned appropriately in an ISO 6 environment to avoid cavity contamination caused particulate migration.

The following concept is proposed based on experiences gained during 20 years of running the ELBE accelerator and on the specification documents for production of XFEL 1.3 GHz cavities:¹⁶⁹

- Non-certified area equipped with car wash, dish washer and dry ice blasting for pre-cleaning

¹⁶⁹ W. Singer et al. (eds.), Specification Documents for Production of XFEL 1.3 GHz Cavities, DESY (2009).

and degreasing to introduce dirty parts into the clean room

- ISO 7 cleaning area for ultra-sonic (US) cleaning and ultra-pure water rinsing (UPWR)
- ISO 6 cleaning area with vacuum oven for mild baking and laminar flow box for ionized N₂ cleaning
- ISO 4 assembly cavity area with elevated floor, rail system and high-pressure rinsing (HPR) cabinet
- ISO 8 for cryomodule and beam line assembly
- UPWR and HPR need a water treatment plant and sufficiently large storage tank

Note: The cleanroom standard ISO 14644-1 has superseded earlier US FED STD 209E standard.



Figure 47: *ELBE cavity tandem in ISO 4 cleanroom after final assembly and leak check.*

SRF test cave

After completion at the manufacturer, the cryomodules undergo a factory acceptance test (FAT) before they are shipped to HZDR. Since the test does not include a high-power performance test at cryogenic temperatures and the transport poses an additional contamination risk to the cavities, a second onsite acceptance test (OSAT) under real operating conditions need to be carried out. For this purpose, a dedicated SRF test cave in a radiation protected area is proposed, that is equipped with 2K helium and 80K nitrogen, particulate free vacuum stations, low and high-power RF and a machine protection system to run a cryomodule safely.

During the test, both cavities were successively subjected to high RF power to determine the quality Q_0 as a function of the acceleration gradient (known as Q_{vsE}) and by this prove the specified performance. The dynamic helium loss (for Q_0) is measured by an electrical heater inside the module. Of course, such a test could also be done at its later installation location in the accelerator. Nevertheless, a suitable test cave would be required anyways. On the one hand, a spare module needs to be tested as well, but once all modules are installed in the accelerator there is no space left. And even more important, repaired or refurbished modules need to be qualified in parallel to DALI beam operation. The same of course applies to a spare SRF gun module. However, as in the latter not only RF parameters are of interest, the SRF cave must also house a diagnostic beam line that allows the SRF gun to be fully characterized in terms of its beam parameters. More details can be found in Section 4.2.5.

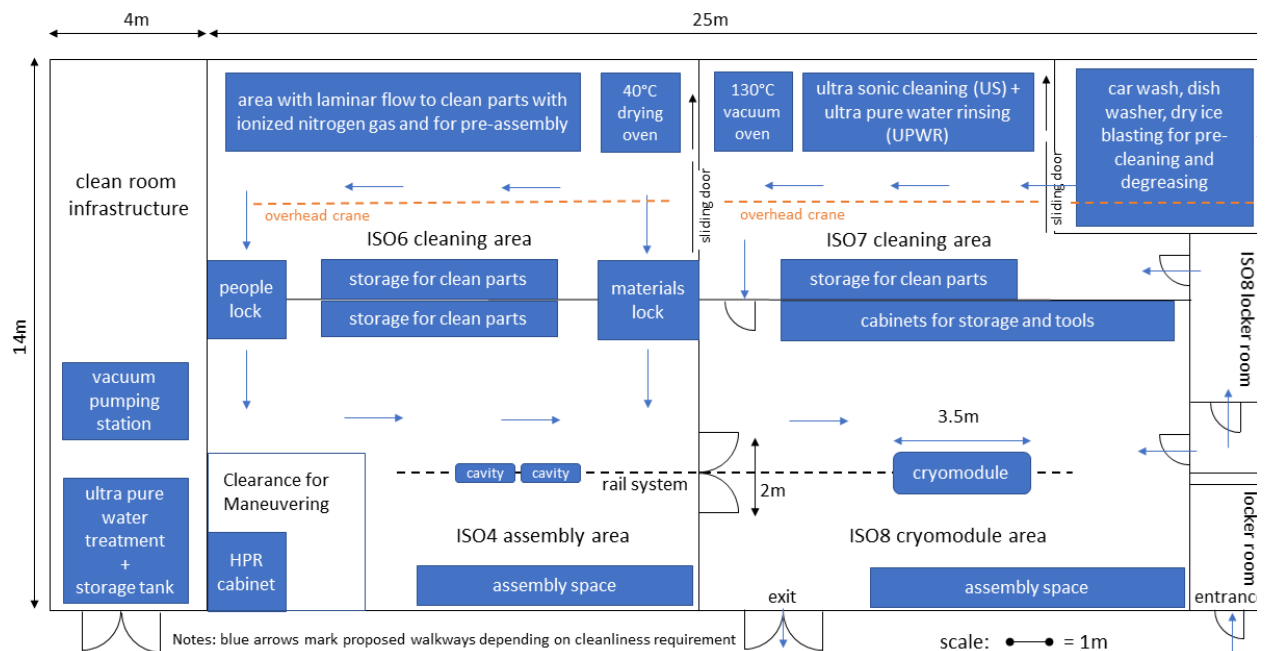


Figure 48: Proposed clean room complex, which infrastructure must be completely maintainable from the outside.

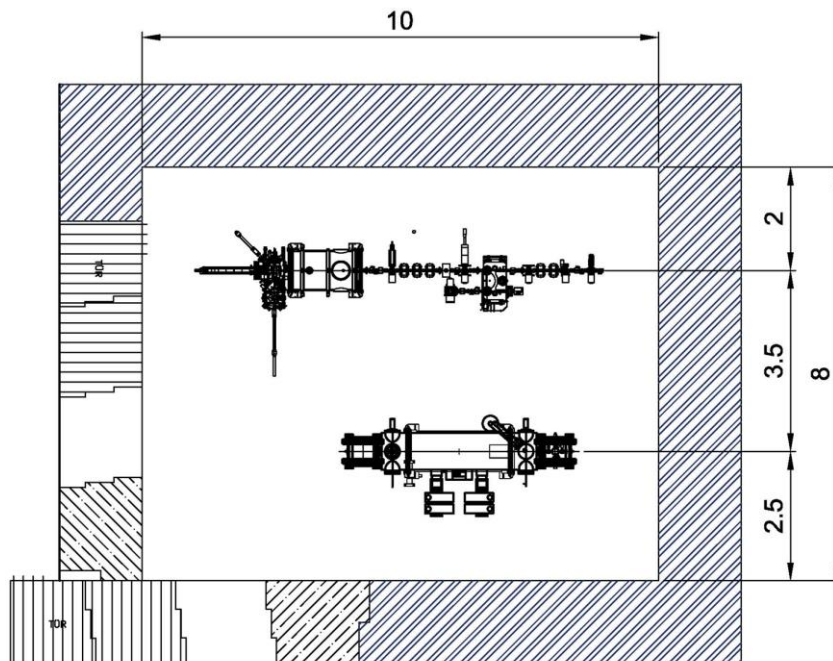


Figure 49: Proposed SRF test cave to qualify both, an ELBE type module and the SRF gun including beam parameters in parallel.

4.3.6 Cryomodule upgrade options and modifications

Research Instruments GmbH is manufacturing the ELBE-type cryomodules under license since 2004. With the exception of the modules for the ALICE ERL in Daresbury, the modules for TARLA FEL in Ankara, MESA ERL in Mainz and PoIFEL in Świerk have been continuously improved, whereas the compactness has remained unchanged (Figure 50). Some of the changes

(especially those marked in green) are of interest for DALI and are therefore summarized in Table 12 below.

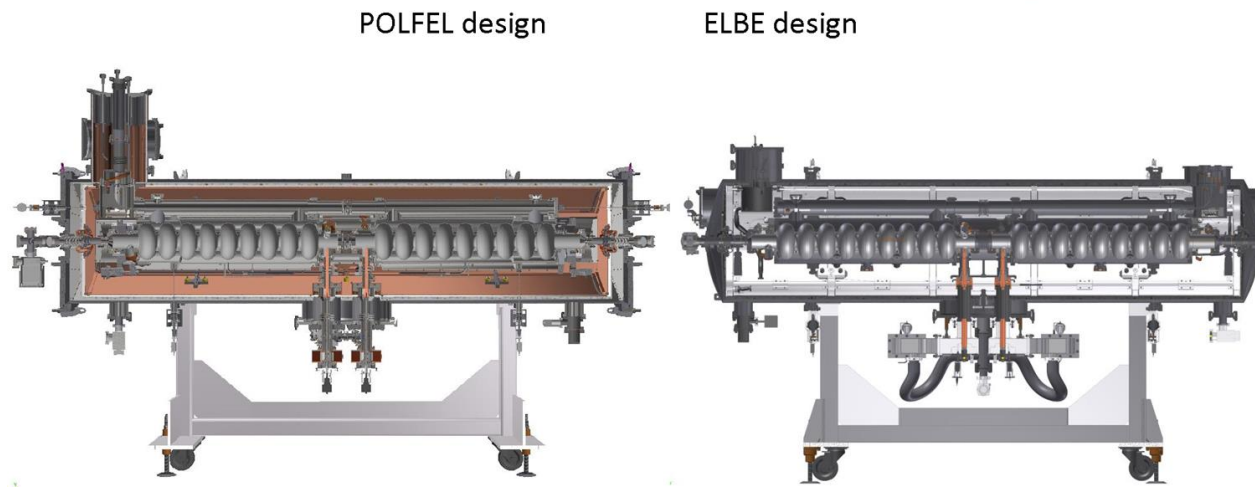
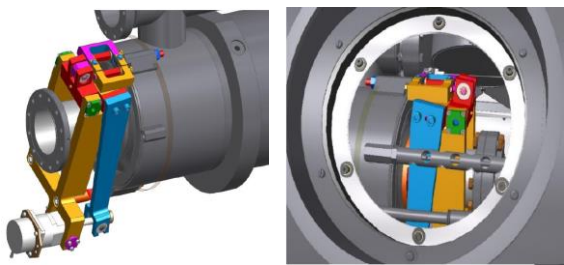
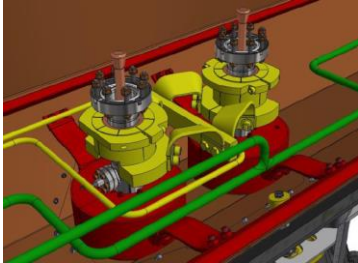
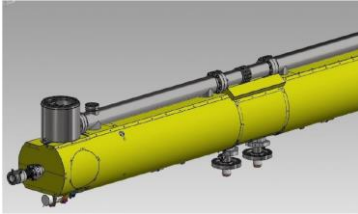
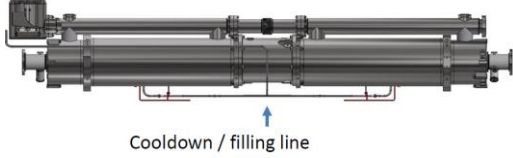
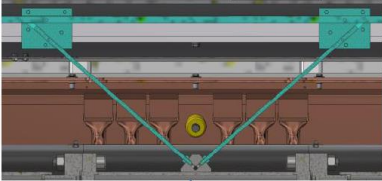


Figure 50: The most advanced ELBE type cryomodule (left) compared to its ancestor (right). Picture by courtesy of D. Trompetter, RI GmbH.

Table 12: Overview of further developments of the ELBE type module that can be considered for DALI. All pictures by courtesy of D. Trompetter, RI GmbH.

	Modification	Comments
	TARLA FEL	
1	Integration of piezo tuner in the ELBE type lever tuner of the cavity.	Solution has not yet been tested, but if it works, the well proven ELBE lever tuner could be reused
	MESA ERL	
2	XFEL Tuner with well proven piezo tuner stack replacing the ELBE lever tuner ^{*)} 	Additional access holes for cold tuner maintenance and slight modification of helium vessel needed, but concept is very well proven for XFEL and LCLS2 tuners ¹⁷⁰ . Motor with gearbox and piezo stacks are available directly from companies (Phytron GmbH and Physik Instrumente, Inc)
3	Replacement of inner Viton sealed gate valve of the cold string by an outer full metal gate valve	Eliminates aging problem of Viton and thus an additional particle source by including cryomodule lid into cold string design, which allows full string assembly in ISO4 cleanroom.

¹⁷⁰ Y. Pischnalnikov et al., 17th International Conference on RF Superconductivity, Whistler, Canada (2015).

		PoIFEL
4	TTF-3 main coupler integration ^{*)} 	Enables of variation of cavity bandwidth and by this adjustment of beam coupling, but less suitable for high CW RF power (>10kW) 5K+70K (18bar helium gas) intercept cooling circuit needed, which effects the thermal shield and the outer magn. shield as well as helium port and helium transfer line (5K,70K in addition to 2K)
5	Increased magn. shielding factor (>100) by additional cold <i>CRYOPERM</i> [®] shield around cavities 	Reduces earth magnetic field from 500 mGauss to below 1 mGauss and more important shields residual magnetic fields inside the cryovessel. But by avoidance of ferromagnetic materials and demagnetization of all cold string attachments a magnetic flux of 10-20 mGauss is achievable without an additional shielding.
6	Symmetrical cooldown line 	Uniform cooldown of both cavities by communicating pipes during filling, state of the art (XFEL, LCLS-II)
7	Improved support structure for cavity string 	O-ring replacement by durable aluminum diamond seals reduces maintenance effort and increases reliability Longitudinal fixation with Invar (1.3912) rods simplifies design but prove of concept needed.

^{*)} Position 2 (XFEL tuner) and position 4 (TTF-3 coupler) were designed and developed by DESY Hamburg. Copyright and intellectual property are exclusively subjected to DESY.

4.4 Magnets

The electron beam transport will look quite similar to the proven design of ELBE. In the preliminary facility layout 30 dipole magnets are needed to reach all end stations. There is no reason to change the established beam line cross-section of 40 mm diameter, so, also the dipole vacuum chambers should follow that size in order to keep smooth inner transitions. Thus, most dipole magnets will look quite similar to the ELBE magnets. A reuse of old magnets will be possible in

only a few cases, though, and will need a refurbishment in particular of corroded water-cooled coils and radiation-damaged plastic parts and hoses.

The needed bending radii and pole-face angles of the dipoles will only be decided by a final beam optical design and may substantially differ from those used at ELBE. In some cases, large dipole gaps are needed to accommodate wider beam lines needed for optical beam transport. All dipoles used to measure beam energy and energy spread will be equipped with NMR magnetic field probes allowing precision measurements of the magnetic field settings.

At least 65 quadrupoles will be needed to periodically re-focus the electron beam and to match different sections of the electron beam transport. For many of them, the existing design of the ELBE quadrupoles is exactly fitting. Quite a few may actually be re-used from ELBE, in particular those from later manufacturing batches with a better suited coil resistance. For some of them larger apertures than that for the standard 40 mm beam lines are needed to accommodate the optical beam. This is especially true for the matching sections in front of the undulators of the FEL oscillator and radiator.

To compensate beam trajectory deviations due to background and stray magnetic fields about 40 steerer pairs (horizontal/vertical) will be needed. With the exception of the thermionic injector we will exclusively use the hybrid steerer designed which was introduced at ELBE when designing the THz facility. These have the advantage of a more compact build and lower stray fields. In those cases where steerers are mounted in close vicinity of larger magnets with extended fringe fields the shunting of these fields by the iron yoke of those steerers needs to be considered in the magnetic design.

The steerers as well as the quadrupoles require only low-power supplies. Emphasis should be put on supplies that allow a sufficiently fast ramping of the current. With the rather low inductance of these devices this is technically possible and allows a great reduction of the beam line setup times and improved reproducibility of a beam-based alignment using automated procedures.

4.5 Undulators

4.5.1 Undulators for the mid-IR source

To cover the wave length range from 10 to 100 μm with the available beam energy up to 50 MeV an undulator with period about 100 mm is needed. It has to deliver a K_{RMS} parameter of minimum 2.0 at a possibly large gap. As was discussed above, the limited free gap inside the undulator vacuum chamber limits the achievable wavelengths due to diffraction losses. To reach a good overlap to the THz source the largest possible wavelength should be realized. Given the diffraction losses lasing above 150 μm seems unlikely.

To explore the limits, we have scaled the ELBE U37 design to the larger period length. It is a hybrid design with $\text{Nd}_2\text{Fe}_{14}\text{B}$ magnets with $B_{\text{R}}=1.30$ T remanence. Using Vanadium Permendur poles a pole surface field of 2.2 T has been reached yielding a maximum $K_{\text{RMS}}=1.37$ at 17 mm gap. Assuming the same pole surface field and relative pole length of 13.5% of the period for a 100 mm undulator a maximum $K_{\text{RMS}}=2.4$ can be reached at 55 mm gap. This allows lasing at 100 μm with 30 MeV beam energy. In principle it may be sufficient to reach $K_{\text{RMS}}=2.0$ to lase at 100 μm with 25 MeV beam energy but this would limit the wavelength scan range at constant energy.

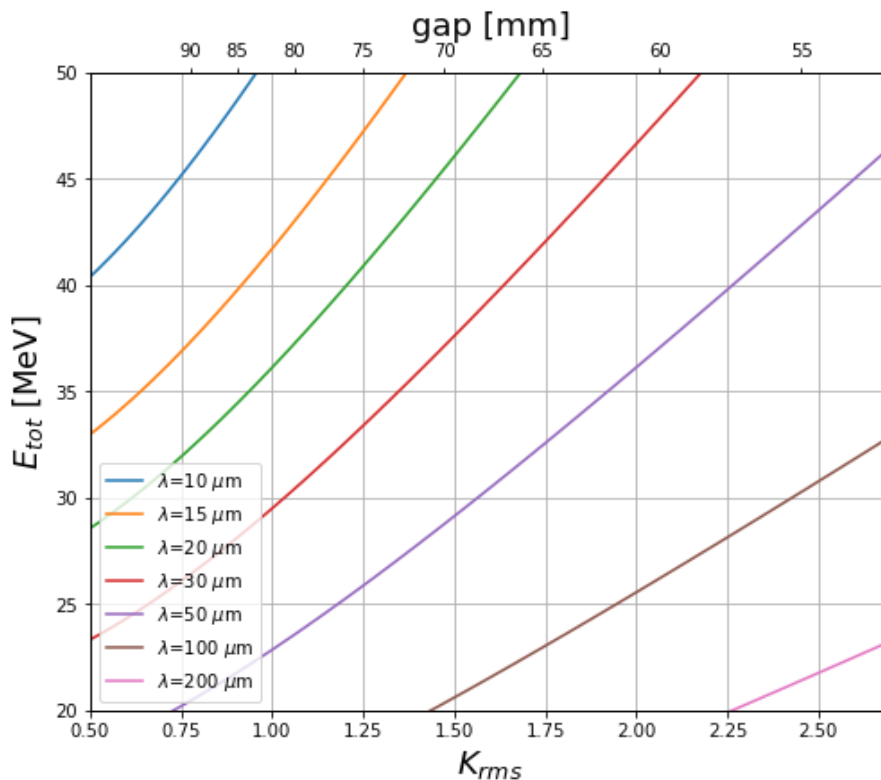


Figure 51: Wavelength tuning range of an undulator with 100 mm period length.

In the design shown here a scan spanning a factor 5 in wavelength could be possible whereas with a more limited undulator parameter only a factor 3 could be reached. A longer undulator period could increase the available K parameter at the same gap. This, on the other hand, greatly reduces the safety margin for truly reaching 10 μm wavelength with the available beam energy as for K below 0.75 or undulator gaps above 90mm the FEL gain drops significantly.

The proposed U100 design pushes the limits of what can be done with room-temperature permanent magnet hybrid designs. It essentially offers the same performance as the ELBE U100 at twice the vacuum gap.

4.5.2 Undulators for the THz sources

For the super-radiant THz sources undulators very similar to the ELBE U300 are needed. In fact, this undulator could be re-used at DALI with minor modifications. It is an electromagnetic design with 300mm period length and reaches a maximum field of $K=8$ at a fixed gap of 100 mm. It has 8 full periods which is approximately the optimum length for reaching the highest THz electric field strength at a radiation bandwidth slightly above 10%. A second undulator delivering a higher spectral brightness on axis should have about 20 periods of the same length.

Some further consideration is required concerning the technology of both undulators. The ELBE U300 works with a power dissipation of ~ 100 kW at full field. The limited effectivity of the power supplies and the necessary cooling circuits further increase the total power consumption of the device. A permanent magnetic or hybrid design would require substantial amounts of magnetic materials but one can get away with using rather low-grade materials. Recently, it was claimed that such a device could be almost equal cost as the present electro-magnet. There would be no need for power supplies or cooling, only a gap-change mechanism is required. Considering the

total cost of ownership over the lifetime a permanent magnet driven design may be the more economic and sustainable alternative.

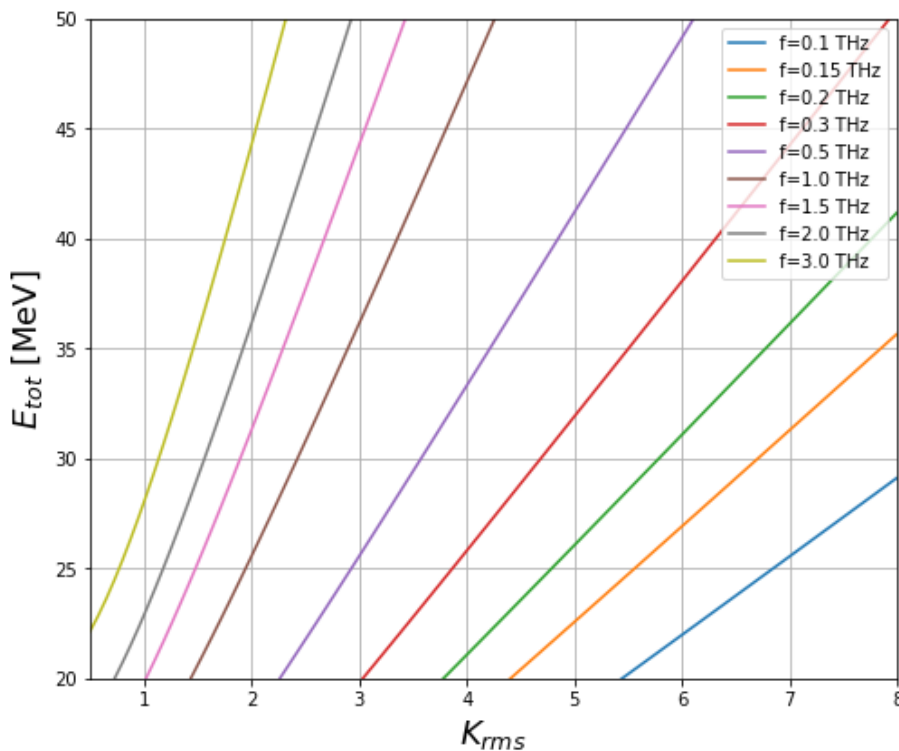


Figure 52: Wavelength tuning range of an undulator with 300 mm period length.

4.6 Beam dumps

After interaction has taken place in the respective secondary radiation sources, the electron beam must be absorbed in a beam dump in such a way that the electron beam power of maximum 50 kW is safely and efficiently absorbed and transferred to a cooling circuit, and as little dose rate background as possible and as few neutrons as possible are produced.

The beam dumps are located at electron beam level within the caves. Additional shielding by boron-loaded polyethylene and lead reduces neutron and gamma-ray radiation dose rates inside the caves. Where needed, the beam dump vacuum and the beam line vacuum are separated by a cooled niobium window.

Two types of beam dump bodies can be considered: either aluminum bodies or graphite bodies. Both variants have been successfully employed at ELBE and many years of experience have been gathered. The two types are presented below and their respective advantages and disadvantages are compared in Table 13.

Aluminum beam dump

The aluminum beam dump consists of a cylindrical highly pure aluminum core (Al 99.6), which has a conical depression with 90° opening angle at the entrance in order to increase the surface area for the impinging electron beam thus reducing local thermal loads. The elemental composition of pure aluminum, here less than 0.5 % of iron and silicon being the main components, significantly reduces long-lasting activation by photo-neutron and neutron capture. The aluminum body has a mass of about 250 kg. Bimetallic Al-stainless steel flanges are welded

onto the aluminum body carrying ultra-high vacuum gaskets. Cooling tubes are cast into the high-purity aluminum core to remove the absorbed heat. The cooling tubes are made of low activatable stainless steel and the cooling water flow rate is about 70 l/min at maximum beam power.¹⁷¹ A major advantage of the aluminum body is that no window would be needed, the aluminum block could be directly connected to the beamline vacuum.

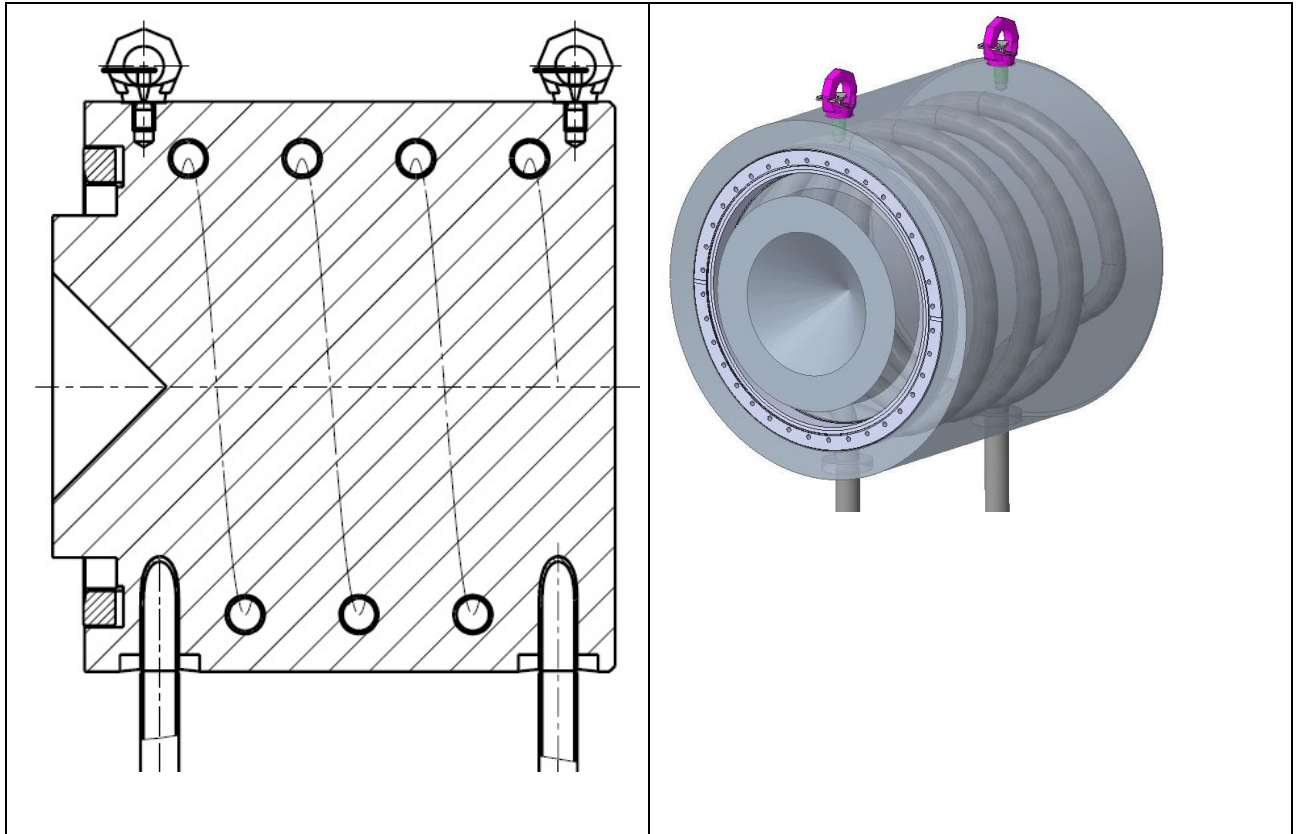


Figure 53: Aluminum body with stainless steel cooling coil entering from below. The electron beam enters from the left.

Graphite beam dump

The graphite beam dump internally consists of a compact core of ultra-pure graphite in the shape of a cylinder, which has a pointed conical depression in the entrance area in order to increase the surface area on which the electron beam impinges, thus, reducing local thermal loads. The graphite body is contained in a stainless-steel vacuum vessel. The cooling water is guided along the wall of the stainless-steel vacuum vessel. The low thermal conductivity of graphite leads to a strong heating of the graphite body up to 1300°C. The heat exchange to the cooling water takes place exclusively by thermal radiation from the graphite surface. Therefore, an uninterrupted cooling water supply for at least 5 hours after switching off the beam is required to exclude a loss-of-coolant accident. The cooling water flow rate is about 70 l/min at maximum beam power.

¹⁷¹ I. Kösterke, Sicherheitsbericht für das Zentrum für Hochleistungsstrahlenquellen zur Erforschung extremer Zustände der Materie im Gebäude 540/542, (2018).

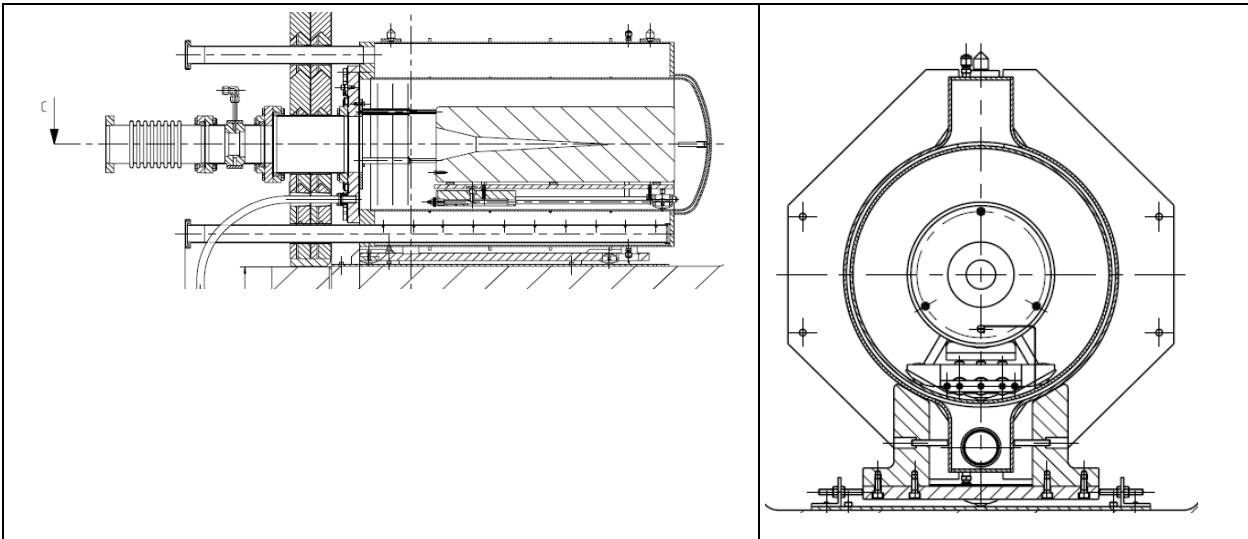


Figure 54: Graphite body with stainless steel vacuum vessel for guiding the cooling water. The electron beam enters from the left.

Table 13: Comparison of the respective advantages and disadvantages of the two beam dump variants.

	Aluminum body	Graphite body
advantages	<ul style="list-style-type: none"> • Very large heat conduction • No post-cooling necessary after beam shutdown • Little activation and neutron production • Vacuum window can be avoided 	<ul style="list-style-type: none"> • Reduced activation by low neutron capture on C-12 and low neutron production from C-13 with 1.1% isotopic abundance • No melting but sublimation beyond 3900 K • Electron beam current can directly be measured
disadvantages	<ul style="list-style-type: none"> • High material purity (Al 99.5) required and bimetallic flange welding • Low melting temperature of 660°C demanding active electron beam wobbling or scattering targets • Electron beam current cannot be measured directly 	<ul style="list-style-type: none"> • Poor thermal conductivity of the material, effective cooling by thermal radiation, only • Post-cooling necessary for several hours requiring active UPS supplies

4.7 Kickers for parallel beams operation

The electron sources can generate beams at a high repetition rate, which opens up the possibility of splitting the beam to different end stations and doing parallel operation. This can be used at DALI to either operate different THz beam lines in parallel (former concept) or operate the THz option with e.g. 100 kHz in parallel with the positron option at 2 MHz.

A drawback of SRF photo injector technology is the generation of significant dark current. Parts of the electrons generated by chance through different processes in the region of the first cell are generated with the much higher resonance frequency of 1.3 GHz of the SC accelerating cells and transported with their fitting energy and phase through the beam line producing a background current at the experimental end stations.

A first approach to solve both problems is to use beam separation technology. This is the transversal deflection structure (TDS) of the beam through a beam separator or kicker often used in combination with a septum magnet in some downstream distance, separating the kicked and un-kicked beam. Table 14 shows different devices with their properties for different applications. As the table suggests, which TDS is best suited for a beam separator depends on the bunch rate, CW beam separation, and the kick voltage. In case of a CW beam, with a high bunch repetition rate, a RF cavity would be a suitable candidate for a beam separator as well as a strip-line kicker, which opens up the choice of separating beams by different patterns. Both concepts have already been developed for future applications at ELBE and will be described in the following.

Table 14: Properties of deflecting structures acting as beam spreaders.

Deflecting structure	Beam energy		Bunch rep. rate		Bunch length		Transvers voltage		Longitudinal kick homogeneity	Design, manufacturing & operation
	$\beta < 1$	$\beta \sim 1$	Hz	> kHz & CW	ps	ns	kV	MV		
Magnets	+++	+	+++	0	+++	+++	+++	0	+++	+
Beam mergers	+++	0	+++	0	+++	+	+++	0	++	+
Dielectric wave guide	+++	0	+++	0	+++	+++	+++	0	+	0
Strip-line kicker	+++	+++	+++	++	+++	+	+++	+++	+++	+
RF cavity	+++	+++	+	+++	+++	0	+++	+++	+	+++

a) Resonant kicker

The main beam parameters and the requirement of a beam separator for the current scenario are provided in Table 15. A detailed study of the different TDS¹⁷² suggested that, a RF cavity is a suitable choice as a beam separator and this is due to its inherent advantages with respect to repeatability of the kick voltage amplitude and phase, and the possibility of CW operation in MHz to GHz range. A comparative study of different RF deflecting cavity (RFDC) design was carried out and the results suggest that the normal conducting RFDC shown in Figure 55 as a suitable

¹⁷² G. T. Hallilingaiah, "Investigation and Development of a Transverse Deflecting Structure: A Beam Separator for ELBE," University of Rostock, 2023

choice for the beam separator. The desired transverse voltage is 300 kV, and this is very much

Table 15: Beam parameters considered for the beam separator design (left) and important normal conducting RFDC parameters are also highlighted (right). Calculated for the former DALI concept with 100 MeV, now for 50 MeV the voltage is reduced to one half and power to a quarter at the same 3 mrad deflection which simplifies the operation conditions.

	Notation	Value	Unit
Beam energy	E_{beam}	100	MeV
Beam velocity constants	γ, β	195, 0.9996	
Bunch charge	Q_{bunch}	1	nC
Bunch repetition rate	f_{brr}	1	MHz
Bunch length	σ_x	1	ps
Transverse emittance	ϵ_n	$\leq 5 \pi$	
Beam size	$\sigma_{x,y}$	0.5 - 1	mm
Kick angle	δ	3	mrad
Cavity width	l_x	274.5	mm
Cavity height	l_y	181.5	mm
Cavity length	l_z	610	mm
Deflecting mode			
Mode frequency	f_{def}	273	MHz
Transverse voltage	V_{\perp}	300	kV
Transverse R=Q	R_{\perp}/Q	5746	Ω
Quality factor	Q	14479	
Peak surface electric Field	E_{peak}	2.741	MV/m
Peak surface power density	S_{peak}	1.34	W/cm ²
Total surface power loss	P_{loss}	785	W

lower compared to transverse voltage of 5MV in the case of LHC crab cavity, therefore a normal conducting copper cavity would be sufficient to achieve the required transverse voltage. Further, this would ease the design, fabrication and operation of the cavity compared to a superconducting cavity. The electric and magnetic field distribution in the deflecting mode are shown in Figure 55. A charge particle gets deflected in the transverse direction due to both the electric and magnetic field, but in opposite directions. However, the transverse force due to electric field is greater compared to magnetic field and the net deflection is along the electric field (vertical plane). For a copper RFDC, an RF power of 785 W is required to deflect a 100 MeV beam by an angle of

3 mrad. To use the cavity for the 2 MHz positron beam option the cavity must be tuned to a slightly different frequency e.g. 274 MHz.

b) Strip-line Kicker

The ELBE strip-line kicker design¹⁷³ uses the common approach with two tapered active electrodes and two ground fenders (see Figure 56). The slight difference is the placing of the two ground fenders in the outer area of the electrodes. The distance between the electrodes was chosen to 30 mm having a balance of lower HV supply and still feeding the electron beam in a homogeneous field area through the kicker (see Figure 57). The design was optimized with the CST package to fit best to 50 Ω impedances, for optimal S-parameters (Figure 58) in the frequency domain as well as having best field flatness (Figure 57) in the significant area between the electrodes. F-parameters from the CST calculation plotted for a frequency range up to 0.5 GHz. In CST F-parameters are renormalized S-parameter for simultaneous excitation.

To understand the effect of the kicker on the charge distribution in a bunch, expressed in the quantity emittance the two influences, wake fields and kicker field were studied. This was done using the CST simulation package. No wake field effect was found up to 1 nC, while the kicker field itself provides a very small contribution of $\epsilon_Y \sim 0.7$ mm/mrad in the y-direction.

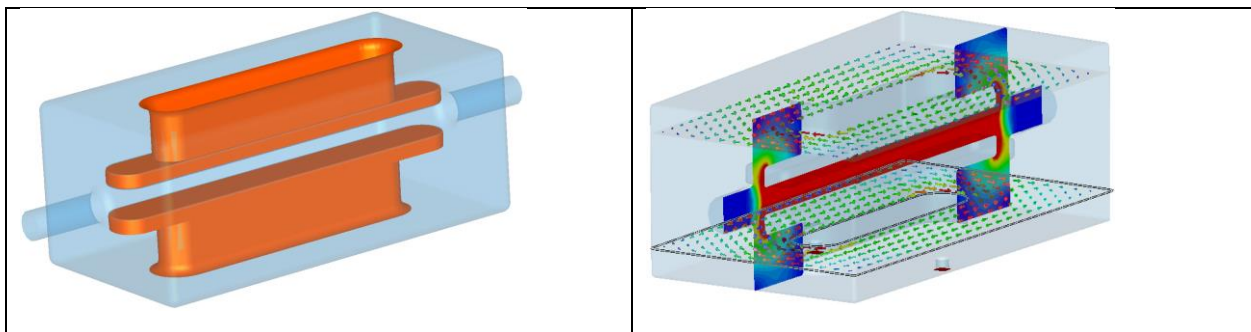


Figure 55: Mechanical design and field strength of the resonant kicker cavity.

An essential component which determines the performance of the kicker is the stability and lifetime of the high voltage generation. For the stability an amplitude jitter of less than 1% is necessary. For the Elbe kicker a high voltage power supply from the company Fidtech was used "FPG 2-500N5X2". The parameters: Maximum amplitude into 50 Ohm - 2 kV, two synchronous output channels, positive and negative, Rise time - 3-5 ns, Pulse duration at 90% - 7-10 ns fixed, Stability in the plateau (flat top) < 1%, Fall time - 4-7 ns, Maximum PRF - 500 kHz, Average output power - 500 W per channel (1kW total power). With this device all required parameters could be verified, except the max. rate at maximum voltage leads to loss of some pulses. This device cannot be operated at maximum power. Also, an operation test over very long periods of time (several months/years) has not been performed so far and would have to be tested for operation on DALI.

¹⁷³ Ch. Schneider, A. Arnold, et al, 10th Int. Particle Accelerator Conf., ISBN: 978-3-95450-208-0

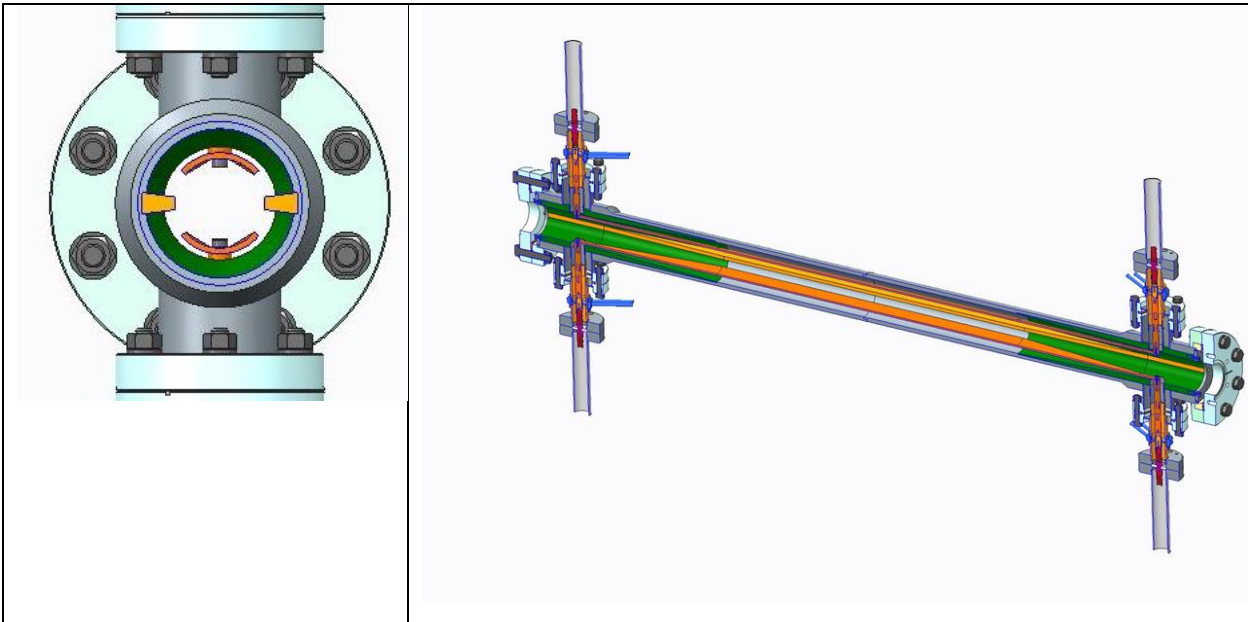


Figure 56: Mechanical design of the ELBE strip-line kicker.

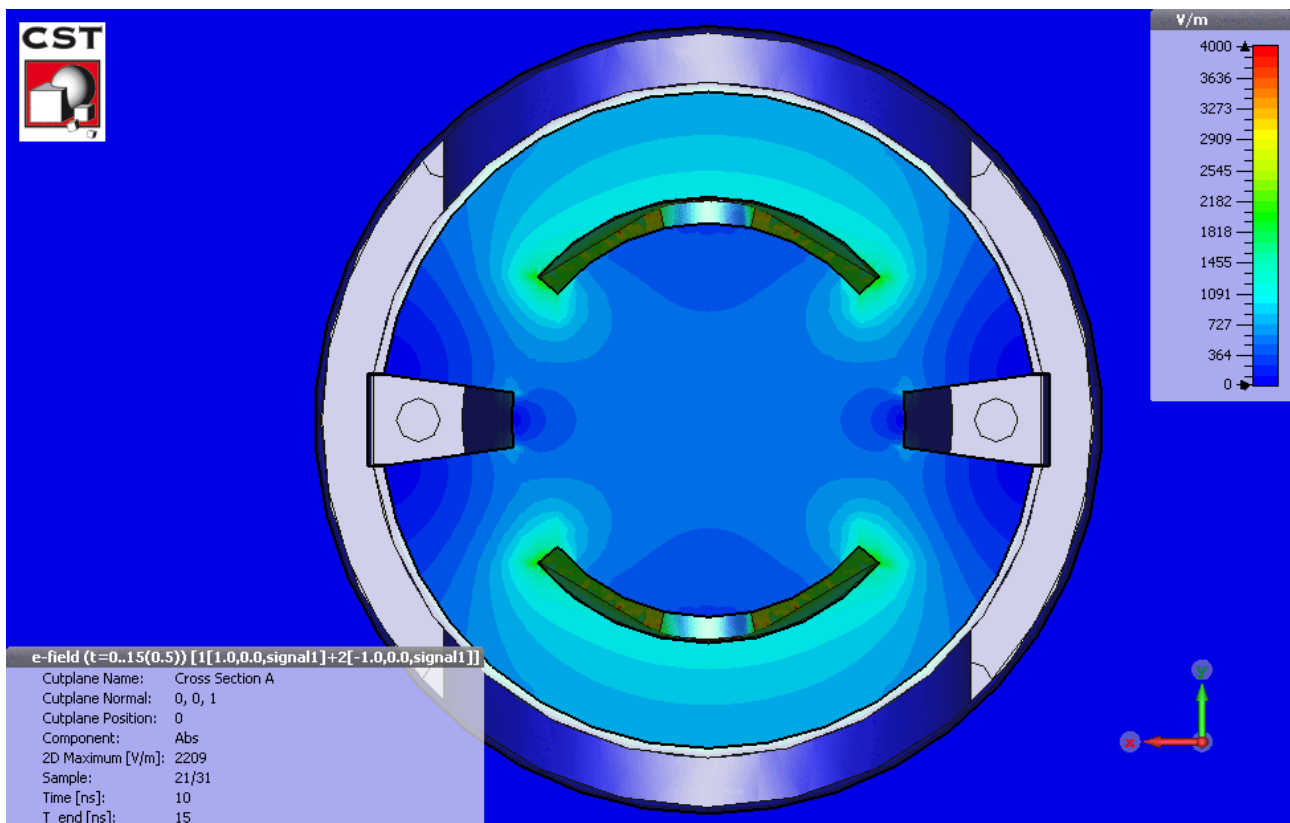


Figure 57: Deflection field strength in the cross-section view.

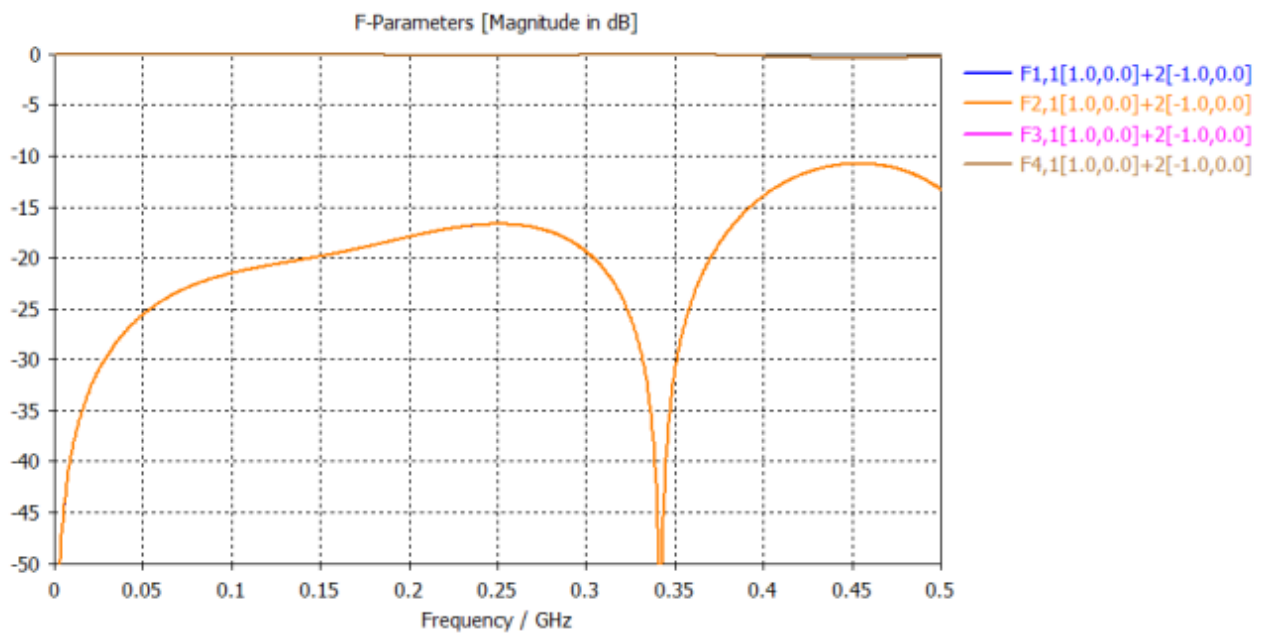


Figure 58: Simulated F -parameters of the strip-line kicker assembly.

c) Dark current suppression

For low-background time-resolved experiments the dark current from the SRF gun or other sources can significantly reduce the signal-to-noise ratio and needs to be suppressed. The dark current can only propagate through the machine if it gets accelerated to nearly the same beam energy as the wanted beam. That means it sits at the same accelerating RF phase position as the main beam but usually fills all RF buckets at 1.3 GHz with low charge. The task of the DCS is to gate the beam such that only the one bucket carrying the wanted bunch can propagate.

Both presented kicker technologies can be used for this task, albeit, in different operation modes. A resonant kicker would be operated in a zero-crossing mode where the wanted bucket passes undisturbed while all others get deflected in one or the other direction and are intercepted by an aperture. Practically, for operating the positron source, a resonant structure operating at an integer fraction of the main accelerator frequency would be detuned by 1 MHz. The resulting beating pattern gives zero deflection at the zero crossings of that 1 MHz beating frequency allowing only the 2MHz repetition rate user beam to propagate.

A strip-line kicker, however, would be used in kicking mode for the wanted beam. It produces short deflecting pulses which duration as well as their repetition rate should be as low as possible to limit the power consumption of the device. Therefore, it makes sense to produce deflecting pulses of few-nanosecond duration at the repetition rate of the wanted beam. The whole deflection then needs to be offset with a magnetic steerer such that in the idle state of the kicker the beam is lost and only the kicked bunches propagate to the experiment.

4.8 High-power RF systems

The high-power RF system amplifies the low-level RF signals described in the next section from Milliwatt to Kilowatt range. These signals are transmitted through wave guide structures and coupled into the accelerating cavities.

The required power is defined by the targeted accelerating gradient in the cavities, the beam current and the cavity bandwidth. In Section 4.3.4, describing the superconducting accelerating modules, a power requirement of 15 kW at nominal current has been defined. In order to allow for controller overhead, helium pressure fluctuations, microphonics and degradation of the power amplifiers, a design target of 20 kW per cavity has been set. In order to allow for a maximum availability and lifetime of power amplifiers, it is good practice to choose a routine working point 1 to 2 dB below maximum output.

The described DALI concept consists of two accelerators that can be combined in a flexible manner. The THz Linac is using three ELBE-like modules, each equipped with two TESLA-type cavities, while the FEL Linac is using two ELBE-like modules. In addition, a high-power amplifier is needed to drive the SRF injector for the THz Linac. In total 11 power amplifiers at 1.3 GHz with a maximum output power of 20 kW each are needed to drive all superconducting cavities of the machine.

In addition, smaller scale power amplifiers are needed to drive the normal conducting bunchers of the FEL injector. There is a large variety of vendors, models and distributors for amplifiers in the 100 W to 1 kW range.

4.8.1 RF power amplifier technology

There are several options to generate kW-level 1.3 GHz signals. In recent years the development of solid-state power amplifiers was pursued on a high level. The availability from different vendors and the level of maturity make them the ideal choice for newly designed accelerators.

Solid state power amplifiers (SSPA) use several amplifier modules, each generating 1- 2 kW of output power, combined in a rack in order to achieve several tens of kW RF power. This makes the systems scalable and comparably easy to maintain.

The systems have proven to be very reliable, since the defect of a single amplifier transistor does not lead to a system failure. The reduced gain is compensated by the other transistors and the repair can be scheduled for the next maintenance phase.

The solid-state amplifiers used at ELBE¹⁷⁴ (see Figure 59) can be a reference for the DALI RF concept. The initial design has been done by Bruker Biospin in 2009 and the systems are in user operation on a high level of reliability since 2012. The RF system branch is now with JEMA¹⁷⁵, France.

Other companies like Cryoelectra GmbH¹⁷⁶ (Germany), R&K Company Limited¹⁷⁷ (Japan) have systems in their portfolio that could fulfil the DALI requirements,



Figure 59: Solid-state power amplifier cabinet with combiner and circulator.

¹⁷⁴ H. Büttig et al., Proceedings of International Particle Accelerator Conference 2014, Dresden, Germany (2014)

¹⁷⁵ Jema Power, <https://www.jema-power.com/range/radio-frequency-amplifiers/>

¹⁷⁶ Cryoelectra, <https://www.cryoelectra.com>

¹⁷⁷ R&K Microwave, <https://rk-microwave.com>

Rohde&Schwarz (Germany) and Trumpf Hüttinger are able to derive suitable devices from their standard product line.

4.8.2 RF waveguide infrastructure

The connection between RF amplifier output and cryomodule is done using WR650 waveguides tailored for 1.3 GHz signals. Waveguides have a much lower intrinsic loss than coaxial cables and therefore are the preferred and well established medium.

After each power amplifier a waveguide circulator need to be installed. It decouples the amplifier from reflected power from the cavity and protects the system RF from damage. The reflected power is dumped into a water-cooled load resistor.

In front of every cavity a waveguide coupler needs to be installed to monitor the forward and reflected power to the cavity. These signals are used to calculate the cavity detuning, monitor the applied power and detect irregular behavior of the superconducting cavities.

4.9 Low-level RF systems

The low-level Radio Frequency (LLRF) system is used to generate the drive signal for the high-power amplifiers that feed the RF driving signal to the buncher and SRF cavities of the accelerator.

It includes a controller that is used to control the electro-magnetic field of the cavities, i.e. the field amplitude and phase. State of the art LLRF systems achieve an amplitude stability of 0.01% and a phase stability of 0.01°. Such requirements have been fulfilled at pulsed machines, e.g. at the European X-Ray Free-Electron Laser (EuXFEL),¹⁷⁸ and at machines operated in CW mode, e.g. at ELBE¹⁷⁹ using state of the art LLRF systems based on the MicroTCA (Micro-Telecommunications Computing Architecture) standard.¹⁸⁰ In both cases open-source firmware and software have been used that are actively supported by the community. Furthermore, commercially available LLRF solutions exist that achieve a similar field stability.^{181,182} They are based on MicroTCA as well.

4.9.1 Digital LLRF

State of the art LLRF systems, as the ones mentioned above, can be divided into two parts. The first part deals with the analog signals, i.e. the cavity pickup antenna signal that needs to be conditioned. Mostly the signal conditioning includes a down-conversion of the RF field frequency (1.3GHz in case of DALI) to an intermediate frequency in the MHz regime. The intermediate frequency is digitized by high-resolution low-noise analog-to-digital converters (ADC).

The second section is the digital processing implemented on a Field Programmable Gate Arrays (FPGA). Typically, the digital processing is based on the real (in-phase or index I) and imaginary (quadrature or index Q) component of the field vector resulting from a digital IQ-demodulation. Various controller types can be implemented in the FPGA, ranging from simple proportional controllers to sophisticated multi-input multi-output controllers.

¹⁷⁸ Branlard et. al., 3rd International Particle Accelerator Conference, New Orleans, USA (2012)

¹⁷⁹ K. Zenker et. al., IEEE Transactions on Nuclear Science **68**, 2326-2333 (2021)

¹⁸⁰ PICMG specification MTCA.4 Rev. 1.0, PICMG (2011)

¹⁸¹ Cerne et. al., Digital RF Stabilization System Based on MicroTCA Technology. <https://www.i-tech.si/>

¹⁸² G. Jug and A. Kosicek, Proceedings of IPAC'10, Kyoto, Japan (2010)

The resulting drive signal (I and Q) is created using high speed digital-to-analog converters (DAC). Those IQ-signals are sent to a vector modulator (VM) that is included in the analog part introduced above.

Usually, the signal conditioning is done on a dedicated module MicroTCA, called rear transition module (RTM), which also includes the VM. The IQ demodulation, signal processing, and signal conversion from analog to digital and vice versa is done on advanced mezzanine cards (AMC). Both types are commercially available in different designs from different manufacturers. This gives flexibility in the implementation of the LLRF system. E.g. for buncher cavities operated at sub-harmonic frequencies the down-conversion is not needed and a direct sampling board can be combined with a standard AMC as used for SRF cavities where a down-conversion board is used.

In summary, a digital LLRF system based on MicroTCA is a flexible system in terms of hardware components as well as in terms of signal processing. The latter can be easily changed thanks to the reprogrammable FPGA, which results in short development cycles.

4.9.2 Alternatives

Compared to digital LLRF systems analog systems provide a low loop-delay. A low latency allows a higher loop gain before negative effects apply, which in turn extends the loop bandwidth of the controller. Individual components are cheap and the systems are rather simple. However, dedicated systems cannot be bought off-the-shelf and need to be custom designed. In terms of performance, the analog LLRF can achieve similar phase and amplitude stability (see e.g. Ref. 179). In comparison to the digital LLRF, an analog system lacks flexibility and the option to apply more sophisticated control algorithms, if needed.

For DALI we prefer a digital LLRF system over an analog LLRF. It meets the requirements and is more flexible, which is mostly relevant if e.g. beam based feedbacks are considered that need to interact with the LLRF system.

Moreover, we prefer open-source firmware and software solutions over commercial solutions. This is more cost effective and flexible when changes need to be introduced to the LLRF, e.g. new feedbacks are implemented. In the past a close collaboration was formed together with DESY for the LLRF software and firmware development.

4.9.3 Long term stability

Along the field detection path, from the pickup antenna via RF cables and the RTM up to the digitization via the ADC, the signal can be altered by length changes or changes of the dielectric constant both introduced by temperature or humidity drifts. Such artificial changes of the detected RF field will be detected by the LLRF. In consequence the RF field of controlled cavity will be changed and like that temperature and humidity drifts affect the accelerating field.

In order to limiting such an effect two methods of passive drift compensation exist. First of all the RF cables have to be chosen carefully. A detailed discussion about the temperature influence on different cable types is shown in ¹⁸³. Furthermore, the cables can be housed in a tube that is flushed with air, that is temperature and humidity controlled.

For active drift compensation, it is possible to inject a calibration signal close to the pickup antenna, e.g. in the RF coupler. This signal is frequency offset with respect to the operating frequency. It will sense the same drift as the cavity signal along the field detection path and it can be used to correct the cavity signal. This method is called two-tone calibration and described e.g.

¹⁸³ K. Czuba and D. Sikora, Acta Phys. Pol. A **119**, 553 (2011)

in ¹⁸⁴. It not only corrects signal drifts in the cables, but also includes drifts on the RTM and of the ADC.

However, in order to achieve ultimate beam stability we will use a beam based feedback, described in Section 4.12. The methods illustrated above will help to minimize the effort by the beam-based feedback to compensate remaining LLRF drifts. They are crucial to keep a stable operation of the beam back feedback and not to drive it to its limits.

4.9.4 Cost estimate

The DALI design includes 6 accelerating modules with 2 SRF cavities per module. Since we propose a single cavity LLRF this amounts to 12 individual LLRF. In addition, the DALI design includes three SRF guns and a thermionic gun. The beam line section of the thermionic gun includes 2 normal conducting buncher cavities, one operated at 1.3 GHz and the other operated at 260 MHz. The latter does not require a down sampling and therefore a direct sampling RTM can be used. In summary, the setup includes 17 LLRF channels. We plan to use four individual crates for the different beam line sections, that might also be placed in different service rooms. Each crate is equipped with two power supplies to guarantee reliable operation by using a power supply redundancy. We plan to use optical uplinks from the MicroTCA Carrier Hub to powerful server computer hardware that is running the LLRF software applications for all LLRF installed in the crate. Alternatively, MicroTCA based computers realized as AMC boards could be used. In that case, we will run at maximum 2 LLRF software applications per AMC due to their limited computing power. Although the option without the optical uplink seems to be the preferred option it has some drawbacks. Namely the limited computing power per AMC computer and the limited network bandwidth. The latter fact is relevant for streaming e.g. DAQ data to a central data storage. Contrary, the server computer hardware allows to upgrade system components over time and offers network links with much higher bandwidth. In addition, one does not depend on MicroTCA vendors and a limited variety of AMC CPUs, but one is open to a huge variety of server manufacturers and available system components.

4.10 Timing system

The timing system generates trigger and clock signals for all accelerator subsystems and user experiments on a picosecond level. It is crucial to control the electron pulse emission from the injectors, LLRF, kickers and the data acquisition of beam diagnostics.

The timing signal generation needs to be locked to the RF master oscillator in order to emit trigger patterns with the correct phase and precise timing with respect to the RF fields or connected oscillators.

State of the art systems use a single timing pattern generator that is source of all timing signals of the machine. The signals can either be send out directly to remote receiver station along the accelerator or translated into a stream of events that can be used to generate specific patterns derived from the event structure. The timing generator and the receivers are usually connected using optical fibers to transport the timing data stream.

There are different commercial and licensed to industry solutions available which offer similar performance.^{185,186} A system that is widely used for accelerators is the Micro Research Finland (MRF) timing system. The hardware is available for different computing platforms like VME and

¹⁸⁴ E. Janas, K. Czuba, U. Mavrič, H. Schlarb, Proceedings of IBIC2016 (2016)

¹⁸⁵ A. Hidvégi et al., 18th IEEE-NPSS Real Time Conference (2012)

¹⁸⁶ Micro Research Finland, <http://www.mrf.fi>

MicroTCA and the main software parts are open source and maintained by the accelerator community. It offers timing system signal generation on picosecond level, drift compensation for the fiber distribution network and a large variety of output modules to generate different logic levels standards.

For DALI a similar system can be applied as it has been for the ELBE accelerator.¹⁸⁷ It will need to control the bunch generation and acceleration of the THz linac and the IR-FEL linac independently, but also aligned to each other to allow the modulation scheme described above. The system will need two event master generators that have to option to run independently but also in a master-slave configuration. This scheme has been implemented for the injector section at ELBE, to allow independent usage of the SRF gun in a dedicated diagnostic beam line, while operation the thermionic injector with the main accelerator. This concept can be extended for the two accelerators at DALI.

Timing system receivers will be placed in different parts of the machine. The LLRF will need to be controlled by a receiver, as well as the gun laser and beam diagnostics. The number of receiver modules is very much dependent from the number and location of all those subsystems and can only be estimated at this point in time. The modular timing system offers a high level of flexibility to extend and modify the system structure and to integrate new hardware requiring timing signals.

4.11 Synchronization and longitudinal feedback systems

In order to explore processes on a femtosecond time scale the synchronization between table-top laser pulses and undulator radiation has to be one the same level of stability. The DALI light sources are designed to generate radiation up to 30 THz which gives a period of 33.3 fs. In order to resolve a single THz cycle a synchronization level of 10 fs or better needs to be achieved.

Core element to define the temporal stability of all photon pulses generated by the accelerator or locked to it, is the radio frequency master oscillator (MO). This device generates low noise signals which are used as a reference for the accelerating field generation, laser synchronization and injector operation.

The reference signals are used at different locations on the accelerator facility, which requires for a synchronization system that compensates all instabilities, introduced by the transport medium exposed to changing environmental conditions.

4.11.1 RF master oscillator

The RF Master Oscillator for DALI has to provide a variety of high frequency signals for the operation of the accelerating cavities. The MO can be a single device or a modular system that is generating the frequencies needed for a dedicated application at the location of use.

The essential frequencies and their application are listed in Table 16. The FEL oscillator has a resonant frequency of 10 MHz which is therefore a central element for the synchronization of connected user lasers. In addition, this frequency can be used as a common lock frequency for a low bandwidth phase lock to a Global Positioning System (GPS) signal, in order to improve the long-term stability of the oscillator system.

Signals for the operation of the LLRF systems are described in the according section and need to be generated locally and re-synchronized to the master oscillator. Special attention has to be spent on the lock bandwidth of every remote oscillator. Noise components of the reference that are within the loop bandwidth can be regarded as common-mode. That means all subsystems

¹⁸⁷ M. Kuntzsch et al., International Beam Instrumentation Conference, Saskatoon, Canada (2023).

follow the low frequency drift of the reference signal and these components can be neglected for the stability discussion. The loop bandwidth is usually set in a range from 100 Hz to approximately 15 kHz. Modern Master Oscillator systems can achieve below 2 fs rms in interval from 100 Hz to 20 MHz.¹⁸⁸

Table 16: Reference oscillator frequencies needed for DALI.

Frequency [MHz]	Application	Comment
10	FEL repetition rate	optional GPS lock
260	Subharmonic Buncher of DC Gun	rate of synchronization system
1300	TESLA cavity resonant frequency	
3900	Harmonic Lock master laser synchronization	

4.11.2 Synchronization system

The low noise RF signals generated by the Master Oscillator need to be distributed to their location of use. Usually, this transmission is done using low loss coaxial cables or by modulating the signal on an optical carrier signal and distribution via optical fibers. Both solutions are prone to jitter and drift introduced by temperature and humidity variations as well as variations caused by mechanical stress. For very short distances and well-defined environmental conditions, e.g. to connect adjacent racks, coaxial cables can be used.

For longer distances actively stabilized fiber connections are preferred to be used. Different flavors of optical synchronization systems have been developed in the last decade.¹⁸⁹ The most advanced and mature system is based on an ultra-low noise femtosecond laser that is locked to the RF master oscillator. The laser pulses are distributed through optical single-mode fibers to the remote stations where the phase of the signal can be used to synchronize subsystems. Part of the signal is reflected back in the fiber and by applying optical cross-correlation techniques the round-trip time is stabilized.

A pulsed optical synchronization system has been installed at ELBE in 2012 and provides reference signals on a 7 fs rms level, which enables high resolution user experiments on the TELBE beam line.¹⁹⁰ The detection method offers a few attosecond resolution, which leads to a jitter below 500 attoseconds and a long-term drift of 3.3 fs rms for the most modern system installed at an accelerator today.^{191,192}

4.11.3 Feedback systems

Longitudinal feedback systems are used to measure residual instabilities on the electron beam or on the photon pulse in a non-invasive manner and to compensate these instabilities using an active feedback loop. The main sources of instabilities are environmental changes like temperature drifts of beam line components, mechanical stress caused by pumps, fans or other kinds of movable devices. A proper system design aims for the reduction of noise and drift

¹⁸⁸ M. Urbanski et al., Low Level RF Workshop (2022)

¹⁸⁹ J. Kim, J. Cox, J. Chen et al., Nature Photonics **2** 733-736 (2008)

¹⁹⁰ M. Kuntzsch et al., International Beam Instrumentation Conference 2014, Monterey, USA (2014)

¹⁹¹ A. Angelovski et al., Physical Review Accelerators and Beams **18**, 012801 (2015)

¹⁹² J. Müller, MT ARD ST3 Annual Meeting, Darmstadt, Germany (2019)

sources. As described in the LLRF section, the passive stabilization of pickup cable ducts reduces the temperature introduced drifts.

In order to stabilize the critical longitudinal electron bunch parameters, like arrival-time, compression and electron energy, a beam-based feedback can be applied. Acquired diagnostic data at different locations at the accelerator is used to analyze the electron bunches and to act on amplitude and phase of the accelerating modules to keep the desired set point. If the bandwidth of a superconducting cavity is limiting the effectivity of the feedback a normal conducting structure can be used to suppress high frequency components. Based on an elaborated machine design and a comprehensive sensitivity study a complex control theory model can be designed. The model will be used to implement a feedback algorithm which reduces long-term drifts as well as fast disturbances. Figure 60 shows a simplified beam-based feedback scheme for a superconducting accelerator using a magnetic bunch compressor. The diagnostic devices are implemented behind the dispersive element while the feedback actuator i.e. the accelerating cavities are in front of the magnetic chicane.

Beam-based feedback systems have proven to achieve less than 6 fs RMS arrival-time jitter on target position and the mid-term goal is to achieve ~ 1 fs stability. A first step in this direction has been done at ELBE and a arrival-time feedback implemented which reduced the electron jitter to be low 20 fs rms jitter.¹⁹³ The majority of the residual jitter is outside of the implemented loop and will be addressed by a more complex feedback system, tailored to the accelerator's noise spectrum.

For the feedback, diagnostics need to be applied that can measure beam properties non-invasively at kilohertz rates with high accuracy. The features of the beam diagnostic elements are a key element for the beam-based feedback and is elaborated more in a dedicated section below.

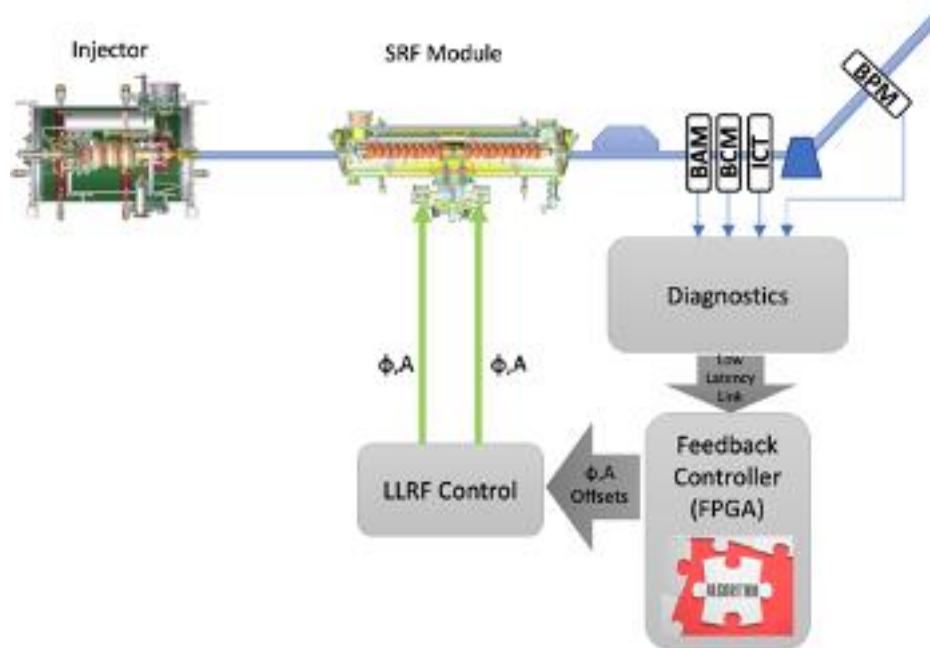


Figure 60: Schematic view of the elements of the feedback loop.

¹⁹³ A. Maalberg et.al., Phys. Rev. Accel. Beams **26**, 072801 (2023)

4.12 Machine protection system

DALI electron beams with an average power of up to 50 kW have a large potential to destroy beam line components on sub millisecond timescale. Such beam loss incidents may in turn cause vacuum inrush along with particles polluting the superconducting RF resonators and injector cathodes. Further, major malfunction of RF systems can cause severe damage to the cryomodules and the helium supply system. Such scenarios could likely cause facility shutdown for weeks to months with very high recovery cost, loss of reputation or user community. It is therefore mandatory to implement a highly reliable, state-of-the-art machine protection system (MPS). It will follow the basic concepts of the ELBE MPS,^{194,195} whereupon all techniques will be subject to a redesign for up-to-date connectivity, control system integration and faster performance.

Machine Protection is understood as a set of organizational measures combined with safety related techniques. These are implemented on different timescales using automated, often distributed subsystems. A preceding, detailed hazard and risk analysis (HRA) and error mode and impact analysis (FMEA) genesis will define the necessary organizational safety measures and the technical design requirements for accelerator subsystems. The remaining risks will be addresses by three levels of machine safety implementation: Hazardous situations are detected and damage is averted by fast interlocks. Machine mode management and instrumentation controls avoid such situations at the best, and authorization and permissions avoid dangerous operational faults on SCADA level.

4.12.1 MPS architecture

Fast Interlocks to shut off the electron beam will be handled by a fast-tripping system (FTS) using FPGA technology, which will be a successor of the existing CPLD based system at ELBE¹⁹⁶. It trips the beam sources and sends out triggers to the timing system for post mortem beam diagnostics. Its distributed I/O stages are configured according to the actual machine mode by the MPS master unit (MU).¹⁹⁷ This core component of the MPS is to host the very basic central beam mode information, such as beam line options, parallel modes, beam timing modes or the main electron beam parameters. It will interface nearly every accelerator sub system such as injectors, vacuum controls, RF controls, beam line and diagnostic controls, as well as the timing system and personnel safety system (PSS). Beam modes will be chosen on SCADA level. The MU has to check beam and timing options for plausibility, deliver this information to all affected subsystems, and ensure secure beam mode changes. Possible implementation platforms are high performance PLCs or FPGA controllers, both combining fast real time behavior with (where necessary), redundancy and failsafe technology. Not least through ELBE, there is broad R&D experience within HZDR in this field. Being a very machine specific core topic, this will be realized in-house.

4.12.2 Beam loss interlocks

Fast interlocks will be generated from beam loss monitors (BLM), beam position monitors (BPM) or differential current monitors (DCM). They are essential to avert machine damage from beam

¹⁹⁴ M. Justus et al., Proceedings of IPAC 2014, Dresden, Germany (2014)

¹⁹⁵ M. Justus, ELBE Maschinen-Interlocksystem: Systembeschreibung, Documentation of the ELBE MPS for approval of operation by federal state authority of Saxony (2019)

¹⁹⁶ M. Justus et al., Proceedings of IPAC 2014, Dresden, Germany (2014)

¹⁹⁷ M. Justus et al., Proceedings of ICALEPCS 2023, Cape Town, South Africa (2023), (to be published)

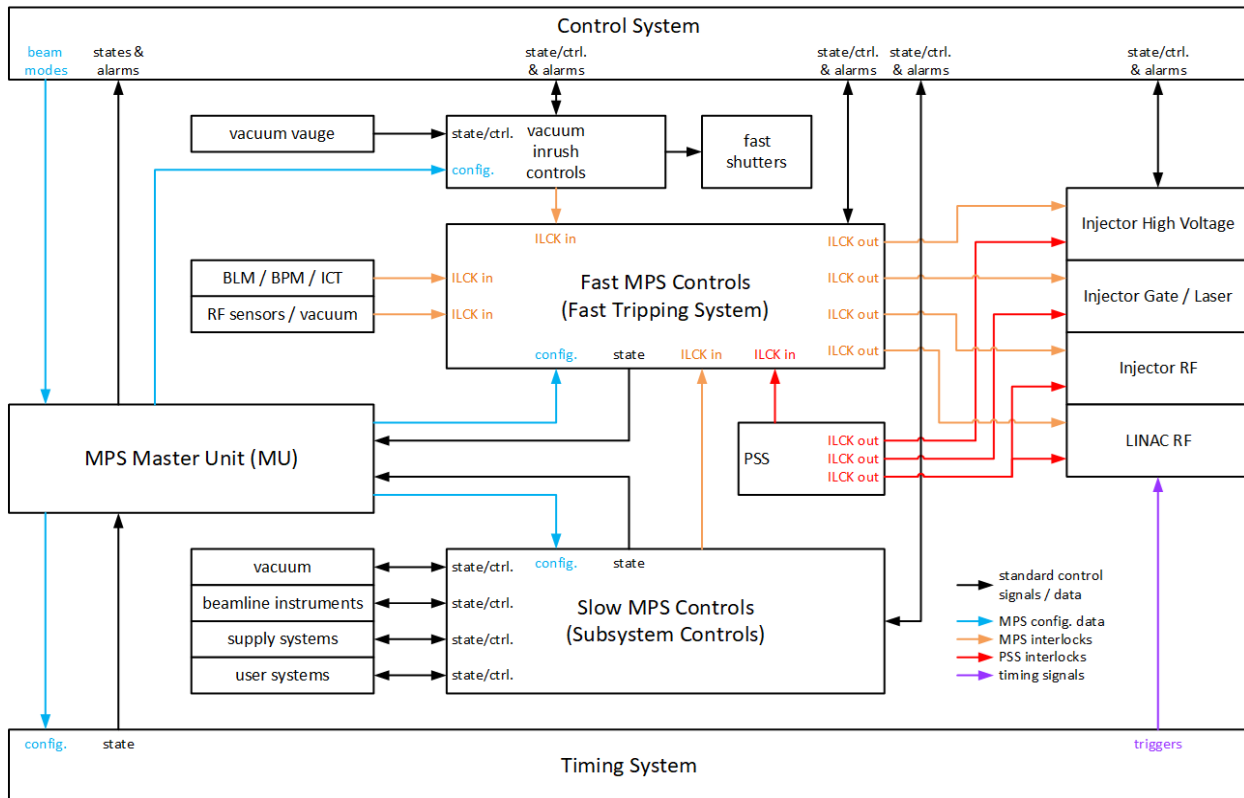


Figure 61: Machine protection system overview.

loss incidents, and will stop beam emission on a sub-millisecond timescale. As utilized very successfully at ELBE, beam loss will be detected by long ionization chamber BLMs¹⁹⁸ along the whole beam transport system, as well as a set of BPMs or ICTs. Sensors and electronics are commercially available for DALI's range of beam parameters and have also been developed in-house at HZDR in the past. Slow interlocks from temperature sensors or leakage current measurement will add an additional layer of safety against slowly emerging loss effects. Standard industrial control technology will block immersive beam line instruments at high power operation.

4.12.3 RF interlocks

MPS for RF systems utilize monitoring of vacuum and cryogenic conditions or RF parameters to instantaneously shut off the RF sources. This will be integral part of the digital LLRF controls, as well as being realized by fast interlocks. PLC controllers will ensure safe operation of the power amplifiers and RF distribution.

4.12.4 Vacuum inrush detection

Sudden severe vacuum incidents are handled by a special set of vacuum gauges, combined with fast shutters to prevent from particle transport into the accelerator cavities. Configurable, autonomously working systems are commercially available and have been used at ELBE.¹⁹⁹ Standard vacuum controls will manage vacuum sectioning, detect slow rise in pressure and handle shutter permissions.

¹⁹⁸ P. Michel, J. Teichert, R. Schurig, Proceedings of 6th European Workshop on Beam Diagnostics and Instrumentation for Particle Accelerators, Mainz, Germany (2003)

¹⁹⁹ M. Justus et al., Proceedings of IPAC 2014, Dresden, Germany (2014)

4.12.5 Radiation damage prevention

A set of radiation monitors at critical locations (i.e. dispersive section, undulators) will be used to optimize beam transport and minimize radiation damage and activation of beam line instruments. This in turn is expected to reduce maintenance effort, replacements and so the overall operational costs.

4.12.6 MPS on operation level

Authorization, limits and permissions will circumvent operational faults that could lead to improper machine states. Any machine safety violation has to trigger a specific alarm to the SCADA system that contains device information, alarm information and timestamp. Subsystems therefore need to be clock synchronized. Alarm and process value logs will be used for failure root cause analysis, so that operators can track back to device failure or operational faults.

4.13 Beam diagnostics

Since the DALI facility will reach a similar parameter space as ELBE, i.e., CW operation, an average beam current of 1 Milliampere, repetition rates of up to 2 MHz, and picosecond bunch length, most of the diagnostics will have specifications similar to the one currently used at ELBE. However, the bunch pattern at DALI will differ from the one at ELBE, as described in Section 4.1.2 (Machine operation, sources and timing). The simultaneous acceleration of interleaved beams targeted at different radiation sources requires beam diagnostics that is able to separately investigate these beams.

For tuning and for detailed characterization of an accelerated beam before it is sent to the radiation production targets at some places short diagnostic beamlines will be installed. This is especially needed for the characterization of the beams delivered by the electron sources but also some high-impedance destructive measurements like the longitudinal phase space mapping need to be placed separated from the high-current beam.

4.13.1 Beam current monitors

For beam current measurements similar methods as at ELBE can be used: Integrating current transformers (ICTs) will enable non-destructive monitoring of the bunch current of all beams. The high bandwidth of the pickup and the fast data acquisition allow the signal acquisition to be gated such that different interleaved beams can be measured independently.

The average current can also be measured as current between the photocathode (i.e., electron source) and the ground, or the beam dump and the ground. The beam line between the electron gun and the accelerating modules will also be equipped with Faraday cups (FCs), which can precisely detect low charges at the cost of destructing the beam. Therefore, the FCs will only be used during facility commissioning and for machine studies.

4.13.2 Beam position monitors

Important characteristics of a beam position monitor (BPM) are position and time resolution as well as total accuracy, geometrical claim, maturity and commercial availability. Different types of BPMs such as button, strip- line and cavity BPMs have been developed in the past. Because of the CW nature of the planned machine and because of its high bunch charge >100 pC while having moderate requirements concerning the resolution (10-100 μm depending on beamline), we will focus on the first two types (Figure 62), only.

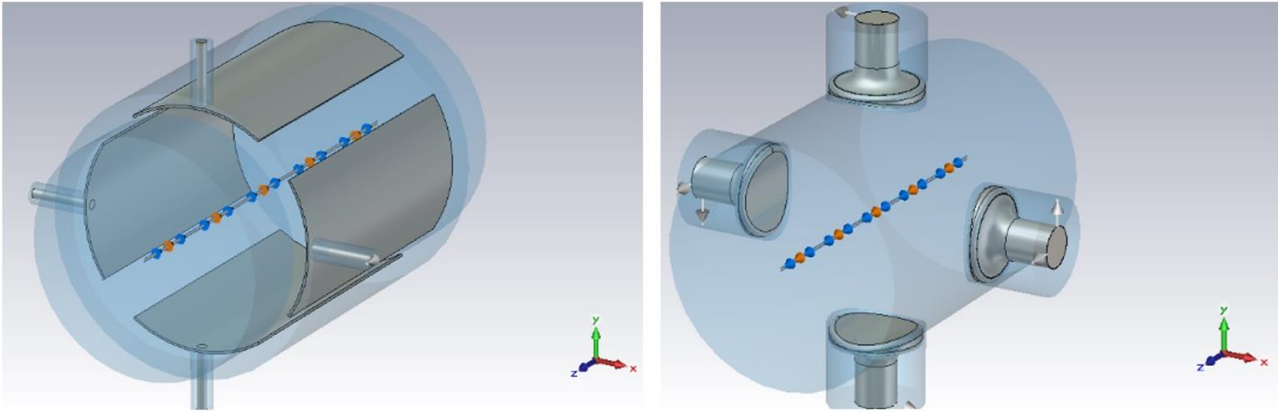


Figure 62: Strip-line (left) and button type (right) pickups for beam position monitoring.

A charged particle beam is always accompanied by electromagnetic field. In the case of a relativistic electron beam this field is perpendicular to the beam direction. If this beam is propagating in a tube with ideally conducting walls, no electrical field is allowed inside the conducting walls. This condition is satisfied, if a so-called image current flows on the inner surface of the wall. The average value of this current as well as the longitudinal distribution and the time structure follow the electron beam structure. Strip-line and button BPMs are probing this image current in the horizontal and vertical plane by either four strip-line or button sensors. By calculating the difference of two opposite signals, the horizontal or vertical beam position can be determined. The sum of all 4 signals is proportional to the beam current.

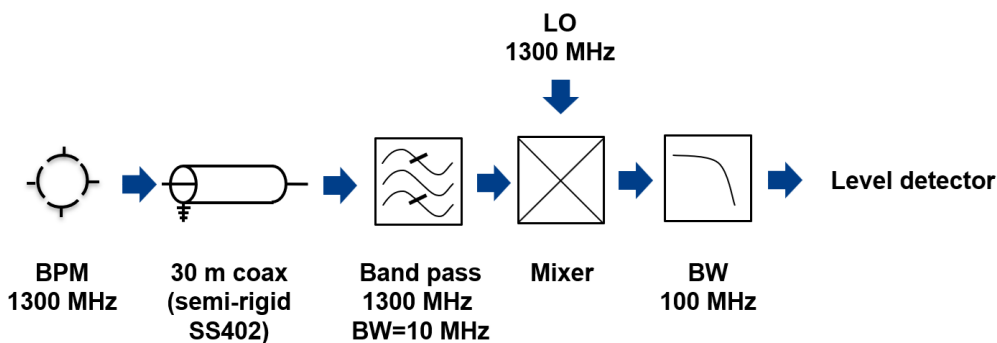


Figure 63: Simple BPM detection scheme for a 10 MHz band pass system such as Libera Single Pass E.

Currently, there is no final decision on the beamline inner diameter. Most likely there will be most sections with 35 mm, but also 50 and 100 mm. In the following the middle is therefore chosen as a compromise, but the signal amplitude can be simply inversely scaled by the dimension. E.g. a 100 mm BPM provides only half the signal amplitude.

Resolution

The resolution is typically limited by the noise of the electronics and the noise figure NF of the rest of the BPM system including cable losses. The resolution limit is defined as beam displacement inversely equivalent to the signal to noise ratio (SNR). In accordance to ²⁰⁰ one obtains:

²⁰⁰ S. R. Smith, et al., SLAC-PUB-7244 (1996)

$$\sigma_x = G \frac{\sqrt{2}\sigma_N}{2I} = \frac{G}{\sqrt{2}} \cdot 10^{\frac{-SNR}{20}} \text{ with } G_{\text{stripline}} = \frac{R_{\text{BPM}}}{2} \frac{\theta/2}{\sin(\theta/2)} \text{ or } G_{\text{button}} = \frac{R_{\text{BPM}}}{2} \quad (10)$$

where R_{BPM} is the radius of the BPM and θ the angular size of its strip-line. In order to estimate the SNR we assume a commercially available bandpass filter system, such as Libera Single Pass E electronics of the company Instrumentation Technologies.^{201,202} Such a system typically consists of a 10 MHz bandpass filter, a mixer for down converting and a lowpass filter + level detector (Figure 63). For signal modelling a Mathcad 15.0 script was used to emulate the BPM signals and its processing towards the level detector. The signal to noise ratio is finally calculated from the peak voltage at the detector, the noise voltage and the noise figure. The latter is conservatively chosen to be $NF=16$ dB, which is the same value as measured for the ELBE BPM.

$$SNR = 20\log(V_{\text{peak}}) - 20\log(V_N) - NF \text{ with } V_N = \sqrt{Z_0 k_B T \cdot B} \quad (11)$$

Finally, Table 17 is summarizing the achievable resolution for different bunch charge and both BPM types. Further improvement of $1/\sqrt{n}$ can be achieved by averaging over n bunches. Based on these results and because of their simplicity, we plan to use button BPMs wherever they are sufficient. Only in case of very strict resolution requirements we will choose a smaller number of strip-line BPMs.

Table 17: Achievable resolutions of a 10 MHz, 1.3 GHz band pass electronic for different BPMs.

all values in μm	requirement	10 MHz band pass electronics			
		50 pC	100 pC	400 pC	1 nC
$\varnothing 50$ mm strip-line	10-100	8.1	4.1	1.0	0.4
$\varnothing 50$ mm button	10-100	63.6	32.0	8.0	3.2

Sensors

For both, strip-line as well as button BPMs, there are no vendors that sell standardized sensors. The design is typically done by diagnostic groups itself while machining is realized by appropriate companies. All design issues are well understood and analytical approaches as well as 2D / 3D codes are used for it.

Examples for strip-line BPMs (see Figure 64):

- ELBE $\lambda/4$ BPM: CF40, strip-line length = 40 mm
- PEFP at KAERI (Korea): CF100, strip-line length = 70 mm²⁰³
- Prototype for ILC and CLIC, built at KEK²⁰⁴

²⁰¹ M. Znidarcic et al., Proceedings of FEL2013, New York, USA (2013)

²⁰² M. Znidarcic et al., Proceedings of LINAC14, Geneva, Switzerland (2014)

²⁰³ Ji-ho Jang et al., Transactions of the Korean Nuclear Society Spring Meeting, 26-27 (2011)

²⁰⁴ R. J. Apsimon et al., Phys. Rev. ST Accel. Beams **18**, 032803 (2015)

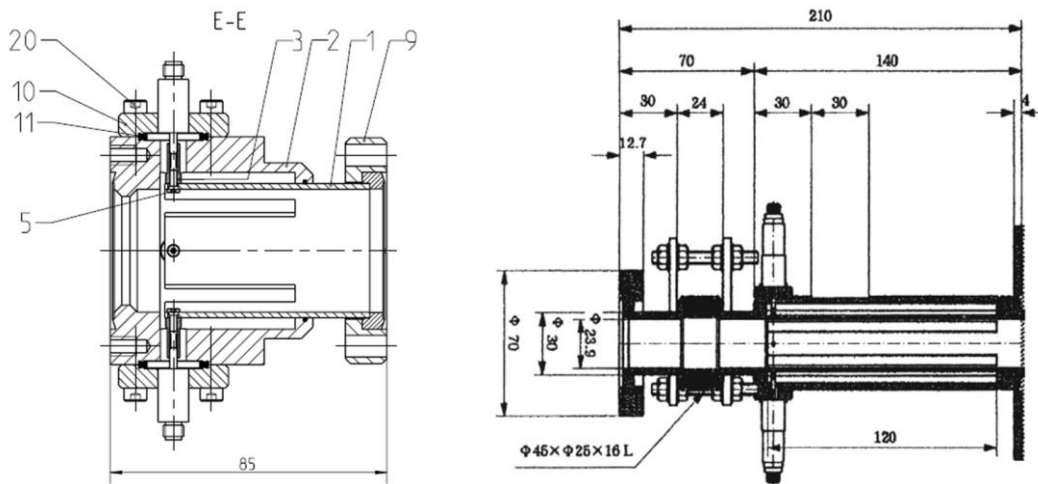


Figure 64: 2D CAD drawing of the ELBE strip-line BPM (left) and a KEK strip-line BPM (right).

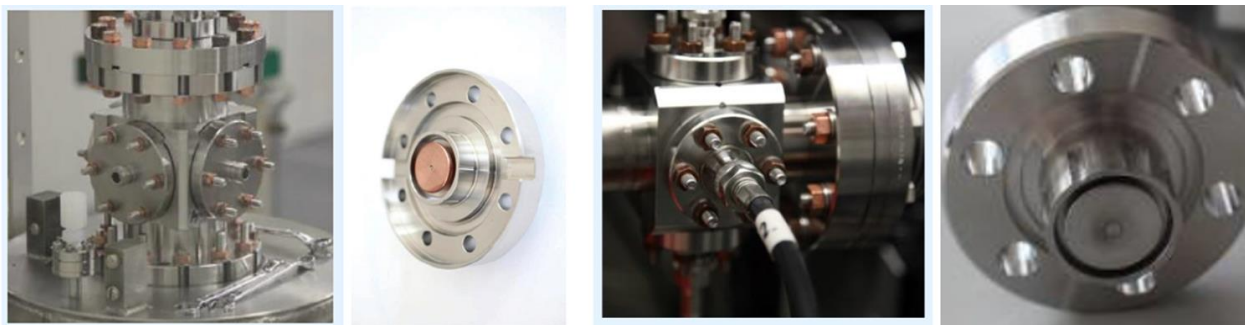


Figure 65: XFEL cold button BPM + pickup (left) and XFEL warm button BPM + pickup (right).

Examples for button BPMs (see Figure 65):

XFEL cold button pickup

- inner \varnothing 78 mm
- total length 170 mm
- button \varnothing 20 mm
- CF25 feedthrough

XFEL warm button pickup²⁰⁵

- inner \varnothing 40.5 mm
- total length 100 mm
- button \varnothing 16 mm
- CF16 feedthrough

BPM electronics

There is a various number of self-made electronics developed by the different labs and institutes (ELBE, XFEL, LCLS, etc.). But in order to reduce development effort and time we are considering a commercial system. The most advanced BPM electronic is offered by Instrumentation Technologies, a hi-tech company that has managed to capture the particle accelerator market and establish itself as a world leader in its particular niche. Its customers include some of the

²⁰⁵ D.M. Treyer et al., Proceedings of IBIC2013, Oxford, UK (2012).

world's leading national research laboratories in Asia, Australia, Europe and the Americas. A very promising all-in-one solution is the Libera Single Pass E, which is a high precision electronics for single pass applications that can handle 4 BPMs at once. Some important data are listed below²⁰⁶
207.

- analog front-end (bandwidth 10 MHz)
- real-time digital signal processing based on μ TCA
- 16-bit ADC, 40 dB dynamic, ≤ 160 MS/s
- high-level software with EPICS interface
- resolution: single bunch $< 10 \mu\text{m}$; CW $< 1 \mu\text{m}$
($\varnothing 20$ mm strip-line BPM at 120 pC)



Figure 66: *Libera Single Pass E.*

4.13.3 Arrival time monitors

Time resolved experiments require a temporal stable photon beam which receives its timing structure directly from the electron beam. Bunch arrival time monitors are a non-destructive detectors which derive the arrival time of the center of mass of an electron bunch. There are mainly two types of detectors.

First is a resonant cavity which is excited by the electron pulses passing through, which leads to ringing of the cavity's resonant frequency.²⁰⁸ By measuring the phase of the ringing signal with respect to a reference, a relative arrival time can be derived with a few-femtosecond resolution. The design is less complex and can be used for beams from single pulses up to high repetition rates. At high repetition rates the single pulse arrival time information cannot be carried out anymore, since the signal cannot ring down before the new bunch arrives. The resulting signal carries a convolution of the arrival time of the current bunch and a number preceding bunches depending on the quality factor of the cavity and the repetition rate of the beam.

Second is an electro-optical monitor which uses a non-resonant button-type pickup to extract a probe signal from the electric field of passing electron bunches. The pickup signal is fed into an electro-optical intensity modulator (EOM) which modulates actively stabilized short laser pulses coming from a laser-based synchronization system. The system allows for single pulse resolved measurements with single digit femtosecond resolution. At ELBE such a system has been deployed using a 40 GHz pickup and 50 GHz EOM which reaches a resolution of 5 fs rms at 200 pC bunch charge.^{209,210} Currently pickup designs and EOMs are under development which will allow for a detector bandwidth of 100 GHz, allowing for better resolution at even lower charge.

For DALI the electro-optical system is preferred, since it allows for higher resolution and is complementary to the laser-based synchronization system.

4.13.4 Beam profile monitors

For the observation of the transverse 2D beam profile beam viewers are foreseen. Screen stations based on single-crystal scintillators (e.g., YAG or LYSO) in conjunction with imaging optics and CCD cameras (all commercially available) are successfully used at electron machines with the

²⁰⁶ M. Znidarcic et al., Proceedings of FEL2013, New York, USA (2013)

²⁰⁷ M. Znidarcic et al., Proceedings of LINAC14, Geneva, Switzerland (2014)

²⁰⁸ A. Brachmann et al., Proceedings of the International Particle Accelerator Conference (2010)

²⁰⁹ A. Angelovski et al., Phys. Rev. Accelerators and Beams **18**, 012801 (2015)

²¹⁰ M. Kuntzsch et al., Proceedings of the International Particle Accelerator Conference (2022)

same bunch charge and similar beam energies. Both the cameras and the screen scintillators need gate/decay times below $0.5 \mu\text{s}$ to distinguish the two electron beams on the screen. Moreover, the actuator opening for the electron beam should be designed to reduce creation of wake fields. Beam viewers might also be utilized in off-axis diagnostics beamlines. A kicker magnet can be used to deflect few bunches in a pulse-stealing mode onto the observation screen to record slow changes in transverse beam size, while the majority of the electron bunches is supplied to user end stations.

Viewers in dispersive sections of the beam transport can be used to measure the energy spread of the beam.

Besides the scintillator screens as beam viewers wire scanners are envisaged: They allow precise measurements of the transverse bunch profile with high dynamic range, allowing to accurately determine the beam halo if needed. Due to their minimal interaction with the beam, wire scanners can be regarded as non-destructive devices.

Measurements of the transverse emittance will be possible using quadrupole scans at the sections with 50 MeV beam energy. At low energies, i.e., after the electron gun, slit masks and so-called pepper pot grid masks will be utilized. It will be possible to determine the beam energy and energy spread on screen station in dispersive sections, both after the gun, and at 50 MeV beam energy.

4.13.5 Longitudinal phase space diagnostics

The DALI design foresees magnetic, nonlinear bunch compressors, where the first- and second-order energy-time-correlations can be modified independently. Tuning the compression requires precise knowledge of the correlation, which demands a transverse deflecting cavity (TCAV) in conjunction with a view screen in a dispersive section for observation of the longitudinal phase space. The TCAV will also give rise to measurements of the bunch length and profile, as well as the transverse slice emittance when used in conjunction with a quadrupole scan method.

Where knowledge of the beam profile is sufficient electro-optical sampling (EOS) methods and THz interferometers^{211, 212} will be employed, as currently done at ELBE.

A detailed mapping of the longitudinal transfer function will be necessary for the non-linear bunch compressors employed in the THz generation. This will be done measuring the transit time through the bunch compressor using two arrival time monitors while varying the beam energy.

4.13.6 Beam loss monitors

For a high-average power machine like DALI the detection of any lost beam currents is of crucial importance to protect the machine from damage. A focused electron beam can melt within less than one millisecond through a stainless-steel beam tube, even small fractions of the beam (less than $10 \mu\text{A}$) can over-heat beam line components like vacuum seals. Beam currents of $1 \mu\text{A}$ when lost over some time lead to radiation damage of all non-metallic parts. Therefore, loss measurements and interlock mechanisms are of great importance. While this loss measurement mostly belongs to the machine protection system it also delivers valuable diagnostic information during beam tuning when the detection of small halo fractions of the beam is important.

At ELBE long ionization chambers made of air-insulated RF cables are used to detect the radiation produced by any lost beams. This design has proven very effective, for large loss values an interlock reaction time of $100 \mu\text{s}$ can be reached, the interlock threshold is set to $1\text{-}10 \mu\text{A}$ of

²¹¹ P. Evtushenko, J. M. Klopff, Proceedings of IBIC2012, Tsukuba, Japan (2012)

²¹² N. M. Lockmann et al., Phys. Rev. Accel. Beams **23**, 112801 (2020)

average loss current depending on the location. Even very small loss fraction down to 1% of the interlock threshold can be reliably detected. One advantage of the mechanical design is that larger segments of the beam line can be covered by a single cable – the segmentation is chosen just fine enough to allow the identification of the beam line section of origin.

In addition, at a few critical positions like small apertures in the beam line localized calibrated radiation dose rate monitors will be installed. These can be of higher sensitivity and also deliver a fast update rate of the signal to be used in automated tuning procedures.

4.14 THz and FEL diagnostics

A key element of setting up and optimizing the machine are photon diagnostics to characterize the optical beams according to the user requirements. Each user experiment will typically specify characteristics such as the peak wavelength, pulse energy or power, and repetition rate. In some cases, users may also have special requirements for band width or pulse duration. It will be important that these photon diagnostics can be operated remotely and independently by the operations staff from the control room. The wide spectral tuning range and different types of sources will require several different types of diagnostics. These optical diagnostics are outlined below for each type of photon source.

4.14.1 Compressed bunch THz sources

The diagnostics for the compressed bunch THz sources are based on experience gained over several years of operating the TELBE super-radiant THz sources. Many of the diagnostic techniques developed at TELBE are based on electro-optic sampling, which utilizes a synchronized NIR tabletop laser to measure the electric field of the THz waveform. The basic principle of EOS is that the electric field of the THz waveform interacts with the NIR laser pulse in a suitable nonlinear crystal via the second-order nonlinearity to modify the polarization of the NIR laser pulse (Pockels effect).²¹³ When the NIR laser pulse is much shorter than the THz pulse, the full THz waveform is measured by scanning the relative arrival time of the THz and NIR pulses using a delay stage, which requires acquisition over many pulses.

In an alternate EOS scheme known as “spectral encoding”, the NIR pulse is chirped and stretched to longer than the THz pulse. It is possible then to “imprint” the entire waveform of a THz pulse onto a single the NIR laser pulse, and because the NIR pulse is chirped, the temporal information from the THz waveform is encoded in the spectral distribution of the NIR pulse. Using a dispersive grating and a linear imaging array, the THz waveform encoded in the spectrum of the NIR laser pulse can be measured directly in a single shot.²¹⁴

Using spectral decoding it is thus possible to measure the entire electric waveform of the super-radiant THz pulse in a single shot, and through a Fourier transform, also obtain the spectral distribution for each THz pulse, but another challenge remains. Because the THz pulse and the NIR pulse are generated from different sources, there is unavoidable timing jitter between these two sources. While advances in timing and synchronization methods continue to improve, the demand also grows for higher and higher temporal resolution. Thus, over several years, TELBE has developed several new methods for measuring the relative arrival time of every THz pulse from the accelerator.¹⁴⁰ All of these methods utilize the single-cycle CDR THz source that is just upstream of the undulator used to generate the super-radiant multi-cycle THz pulses. Because the CDR pulse and the multi-cycle THz pulse from the undulator are generated from the same

²¹³ Q. Wu and X.-C. Zhang, Appl. Phys. Lett. **67**, 3523-3525 (1995)

²¹⁴ Z. Jiang and X.-C. Zhang, Appl. Phys. Lett. **72**, 1945-1947 (1998)

electron bunch, they arrive in the lab essentially jitter-free and the CDR pulse can be used to determine the arrival time of the THz pulse from the undulator relative to the NIR laser pulse.

By utilizing the same NIR laser for diagnostic measurements and user experiments, it is thus possible to determine the arrival time of every THz pulse relative to the NIR sampling pulse at the user experiment. Also recently, a method to provide NIR laser pulses that are intrinsically synchronized to the THz pulses has been commissioned.²¹⁵ For this method, the NIR laser pulse is stretched to be much longer than the single-cycle CDR pulse which is then used to “slice out” a part of the NIR pulse to produce a short laser pulse that is intrinsically synchronized to the THz pulses from the accelerator. This new method eliminates the need for post-processing of the measurement data. The layout of a typical measurement scheme using the super-radiant multi-cycle THz pulses is shown in Figure 67 adapted from Ref. 140.

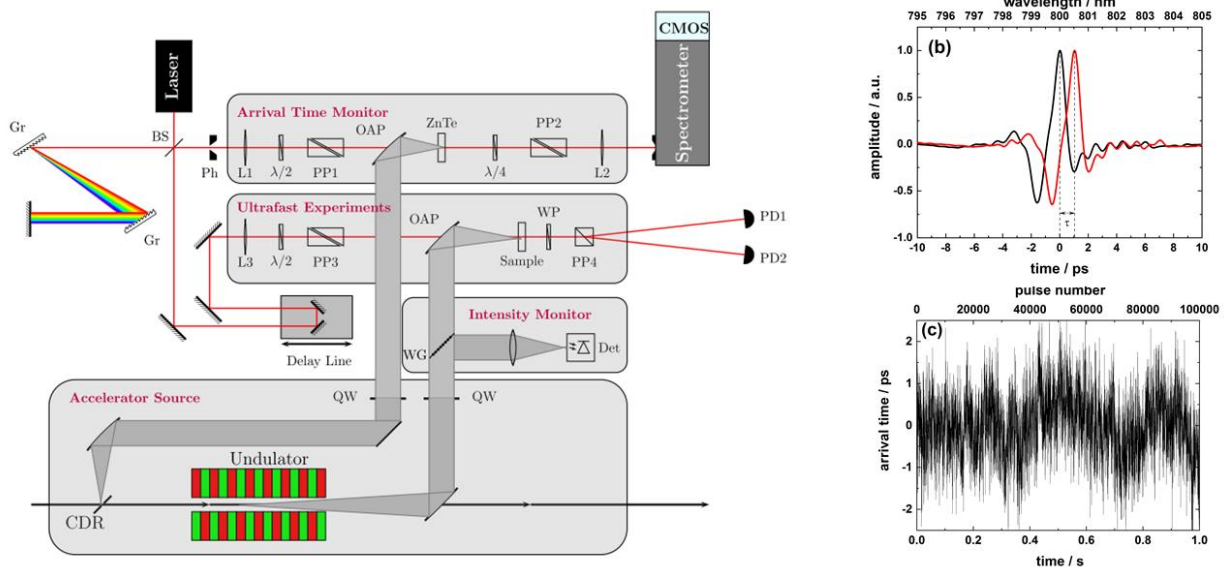


Figure 67: Pulse-to-pulse detection scheme. (a) Schematic of the experimental setup at TELBE. (b) Spectral-decoding-type electro-optic sampling traces of 2 pulses from the diffraction radiator with an arrival time-difference of $\tau = 1.03$ ps. (c) Pulse-resolved arrival time jitter recorded over 1 s, that is, 10^5 laser shots.

In addition to the EOS-based measurements, other instrumentation for measuring the pulse energy or average power will be used. A simple and fast monitor can be provided by specially instrumented pyroelectric sensors such as the fast pyro detectors from DESY, which have sufficient electronic bandwidth to generate a short voltage pulse proportional to the energy of each THz pulse. These detectors are already in use to monitor the TELBE beam “in situ” from a beam splitter in the lab and can be monitored either with an oscilloscope in the time-domain, or with a spectrum analyzer to look for unwanted noise in the frequency domain. An alternative to the fast pyroelectric detectors are Schottky diodes for frequencies up to about 2 THz²¹⁶ or field effect transistor (FET) devices.²¹⁷

In addition to these ultrafast metrology methods, it is also beneficial to utilize more customary instrumentation. By operating the DALI sources at high repetition rates, it is possible to use standard calibrated power or energy meters such as the 3A-P-THz thermopile sensor from

²¹⁵ M. Chen et al., Opt. Lett. **43**, 2213-2216 (2018)

²¹⁶ <https://acst.de/product/3dl-12c-ls2500-a1-a1m/>

²¹⁷ S. Regensburger et al., IEEE Transactions on Terahertz Science and Technology **9**, 262-271 (2019)

Ophir²¹⁸ or the PTB calibrated sensors from SLT Sensor- und Lasertechnik GmbH.²¹⁹ This simple power measurement is ideal for coarse tuning of the accelerator when setting up the machine and can also provide a feedback signal for beam-based feedback to correct for slow drifts that affect machine performance. Furthermore, since both types of sensors are provided with a calibration (3A-P-THz: factory calibration, SLT: PTB calibration), they can provide an accurate reference and cross calibration for measurements of optical parameters such as pulse energy, peak electric field, fluence, etc.

Finally, the spatial mode distribution can be measured with a PyroCam beam profiling camera.²²⁰ The PyroCam is an ideal imaging device that is sensitive over the entire THz, IR, and visible spectrum. It is thus also eminently useful for establishing co-alignment of the THz source and visible alignment lasers.

4.14.2 Modulated bunch THz sources

The diagnostic methods for the modulated bunch THz sources will also utilize EOS methods and instrumentation similar to the metrology systems for the compressed bunch sources, but with some modifications. The spectral range (2 – 30 THz) will put more demands on the nonlinear crystal (optical transmission, phase matching, and bandwidth) as well as the pulse width of the NIR laser (sampling and spectral bandwidth). Considering the latter, it will be necessary to have a NIR laser pulse of 10 fs or less, but such laser pulse widths are readily available now. Regarding the nonlinear crystal, GaP provides good performance up to about 10 THz, above which a Reststrahlen band causes the crystal to be too highly absorbing. It has been demonstrated though that a very thin ZnTe crystal polished to a thickness of 30 μm is effective up to 37 THz.²²¹

As with the compressed bunch THz sources, it will be necessary to have a means for measuring the relative arrival time between the THz pulses and the NIR table-top lasers in the user labs. In this case, the timing reference will be performed in a slightly different method. The fundamental difference is that rather than a single-cycle pulse, the modulated bunches would generate a multi-cycle pulse from a diffraction radiator. But, in an effort to preserve modulation structure on the electron bunches between the modulator and radiator, a diffraction radiator is not preferred. Instead, the coherent edge radiation (CER) from the dipole magnet upstream of the radiator would provide a completely non-perturbative means to generate a timing pulse. Because of the multi-cycle waveform of the CER radiation from the modulated bunches, the timing signal would likely be derived not from the peak of the waveform, but by measuring the timing of a zero-crossing of a specific cycle within the waveform.

The fast detectors planned for the compressed bunch THz sources (i.e. pyroelectric, Schottky, FET) have limited sensitivity for the higher spectral frequencies, so an alternative detector would be to use a superconducting transition edge hot electron bolometer (HEB). We are currently using a Type 2 HEB from Scontel²²² for pulse-to-pulse detection of the FELBE FELs. That detector provides up to 200 MHz electronic bandwidth and high sensitivity over the entire spectral range of the two FELBE FELs (1.6 – 60 THz), and thus would also be ideal for the modulated bunch THz sources of DALI.

The average power sensors from Ophir and SLT are also rated and calibrated for operation over the spectral range of all of the DALI sources and thus will similarly provide reference and cross

²¹⁸ <https://www.ophiropt.com/en/f/3a-p-thz-high-sensitivity-thermopile-sensor>

²¹⁹ <https://www.pyrosensor.de/THz-Detectors-Accessoires-924551.html>

²²⁰ <https://www.ophiropt.com/en/f/pyrocam-iihr-gige-laser-beam-profiler>

²²¹ Q. Wu, and X.-C. Zhang, *Appl. Phys. Lett.* **71**, 1285-1286 (1997)

²²² <https://www.scontel.ru/terahertz/>

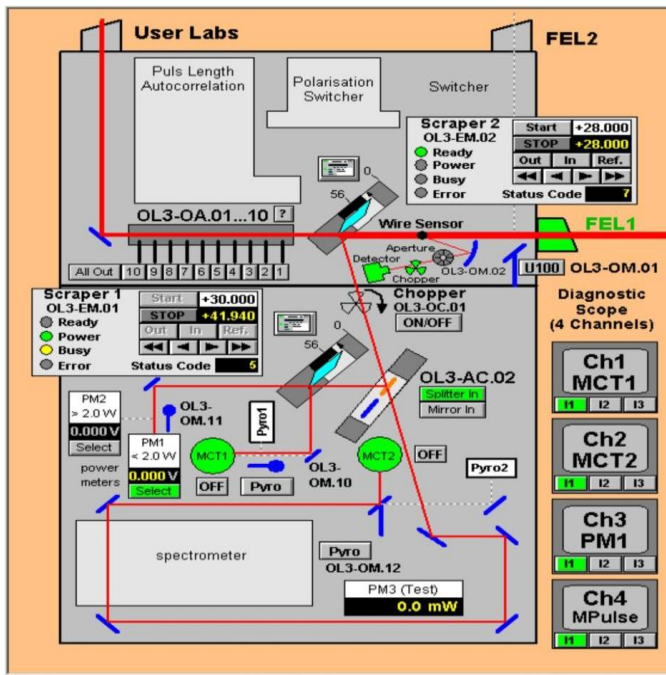


Figure 68: Layout of existing diagnostics for FELBE FELs.

calibration measurements that are critical for accurately characterizing the THz beam for the users. Similarly, the PyroCam operates over the entire spectral range of all DALI sources and will provide important measurements of the spatial profile of the THz beam and also aid with alignment of the THz beam and visible alignment lasers.

4.14.3 FEL oscillator

For diagnostic metrology of the FEL oscillator, we plan to utilize much of the same diagnostics that have proven to be effective for the FELBE FELs (see Figure 68).²²³ The primary diagnostic for optimizing lasing is average power, which is measured with standard thermopile laser power sensors. For operation in macro-pulse mode, such as during initial setup of the beam, more sensitive pyroelectric or liquid nitrogen cooled MCT detectors will be used.

For spectrum measurements, a grating spectrometer with multiple gratings provides a robust method for measuring the FEL spectrum.²²⁴ The spectrometer can be operated in scanning mode with slits and a single element detector or with a linear array (typically pyroelectric). In either case, the spectrum measurements provide an average measurement, not a shot-to-shot measurement.

For shot-to-shot measurements, two types of EOS methods are proposed. A simple method by Ilyakov et al. for shot-to-shot measurement of the carrier envelope phase (CEP) has been demonstrated with the FELBE FEL.²²⁵ In the method by Ilyakov, the CEP of the FEL pulse is measured with a single NIR laser pulse overlapped with the FEL pulse in an appropriate nonlinear crystal and thus can be rather compact and requires only two voltage channels on a fast ADC (see Figure 69). Another method based on the “time-stretch”²²⁶ and “phase diversity”²²⁷ concepts

²²³ W. Seidel et al., Proceedings of FEL 2016, Berlin, Germany (2006).

²²⁴ <https://www.princetoninstruments.com/products/spectrapro-family/spectra-pro-hrs>

²²⁵ I. Ilyakov et al, Optics Express **30**, 42141-42154 (2022)

²²⁶ E. Roussel et al, Scientific Reports **5**, 10330 (2015)

²²⁷ E. Roussel et al., Light: Science & Applications **11**, 14 (2022)

of Roussel et al. has recently been tested with the FELBE source. This method utilizes features of the spectral decoding method in that the NIR laser pulse is chirped and stretched before interacting with the FEL pulse in a nonlinear crystal. Then the NIR laser pulse with the waveform of the FEL pulse imprinted onto the temporal and spectral distribution is stretched over multiple orders of magnitude so that the modulation from the FEL waveform can be measured in the time domain with a fast photodiode and a fast oscilloscope or ADC. The advantage of this method is that the entire FEL waveform is acquired in a single shot. The disadvantage is that the optical layout is more complex and the signal acquisition and processing can only be performed on a shot-to-shot basis in short bursts. Both methods of Ilyakov and Roussel will require pushing the spectral range of the nonlinear crystal and NIR laser pulses of less than 10 fs, so both methods still require more testing and investigation. It will be of great importance to have diagnostic metrology capable of measuring the shot-to-shot CEP of the FEL pulses since this will determine the CEP of the radiation from the modulated bunches.

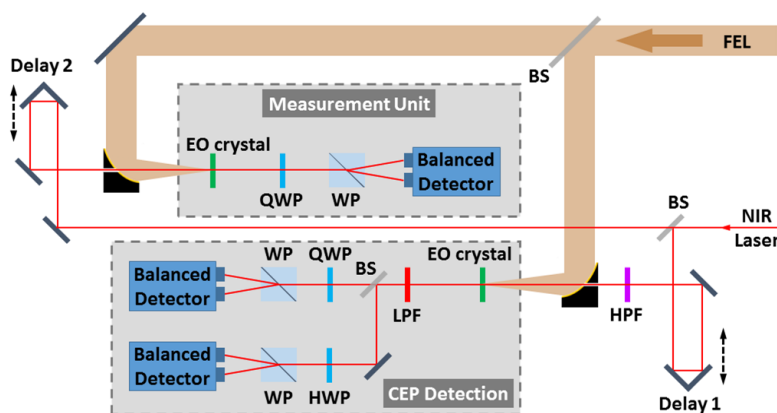


Figure 69: Layout of the method for shot-to-shot detection of the CEP of each FEL pulse.

It is also planned that the Scontel HEB detector described above will continue to be used for shot-to-shot pulse energy measurements as well as a PyroCam for beam profiling and alignment tasks. Calibrated sensors from Ophir or SLT will be used for reference and cross calibration purposes of power measurements and other optical characterizations that are critical for user measurements. An FTIR spectrometer will provide an accurate means of cross calibration for the grating spectrometer.

4.15 Control system

The control system is a central part of DALI. It denotes the domain-specific IT infrastructure, which allows one to remotely control and to survey all devices and mandatory subsystems, essential or useful for operation, states and transitions of the accelerator complex.²²⁸ Important subsystems are the personnel safety system, the machine protection system (MPS) and the timing and synchronization system.

The implementation of those subsystems will rely on different hardware platforms like Programmable Logic Controllers (PLC, see Section 4.13) or MicroTCA (see Section 4.10) and different field buses that need to be integrated.

²²⁸ R. Müller, Control Systems for Accelerators, Operational Tools (2015)

4.15.1 Existing solutions

Over the last decades two control systems were well established in the domain of particle accelerators and synchrotron light sources – Tango²²⁹ and the Experimental Physics and Industrial Control System (EPICS)²³⁰. Both are high-performance control systems developed by global collaborations providing mature and reliable toolkits. They are freely available and detailed documentation as well as community support are available. Both, provide a driver database that offers support for commonly used devices.

A survey²³¹ among 15 different accelerator facilities with 22 participants was conducted in preparation of this document. It confirmed that the majority of the centers are using EPICS (46%) and Tango (27%). The overall satisfaction with their control systems was above 80% and the satisfaction with the community support was rated with seven in case of EPICS and 8.5 in case of Tango on a scale ranging from 0 (unsatisfied) to 10 (totally satisfied). Apart from the community support several experienced companies offer expertise in software development for both EPICS and Tango. This allows for outsourcing the developments of certain control system components, like e.g. hardware driver development. At ELBE we have made good experiences in case of COYLAB²³², who developed the MRF based new ELBE timing system (see Section 4.11). In the survey it turned out that many participants used support from industry partners.

Table 18: Example control system configuration for EPICS and Tango covering the most important control system components. For details about the different components listed in the table (see Refs. 233,234).

	EPICS	Tango
Human machine interface	Control System Studio	Sardana
Alarm system	BEAST	PANIC
Archiving	Archiver Appliance	HDB++
Logbook	Olog	e-logbook
Snapshot	MASAR	SNAP+Bensikin

Table 18 shows an example configuration of the most important control system components. In case of EPICS all components are integrated in the human machine interface (HMI) of EPICS called Control System Studio (CSS).

In our survey we found that most EPICS users use a similar configuration and e.g. all were using the EPICS Archiver Appliance for archiving. In case of Tango, often multiple solutions exist, e.g. for archiving the legacy archiving system HDB exists. On top there are multiple GUI programs to access the archived data, whereas with EPICS everything is included in CSS. This was reflected in our survey too, where the Tango configurations were more diverse.

In terms of interfaces both EPICS and Tango provide a rich set of options. For interfacing with the control system, in order to allow e.g. scripting, both EPICS and Tango provide bindings for Python

²²⁹ Tango Controls, <https://www.tango-controls.org/>

²³⁰ EPICS Controls, <https://epics-controls.org/>

²³¹ R. Steinbrück, K. Zenker, Proceedings of ICALEPCS 2023, Cape Town (2023) (to be published).

²³² Cosylab, Control System Laboratory, Gerbičeva ulica 64, SI-1000 Ljubljana

²³³ Tango Documentation, <https://tango-controls.readthedocs.io/>

²³⁴ Control System Studio Services, <https://controlsystemstudio.org/services/>

and C++ exist. Those two computing languages are the most common languages used by the survey participants. The protocols used for scripting are the control system internal protocols - Channel Access or PV Access in case of EPICS and Common Object Request Broker Architecture (CORBA) or ZeroMQ in case of Tango.

Both control systems include a mechanism for access control based on users and user groups. It allows to set access rights based on global settings that apply to all process variables in the system, down to setting access rights for single process variables. As confirmed by the survey the control system typically is operated in a dedicated network, that is secured by a firewall and can be accessed only via gateway access points.

In order to interface other subsystems common industry protocols like OPC UA or modbus are supported. The survey showed that interfaces to industry protocols are used by all participants independent of the used control system.

The above shows that both EPICS and Tango provide all tools, that are from a technical stand point equally suited to build a control system for DALI. However, in the following general and site-specific arguments are discussed, that are not technical but cover other aspects that need to be taken into account when deciding on the DALI control system.

4.15.2 Considerations for DALI

In Europe recent accelerator project are using EPICS, which opens up synergies and DALI could benefit from the experiences of those projects especially as they use subsystems that are similar to DALI. The European Spallation Source (ESS) is using a MRF based timing system based on EPICS,²³⁵ which is similar to the proposed DALI system (see Section 4.11). The control system of the MESA accelerator in Mainz is EPICS, too. MESAs LLRF system²³⁶ is similar to the DALI LLRF (see Section 4.10).

Independent of specific accelerator subsystems, in general the EPICS driver base is the largest compared to other control systems.²³⁷ This results in a reduced development time of the control system. At HZDR competence in EPICS is available and recent projects at HZDR, like the Helmholtz Accelerator Mass Spectrometer Tracing Environmental Radionuclides (HAMSTER) are using EPICS as well. Finally, at ELBE the recently implemented new timing system and the THz optical beam line control already use EPICS. Also, the LLRF system¹⁷⁹ can easily be switched to EPICS thanks to the ChimeraTK framework that allows to implement control system independent applications.

All the above arguments support preference of EPICS over Tango as the control system for DALI. However, a final decision has to be taken only in the next phase of the DALI project.

4.16 Vacuum system

The vacuum system is required to transport the electron beam from the source (injector) to the individual experimental caves with negligible losses due to particle interaction. The beam line dimensions have to allow for steering and focusing the electron beam without getting too close to the wall. According to the DALI concept, the average electron beam current resembles that one specified for ELBE accelerator. In addition, vacuum quality requirements are similar. Critical parts

²³⁵ J.J. Jamróz, J. Cereijo García, T. Korhonen and J.H. Lee, International Conference on Accelerator and Large Experimental Physics Control Systems (2020)

²³⁶ J.N. Bai, K. Aulenbacher, J. Diefenbach, P. Echevarria, F. Fichtner and R.G. Heine, Proc. 29th Linear Accelerator Conference (LINAC'18), Beijing, China (2019)

²³⁷ R. Müller, Control Systems for Accelerators, Operational Tools (2015)

like injectors and linacs demand for higher vacuum than downstream beam line parts next to the radiation sources.

Therefore, it is reasonable to design the DALI vacuum system based on the technologies that are proven to work at ELBE during the last decades of successful operation. Fundamental parameters are the DN 40 beam tube diameter and the use of stainless steel 1.4301 for the major parts of the beam guidance system including pipes, flanges, pumps and others. Greater tube diameters and aluminum vacuum chambers are still an option for critical parts with high radiation exposure or beam dynamics needs. However, due to technological challenges with respect to production and maintenance this will be more an exception than a rule. Thus, the selection of vacuum components for DALI can be deduced from ELBE machine design. Numbers and costs are estimated by scaling. Vacuum components for optical beam transport are not taken into account here. They are part of the design of these distinguished machine parts.

The currently planned length of the DALI electron beam line is in the range of 160 meters comparable to ELBE with a total beam line length of 150 meters. The required vacuum in the beam line is in the range of $1\text{E-}10$ to $1\text{E-}8$ mbar depending on the position in the beam line, which corresponds to a value in the ultra-high vacuum (UHV) range.

All flanges and components connected in the UHV are sealed with CF gaskets in accordance with ISO 3669 2017. Oxygen-free, high-purity copper is used as the sealing material. All connections in high vacuum (HV) or fine vacuum (VV) ($> 10^{-9}$ mbar) are made with elastomer seals. Sealing materials are VITON or EPDM according to ISO-KF.

The entire beam line has a modular design, based on frames made off aluminum profiles and aluminum welded assemblies. These allow the beam line components to be aligned in all axes at approx. 1400 mm above floor level.

The basis for generating the ultra-high vacuum is formed by pumping stations at several points throughout the beam line, consisting of a 3-stage pump module:

1. diaphragm pumps up to 1 mbar (fine vacuum)
2. turbomolecular pumps up to 10^{-6} mbar (high vacuum)
3. ion getter pumps up to 10^{-9} mbar (ultra-high vacuum)

These are switched in stages to achieve an ultra-high vacuum at the end. Cold cathode gauges in the UHV range or Pirani gauges for the fore-vacuum are used for monitoring.

With respect to machine protection a fast-closing valve system will prevent injectors and linac modules from contamination in case of vacuum incidents. A dedicated commercial system of fast gauges and shutters together with the required controllers will be used for this purpose (see also Section 4.12.4).

There are stringent requirements for the cleanliness of the beam line and its components. For this purpose, clean rooms of clean room class 4 are required for assembly and clean room class 6 for cleaning. The cleaning of the beam line components should be automated by robots in 24/7 mode in order to achieve a high level of cleanliness and short processing times. For assembly and maintenance work in the beam line area, automated mobile "white" pumping stations ("pump and purge") could be used to minimize the use of personnel for this work.

4.17 Radiation safety / shielding

The operation of the accelerators and secondary radiation sources with the planned beam and radiation parameters will only take place in shielded caves. The concrete shielding of the caves will be dimensioned in such a way that the photon and neutron radiation resulting will be reduced to an acceptable level, not exceeding the limit values of dose and dose rate for the neighboring controlled areas, monitored areas or normal areas. If concrete shields are not sufficient at individual locations, e.g. at beam dumps or targets, additional local shields (lead, concrete, PE) will be installed. Cables and media pipes will be guided into the caves through radiation chicanes. To reduce the required space, radiation protection gates will be used to access the caves. During beam operation, the gates will be closed and the caves will have restricted area status. A security search system will be used to ensure that no persons will remain in the caves to be closed. For dimensioning these shielding elements detailed numerical simulation calculations for different situations will be necessary (i.e. target irradiation, beam dump irradiation, beam loss).

During beam operation, materials in the caves can get activated and cause increased dose rate values after beam operation. Component activations with high activities are registered by detectors in the caves. The gates can then remain closed until dose rates have undergone a certain level that allows access. Any access after accelerator operation and handling activated components from the caves will be carried out by qualified personnel only and requires use ODF suitable mobile dose rate meters. Activated parts which are brought out of the caves must be temporarily stored in a special shielded a controlled area for decay.

Due to the expected radiation dose rates, employees working at the accelerator site will have to be occupationally radiation exposed personnel according to the effective radiation protection legislation. The monitoring of the permissible dose values is carried out with suitable personal dosimeters. Radiation safety training for all involved personnel has to be carried out annually as well as on demand.

To build and run an accelerator facility require approvals by governmental authorities in advance, as well as constant supervision of compliance with approval requirements during operation. This requires sufficient personnel qualified in radiation safety. Due to the many years of operation of ELBE and other radiation safety-relevant facilities at HZDR, there is already a well-established radiation safety infrastructure on site.

4.18 Personnel safety system

Operating a superconducting linear accelerator in CW regime means to create very intense levels of ionizing radiation in the vicinity of the machine by RF field emission, beam loss effects or beam dumping. Dose rates in the accelerator caves can be lethal on a timescale of seconds to minutes. Other severe dangers to personnel emerge from high voltage installations, laser system, use of technical gases or kilowatt RF fields. These aspects are well known and understood from 25 years of ELBE operation.²³⁸ Based on a detailed HRA according to the effective corpus of legislation (standards like EN/IEC 61508, EN/IEC 62061 or EN/ISO 13849), both organizational and technical measures have to be defined to reduce harming risks for personnel down to an acceptable level.

For laser safety, oxygen monitoring or shielding of high voltage installations, straight-forward safety solutions or commercial systems are standard and available. As ELBE is, DALI will be a multi-option machine, supposed to allow access to controlled areas, while other areas are access restricted and in operation. Thus, the radiation safety related part of the PSS is going to be more

²³⁸ M. Justus et al., Proceedings of ICALEPCS 2013, San Francisco, USA

complex and will require a safety PLC based, distributed system with a safety implementation level up to SIL 3 (or performance level PL e, respectively). The main functions of the PSS will be to prevent people from staying or being left in restricted areas and protecting people from direct radiation exposure or incorporation of activated air in controlled or monitored areas. This is achieved by a safety search system for the caves and monitoring of dose rate meters, dedicated bending magnets, beam shutters, radiation doors, emergency stop buttons and the air ventilation system. In case of an interlock, all related sources of radiation (injectors, RF accelerators) will be shut down safely. The PSS must therefore be an autonomous system from field level to GUI, with interfaces to the SCADA system, auxiliary facility systems, access control and the MPS. The safety implementation level (SIL) of each individual safety function entails special design requirements on the involved sensors and instrumentation (MTBF, redundancy, SIL compliance). The system as a whole is expected to be subject to external expert review within the approval procedure for operation of DALI. There is sufficient longtime experience and engineering capabilities at HZDR in designing the PSS,²³⁹ as well as proven contractors for implementation.

4.19 Cryogenic system

The main task of the cryogenic system is to provide the cooling power for the superconducting accelerator structures. These are mainly the liquid helium cooling below the lambda point and the cooling shield supply to the cold, distribution, sub cooler boxes and the transfer lines. The figure of merit for the cooling system is the maximum power that the number of SRF modules and the distribution system will consume. Table 19 shows some estimations for the accelerator modules and the liquid Helium distribution system. For the dynamic load of the acceleration module (accelerator modules) based on ELBE experience with some margin of safety is the most likely choice. For accelerator cryo-modules, valve boxes and transfer line system also common numbers are given. All adding up to around 600 W@1.8 K. Nevertheless, an additional margin

Table 19: Power consumption scenarios of the acc. modules and distribution system.

		ELBE-Operation	Scaled to DALI
	Dynamic load	Power [W]	Power [W]
6x	Accelerator cryo-module	50	300
3x	SRF gun module	35	105
			405
Static load			
9x	Acc. Module	10	90
2xx	Distribution valve box	10	20
5x	Sub cooler valve box	10	70
180m	Transfer lines	0.2 W/m	36
	Sum		601

²³⁹ M. Justus, "ELBE Zentrum für Hochleistungsstrahlenquellen: Personensicherheitssystem - Systembeschreibung", documentation of the ELBE PSS for approval of operation by federal state authority of Saxony, V5.1, 2022, Dresden, Germany

for plant degradation between maintenance intervals and some buffer for upgrading the SRF structure has to be planned.

For the structure of the cryo-system, two models for DALI are conceivable, which are both used at accelerator facilities. Model 1 (named here "in-line") refers to a supply line from which the supply of the cryogenic modules is organized with "identical" outlet or distribution boxes, it is a kind of sequential distribution normally used for larger cryomodule system. Advantages are e.g. identical construction of the distribution or sub cooler box as well as a possible slim design of the boxes, which is to be considered by the reduced available space in and over the Caves. Disadvantages are e.g. cool down and operation are only possible for the whole system. Model 2 (named here "branching", see Figure 70) would be a tree like structure in which individual outlet boxes can release and close access - so that a selective cool-down and operation is possible. In principle, this would require more boxes, but several modules could be connected to one end box, so that some boxes could be saved. Disadvantage is the larger space requirement of the boxes. Even if it is for cryo-systems rather favorable to plan as little as possible cold and warm-up cycles, there are two important points which are to be considered for the DALI system, operating regime and energy saving options.

The cryo-system function of DALI can be divided into four basic sections: ERL FEL, THZ, SRF test and UED. Specifically, the SRF Test and UED functions could have cool down and operating cycles independent of the rest of the accelerator operation. The Intake power of the entire accelerator facility is to a considerable extent determined by the helium refrigeration system. While keeping the cryogenic system cold generally allows only a limited dynamic adjustment of the power consumption. A controllable operation of individual cryogenic sections would allow a significantly larger savings potential. A step in this direction would be the implementation of two separate low-pressure circuits and the selection of cry-section via an appropriate distribution-box-design and -system. This would favor the branching solution. Therefore, the additional conditions for the SRF modules specify the overall plant conditions: Cooling regime, operating regime, pressure stability. As stated in the previous paragraph, the optimal cooling and operating regime is the implementation of two under pressure circuits. The first circuit has the sections either IR, THz, Test or IR and THz or Test. The second under pressure system would be the optional UED

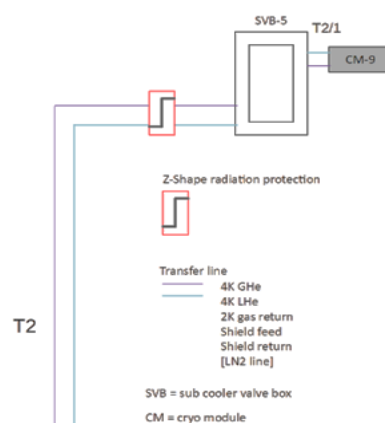
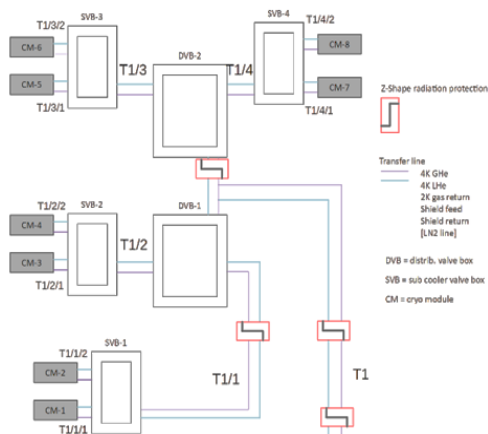


Figure 70: Acc. Helium supply Low pressure circuit I: Tree like branching structure for separate cool down and operation.

Figure 71: Low pressure circuit II: UED lab.

branch. The pressure stability must be in the range of ± 0.1 mbar for both under pressure sections.

4.20 Power and auxiliary supplies

The required media supply to operate DALI is very comparable to ELBE. An electrical energy connection with approximately 4 MVA is required. An uninterruptible power supply (UPS) systems, backed up by a diesel generator will be used to ensure the operation of the helium refrigeration system, critical vacuum systems, the personnel safety systems, as well as control system and IT/OT infrastructure during main power failures. This is essential to avoid degrading of the accelerator cavities and to quickly recover user operation after power outages.

For cooling of technical systems like cryogenics, beam dumps, beam line magnets, power supplies and other components a cooling capacity of about 1 MW at a flow temperature of $28\text{ }^{\circ}\text{C}$ is required. Depending on how the cooling water is used in the radiation protection areas, the water circuits must be separated into potentially activated and non-activated circuits. Cooling water should be deionized.

The helium refrigeration system has a closed helium circuit. Tanks with approx. 10000 l are required to store additional helium gas. Liquid nitrogen is also used mainly to operate the cryogenic system. A storage tank of at least 80 m^3 is to be provided.

A compressed air supply with a capacity of approx. 2000 l/min at 8 bar is needed. Compressors should be redundant and critical components that need to be pressurized for machine protection reasons (i.e. dedicated vacuum shutters) will be backup up by individual pressure reservoirs.

For different experimental setups and optical transport systems, industrial gases like argon or nitrogen will have to be supplied as a laboratory installation.

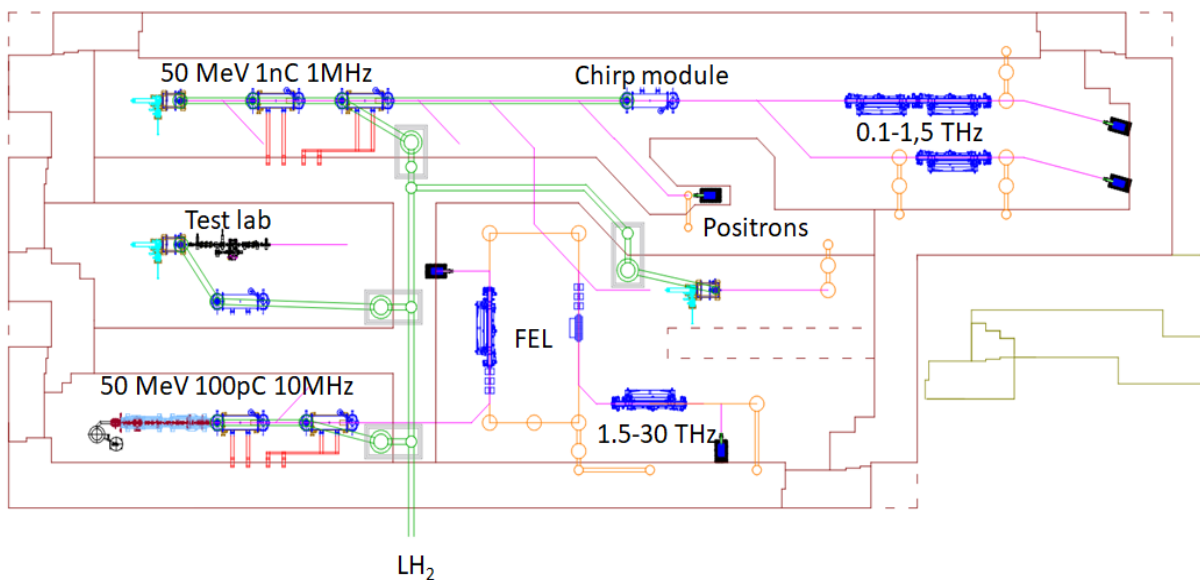


Figure 72: DALI machine layout. Integration of all radiation protection areas on the ground floor of the existing ELBE building.

4.21 Integration into a DALI building

There are basically two options for integrating the DALI accelerator and the user laboratories. Firstly, the existing ELBE building can be used. The floor space available in the existing ELBE building would be sufficient for all DALI components relevant to radiation protection, such as electron injectors, beamlines, accelerator modules and beam dumps. The laboratories for high-power lasers, which are also in the current ELBE building, could be retained. Figure 72 shows the possible integration of the DALI accelerator with THz and positron generation including a test laboratory in the associated radiation protection rooms. The room layout allows the separate operation of both accelerators and the gun or accelerator modules in the test laboratory. This means that during the operation of one of these accelerators, the other rooms can be entered after appropriate radiation protection measures (closed beam shutter and prevention of a direct beam on the beam shutter). The radiation protection walls and radiation protection gates shown in the figure cannot be taken from ELBE and must be rebuilt for DALI. To do this, around 80% of the radiation protection walls for ELBE and the neutron laboratory must be dismantled. The area of the ELBE available for the high-power laser is not affected by this layout and can be retained. Figure 73 shows the room layout in the first upper floor (above the radiation protection areas). A large part of the control technology, the power and high-frequency supply as well as the user laboratories for THz and positron experiments are provided here.

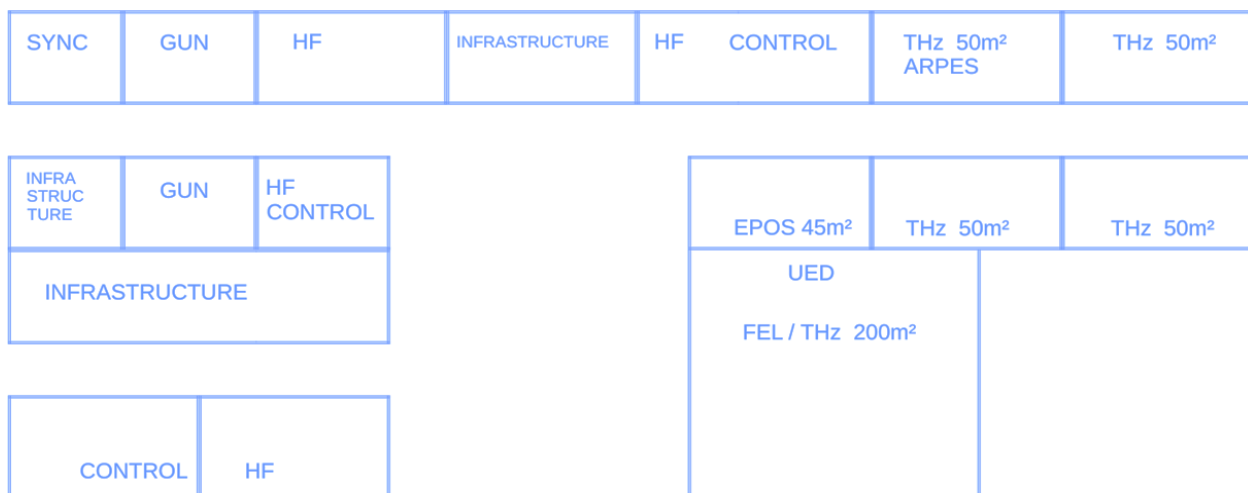


Figure 73: Rooms for technical equipment and user laboratories on the first floor.

The total height to the ceiling of the laboratory rooms on the first floor is increased by approx. 1.4 m compared to ELBE due to the necessary radiation shielding of the ceiling (3 m instead of 1.6 m). Since the existing ELBE hall cannot be increased in height from an economic point of view, over the new DALI laboratories it is not possible to use the existing hall crane. As an alternative, for transporting heavy equipment and materials to the first floor an elevator needs to be provided.

In addition to the existing ELBE building, laboratory and storage areas as well as areas for clean rooms of approx. 2000 square meters are required. Since extensions for such areas are not

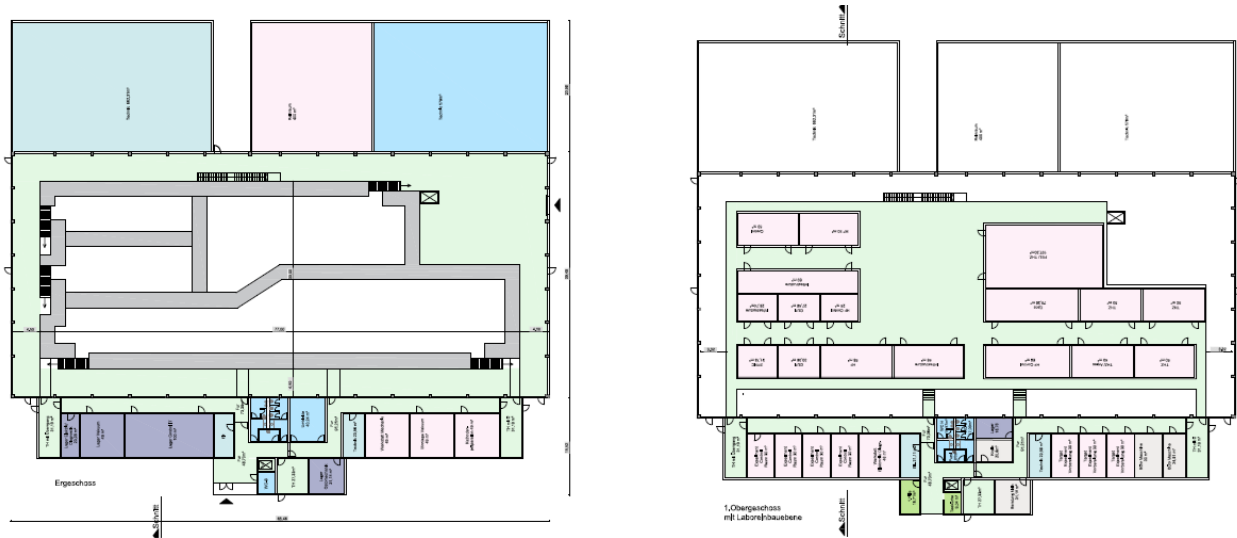


Figure 74: Layout of the new DALI building with all necessary areas for the accelerators and laboratories (no additional areas necessary on the HZDR campus).

possible on the ELBE building, a corresponding new building must be built at another location on the HZDR campus. In addition, for the period of reconstruction, an area of approximately 200 square meters must be made available in the existing ELBE hall for users to carry out experiments with table-top lasers. The total costs for the dismantling of the ELBE-specific installations, the installation of the accelerator vaults and laboratories for DALI and the construction of additional laboratory and storage areas outside the ELBE building amount to 86,2 M€. A disadvantage of using the existing ELBE building compared to a completely new building would be the interruption of user operations for several years during the transition from ELBE to DALI.

Alternatively, DALI can be integrated into a new building to be built. Figure 74 shows the ground floor and first floor of a potential new DALI building. This scheme accommodates all areas of the accelerator facility, user laboratories, clean rooms and storage. The construction cost for such a new building would be approx. 84 M€. There are several options, where such a building could be erected on the HZDR campus, Figure 75 shows possible locations.



Figure 75: Possible locations for a new DALI building on the HZDR campus.

5 Strategic Importance and Impact

5.1 Strategic importance of DALI

The science-driven development of technology and instrumentation (“enabling technologies”) is a *conditio sine qua non* for realizing internationally outstanding science. Moreover, there is a growing demand for high-field THz beams for a large variety of scientific applications like the investigation of complex systems and processes spanning from functional and quantum materials to biological systems and chemistry. Using long-wavelength electromagnetic radiation in the MIR and THz regimes with tailored characteristics (frequency, polarization, bandwidth) to control selected degrees of freedom in complex materials in their ground state (e.g. bond length or bond angle) is a complementary approach to the investigation of matter and materials compared to the one adopted by other analytical facilities, such as synchrotrons or X-ray FELs.

There is a growing demand for facilities with these capabilities, combining a wide wavelength range with a high versatility in beam characteristics. At HZDR, this can be seen in the high user demand for beam time at the pilot facility TELBE. Different institutions worldwide are working on the implementation of new facilities or the upgrade of existing ones to satisfy this demand. The DALI facility, conceived as a further development and successor of ELBE, will be the only system worldwide to generate the strongest achievable THz fields at high and flexible repetition rates, allowing selectable pulse shapes, bandwidths, polarizations, and pulse delays in CW mode. It will provide high-field THz beams of unprecedented brightness and repetition rate, plus an UED probe as well as a positron source. Realizing and operating DALI will keep HZDR in a worldwide unique position as was emphasized by an international expert panel in the Strategic Evaluation of the Helmholtz programs, where DALI was presented:

“Strengthen the commitment to THz methodology and science even more to become a world leader in the ongoing ‘THz revolution’.”

“DALI (Dresden Advanced Light Infrastructure), the upgrade of ELBE, is part of Helmholtz photon science road map and will extend the capabilities of strong-field THz. It will become a world-leading THz facility.”

5.1.1 Strategic importance for HZDR and the Helmholtz Association

DALI’s expected contributions will be in the core of HZDR’s mission: The long-term goal of HZDR is to conduct cutting-edge research in the fields of Energy, Health, and Matter. Strategic collaborations with both national and international partners allow us to address some of the pressing challenges faced by modern-day industrialized society by providing knowledge and technologies for the next generations in order to:

- support the transition to sustainable industry through resource and energy efficiency,
- develop radiation based diagnostic and therapeutic methods to combat cancer, and
- research future materials and technologies under extreme fields and develop them to the point of application.

The capabilities of DALI in the THz region perfectly match the strength of the research activities of HZDR. It will certainly attract outstanding scientists in this field, not only as users but also as staff members of HZDR, potentially financed by ERC, Emmy-Noether, or other renowned grants supporting the setup of young investigator groups. Similarly, the positron source mirrors strong in-house research focus. In addition to the existing expertise mainly centered around two HZDR institutes (Radiation Physics, Ion Beam Physics and Materials Research), great interest in DALI

has also been expressed by several other institutes, such as the Institutes of Resource Ecology, and CASUS, Center for Advanced System Understanding. We anticipate that DALI will play an increasing role for the research activities also of these HZDR institutes.

HZDR developed, constructed, and operates the unique large-scale user facilities Ion Beam Center (IBC), Helmholtz High Magnetic Field Laboratory Dresden (HLD), and especially the ELBE Center for High-Power Radiation Sources, of which the IR-FEL FELBE and the pilot THz laboratory TELBE are part of, for the benefit of an international user community. Moreover, it is implementing and already operating the Helmholtz International Beamline for Extreme Fields (HIBEF) at the European XFEL. DALI, as the planned successor of ELBE, where more than 70% of the available beam time is granted to external users, is an important cornerstone for upgrading the technologies and broaden the experimental possibilities for the international scientific community.

As an integral partner in the Helmholtz Program *Matter and Technologies*, HZDR has strong research activities in the further development of current accelerator-based technologies as well as in research on novel accelerator technologies, especially laser-based ones. In the research field of computing, data management, and data analysis, HZDR is one of the internationally leading institutions. Here, the center is strongly linked to other players within the Helmholtz Association across the different Research Fields and beyond. Moreover, HZDR is a founding partner and the hosting institution of CASUS, Center for Advanced Systems Understanding.

Photon Science Roadmap: Spectral Regimes

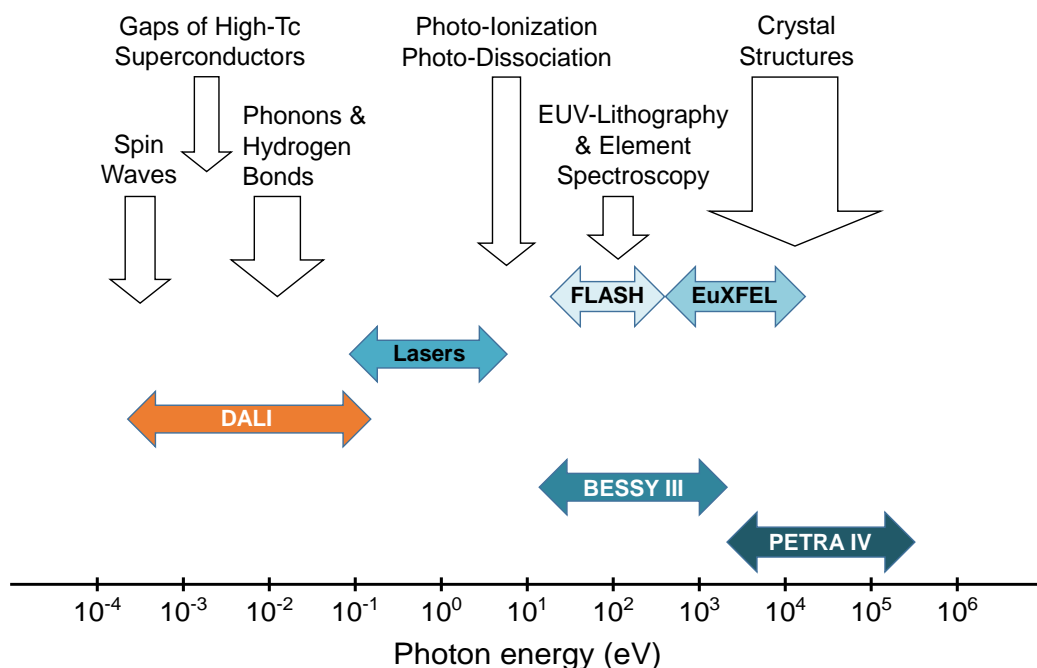


Figure 76: Photon science facilities in Germany: spectral ranges, and important application fields. Particularly notable is the complementarity of the covered photon energy ranges of the FEL facilities European XFEL, FLASH2020+, and DALI, which are devoted to ultrafast science, nonlinear phenomena, and high-energy-density physics, as well as of the synchrotron facilities BESSY III and PETRA IV, dedicated to spectroscopic applications.

The DALI project, as the successor of the ELBE facility, is a central element of HZDR's strategy to integrate newly developed technologies from its research with the program into large-scale facilities in order to provide novel experimental capabilities to the international user community from science and industry.

The Helmholtz Program *From Matter to Materials and Life* is dedicated to the development, construction, and operation of world-class photon, neutron, ion, and highest-field facilities (LK II) for the benefit of an international scientific user community, as well as to basic and applied research utilizing and further exploiting these facilities. DALI will be a user facility within the Program and complement its facility portfolio, especially regarding the photon energy range (see Figure 76). The unique experimental capabilities of DALI will allow for novel applications comprising all Research Topics of the Program. Here, DALI will be in a worldwide leading position in the research on highly complex systems with large-scale infrastructures, embedded in versatile international user communities, and collaborating with major user facilities in Europe and worldwide.

According to its mission, the Helmholtz Association is dedicated to solving the major challenges facing society, science, and economy by conducting high-level research in the strategic programs within its six Research Fields and to studying highly complex systems together with national and international partners using large-scale facilities and scientific infrastructure. This positioning of Helmholtz is unique in the German science system, and only Helmholtz has the resources and expertise to develop and operate user facilities at this scale. To maintain an internationally leading position and fulfill the demands of the user community, it is mandatory to renew and upgrade the facility portfolio on a regular basis. To this end, the Research Field *Matter* of the Helmholtz Association recently initiated a Photon Science Roadmap to plan, prioritize, and synchronize the facility upgrades and new-builds in the field of photon science planned for the fourth PoF period and beyond. The Roadmap aims at finding a common strategy, raising synergies, optimizing the effort of resources and competences, and harmonizing the financial planning over the implementation phase of the different projects PETRA IV, DALI, and BESSY III (see Figure 76 for the respective spectral ranges of these facilities).

5.1.2 Strategic importance for the region, Germany and Europe

The future research infrastructure DALI will be the only multi-user large-scale research infrastructure of this size in the eastern part of Germany outside of Berlin and thus a regional and national lighthouse project. Science at Dresden, represented by the research network DRESDEN-concept of several research and cultural institutions centered on the TU Dresden as one of Germany's Universities of Excellence will strongly benefit of such a facility. Already now, groups from TU Dresden and others have expressed interest in engaging at DALI utilizing a funding instrument called "Verbundforschung", which allows university research groups to set up instruments or experiments at German large-scale research infrastructures. With a wider focus on the border triangle including Poland and the Czech Republic, only ELI Beamlines, one of the sites of the Extreme Light Infrastructure (ELI), will in the future have a similar importance as an international user facility, however targeting a completely different user community. In this way, the attractiveness of Dresden will strongly benefit from DALI as a magnet for outstanding researchers as well as for young talents, reaching far beyond the borders of the actual city and of Saxony.

In the field of accelerator-based light sources, a revolution in the achievable beam properties is currently taking place, and many facilities, including the ones in the Helmholtz Association, are planning or already implementing respective upgrades. With this development, the Helmholtz Association, as the operator of large-scale research infrastructures for Germany, also secures

the international competitiveness of its facilities, as can be seen in the Helmholtz Photon Science Roadmap. The full operation of the European XFEL and the upgrades of the existing accelerator-based light sources in Germany will create new opportunities for scientists in Germany, but also exhibit a substantial attraction to scientists worldwide. As a long-wavelength radiation source, DALI is a worldwide unique facility. It will complement the available spectrum of electromagnetic radiation generated by accelerator-based light sources. DALI will enable the control of selected degrees of freedom to foster a deeper understanding of matter and materials, complementing investigations performed with other light sources.

DALI is conceived as a very flexible facility, being operated on the one hand as a typical user facility, yet offering external user groups and consortia the possibility to establish their own experimental stations. This format, well established in the Helmholtz Association, is expected to be particularly attractive for other German research organizations and universities. Moreover, DALI will also have an impact on industry. On one hand, this will be through the construction process itself. On the other hand, the realization of DALI will require several new developments in accelerator and detector technologies in cooperation with industrial partners. Furthermore, DALI will offer various access routes for users from industry to enable the exploitation of its unique capabilities for industrial research.

The future of German large-scale facilities lies in the full implementation of the European Research Area, with the removal of any national borders in science, the free flow of knowledge, and the possibility to recruit the best and most motivated researchers and facility staff members from anywhere in Europe. As vital as the right ecosystem is European collaboration. The EU supports these collaboration activities by funding tools like the “Integrating Activities”. Prominent present or past examples for funded activities in an infrastructure context are LaserLab Europe, IA-SFS, ELISA, CALIPSO, and CALIPSOplus. LEAPS, the League of European Accelerator-based Photon Sources, is an example of a sustainable, long-term collaboration of European research infrastructures independent of European framework programs and covering a substantially broader scope than the Integrating Activities. Here, ELBE – Center for High-Power Radiation Sources, the predecessor of DALI, has been a member since the first day.

The goal of LEAPS is to establish roadmaps for technological developments and facility upgrades of the European accelerator-based light sources and to join forces and contribute complementary expertise in order to establish and maintain European accelerator technology as a global benchmark. Within LEAPS, DALI is listed among the recognized future upgrades. DALI will be the leading accelerator-based THz facility in Europe and worldwide able to offer access to THz beams of the unprecedented characteristics elaborated in the present document. In particular, it will be a unique facility in LEAPS, meeting a multitude of user requirements; no other facility is able to satisfy.

In parallel, the European Strategy Forum on Research Infrastructures (ESFRI) defines the facilities that are considered as being of highest strategic interest for Europe. The ESFRI roadmap obviously needs to be aligned with national roadmaps. In turn, the impact and importance of DALI in the Helmholtz Association and in Germany must imperatively entail a comparable importance for Europe as a whole.

5.1.3 Uniqueness in a worldwide context

The DALI project aims at constructing a worldwide unique infrastructure for scientific research in the fields of materials science, chemistry, life sciences, using linear and nonlinear spectroscopy in the THz spectral range. The focus will be on converting the concept of superradiant generation of high-field THz pulses at high repetition rates into an internationally important multi-user facility.

An UED and a positron source are also part of the concept. Finally, DALI will be constructed on a campus with and in vicinity of the high power laser laboratory and HZDR's high magnetic field laboratory (HLD). The competence and experience with high-power laser systems and strongest magnetic fields are a strong asset.

Among the major existing or planned photon science facilities in Germany, the spectral ranges of the BESSY III and PETRA IV synchrotrons as well as the FEL facilities European XFEL, FLASH, and DALI are complementary to each other (see Figure 76), and these facilities together would therefore serve the scientific community in an optimal way. While BESSY III and PETRA IV are primarily used for diffraction and spectroscopic investigations, the much shorter (femtoseconds to few picoseconds) and more intense pulses of DALI, FLASH THz, and European XFEL also allow experiments that focus on high-excitation phenomena, optical nonlinearities, or high time resolution.

The underlying key technology of DALI is superconducting radiofrequency (SRF) electron acceleration technology, which over the past two decades has been developed to maturity mainly in Germany in projects such as the European XFEL and the ELBE facility. The SRF acceleration technology enables the provision of highly intense low-energy (meV) and long-wavelength photon pulses with unique characteristics. As such the DALI facility is complementary to short-pulse X-ray sources such as the European XFEL that are based on the same technology and that provide high-energy (keV) photon pulses of extremely short wavelengths for the investigation of complex processes based on the measurement of the molecular and atomic structure. The intense low-energy photon pulses generated by the DALI facility will enable an alternative complementary and essential method to access and measure phenomena that exist far from equilibrium. The low-energy photon pulses with their tailored characteristics (frequency, polarization, bandwidth) allow for the controlling of selected degrees of freedom in the underlying materials in their ground state, such as bond length and bond angle, with "surgical" precision. This enables the direct clarification of the connection, for example, between structure and function in a unique manner.

In the following, the complementarity and competitiveness of DALI are compared with large-scale existing and planned infrastructures in the European and international context.

THz: So far, only very few pilot facilities for high-field THz experiments exist worldwide (see Table 20), and their parameters remain far below the target parameters aimed for at DALI. Up to now, DALI is the only planned user facility for research with high-field THz pulses reaching hundreds of $\mu\text{J}/\text{pulse}$ and frequencies up to 30 THz that will be based on a CW SRF accelerator. This goal carries forward the achievement of the TELBE source at the existing ELBE facility of HZDR as the worldwide first dedicated user facility based on CW SRF electron acceleration delivering μJ energy pulses at frequencies up to 2 THz. The parameters of the DALI sources would open the possibility to explore new high-field driven phenomena and also to build upon recent groundbreaking experiments (e.g. in the field of selective chemistry), which impressively demonstrate the potential of a facility such as DALI.

In comparison to the DALI project, most already existing or planned accelerator-based facilities, such as FLASH2020+ (DESY, Hamburg, D), FLUTE (KIT, Karlsruhe, D), FELIX (Radboud University, Nijmegen, NL), CLIO (CLIO, Orsay, F), TARLA (Ankara University, Ankara, TR), NovoFEL (Budker Institute of Nuclear Physics, Novosibirsk, RUS) are complementary.

LCLS-II (SLAC, Stanford, USA), CTFEL (CAEP, Chengdu, PRC), or PoFEL (Otwock, PL) are facilities comparable to DALI and for which a CW upgrade is foreseen. Nevertheless, DALI is a dedicated CW machine based on more than 20 years of experience with that technology at ELBE.

Table 20: Other accelerator-based THz facilities.

Name (Location)	Type	Status	Comment
FELIX (Nijmegen, NL)	FEL	Operating	<ul style="list-style-type: none"> • Four FELs • Simultaneous operation of three FELs possible • Largest MIR-THz FEL user facility worldwide • Normal-conducting, non-CW • One FEL with extremely long wavelengths (up to 1,500 μm or 0.2 THz)
CLIO (Orsay, F)	FEL	Operating	<ul style="list-style-type: none"> • Normal-conducting, non-CW
NovoFEL (Novosibirsk, RUS)	FEL	Operating	<ul style="list-style-type: none"> • Normal-conducting • CW at MHz repetition rates
CTFEL (Chengdu, PRC)	FEL	Operating	<ul style="list-style-type: none"> • Superconducting • CW at MHz repetition rates planned • Restricted to few THz (<4 THz)
PoIFEL (PL)	FEL	Planned	<ul style="list-style-type: none"> • Similar to ELBE with superradiant THz
FHI-FEL (Berlin, D)	FEL	Operating	<ul style="list-style-type: none"> • No user facility • Only MIR • Normal-conducting, non-CW
TARLA (Ankara, TR)	FEL	Under construction	<ul style="list-style-type: none"> • Copy of ELBE • CW operation planned
LCLS-II (Stanford, USA)	FEL	Under construction	<ul style="list-style-type: none"> • Hard X-ray FEL with additional THz source • Superconducting, CW
FLASH2020+ (DESY, D)	FEL	Planned	<ul style="list-style-type: none"> • XUV FEL with additional THz source • Superconducting, non-CW
TeraFERMI (Elettra, Trieste, IT)	CDR	Operating	<ul style="list-style-type: none"> • Single cycle (< 4 THz), low repetition rate

Over the last decade, **laser-based sources** with considerable intensity have been developed. They exploit nonlinear optical processes, most commonly optical rectification and difference frequency mixing in nonlinear crystals and generation in air plasmas excited by near-infrared and second-harmonic radiation. Photoconductive emitters, which are the most efficient THz sources for compact systems employing high-repetition-rate laser oscillators with near-infrared pulse energies in the few nJ range, are not well-suited for very intense THz generation due to screening and other saturation effects.

Most intense laser-based sources deliver single-cycle broadband pulses. The spectral bandwidth depends on the crystal used for radiation generation, as these polar materials feature strong phononic absorption. In cooled LiNbO_3 crystals operated in tilted-phase-front geometry, very efficient optical-to-THz conversion in the range of a few percent can be achieved under optimum conditions. However, the spectral range is limited to ~ 2 THz. Organic crystals such as DAST, OH1, and DSTMS provide larger bandwidth, with some dips due to absorption lines. In GaP spectra, up to 7 THz can be generated. GaSe crystals can provide pulses way up to MIR frequencies, but at rather low conversion efficiency. In air plasmas, broadband, gapless THz spectra can be generated, basically limited by the duration of the excitation pulses and the phase stability of the second-harmonic generation. The conversion efficiency of the process is about two orders of magnitude lower compared to the LiNbO_3 crystals.

In recent years, intense narrowband sources based on laser excitation have also been developed. They rely on difference frequency mixing of two near-infrared pulses with tunable frequency offset or utilize periodically poled nonlinear crystals (or both). Such systems provide carrier envelope

phase stable multicycle THz pulses with a spectral width depending on the particular design of the system, typically in the 10% range.

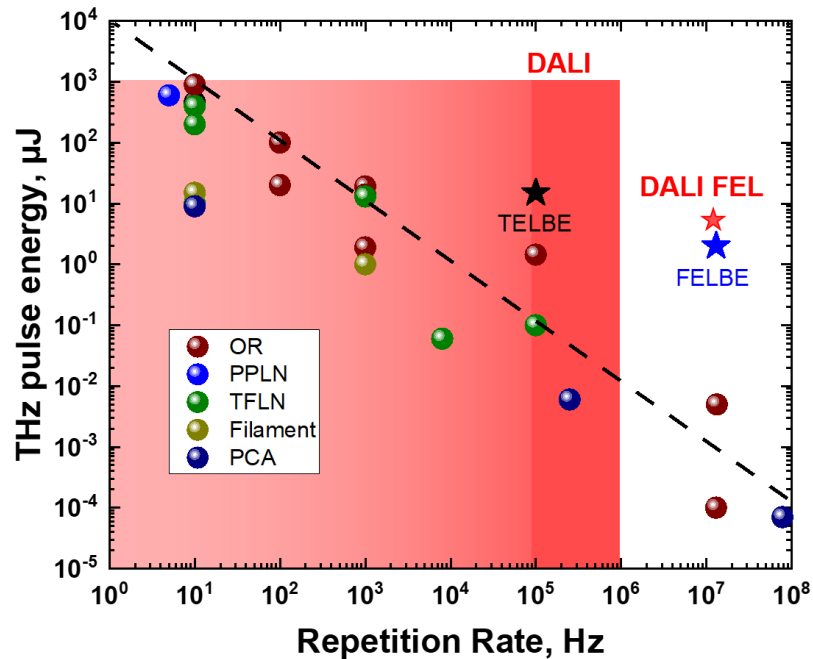


Figure 77: THz pulse energies versus repetition rate of intense THz sources utilizing excitation with intense near-infrared lasers. The sources use periodically poled LiNbO_3 (PPLN),²⁴⁰ thin-film LiNbO_3 (TFLN),^{241,242,243,244,245,246} other crystals for optical rectification (OR),^{247,248,249,250,251,252,253,254} plasma filaments,^{255,256} or photoconductive antennas (PCA).^{257,258,259} For comparison, the black and blue stars mark the pulse energies of TELBE and FELBE, respectively. The dashed line indicates 10 mW average power.

A few years ago, near-infrared laser oscillators operating at several MHz repetition rate and providing more than 1 kW average output power have entered the market. They are enabled by

- ²⁴⁰ S. W. Jolly et al., Nat. Commun. **10**, 2591 (2019)
²⁴¹ J. A. Fülöp et al., Opt. Express **22**, 20155 (2014)
²⁴² X.-J Wu et al., Opt. Express **26**, 7107 (2018)
²⁴³ K. L. Yeh et al., Appl. Phys. Lett. **90**, 171121 (2007)
²⁴⁴ S.-W. Huang et al., Opt. Lett. **38**, 796 (2013)
²⁴⁵ M. Kunitski et al., Opt. Express **21**, 6826 (2013)
²⁴⁶ M. C. Hoffmann et al., Opt. Express **15**, 11706 (2007)
²⁴⁷ C. Vicario et al., Opt. Lett. **39**, 6632 (2014)
²⁴⁸ M. Shalaby and C. P. Hauri, Nat. Commun. **6**, 5976 (2015)
²⁴⁹ C. P. Hauri et al., Appl. Phys. Lett. **99**, 161116 (2011)
²⁵⁰ A. Sell et al., Opt. Lett. **33**, 2767 (2008)
²⁵¹ F. Meyer et al., Opt. Express **27**, 30340 (2019)
²⁵² B. Liu et al., Opt. Lett. **42**, 129 (2017)
²⁵³ P. L. Kramer et al., Opt. Express **28**, 16951 (2020)
²⁵⁴ F. Meyer et al., Opt. Lett. **45**, 2494 (2020)
²⁵⁵ T. I. Oh et al., New J. Phys. **15**, 075002 (2013)
²⁵⁶ K. Y. Kim et al., Nat. Photon. **2**, 605 (2008)
²⁵⁷ X. Ropagnol et al., Opt. Express **24**, 11299 (2016)
²⁵⁸ M. Beck et al., Opt. Express **18**, 9251 (2010)
²⁵⁹ N. T. Yardimci et al., Sci. Rep. **7**, 4166 (2017)

advances in laser technology, in particular the emergence of thin-disk and slab lasers. Such lasers are also highly attractive for THz generation, and there is rapid progress in the optimization of THz systems based on these sources. However, these systems are limited by the rather low intrinsic efficiencies of the THz generation processes. Pulse energies in excess of 100 μJ at repetition rates above 100 kHz require multi-kilowatt laser systems and extremely robust nonlinear media. The technical realization of such THz sources will require dedicated, costly facilities, and they will therefore only be available to a limited number of users. Even if methods are found to make the nonlinear media immune to the necessarily large pump powers, the limitations in frequency range and spectral brightness compared to accelerator-based sources will remain significant.

The recent developments are summarized in Figure 77, which shows a few general trends:

- Currently, the best systems line up around the 10 mW average power line.
- Systems for pulse energies $>10 \mu\text{J}$ are limited to repetition rates of 1 kHz and below. The high-power systems at repetition rates of 10 Hz and 100 Hz cannot be optimized much more, as they are limited by the damage threshold of the nonlinear crystals.
- Optimizing systems for higher repetition rates relies mainly on proper heat management. Here, in particular for the very recent $>10 \text{ MHz}$ systems, one can still expect progress.

The progress in laser-based sources is relevant for DALI in the following ways:

- **Competition:** It has to be ensured that DALI has outstanding parameters with respect to spectral coverage and pulse energy far out of reach of laser-based sources. As discussed above, even with optimistic estimation of progress of such sources, DALI will cover a frequency range that is out of reach of laser-based sources, with pulse energies that are at least two orders of magnitudes larger than future laser-based systems operating in the 100 kHz repetition rate range.
- **Complementarity:** Laser-based sources for intense broadband radiation are ideal to complement DALI. A state-of-the-art system matching the repetition rate of DALI and synchronized to DALI will be available at the user stations for two-color pump–probe experiments.
- **Shaping the user community:** As intense laser-based sources become more widely available, the number of top scientific studies at such systems will grow. At DALI, experienced users will benefit from orders of magnitude higher pulse energy for their top-class experiments. Overall, DALI can host the most exciting experiments from a dynamic, diverse scientific community.

Positrons: Only a few installations for positron annihilation lifetime spectroscopy exist so far. The majority of them are installed at research reactors making use of high-intensity gamma rays from neutron capture reactions, which are in turn employed to generate positrons through the pair production mechanism. HZDR operates the only positron source at a superconducting accelerator so far. While continuous positron beams with high average fluxes exist at several research reactors, the necessary beam chopping and beam bunching systems required for a pulsed positron beam reduce the initial positron flux by orders of magnitude. The available CW pulsed beams with tailored repetition rates – only feasible with superconducting accelerator technology – allows us to go far beyond reactor-based sources. Reactor-based pulsed-beam positron sources are typically operated at fixed frequencies of several 10 MHz, thus limiting maximum positron lifetimes without pulse-to-pulse overlap to below about 2 ns. Therefore, reactor-based pulsed positron beams can neither be used for materials research of porous structures (e.g. low-

k dielectrics for CMOS devices, membranes, etc.), nor for materials with large open-volume structures (polymers, organic compounds, etc.). Accelerator-driven sources therefore constitute a preferable solution spanning all existing positron or positronium lifetimes.

Table 21: *Worldwide positron facilities.*

Name (Location)	Type	Pulsed beam intensity	Repetition rate Max. e ⁺ lifetime	Status
KURAMA ²⁶⁰ (Kyoto Univ., Japan)	Research reactor	7 x 10 ³ e ⁺ /s	30 MHz 2 ns	Online after safety upgrades
PULSTAR ²⁶¹ (North Carolina State Univ., USA)	Research reactor	1 x 10 ⁶ e ⁺ /s	50 MHz 1.2 ns	Under construction
FRM II, ²⁶² sources NEPOMUC ²⁶³ and PLEPS (MLZ, Germany)	Research reactor	1 x 10 ⁵ e ⁺ /s	50 MHz 1.2 ns	Operational, user facility
Electron LINAC (AIST, Tsukuba, Japan)	NC LINAC	2 x 10 ⁴ e ⁺ /s	37.5 MHz 1.6 ns	Reconstructed, SC LINAC abandoned
ELBE, source EPOS ²⁶⁴ (HZDR, Germany)	SC LINAC	1 x 10 ⁶ e ⁺ /s	1.6 MHz 38 ns	Operational, user facility
CEBAF (Jefferson Lab, USA)	Microtron SC LINAC	–	–	Under consideration, polarized e ⁺ source

The consideration of complementary and competing facilities presented here does not comprise dedicated **laser laboratories**. Existing or planned infrastructures comparable to the high-power laser laboratory of HZDR are BELLA (LBNL, Berkeley, USA), CALA (LMU/TUM, München, D), CILEX Apollon (CEA, Saclay, F) and ELI Beamlines (Dolní Brežany, CZ), among others.

5.1.4 Attractiveness to external users

As a research infrastructure with a unique portfolio of THz radiation sources, DALI will contribute to strengthening the leading position of Germany in photon science. In a similar way to the European XFEL or LCLS, DALI will constitute a magnet for highly recognized scientists from all over the world in this rapidly expanding research field and lay the foundation for numerous scientific and technological breakthroughs. Apart from access to a world-leading research infrastructure at the cutting edge of technology, young researchers will benefit from the interdisciplinary environment and from collaboration with leading research groups in their field.

The focus of DALI is on the generation of superradiant high-field THz radiation with unique parameters regarding pulse energy, repetition rate, and control of the pulse form. It will be the only facility worldwide to produce THz fields with pulse energies between 100 μJ and 1 mJ and high and flexible repetition rates between 100 kHz and 1 MHz while offering selectable bandwidths, polarizations, and pulse delays. Complementarily, access to positron and electron sources will be offered, too. The facility will be operated in parallel with the already existing research infrastructures at HZDR, such as the high-power lasers DRACO and PENELOPE, and the High Magnetic Field Laboratory Dresden (HLD). Request for high-field THz radiation,

²⁶⁰ A. Yabuuchi, et al., J. Phys. Conf. Ser. **791**, 012013 (2017)

²⁶¹ A. I. Hawari et al., AIP Conf. Proc. **1099**, 862 (2009)

²⁶² P. Sperr et al., Appl. Surf. Sci. **255**, 35 (2008)

²⁶³ C. Hugenschmidt et al., JLSRF **1**, A22 (2015)

²⁶⁴ R. Krause-Rehberg et al., Appl. Surf. Sci. **252**, 3106-3110 (2006)

presently still limited to a few expert groups, currently experiences a huge increase triggered by a number of groundbreaking results obtained with this radiation. Already now, the running THz source TELBE is only able to fulfill a fraction of the requests for beam time. With DALI coming online, the user community of the new facility is expected to reach a size comparable to the user community of a medium-size synchrotron storage ring.

The worldwide unique characteristics of DALI will result in an increase of the fraction of international users. Estimates result in a forecast of as much as 50% of the users coming from universities and research centers from outside Germany. However, this estimate strongly depends on whether competing facilities will be built in Asia or America in the coming years, at least. The following distribution across scientific disciplines is expected: 40 – 50% physics and materials science, 20 – 30% chemistry, 20 – 30% biology and medicine, and 10% accelerator physics and detector research. Based on our experience with the existing ELBE facility and considering the numbers from the user facilities of the Helmholtz Association, about 50% of the users will come from universities, 45% from non-university research institutions and from international research infrastructures, and up to 5% from industry. The target is an external usage of around 75%, the remaining 25% being granted to in-house users from HZDR and to users from other Helmholtz centers.

5.2 Impact of DALI

DALI will fill a large energy gap in the covered photon energies left open by the other accelerator-based light sources that are currently operated or expected to become operational in the near future in Germany. Complementarily, Chapter 2 presents a kaleidoscope of scientific challenges ready to be tackled as soon as DALI will provide the required research infrastructure. The impact of DALI on research fields ranging from solid-state physics and materials sciences to chemistry, molecular biology, and medicine thus appears to be evident. However, considering the research topics relying on the availability of DALI, it becomes obvious that most of them have implications on human life. Results of experiments in solid-state physics and materials science will advance information technologies. Being able to watch biological processes in real time lays the foundation for a full understanding of the processes influencing health and diseases. This knowledge will constitute the basis for developing efficient approaches to fight diseases originating from processes running on the molecular scale.

However, the impact of DALI will go beyond science and benefits for humankind resulting from scientific findings. The uniqueness of the facility will attract researchers not only from Germany, but also from all over Europe and even worldwide. Some will come as users, staying for a limited amount of time, but others will come and stay, contributing to an enrichment of the city of Dresden and the whole region by new cultural aspects and alternative approaches for tackling challenges and finding solutions. This development will foster intercultural communication and mutual understanding and respect and could contribute to Dresden earning a high reputation as a modern and cosmopolitan city, which will further increase its overall attractiveness.

5.2.1 Regional and supra-regional economic effects

Interaction with industry is becoming increasingly important for all large research infrastructures. In this collaboration, industry may play different roles, as supplier, user, or partner in co-developments. The experience of research infrastructures that are particularly active in fostering interactions with industry and small and medium enterprises (SMEs) and have a long-standing experience therein, such as DIAMOND in the UK or ESRF in Grenoble, shows that the focus needs to be on the local ecosystem around the facilities. DALI will be in the promising situation to

be surrounded by established high-tech industry in Dresden, but also by a variety of smaller companies in the region. The geographical situation close to Poland and to the Czech Republic will offer the opportunity to also reach out to companies outside Germany. Complementarily, the possibility for industry to get access to DALI for boosting their own competitiveness on the global market will contribute to the attractiveness of Dresden as a promising site for industry.

A new facility such as DALI, with challenging goals with respect to technical and technological performance indicators, cannot rely on existing and commercially available technology alone. New developments, to major part also requiring substantial research activities, will be needed. DALI will obviously benefit from the results of these research activities. However, accelerator-based light sources, being they synchrotrons, FELs, or sophisticated THz sources such as DALI, have similar requirements in many aspects. DALI will take suitable measures to protect the knowledge resulting from the new developments. Possibilities to found start-up companies that commercialize a particular product or knowledge transfer to established supplier companies will be investigated. As a research infrastructure is constantly subject to upgrades of specific part, knowledge transfer remains important over the whole life cycle of the facility.

The technological challenges related to the construction of DALI will attract the interest of highly specialized companies in particular. The possibility to apply pre-commercial procurement and public procurement procedures for innovative solutions will be investigated in order to trigger development activities ensuring that, when becoming operational, DALI will be at the cutting edge of technology. However, this will not be the end of the story. Also during the operation phase, specific project ideas will require technological developments that fulfill very demanding requirements. DALI staff, potentially in collaboration with the respective users, might carry out those developments or they will be co-developments with industrial companies that will contribute a particular expertise. In many cases, the impact of the instrumentation, device, or produce will go far beyond the particular research project, and commercialization will be a logical further step.

Access to DALI for proprietary use will be offered from the beginning. However, we expect the request for access to start at a relatively low level and to ramp up over a period of several years. Experience from the present pELBE beamline shows that, already now, there is a strong interest in the use of positrons for materials characterization in applied research, in particular for materials exhibiting a porous structure. Due to the currently still limited amount of beam time at the positron beamline and the lack of sufficient personnel, we have refrained from advertising the unique potential of positron annihilation lifetime spectroscopy for materials characterization to industry. Broadly advertising this opportunity as soon as DALI will be operational is expected to result in an immediate onset of corresponding request.

A few prominent examples of applied research using THz radiation, respectively, have been discussed in Chapter 2. They bear great potential for industrial application. To lower the subjective barrier that prevents industry users from requesting access to large research infrastructures, “twinning beam times” will be offered. These will be joint beam times of an industry user with a beamline scientist, investigating a few typical test samples, but of low strategic importance for the industry user, thus enabling publication of the results. In this way, these “twinning beam times” are to be considered as non-proprietary research and can be offered to the users free of charge.

The DALI advisory boards will include experts on outreach to industry. Based on their own long-standing experience, these persons will play the role of mentors during the first years.

The costs of access to DALI for proprietary research will be charged to the respective user based on full-cost accounting. This process will be managed by the HZDR Innovation GmbH, a spin-off company of HZDR handling industry access to the research infrastructures of HZDR.

5.2.2 Sustainability

At the HZDR, the topic of "sustainable construction" has been gaining more importance for many years. Moreover, this aspect is increasingly included in the realization of projects. Therefore, an additional position with an expert for sustainable construction was established in the construction department of the center. This expert carries out the sustainability assessment of all suitable new buildings and renovation projects using the Sustainable Building Assessment System (Bewertungssystem für Nachhaltiges Bauen, BNB). The assessment system is a holistic evaluation of the sustainability quality of buildings, which was developed by the Federal Ministry of Housing, Urban Development and Building (Bundesministerium für Wohnen, Stadtentwicklung und Bauwesen) in cooperation with the German Sustainable Building Council (Deutsche Gesellschaft für Nachhaltiges Bauen). Additionally, an optimization tool was developed that is used during planning and construction to evaluate and track the sustainability goals set at the beginning of the project.

The life cycle of a building is considered over 50 years, starting with the planning and construction, through the use phase to the deconstruction of the building. Approximately 164 sub-criteria have to be evaluated and a bronze, silver or gold seal of approval is to be sought. The consistent application of sustainability criteria in the construction of new buildings, the consideration of energy optimization potential in the renovation of buildings and their transfer to optimal, efficient operation are anchored in the continuation of the campus master plan at the HZDR site in Dresden-Rossendorf.

At the HZDR, a variety of approaches and developments have existed for years with regard to climate protection and the efficient use of energy. These have been developed within the framework of the previous master plans and have been continuously updated and implemented accordingly. Climate protection in this context especially aims to reduce the use of fossil resources. Nevertheless, research sites are energy-intensive. This makes the sustainable and holistic use of energy highly important. In holistic terms, this means that efficient measures on new buildings and existing buildings are to be optimally combined and planned together with plant engineering measures, taking into account economic efficiency. The implementation of all low energy consuming measures will be closely discussed with best practiced facilities such as KARA at KIT.

5.2.3 Public acceptance, stakeholder and communication

As discussed before, DALI will attract considerable attention far beyond the region of Dresden. The facility will be built using public money, i.e. money from taxpayers, and therefore HZDR clearly owes to the public to present its vision, to report exciting results in a comprehensible form, and to open its doors from time to time, welcoming everybody interested in seeing what such a facility really looks like. HZDR is aware of this responsibility and it will invest a lot of effort in tackling this challenge. Dresden being a city with a large university, many non-university research institutes, and several high-tech industry sites, the public may be considered as being rather open to research and to new research facilities contributing to the worldwide attractiveness and visibility of Dresden. Nevertheless, HZDR is aware of the trust that this acceptance of huge investments in research infrastructures represents and will take its obligation to maintain close links to the public very seriously.

The center will develop a specific communication strategy for DALI, taking into account the portfolio of target groups that is specific for this new facility. A website for DALI will be set up, including a news section in which recent scientific breakthroughs, but also events of general interest will be promoted, offering the choice between a version targeting scientists in the field

and one aimed at the public. Another section will target industry users. This will be complemented by a description of the facility for potential academic users of the facility and one with less detail for any interested person. The user section will be short and mainly linked to the general user site of HZDR. In addition to the website, the HZDR will investigate the potential of social media in the context of DALI, a concept will be developed and applied in a suitable way. The center will keep contact with local newspapers, but also the supra-regional press to offer them interesting news and results related to DALI. The possibility of visiting the site will be organized in collaboration with the PR office of HZDR.

The stakeholder strategy adopted by DALI will start with a stakeholder analysis. HZDR will revise it annually following an update of this analysis and a critical review of the tools used to keep stakeholders informed and to make them part of a DALI community. A first approach will be the production of a periodic DALI newsletter with articles presenting a selection of particularly interesting user experiments, including short portraits of the respective users. In addition, there will be news on the facility, on prominent visits by officials from politics, or on talks by renowned scientists interested in DALI, as well as reports on targeted past or future workshops.

As users are a most prominent group among the stakeholders, dedicated workshops will be offered to ensure the experiments at DALI being carried out by well-trained users able to exploit the full potential of the facility. A user meeting will be organized every year, with a user prize to be awarded every year.

To attract users from industry and promote the great opportunity that access to DALI may offer for industry and SMEs, information days will be organized several times per year. In addition, an industry liaison officer for DALI will be hired, integrated in HZDR's innovation and transfer team. This person will visit the small and big companies in the wider region, ask for their needs, and explain what DALI is able to offer. These visits will be complemented by participation in fairs. In these activities, HZDR will tie in with existing activities on the European level, e.g. the European Analytical Research Infrastructures Village EARIV (<https://www.eariv.eu/>), which emerged from a collaboration of various EU projects of the large-scale research infrastructures in Europe.

6 DALI Project Management

6.1 Planned governance structures (during construction & operation)

HZDR as a center will be responsible for the implementation and operation of the future DALI research infrastructure. This means that DALI will be legally and organizationally an integral part of the registered association Helmholtz-Zentrum Dresden – Rossendorf e.V. As a member of the Helmholtz Association, HZDR is itself integrated into the Helmholtz strategy and Research Fields (currently *Energy, Health, and Matter*). The strategic orientation of the future DALI facility will therefore be a central element of these overarching strategies. The DALI strategy and the facility's performance will be evaluated in the context of the Helmholtz Association's scientific and strategic evaluations (as done for the fourth period of the Program-oriented Funding at the beginning of 2020). As a user facility within the Helmholtz Association, DALI will be subject to the respective strict requirements of the association (see Section 6.2).

6.1.1 Management during the DALI project phase

The management structure of DALI is organized in a PRINCE2-like scheme. The DALI Steering Committee, representing the Customers, the Executive, and Service & Support supervise the project. The Customers are the DALI Executive Board, which is constituted by the directors of the institutes responsible for the implementation and later operation of the facility, the Scientific Head of DALI, and representatives of potential internal (corresponding HZDR institute directors) and external users. The Executive is identical to the HZDR Board of Directors. The heads of the required organizational units in administration, central departments, and staff of the board (i.e., finance, procurement, construction, safety, IT, etc.) constitute Service & Support.

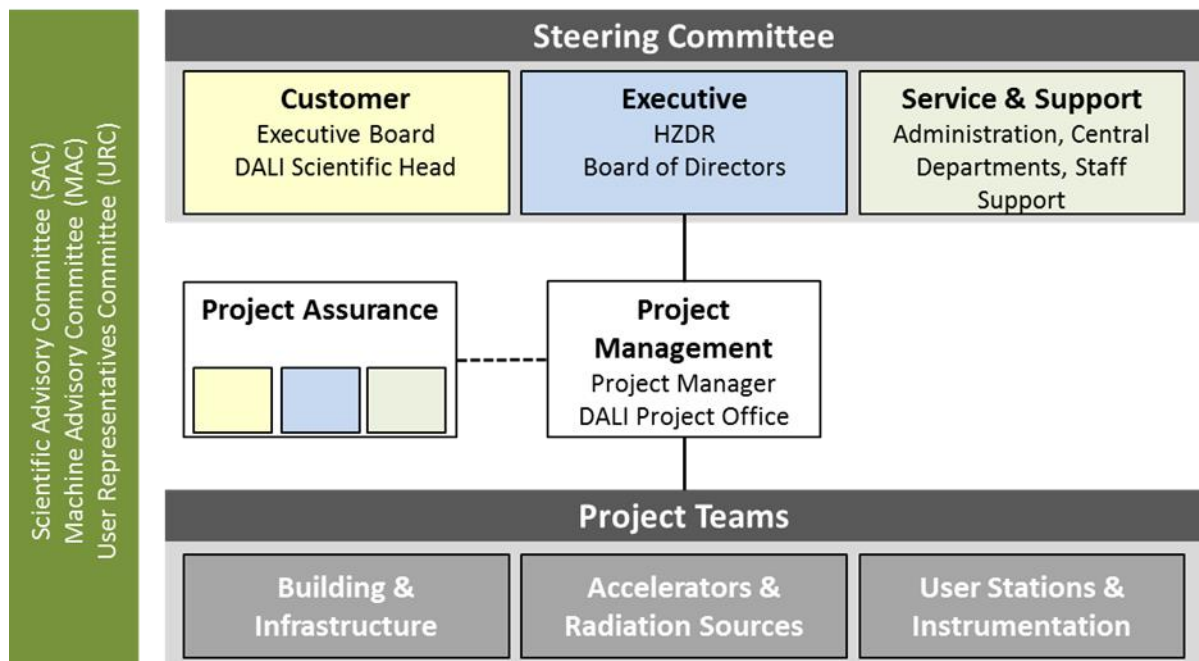


Figure 78: Organizational chart of the DALI project.

A project manager appointed by the HZDR Board of Directors and supported by the DALI Project Office leads the project. This Project Management coordinates the project teams working on the different work packages (not shown here) under the three main pillars Building & Infrastructure,

Accelerators & Radiation Sources, and User Stations & Instrumentation. This work of the Project Management is monitored by a Project Assurance constituted by representatives or delegates of the Customers, the Executive, and Service & Support, which directly reports to the Steering Committee.

Three different committees advise the project organization as a whole: a Scientific Advisory Committee (SAC), a Machine Advisory Committee (MAC), and a User Representatives Committee (URC). Moreover, the project status will be reported to HZDR’s advisory and supervisory bodies on a regular base as well as to external reviewers who give their advice and feedback to the Steering Committee. The entire structure of the DALI project is shown in Figure 78.

6.1.2 Management during the operation phase

The DALI Management Board, consisting of the DALI Scientific Head and the directors and lead scientists of the involved institutes (Institute of Radiation Physics, Institute of Ion Beam Physics and Materials Research), will be responsible for the operation of DALI. Here, the Scientific Head serves as the Facility Head and is responsible for the further development of the facility. Moreover, he/she acts as representative of the facility within the research and user community. The Management Board directly reports to the HZDR Board of Directors. Three specific advisory boards – MAC, SAC, and URC – of the facility, whose heads hold an observer status in the Management Board will provide their advice and assistance.

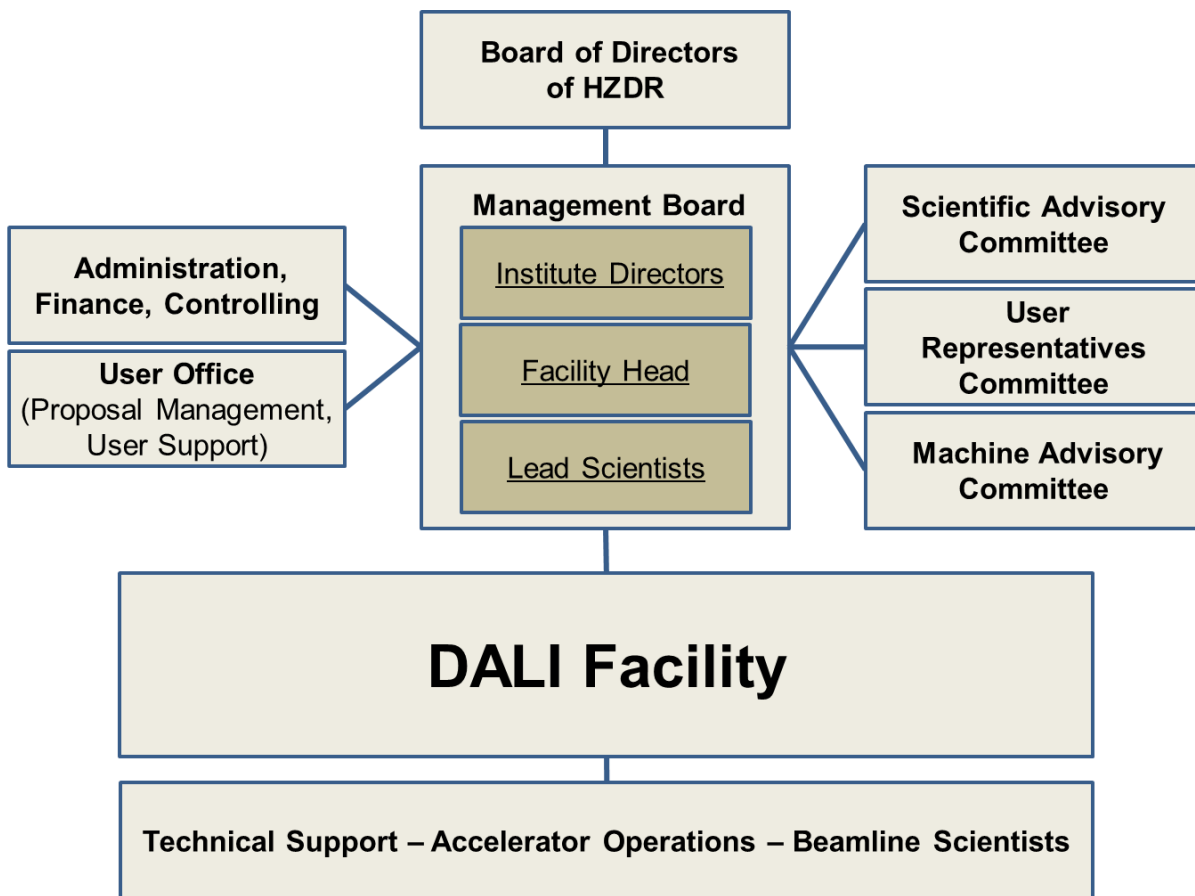


Figure 79: DALI organizational chart.

The operation of the accelerator and the beamlines at the facility as well as the organization of the user support are under the responsibility of the Institute of Radiation Physics, while the responsibility for the experimental user stations will be shared between the Institute of Radiation Physics and the Institute of Ion Beam Physics and Materials Research. The service units of HZDR will provide basic technical, logistical, IT, and development support. The corresponding organizational chart is shown in Figure 79. With substantial financial participation of national or international partners (e.g. by taking charge of a user station), the governance of the infrastructure will be adjusted accordingly.

6.2 Operation regime, access management and user operation

DALI will be operated on a 24/7 basis. These operations are planned based on the experiences acquired at ELBE over the last 20 years. At ELBE, there are four 11 weeks long user runs per year separated by two weeks long shutdown periods in between. During user run, the machine is operated in a fixed shift pattern. The users come in two shifts per day (06-18 and 18-06), while for the operators there are three shifts (06-14, 14-22, 22-06) during weekdays and two shifts (06-18) on Saturdays and Sundays. The operator personnel consist of qualified full machine operators, plus scientists, engineers and technicians. There are always two operators on shift. This is required by the radiation and occupational health and safety authorities. Moreover, this a proven necessity for highly available user beam operations.

In the framework of the Program-oriented Funding (PoF) of the Helmholtz Association, DALI will be operated as a “Leistungskategorie II” (LK II) infrastructure, therefore having to meet the following criteria:

- more than 50% external users from outside the Helmholtz Association
- operating costs (on full costs basis) at least 5 M€ per year
- transparent user selection process based on a peer-review procedure by an external selection committee

At DALI as many as 12 different experimental stations will be offered to users (see Chapter 3), where it is planned to operate more than one beam line in parallel to maximize user beam time. The aim is to achieve an average overbooking factor of 2 or higher, corresponding to request for beam time exceeding the available user beam time by a factor of 2 or higher.

Access to DALI for users will be granted in a transparent proposal process. Two calls are issued per year in the spring and fall, respectively. Users apply for beam time using a web-based system (GATE) that also regulates safety trainings and campus access. Proposals are then peer reviewed by a scientific advisory committee, where three members assess it independently. Selection criterion is primarily scientific excellence. In the case of equal ranking, criteria aiming at supporting in particular Ph.D. students and young scientists, scientists from the Widening Countries in Eastern and south-eastern Europe, and women scientists in STEM (science, technology, engineering, and mathematics) fields are taken into account, too. Beam time, respectively number of shifts, is assigned according to the ranking established by the review committee. Shifts are then allocated into a beam time plan by a local beam time panel.

Around 25 % of all shift are used for machine development, preparation of settings and beam setup. Moreover, the shutdown periods are used for maintenance and commissioning of new machine parts. Then user beam operations is suspended and there are no shifts.

Overall, access to DALI complies with the recommendations of the European Charter for Access to Research Infrastructures.²⁶⁵ In addition, terms and conditions for access to research infrastructures at HZDR as well as a data policy are in place and available to the users.

Access to DALI is free of charge for non-proprietary research by users from universities and research institutions. Results are requested to be published. Industry users will be charged for the beam time on an absorbed costs basis.

Apart from a DALI website for the community, an annual user meeting will be established in order to provide a platform for user to share experience, meet, and start new collaborations. Users will be invited to present their experiments, results, and most recent publications. These meetings will also be used to stimulate direct discussion between users, beamline scientists, and facility operators on the feasibility of new ideas, potential issues hampering smooth and successful beam times, technical problems, and, from a strategic point of view, requests for upgrades enabling access to new realms of science.

6.3 Building options

As described in Section 4.21, there two options for the DALI building, which had been analyzed. Variant 1 is the reuse of the ELBE hall after modification, variant 2 is the construction of a new building, both under the requirement that the high-power laser laboratories (comprising DRACO, PENELOPE and ATHENA) will remain. Both variants have their technical and logistical challenges. Moreover, in both cases, the capacities of the operational and scientific staff needed are similar and the burden during the implementation of DALI is comparable. Even the cost estimates are on nearly the same level of around 86 Mio. €. Nevertheless, the dark time, where there is no longer ELBE beam and still no DALI beam available, is shorter in variant 2. Therefore, although variant 1 is more sustainable, HZDR prefers the construction of a new DALI building by now. This will allow the existing ELBE facility to be operated for as long as possible during the construction of the new hall and the implementation of the radiation sources. To further minimize the downtime of the facility, the sources can be commissioned one after the other. Once ELBE operation has ended, some components of ELBE will be refurbished for utilization at DALI. The former ELBE building will continue to host and support the existing high-power laser laboratory, and the newly vacated space in the hall will later be used for other scientific purposes. Accordingly, in the following (Sections 6.4ff and Chapter 7 on finance) only this variant will be discussed. However, both options will be worked out further and revised during the TDR phase, leading to a final decision at its end.

6.4 Schedule and work breakdown structure

The project is divided into several phases, as shown in Figure 80. A very initial concept was developed in 2015-16, followed by a phase through 2020 in which preliminary technological studies were conducted. At the end of this phase, the conceptual design of the DALI system was developed and documented in the Pre-Conceptual Design Report (Pre-CDR), which was evaluated positively in the first phase of the process to add DALI to the Helmholtz Roadmap for Research Infrastructures (2021). In a subsequent phase, a more detailed Conceptual Design Report (CDR) was prepared and submitted in 2023 (this document). Its evaluation mid of 2024 will finish phase two of the Helmholtz Roadmap process and is requirement to successfully apply for inclusion in the German National Roadmap for Large-Scale Infrastructures.

²⁶⁵ <https://data.europa.eu/doi/10.2777/524573>

Furthermore, the CDR will form the basis for a Technical Design Report (TDR) to be prepared between 2024 and 2025. In parallel, project approval for the German National Roadmap for Large-Scale Infrastructures will be initiated as soon as its call will be published. By now, the timeline as well as the specific requirements for this process are unclear, due to a planned revision of the procedure by the BMBF.

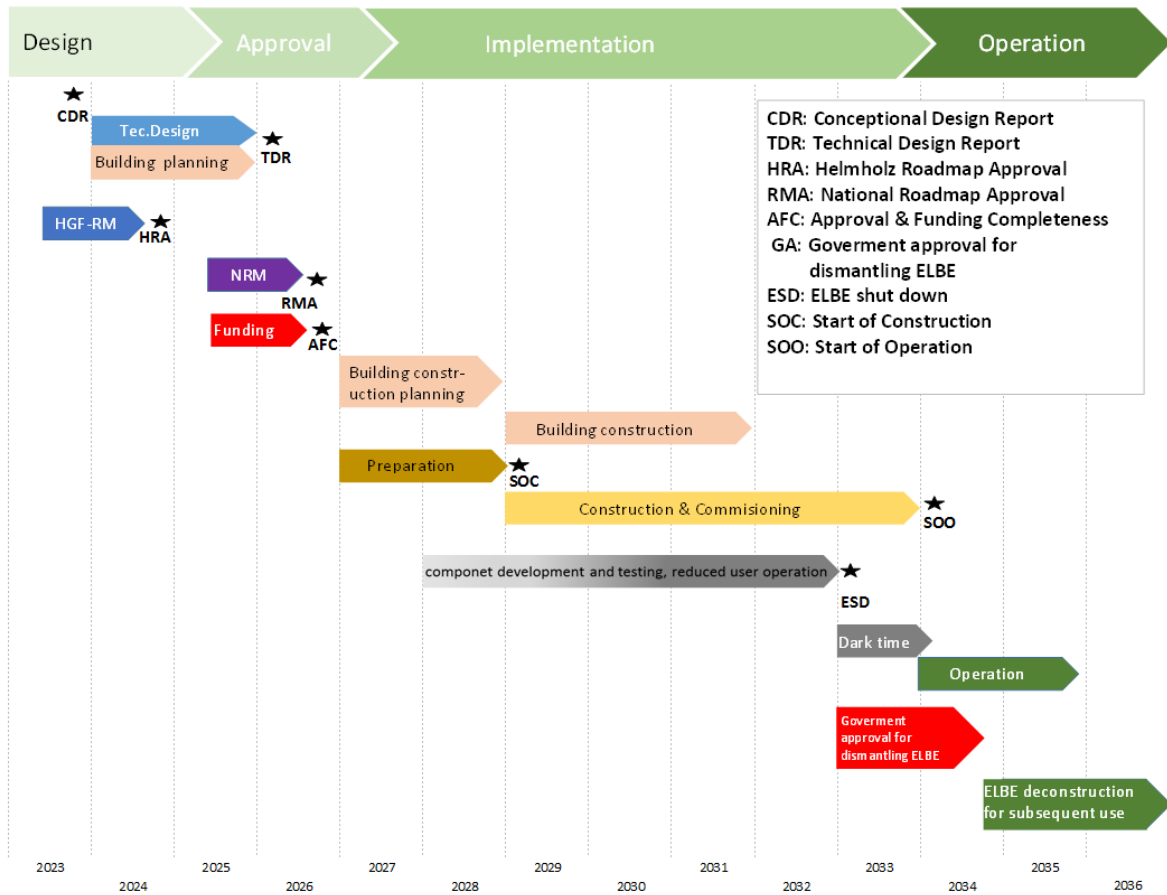


Figure 80: Schedule of the DALI project (based on construction start in 2027).

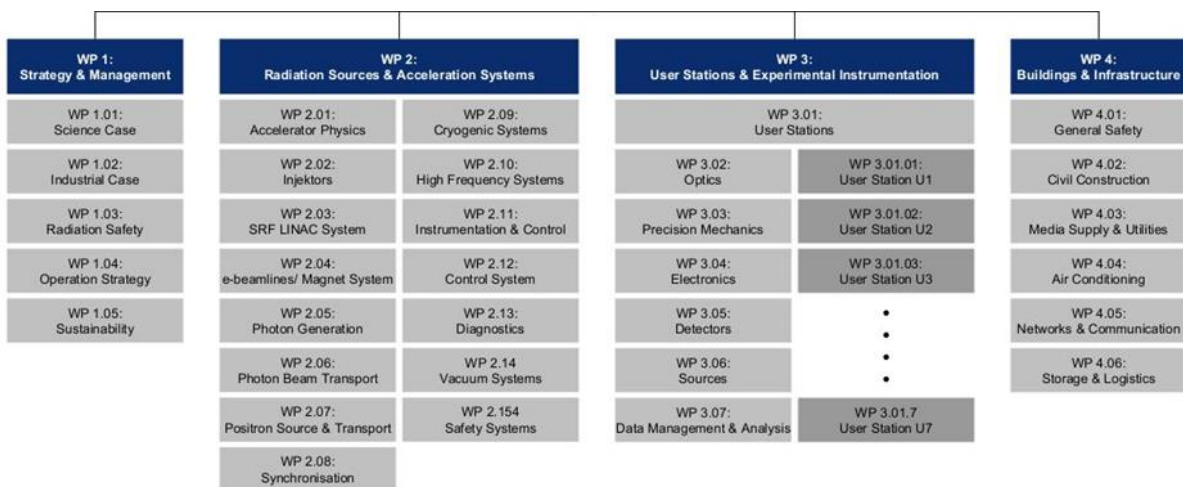


Figure 81: DALI work breakdown structure.

Under the assumption of having the permission and funding for starting the project in 2027 the implementation phase will extend for seven years until 2033, including preparation, construction, and commissioning (see below). During this phase, ELBE will continue regular user operation until end of 2032, with full operation of DALI being planned for 2034. The dark time will last for approx. one year. The facility is expected to operate beyond 2050 (not shown in Figure 80).

6.5 Risk management and mitigation

6.5.1 Technical risks

On the technical side, we are confident in the predictive capabilities of the modern numerical codes used to calculate beam dynamics and design beam transport systems. Numerical and analytical modeling tools for MIR-THz and undulator radiation are well understood and robust. The beam transport magnets, including the undulators required for the project, will rely on standard, commercially available technology, as will the vacuum system. We are also entirely comfortable with the beam diagnostics and control systems required for the realization of such a project. The SRF accelerating modules of the ELBE design and the cryogenic system including the liquid-helium cryogenic plant would be acquired commercially. We also have a long-standing in-house expertise with secondary positron sources at ELBE, the FRM II reactor in Garching, the HOR reactor in Delft, and several radioisotope-based beams.

The primary technical risk for the MIR-THz source is the realization of a robust electron source capable of delivering a beam with a large bunch charge (≥ 1 nC) at a high pulse repetition rate of 1 MHz and suitable for strong bunch compression and the modulated-beam approach. There are several electron guns, from which one can reasonably expect the required beam parameters. Some of these options, according to calculations, should be capable of generating such a beam in their present state. Others would need an improvement of their parameters, for instance of the accelerating field gradient. Until the necessary beam parameters are demonstrated in a laboratory, the risk remains that the improved parameters cannot be reached. Besides, the experience with electron gun developments in many laboratories shows that an appreciable amount of time is often required for a significant improvement of the gun parameters. The failure to deliver beam with the required parameters would lead to an operation with smaller bunch charge, hence reduced MIR-THz pulse energy (field amplitude), where the pulse energy depends quadratically on the charge.

The following are considered to be secondary technical risks:

- Micro-bunching instability (μ BI) leads to an increase in longitudinal emittance and limits the compressibility of the beam. The existing μ BI theory used for the estimations in this report is linear and one-dimensional (1D). Space-charge effects, which play a key role in μ BI, might however have significant nonlinear components and are not 1D. Numerical modeling of μ BI is also challenging because numerical artifacts tend to be larger than the μ BI effects. A robust but very time-consuming approach could be to use the real number of particles for the numerical calculations of the beam dynamics, which is within the capability of modern modeling tools when used on cluster supercomputers.
- This proposal assumes the operation of ELBE-type accelerating modules with an accelerating gradient of at least 12.5 MV/m. This is somewhat higher than presently used at ELBE. We do not consider this to be a major risk, since the gradient design goal of another large-scale CW SRF accelerator facility (LCLS-II) is higher and expected to be met. Nevertheless, cryomodule assembly is a delicate technology, and design demonstration with the modified cryomodule is necessary to eliminate the risk.

- The UED probe beam must have a very small transverse emittance. Beam dynamics modeling of the 1.3 GHz, 3.5-cell SRF electron gun at HZDR with the present accelerating field gradient show that the required emittance is within the system capabilities. Here again, we must take into account the experience with low-emittance gun developments, which shows that significant experimental efforts might be necessary to experimentally achieve the beam parameters predicted by modeling.
- Synchronization of the table-top laser systems and beam-based photon sources with a residual temporal jitter of less than 100 fs RMS is necessary within this project. Among the key components of the synchronization system are the synchro-locks of the table-top lasers. These are required for operation with an accuracy of better than 50 fs RMS. Although a comparable synchronization level has been demonstrated in dedicated experiments, this is not yet a technology that could be routinely applied for facility-scale installation.

6.5.2 Other risks

The ambitious performance goals of the DALI facility approach the limits of the present state of the art of accelerator physics and technology, and considerations of risks in this highly complex project are mandatory. For this reason, the DALI project will be realized along the guidelines of the HZDR rule B 310 "Project Management Manual".

Risk of serious conceptual flaws – The risk of serious conceptual flaws is counteracted very efficiently by thorough analyses and detailed studies performed by the highly experienced accelerator design team in the HZDR department Radiation Source ELBE. A continuous exchange with other colleagues in the worldwide accelerator community and with the Scientific Advisory Committee for the Radiation Source ELBE is extremely valuable to avoid safely overlooking design mistakes or missing opportunities for further design optimization. Participation of team members in workshops and conferences related to MIR-THz radiation sources and other key technologies as well as in advisory committees of other projects is also important in this respect.

Schedule risks – One important aspect of the mitigation of schedule risks is a tight follow-up on all critical milestones in all phases of the project. This includes the supervision of the manufacturers of accelerator and beamline components and is the main task of the (external) project manager. The organization of the project and the applied tools and procedures for project follow-up enable the project management to have a complete overview of schedule-critical issues at any point in time.

Cost risks – See Section 7.7 in the following chapter.

7 Financial Framework

7.1 Project scope

The DALI project comprises the construction, commissioning, and operation of a new facility for high-power THz sources as well as positron and UED sources. The project essentially consists of six major subprojects:

- **THz source:** see Section 4.1.5 and 4.1.6
- **Positron source:** see Section 4.1.8
- **UED electron source:** see Section 4.1.9
- **Experiments:** The photon experimental facilities will comprise five THz user stations that will receive beam from the DALI THz sources (up to two can be used in parallel). Additionally, the beams of numerous synchronized table-top laser sources will be distributed to all of the photon user stations. An HHG source will also be available for one of the THz stations. The UED electron source described above will also be available together with the DALI THz and table-top sources. For positron experiments, two user stations and one versatile open-beam port for experimental setups from users will be set up. See Section 1.3 for an overview and Chapter 3 for a more detailed description.
- **Civil construction:** The facility requirements for DALI are distinct from the ones of the current ELBE building. Different civil construction plans have therefore been considered, including an entirely new building as well as different reconstruction scenarios entailing a modification and extension of the existing ELBE building. The costs were taken into account as well as the anticipated downtime of the facility (“dark time”) and the effects on adjacent facilities, such as the HLD and the high-power laser laboratory. Eventually, the construction of a completely new building was determined as the best option, by now. For details, see Sections 4.21 and 6.3.

The DALI project is divided into three major phases from an organizational and financial point of view. A first design phase for the compilation of the CDR (this document) is finished. It is followed by a technical design phase for the preparation of a TDR. The DALI implementation phase comprises the preparation, construction with production of components, installation, and final commissioning of the facility. After this, DALI will enter the regular operation phase.

7.2 Project costs

In the following, the costs of the major elements of DALI are described in more detail. Table 22 at the end of this section shows the cost estimation for the facility

THz source: The THz source comprises the two injectors, the low-level and power RF sources, the electron beamlines, as well as the LINAC modules for the production and preparation of the electron beam. Three components – two superradiant undulators, which are operated in a modulated and an unmodulated mode, respectively, as well as an FEL oscillator – are used for photon production. Subsequently, photon beamlines transport and distribute the THz beams to the user stations.

UED source: The ultrafast electron diffraction source comprises a highly integrated combination of a specific UED injector and a dedicated beamline.

Positron source: The High-intensity Positron Source (HiPS) will be installed behind the THz undulator beamlines, thus serving as a beam dump for the electron beam. The technology will be based on the experience with the liquid-lead loop at ELBE's neutron time-of-flight source nELBE. The unique liquid-metal electron-to-bremsstrahlung converter combines a high power density with an effective bremsstrahlung yield. Both a magnetic transport system for low-energy positrons (realized at ELBE) and a fully electrostatic transport system (realized at the TU Delft reactor) are possible concepts for the positron beamlines to the user stations. Details will be worked out at least for the TDR.

Experiments / user stations: Due to the current stage of the planning process, the costs of the user stations are not yet distinguished for the different experiments. The total costs for this position are given using a general estimate per user station. Details will be worked out at least for the TDR.

Civil Construction: Base for the cost estimate here is the assumption that HZDR will construct a completely new DALI building (for details, see Sections 4.21, 6.3 and the corresponding paragraph in Section 7.1). However, the analysis of a reconstruction scenario revealed similar numbers.

Other: Further positions comprise cryogenic systems, vacuum and mechanical systems, electron beam diagnostics, instrumentation and control, synchronization and timing, personal safety systems, auxiliary systems as well as computing infrastructure and data management.

Table 22: Cost estimation for the DALI facility (given in T€)

Position	Cost estimate [T€]
Radiation Sources	4,500
FEL DC- thermionic injector	500
1nC SRF gun (w/o UED)	6,500
SRF linac system (cryo-modules, high-power RF, LLRF)	19,000
Beam transport (magnets and power supplies)	4,000
Vacuum and mechanical systems	5,000
Electron beam diagnostics (including beam-based feedbacks)	5,000
Instrumentation and control (including software engineering)	3,500
Synchronization and timing	2,000
Cryogenic systems	31,000
User laboratories and photon beam transport	32,500
Personal safety systems (Radiation safety - Laser safety - ODH)	2,000
Auxiliary systems (cooling, gasses)	4,500
Positron source and transport	5,500
UED system	7,000
Computing infrastructure & data management	10,500
Building (new)	86,000
total	229,000

7.3 Cost profile

Table 23 shows the cost profile over the implementation period. Values that are more accurate will be worked out during the TDR phase and should be available by the end of 2025. From today's point of view, there are no exact figures for the annual distribution of the required funds, but some boundary conditions can already be given now under the assumption of the planned schedule (see Section 6.4), and based on a 2023 price index.

Table 23: Cost profile for the DALI implementation (given in T€).

Phase	Implementation phase							Total
	Preparation		Construction, Installation, Commissioning					
Year	1	2	3	4	5	6	7	
Costs [T€]	4,000	14,000	25,000	41,000	39,000	65,000	41,000	229,000

7.4 Operational costs

DALI will be an upgrade/replacement of the existing ELBE facility, which HZDR intends to operate according to the same financial scheme as ELBE, namely as a LK II facility. The conditions for access will be the same as for ELBE: free access for all academic users, who will be granted beam time for experiment proposals via a peer-review process, and a full cost recovery model for all other users including from industry. The expected operating costs for DALI can therefore be estimated with reasonable accuracy from the costs for the present ELBE facility. Nevertheless, this requires knowledge of the detailed DALI setup, which will be available with the TDR. As a first coarse estimate the operational costs for the DALI facility are assumed to amount to 23,000 T€ per year.

7.5 Costs of the phase-out

The DALI facility will be an important part of the strategy of HZDR and the Helmholtz Research Field Matter. It will serve as a central large-infrastructure facility for a user community from Germany, Europe, and beyond, coming from a wide spectrum of scientific fields. A dismantling of the facility would lead to a strategic reorientation of research not only at HZDR, but also within the entire German user community for THz radiation. Nevertheless, in the TDR preparatory phase until the end of 2025, an estimation will be done of the resources needed for dismantling the facility. It is assumed that DALI will be available to users for more than 20 years. The analysis for the dismantling will concentrate primarily on the materials used and their disposal. Since such an estimate requires the detailed data for setting up DALI, a valid estimation for the phase-out period will only be possible in the context of the final TDR.

7.6 Funding scenarios

A detailed financial planning of the project will be part of the TDR. The costs for the development of this document, which are mainly personnel costs as well as costs for the construction design, will be covered by HZDR. The application for inclusion of DALI in the Helmholtz and German National Roadmaps is motivated by the request for financial support for building the facility. The

anticipated required budget of 229 M€ is far beyond the financial capacity of HZDR in particular and of the Helmholtz Association in general.

Like the ELBE operating costs, the costs for running the DALI facility will be covered by HZDR in the format of the established LK II funding for prominent Helmholtz user facilities. However, whereas the operational costs for ELBE, prospectively budgeted for the time when DALI will enter user operation and ELBE will have been shut down, amount to around 13 M€ per year, the annual cost for running DALI will rather be on the order of 23 M€. To cope with this challenge, HZDR will use the construction phase of DALI to develop a clear strategy for the research activities of the center to be pursued in the future. This will result in a streamlining of the activities around DALI as the future core of the center, related to a transfer of budget to the LK II funds to cover the operational costs of the new facility.

7.7 Economic risk assessment

In the following, those risks are discussed that could have a significant impact on the project. First, DALI cannot be realized funded by the Helmholtz Association or HZDR alone. External funding is needed, like a dedicated project funding, e.g. via the National Roadmap. Other important risks are primarily those directly attributable to the prices of the required components and services on the market at the time they are needed. Here, we see a very high volatility due to the recent crisis. In addition, there are risks of technical nature (see Section 6.5) or delays in delivery that could lead to additional costs. Therefore, the risk assessment during the implementation phase comprises all the potential risks for the project including the possible economic impacts. In the following, potential risks will be discussed here in a quite generic way. In the upcoming years, these risks will be further evaluated and specified. A precise risk assessment will be part of the TDR.

Civil construction: Construction companies often do not accept contracts from the public sector due to the high bureaucratic hurdles. The lack of competent specialists may cause delays in the construction of the building. Moreover, availability of construction materials, due to disrupted supply-chains is a serious problem affecting the prices, too. Nevertheless, a major risk is the volatility of prices in this sector in the last years. This makes estimating the cost increase risk in this sector difficult.

Accelerators and radiation source systems: The main economic risks for the accelerators and the radiation source systems – apart from what has already been discussed in general – lies in two areas. These are i) the cost of the cryogenic plant (large helium liquifier) and ii) the cost of the accelerating cryomodules of the SRF LINAC. Both base on the low number of manufacturers for these products, having a long orders lists and strong leverage to determine the prices.

Experiments: Regarding the experimental stations, there is the risk of cost increase due to delays in the construction process and due to changing requirements for the technical specifications of the facility over the course of time. Cost increases due to changes in statutory regulations, for example additional and new requirements regarding environmental and radiation protection, are a possibility, but presently not foreseeable.